

52227

132

LAUR-95-3468

October 1995

***Natural Background Geochemistry and
Statistical Analysis of Selected Soil Profiles,
Sediments, and Bandelier Tuff,
Los Alamos, New Mexico***

***Edited by
Patrick A. Longmire
David E. Broxton
Steven L. Reneau***

Los Alamos Environmental Restoration
Records Processing Facility



ER Record I.D.# 52227

Los Alamos

*Los Alamos National Laboratory is operated by the
University of California for the United States
Department of Energy under contract W-7405-ENG-36.*



7145

Received by ER-RPF

FEB 09 1996

Dic

DRAFT DOCUMENT

NATURAL BACKGROUND GEOCHEMISTRY AND STATISTICAL ANALYSIS OF SELECTED SOIL PROFILES, SEDIMENTS, AND BANDELIER TUFF, LOS ALAMOS, NEW MEXICO

Revision Date: September 28, 1995

by

Patrick Longmire, CST-7; David Broxton, EES-1; and Steven Reneau, EES-1
Editors

EXECUTIVE SUMMARY

The investigations compiled in this draft report describe elemental background concentrations for 24 analytes in soils, sediments, and the Bandelier Tuff at Los Alamos National Laboratory. Results of these investigations form the basis for statistical analysis for risk and screening analysis for the Environmental Restoration Project and are required as part of the RCRA corrective action process developed by the US Environmental Protection Agency (EPA). These investigations included studies of geochemistry, soil characterization, stratigraphy, and geomorphology. These investigations were conducted in support of the Resource Conservation and Recovery Act (RCRA) Facility Investigation for Los Alamos National Laboratory. Results of these investigations have relevance to all Laboratory field units and operable units.

The Wilcoxon rank sum test and box plots are used to determine if there is a significant chemical difference between soil horizons, sediments, and mapping units of the Bandelier Tuff. Values of upper tolerance limits (UTLs) in soils, sediments, and the Bandelier Tuff for naturally-occurring metals, nonmetals, and radioisotopes of K, Th, and U (excluding sediments) at the Laboratory are presented.

Approximately 250 background soil samples have been collected adjacent and within the Laboratory boundary. Soil samples were partially digested using HNO_3 and completely digested using HF, providing total element concentration, prior to analysis following EPA SW846 methods. Total element concentrations in 75 soil samples were also determined by x-ray fluorescence and instrumental and delayed neutron activation analysis. Background-elemental concentrations in soils on the Pajarito Plateau vary with parent material, the degree of soil development, and other factors. Well-developed soils containing B horizons have higher concentrations of trace elements than weakly developed soils found on the Pajarito Plateau. The B horizons in background soils generally contain higher concentrations of iron hydroxides, clay minerals, and trace elements relative to A and C horizons. No

DRAFT DOCUMENT

additional Laboratory background data are needed for B horizons (134 samples) present on mesa tops; however, we recommend additional characterization of A and C horizons because a small number of samples (<30) are present in the data set for mesa top soils. We recommend that additional soil samples be collected and characterized from A, B, and C horizons for slope and canyon bottom soils.

Several soil profiles characterized on mesas at TA-63 and TA-67 contain anomalous concentrations of U within the several A horizons. These horizons apparently have received wind-blown U that possibly was derived from Laboratory firing sites. These U data collected from the A horizons at TA-63 and TA-67 are not included in the background-elemental data set for the Laboratory.

An initial 16 background sediment samples have been collected from Ancho Canyon and Indio Canyon at Technical Area 39. Systematic variations in elemental background concentrations in sediments occur between different geomorphic settings and different particle sizes. The lowest concentrations of most elements occur within coarse, well sorted sands in active stream channels and the concentrations of most analytes generally increase with decreasing particle size characterized by larger surface areas. These differences indicate that the best comparison of potentially contaminated sediments to background should utilize the most comparable subset of the Laboratory background data set. Analyte concentrations in sediments are generally lower than those associated with B horizons in soils, but are comparable to elemental concentrations within A and C horizons. We recommend that additional background sediment samples be collected and chemically characterized from several canyons at the Laboratory representative of the different geologic-geomorphic conditions.

A total of 251 bulk rock samples was collected to characterize the chemistries of bedrock units on the Pajarito Plateau. Total element concentrations were determined for 208 samples by x-ray fluorescence and 38 samples by instrumental and delayed neutron activation analysis to determine the chemical variability of the bedrock units. Based on these analytical methods, a representative suite of 106 samples was selected for analysis by EPA SW846 methods, using HNO₃ digestion techniques, for their leachable concentrations of inorganic analytes. The spatial coverage and population size of background chemistry samples for the Bandelier Tuff are considered adequate for defining background screening values for units Qbt 1g, Qbt 1v, Qbt 2, and Qbt 3 of the Tshirege Member. These tuffs are the most widespread rock units on the Pajarito Plateau and make up the bedrock at the majority of the Laboratory's potential release sites. No additional background data are needed for these units. We recommend additional characterization of Qbt 4 because so few samples of this unit are included in the present data set. Preliminary background screening data are presented for pre-Tshirege rock units (tephras and volcanoclastic sediments of the Cerro Toledo interval, the upper part of the

DRAFT DOCUMENT

Otowi Member of the Bandelier Tuff, and dacitic lavas of the Tschicoma Formation); we recommend that these data be supplemented by local background data on an as needed basis.

DRAFT DOCUMENT

NATURAL BACKGROUND GEOCHEMISTRY AND STATISTICAL ANALYSIS OF SELECTED SOIL PROFILES, LOS ALAMOS, NEW MEXICO

by

Patrick Longmire, CST-7; Eric McDonald, EES-1; Randy Ryti, Neptune and Company, Inc.; Steven Reneau, EES-1; and Paula Watt, Univ. of New Mexico

ABSTRACT

During 1993, fourteen soil profiles were characterized and sampled to enlarge the background-elemental database (Longmire et al., 1995) for Los Alamos National Laboratory (hereafter referred to as the Laboratory). Prior to chemical analyses, soil samples are partially digested primarily using HNO_3 at pH 1, which provides element concentrations in acid-soluble solid phases such as calcium carbonate, solid organic matter, clay minerals, and ferric hydroxides. Aliquots of the same soil samples are also completely digested using HF, providing total element concentrations. These soil digestion procedures provide a comparison of elements incorporated within the primary silicate minerals (total digestion) with those elements concentrated in surface coatings formed during soil genesis (partial digestion). Analytical methods consisted of inductively coupled plasma spectroscopy, atomic absorption, and ion chromatography. In addition, several soil properties, including texture, bulk density, organic matter, cation exchange capacity, and extractable iron oxides, were analyzed using standard soil characterization techniques.

Approximately 250 background soil samples have been collected adjacent and within the Laboratory boundary. These samples have been analyzed for 24 metals and non-metals relevant to the Environmental Restoration Project. No additional Laboratory background data are needed for B horizons (134 samples) present on mesa tops; however, we recommend additional characterization of A and C horizons because a small number of samples (<30) are present in the data set for mesa top soils. We recommend that additional soil samples be collected and characterized from A, B, and C horizons for slope and canyon bottom soils.

Background-elemental concentrations in soils on the Pajarito Plateau vary with parent material, the degree of soil development, and other factors. Well-developed soils have higher concentrations of trace elements than weakly developed soils found on the Pajarito Plateau. The B horizons in background soils generally contain higher concentrations of iron hydroxides, clay minerals, and trace elements relative to A and C horizons. In addition, variations in soil-elemental concentrations are related to climate, topography, and to the parent

DRAFT DOCUMENT

materials, which include alluvial fan deposits, sheet wash material, colluvium, wind-blown sediment, El Cajete pumice, and the Bandelier Tuff.

Soil profiles characterized on mesas at TA-63 and TA-67 contain anomalous concentrations of U within the several A horizons. These horizons apparently have received wind-blown U that possibly was derived from Laboratory firing sites. These U data collected from the A horizons at TA-63 and TA-67 are not included in the background-elemental data set for the Laboratory. The B and C horizons are less affected by the anthropogenic U and these horizons generally have U concentrations similar to other background soil horizons reported by Longmire et al. (1995).

Comparisons of site data to background data are needed as part of the Resource Conservation and Recovery Act (RCRA) corrective action process developed by the US Environmental Protection Agency (EPA). The Wilcoxon rank sum test and box plots are used to determine if there is a significant chemical difference between soil horizons. Results of statistical analyses, including calculation of a horizon-specific upper tolerance limit (UTL) for each element, are presented in this report. The UTL is equal to the mean plus the standard deviation multiplied by k-factors (one-sided normal tolerance factors), using the 95th percentile at 95% confidence. For elements that are normally distributed without any data transformation and the elements that are normally distributed after a square root transformation, UTLs were calculated using the following equation:

$$UTL_{0.95,0.95} = \text{mean} + \text{standard deviation} * k_{0.95, 0.95}$$

The k-factor is dependent on the number of background samples. The UTLs for log-normally distributed elements are estimated by a simulation process. The calculated UTL results were screened to ensure that the estimated UTLs were not artificially inflated due to a small sample size. Site data greater than the UTL-calculated threshold value are considered to exceed the normal maximum background concentration for a particular element. Values of UTL in soils, including A, B, and C horizons, for naturally-occurring metals, nonmetals, and radioisotopes of K, Th, and U at the Laboratory are presented below.

DRAFT DOCUMENT

Analyte	Soil Horizon			All Data
	A	B	C	
Aluminum	26600	43600	38700 *	38700
Antimony	0.5	1	ND	1
Arsenic	6.99	8.12	6.58	7.82
Barium	263	321	286	315
Beryllium	1.41	1.91	1.95 *	1.95
Cadmium	1.4	2.7	ND	2.7
Calcium	4030	6480	5930	6120
Chlorine	25.0	78.2	170	75.9
Chromium	19.3 *	19.0	17.0	19.3
Cobalt	31.0	14.8	41.2	19.2
Copper	30.7 *	29.2	22.2	30.7
Iron	18100	21800	18500	21300
Lead	28.4	22.3	21.9	23.3
Magnesium	3460	4480	4610 *	4610
Manganese	1000	673	463	714
Mercury	ND	0.1	0.1	0.1
Nickel	12.2	16.0	13.3	15.2
Potassium-TOTAL	33200	33400	41800	35000
Potassium	3070	3420	3410 *	3410
Selenium	0.7	1.3	1.7	1.7
Sodium	602	798	2680	915
Sulfate	42.7	249	712	317
Tantalum	ND	ND	ND	ND
Thallium	0.4	1	0.6	1
Thorium	13.3	15.0	12.3	14.6
Thorium-TOTAL	20.5	22.7	25.3	22.6
Uranium	1.87 *	1.72	1.36	1.87
Uranium-TOTAL	5.10	5.34	6.58	5.45
Vanadium	42.8	42.0	32.0	41.9
Zinc	47.1	51.5	50.8 *	50.8

* Values were trimmed to the all data UTL to eliminate inflated UTLs.

ND = Not detected. Units are mg/kg.

DRAFT DOCUMENT

INTRODUCTION

Determining environmental impacts to surface waters, groundwaters, soils, sediments, and bedrock (Bandelier Tuff) at the Laboratory requires knowledge of background-elemental chemistry of geological and hydrological media. Background media are defined as soils, sediments, rocks, surface waters, and groundwaters unaffected by Laboratory operations. Longmire et al. (1995) reported initial background elemental concentrations in selected soils and the Bandelier Tuff. Broxton et al. (this report) provide additional background elemental data for the Bandelier Tuff. Statistical and geochemical comparisons of background samples with contaminated or non-background samples are needed to identify and evaluate environmental contamination. The purpose of the soil characterization studies presented in this report is to determine the nature and variability of background-elemental concentrations and soil parameters within different soil horizons for a variety of soil profiles at the Laboratory, enlarging the earlier database of Longmire et al. (1995).

During 1993, fourteen soil profiles were characterized and sampled to determine background-elemental concentrations and their relation to soil characteristics (Watt, 1995, McDonald, unpublished). One hundred and thirty-nine soil samples were submitted for chemical analyses using methods approved by the USEPA, Laboratory, and Soil Survey Staff (1981). Soil samples were analyzed for both total element and partial element concentrations by digesting soil samples using hydrofluoric acid (HF) and nitric acid (HNO₃), respectively.

Geochemical characteristics of soils on the Pajarito Plateau vary widely and are related to local variations in parent material, topography, soil age, surficial processes, climate, and vegetation. The sites of detailed soil sampling and analysis in this study were chosen to provide chemical data for soils not sampled previously and to evaluate the physical and chemical variability in soils in several soils series previously described by Nyhan et al. (1978). Soil characterization data for these soils reported in Watt (1995) are presented in detail in this report. These soils formed in a wide variety of geomorphic settings and the setting of each sample site was described to provide a better understanding of controls on the variations in soil development.

This investigation contributes to the Environmental Restoration (ER) Project, by providing additional background-elemental data that can be used in conjunction with screening action levels (SALs) in risk-assessment calculations for different contaminants. These background-elemental data are useful in developing sampling and remediation strategies at sites, to understand processes controlling contaminant transport, and to distinguish between contaminated and non-contaminated media. These data may also be used to establish cleanup levels for sites to be remediated. Recommendations are

DRAFT DOCUMENT

provided for sample collection, sample preparation and analyses, and statistical and geochemical interpretation of soils data.

This report (1) summarizes results of soil characterization studies conducted by Watt (1995) and McDonald (unpublished data); (2) describes analytical and statistical methods used to define and characterize background chemical (analyte) distributions in soils; (3) discusses soil development (pedogenesis) and soil chemistry relationships; and (4) describes how these background data may be statistically compared to the background-elemental data set for soils provided by Longmire et al. (1995) and to non-background (potential release site) or contaminant analytical data. In addition, this report addresses characterization studies outlined in the Laboratory's Hazardous and Solid Waste Amendments (HSWA) permit, Task III (Facility Investigation), Section A. (Environmental Setting), Number 2. (Soils), Items a, b, f, g, i, k, l, m, p, and q.

SAMPLING SITES AND METHODS

Sampling Sites

Fourteen soil profiles at seven different areas were described in the field and soil samples were collected for chemical analyses. The soil sample sites included mesa tops (TA-51, TA-63, TA-67), a canyon bottom (Ancho Canyon (AC-1), and fans and colluvial slopes in the western part of the Laboratory (Water Canyon (WC), TA-16). Vegetation ranges from Ponderosa pine forests in the wetter, western part of the Laboratory to pinon-juniper woodland in the drier, central part (Table 1, Figure 1). The parent materials for the soils included weathered and eroded Bandelier Tuff, alluvium partially derived from Tschicoma dacite in the Sierra de los Valles, wind-blown dust, and El Cajete pumice. All sites were within the soil mapping area of Nyhan et al. (1978), and include six of their thirteen soil series, although the sample sites were not necessarily typical of soils within each series as described by Nyhan et al. (1978).

Descriptions of soil samples are provided in Table 2. Areas selected for detailed soil characterization described by Watt (1995) and McDonald (unpublished data), with the number of soil profiles, include: Site 1, TA-39 in Ancho Canyon near State Route 4 (one profile: AC-1); Site 2, Water Tanks along State Route 501 (two profiles: TA-16-1, -2); Site 3, TA-16 along West Jemez Road near intersection of State Route 4 and State Route 501 (west gate) (one partial soil profile: LA-4); Site 4, TA-51 (one soil profile); Site 5, TA-63 (four soil profiles: 1A, 2, a, c); Site 6, TA-67 at the proposed Mixed Waste Disposal Facility (MWDF) (five soil profiles: E1, E1-2, E3, W1, W5); and site 7, Virgin Mesa (southwest of Jemez Springs and west of the confluence of the Jemez River and the Rio Guadalupe). Although complete soil profiles were described, only a subset of samples were submitted for background geochemistry (LA-4,

Table 1. Summary of Soil Sample Sites.

Sample Site	Technical Area	Elevation (ft)	Vegetation	Topographic Setting	Surficial Material
1. Ancho Canyon	TA-39	6270	Ponderosa pine	canyon bottom	Holocene alluvium (last 5000 years)
2. Water Tanks Trench	TA-16	7750	Ponderosa pine	base of scarp	pre- El Cajete to late Holocene colluvium
3a. Water Canyon, (north)	TA-16	7560	Ponderosa pine	base of scarp	Holocene colluvium over fan
2b. Water Canyon,(south)	TA-16	7580	Ponderosa pine	old fan	Pleistocene alluvium
4. Mesita del Buey	TA-51	7020	piñon-juniper	mesa top	thin post El Cajete (?) soils
5a. Pajarito Road, Trench 1	TA-63	7200	grass	mesa top	thick pre and post (?) El Cajete soils
5b. Pajarito Road, Trench 5-1	TA-63	7200	grass	mesa top	thin post El Cajete (?) soils
5c. Pajarito Road, Trench 5-2	TA-63	7200	grass	mesa top	thin post El Cajete (?) soils
5d. Pajarito Road, Trench 5-3	TA-63	7200	grass	mesa top	thin fracture fill
6a. Pajarito Mesa, Trench E1	TA-67	7240	Ponderosa pine	mesa top	pre- and post El Cajete soils
6b. Pajarito Mesa, Trench E3	TA-67	7210	Ponderosa pine	mesa top	pre- and post El Cajete soils
6c. Pajarito Mesa, Trench W1	TA-67	7250	Ponderosa pine	mesa top	pre- and post El Cajete soils
6d. Pajarito Mesa, Trench W5	TA-67	7290	Ponderosa pine	mesa top	pre- and post El Cajete soils
7. Virgin Mesa, Jemez Springs			Ponderosa pine	mesa top	

SANTA FE NATIONAL FOREST

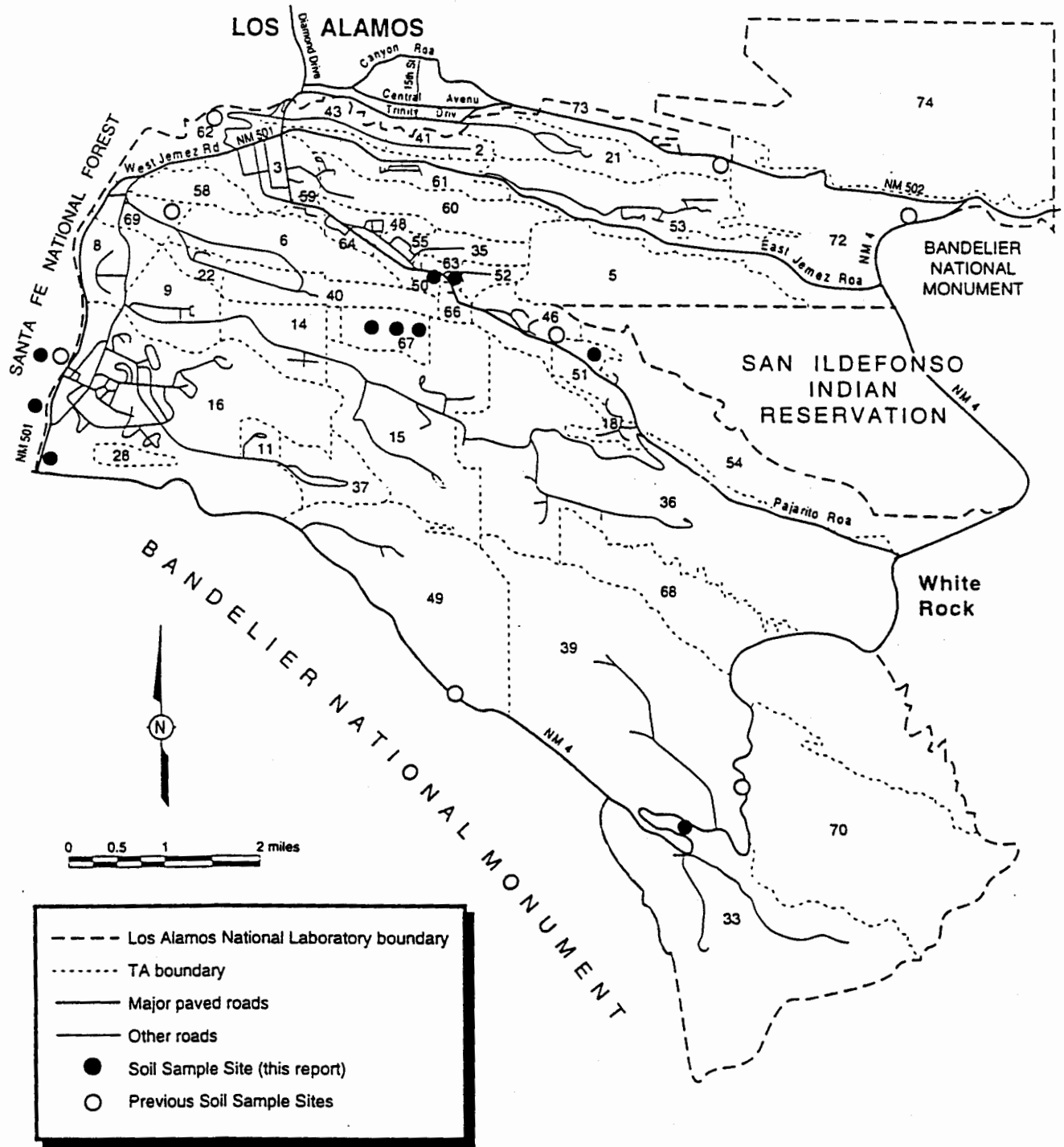


Fig. 1. Map of Los Alamos National Laboratory showing soil sample sites.

DRAFT DOCUMENT

TA-67-E1, TA-63-2). Several soil samples were collected from each horizon (termed colocated sample) at several sites. These localities allowed partial sampling of various degrees of soil development that occurs on the Pajarito Plateau and an evaluation of the variability in soil characteristics and chemistry within several soil series previously described by Nyhan et al. (1978). At each location, soil samples were collected at different depths (0 to 354 cm) corresponding to the different soil horizons and weathered Bandelier Tuff.

Field Methods and Soil Characterization

Soils were described and sampled from exposures in trenches, sides of drainage channels, and road cuts. For each soil horizon, a single, representative bulk sample of approximately one kilogram (kg) was collected. Field descriptions were made according to guidelines and standard procedures for characterizing soils described in Birkeland (1984) and Soil Survey Staff (1981). Collection and analysis of soil geochemical and morphological data were based on these vertically stratified samples. Soil samples were analyzed at the Quaternary Laboratory at the Department of Earth and Planetary Sciences, University of New Mexico, for chemical and physical properties. Procedures for these analyses are contained in Watt (1995), Soil Survey Staff (1981), and Methods of Soils Analysis (American Society of Agronomy, 1986). Soil horizons were classified and characterized according to their texture, consistency (wet/dry), particle-size distribution, color, clay-size content, calcium-carbonate content, organic-carbon content, soil pH, cation exchange capacity (CEC), citrate-bicarbonate-dithionite extraction for iron oxides and iron oxyhydroxides, oxalate extraction for iron oxyhydroxides, and bulk density (Watt, 1995; Watt and McFadden, 1992). Soil samples were passed through a 2.0 mm (20 mesh) sieve to remove pebbles and roots. Soil samples were either air-dried or dried in a forced-air circulation oven at 105°C for 24 hours. All equipment was cleaned and sterilized between each sample preparation.

Sample Digestion and Analytical Techniques

The elements antimony (Sb), arsenic (As), barium (Ba), beryllium (Be), chromium (Cr), lead (Pb), manganese (Mn), mercury (Hg), thorium (Th), and uranium (U) are of primary concern to the ER Project because numerous potential release sites (PRSs) and solid waste management units (SWMUs) at the Laboratory may contain elevated concentrations of these elements. Other elements and compounds of secondary importance to the ER Project include aluminum (Al), cadmium (Cd), calcium (Ca), cesium (Cs), chlorine (Cl), cobalt (Co), copper (Cu), iron (Fe), magnesium (Mg), potassium (K), selenium (Se), sodium (Na), strontium (Sr), sulfate (SO_4^{2-}), tantalum (Ta), thallium (Tl), titanium (Ti), vanadium (V), zinc (Zn), and zirconium (Zr). Radioactive isotopes were not

Table 2. Soil Sample Location and Soil Horizon Collected During Soil Background Investigation.

<u>SOIL PROFILE</u>	<u>SAMPLE NUMBER</u>	<u>SOIL HORIZON</u>	<u>SOIL PROFILE</u>	<u>SAMPLE NUMBER</u>	<u>SOIL HORIZON</u>
Ancho Canyon (1)	2080	A2	TA-63a	2114	A2
	2082	Bw1		2150	Colocated
	2083	Bw2		2115	Bw1
	2084	Bw3		2151	Colocated
	2081	Btb		2152	Bw2
	2085	Bwb		2116	CB
	2088	Ckq		2153	Colocated
	2087	C'		2117	fracture fill
	2086	C	TA-63c		
TA-16 South-1				2118	A1
	2090	Bt4b		2154	Colocated
	2091	Bt5b		2119	A2
	2092	Bt6b		2120	Bw1
	2093	Bt7b		2155	Colocated
	2094	Bt8b		2121	Bw2
	2095	Bt9b		2122	Bw3
	2089	BCb		2156	Colocated
TA-51			TA-63-1A		
	2096	BA		2100	A1
	2098	Bw		2101	A2
	2097	BC		2104	Bw
TA-63				2103	Bth
	2099	Bwb		2102	Btb

Table 2. Soil Sample Location and Soil Horizon Collected During Soil Background Investigation.

<u>SOIL PROFILE</u>	<u>SAMPLE NUMBER</u>	<u>SOIL HORIZON</u>	<u>SOIL PROFILE</u>	<u>SAMPLE NUMBER</u>	<u>SOIL HORIZON</u>
TA-63-2			TA-16, Water Tanks Trench, TA-16-2 (con't)		
	2113	Bw		2212	Colocated
	2149	Colocated		2129	Bt5b2
	2107	Bth		2213	Colocated
	2144	Colocated			
	2108	Bthk	TA-16, Water Tanks Trench, TA-16-1		
	2145	Colocated			
	2109	Btk1		2135	C1b1a
	2146	Colocated		2112	C2b1a
	2110	Btkb1		2134	C3b1a
	2147	Colocated		2130	Bt1b1b
	2111	Btkb2		2215	Colocated
	2148	Colocated		2208	Bt1b1c
	2105	Btb1		2123	Colocated
	2142	Colocated		2131	Bt2b1b
	2106	Btb2		2216	Colocated
	2143	Colocated		2132	Bt2b1c
TA-16 Water Tanks Trench, TA-16-2				2217	Colocated
	2124	Bt1b2		2133	Bt3b1c
	2209	Colocated		2218	Colocated
	2126	Bt2b2	TA-16 South-2		
	2210	Colocated		2137	Ap
	2127	Bt3b2		2139	Bt1
	2211	Colocated		2140	Bt3
	2128	Bt4b2		2141	Bt4
	2125	Bt2		2138	BC
	2214	Colocated		2136	2C

Table 2. Soil Sample Location and Soil Horizon Collected During Soil Background Investigation.

SOIL PROFILE	SAMPLE NUMBER	SOIL HORIZON	SOIL PROFILE	SAMPLE NUMBER	SOIL HORIZON
TA-67 E1-1	2159	A	TA-67 W1	2186	A1
	2160	BA		2219	A2
	2163	Bw		2189	A3
	2161	Bt1		2190	BA
	2162	Bt2		2188	Bw1
	2158	2Bwb		2192	Bt1
	2157	2BCb		2193	Bt2
TA-67 E3	2172	A		2187	Btkb
	2164	2BAb1		2194	E/Bb
	2167	2Bt1b1	TA-67 W5	2191	B/CR
	2168	2Bt2b1		2183	A
	2165	2BC1b1		2184	BA
	2166	2BC2b1		2175	2Bt1b1
	2169	3Bt1b2		2176	2Bt2b1
	2170	3Bt2b2		2177	2Bt3b1
	2171	3Bt3b2		2173	2BC1sb1
				2174	2BC2sb1
				2178	2BAb2
				2179	3Btb2
				2181	4CBt1b3
				2182	4CBt2b3
				2180	4C1b3
				2185	4C2b3

Table 2. Soil Sample Location and Soil Horizon Collected During Soil Background Investigation.

<u>SOIL PROFILE</u>	<u>SAMPLE NUMBER</u>	<u>SOIL HORIZON</u>
TA-67E1-2	2199	Btkb1
	2203	Bt1b1
	2195	Bt2b1
	2196	Bt3b2
	2197	Btk1b2
	2198	Btk2b2
	2202	E/Btb1
	2201	E/Bt2b1
	2200	CR
Virgin Mesa	2204	BA
	2205	Bt
	2206	Bw
	2207	CB

DRAFT DOCUMENT

analyzed in this investigation because the Laboratory (Group ESH-18) performs annual sampling of soils and sediments in background (equivalent to fallout activities of radionuclides) and facility areas for these constituents. It is possible that additional sampling of background soils for radionuclides will be conducted in the future.

Following sample preparation, soil samples were submitted to CST-9 for chemical analyses using EPA-SW846 methods and other analytical techniques available at the Laboratory. These include inductively coupled plasma mass spectrometry (ICPMS), inductively coupled plasma emission spectroscopy (ICPES), electrothermal vapor atomic absorption (ETVAA), cold vapor atomic absorption spectroscopy (CVAA), and ion chromatography (IC) analyses. Chemical data obtained for this investigation are stored and are available at the facility for information management analysis and display (FIMAD). Table 3 provides a listing of each analyte and appropriate analytical techniques. The procedures used for these analyses are described in detail in EPA (1986), Gautier and Gladney (1986), and Gladney et al. (1980, 1981). Quality assurance was provided by concurrent analysis of different National Institute of Standards and Technology (NIST), EPA, and United States Geological Survey (USGS) reference materials described by Gladney et al. (1981). Quality control samples including duplicates and spiked samples were analyzed at frequencies specified by the U.S. EPA (1987).

Soil samples were analyzed for total-element concentrations following complete digestion using concentrated HF, HClO₄, and HNO₃ (LANL Method EI 143, digestion ((total)/-soils, sludges, and sediments). Aliquots or splits from the same samples were also digested using concentrated HNO₃, HCl, and H₂O₂ (EPA Method 3050A) and were analyzed for the same elements using EPA-SW846 methods, including ICPES, ICPMS, IC, and ETVAA. In all instances, element concentrations from HNO₃ digestion are less than the total-element concentrations. The lowest detection limits for specific elements and species using ICPES, ICPMS, IC, and ETVAA were 0.08 (Be) , 0.12 (Ta), 12 (sulfate), and 0.3 (As) ppm, respectively (see Table 8). Precision values for Be, Ta, sulfate, and As were $\pm 10\%$, $\pm 10\%$, $\pm 10\%$, and $\pm 20\%$, respectively. Precision values for all of the other elements were $\pm 10\%$.

Element leaching from soils is evaluated by comparing analytical results from HNO₃ digestion to those obtained from HF digestion. Large differences in concentrations of the total element and HNO₃-digested samples suggest that minimal redistribution of elements from primary silicates to secondary surface coatings has occurred and most of the element is chemically bound or tied up within the primary silicate minerals. Small differences in element concentrations between HNO₃-digested samples and total-element analyses suggest that elements have been largely mobilized and concentrated on surfaces and/or coprecipitated with acid-soluble phases including ferric hydroxide, ferric

TABLE 3. EPA-SW846 and LANL Analytical Techniques Used in LANL Background Soil Investigation.

Element	Technique	Element	Technique
Al	ICPES	Mg	ICPES
As	ETVAA	Mn	ICPES
Ba	ICPES	Na	ICPES
Be	ICPES	Ni	ICPES
Ca	ICPES	Pb	ICPES
Cd	ICPES	Sb	ICPES
Cl	IC	SO ₄	IC
Co	ICPES	Ta	ICPMS
Cr	ICPES	Tl	ICPMS
Cu	ICPES	Th	ICPMS
Fe	ICPES	U	ICPMS
K	ICPES	V	ICPES
		Zn	ICPES

ICPES, inductively coupled plasma emission spectroscopy

ICPMS, inductively coupled plasma mass spectrometry

IC, ion chromatography

ETVAA, electrothermal vapor atomic absorption spectroscopy

DRAFT DOCUMENT

oxyhydroxide, calcium carbonate, solid organic matter, and clay minerals such as smectite and kaolinite. Many trace and major elements, including Al, Ba, Na, K, U, and Th, are structurally incorporated within primary mineral lattices and amorphous solids (primarily glass). Subsequently, HF digestion of a sample results in higher concentrations for some elements relative to a partial digestion using HNO_3 . Other trace elements, including As and Be, are mainly concentrated on surfaces of soil particles, consisting of clay minerals and ferric oxyhydroxide-ferric hydroxide (termed iron oxides) in well-developed soils, through adsorption processes. Under these circumstances, HF and HNO_3 digestions yield similar analyte concentrations. Therefore, the type of digestion (extraction) of environmental samples strongly influences analytical results. Consistent and appropriate digestion procedures should be used to allow comparability of data.

GEOMORPHIC SETTINGS AND GENERAL SOIL HORIZONS

The soils sampled in this investigation include a range of geomorphic settings and ages, both of which influence soil development and soil chemistry. Most sampled soils are collected from mesa tops in the central portion of the Pajarito Plateau, and are developed in a variety of materials that can include components of locally weathered Bandelier Tuff, the ca. 50-60,000 yr old El Cajete pumice (Reneau et al., 1995), and wind-blown sediment. The strongest soil development, and the highest concentrations of most trace elements, are found in soils that are older than the El Cajete pumice. Other geomorphic settings sampled in this study are colluvial slopes at the base of the Pajarito fault scarp, a young stream terrace on the eastern Pajarito Plateau, and an old alluvial fan on the western Pajarito Plateau. Elevations of the study sites range from 6270 to 7750 ft, and vegetation includes both Ponderosa pine forest and pinon-juniper woodlands (Table 1).

Site 1. Ancho Canyon, TA-39

The Ancho Canyon sample site is a stream-cut bank that exposes Holocene alluvium below a 2.4 m high terrace. The site was mapped as part of the Totavi series by Nyhan et al. (1978). Ancho Canyon above this point entirely drains the Tshirege Member of the Bandelier Tuff, and the source for sediments is thus eroded tuff plus other material contained within eroded soils (such as wind-blown sediment and El Cajete pumice). Sedimentary layers exposed in this bank include both relatively well-sorted coarse sands and gravels that represent channel deposits, and poorly-sorted mixtures of pumice-rich sand, silt, and clay that represent floodplain deposits (Figure 2: sketch of general stratigraphy + radiocarbon dates). Radiocarbon analyses of charcoal

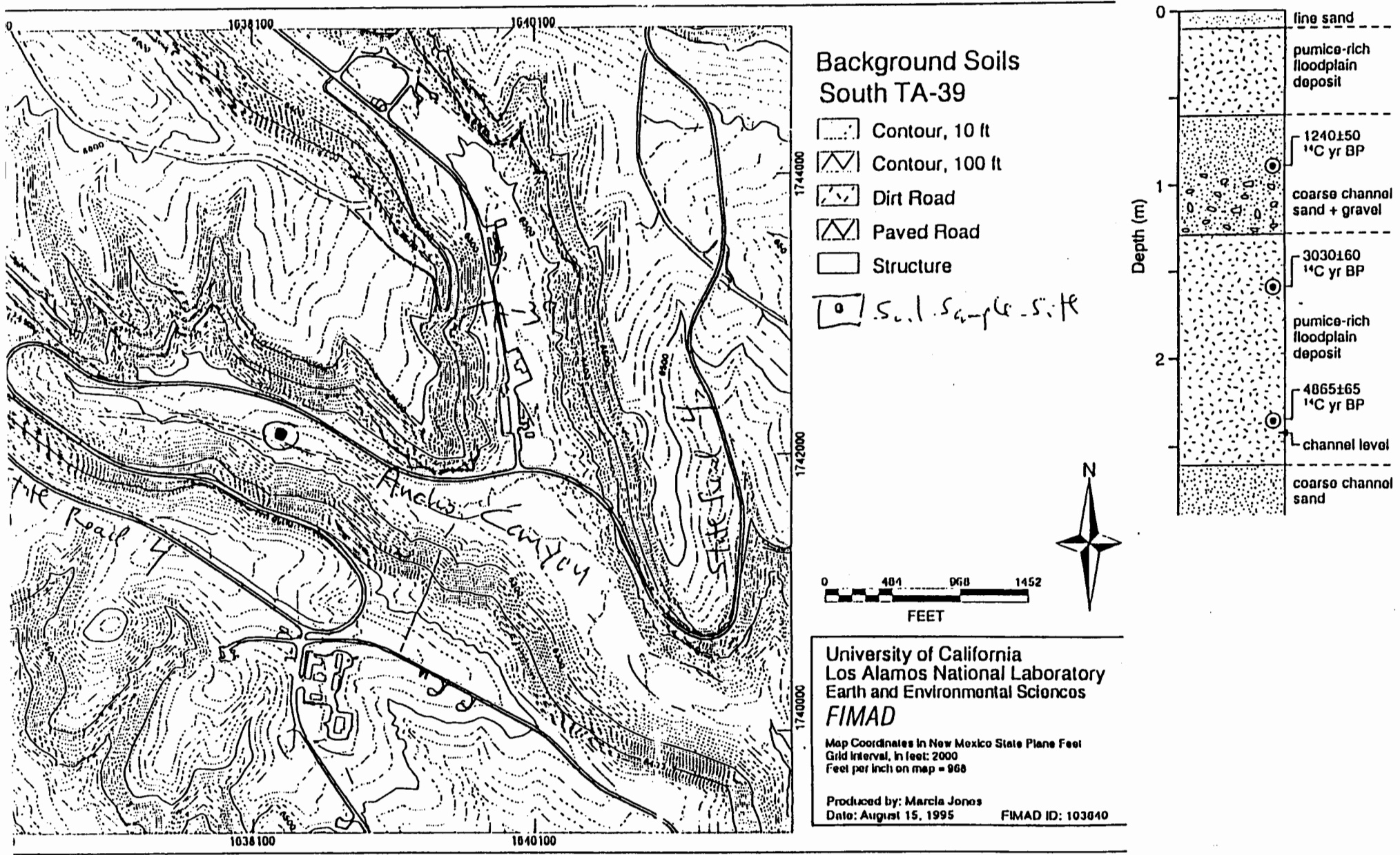


Fig. 2. Map showing location of soil sample site in Ancho Canyon.

DRAFT DOCUMENT

fragments collected from these sediments indicate ages of 3000 to 5000 ^{14}C yrs for a buried floodplain deposit at depths of 1.6 to 2.4 m, and an age of about 1200 ^{14}C yrs for an overlying channel deposit at a depth of 0.9 m. This sample site may be representative of many canyon-bottom sites at the Laboratory, particularly in canyons that originate on the Pajarito Plateau and entirely drain Bandelier Tuff, although the chemistry will probably vary with the age of the sediments.

Site 2. Water Tanks Trench, TA-16

The sample site is south of Canon de Valle at the base of the Pajarito fault scarp, in a trench excavated as part of paleoseismic investigations (Figure 3, location map; Wong et al., 1995). The trench exposed a sequence of colluvial deposits of varying age and degree of soil development, and also a pure layer of El Cajete pumice (Figure 4: sketch of trench stratigraphy). One soil profile from this trench, above the pumice, was previously analyzed and is presented in Longmire et al. (1995). In this study, two colluvial layers beneath the pumice were sampled farther west in two locations. The lowest colluvial layer has pedogenic features associated with strong soil development indicating a relatively longer period of soil development than the other colluvial layers exposed in the West Jemez Road trenches. The site was mapped as part of the "Rock Outcrop-Pines-Tentrock Complex" by Nyhan et al. (1978). This pit exposed 1.7 m of fine-textured Holocene colluvium or fan sediment that was derived from a possible fault scarp and deposited on top of a stream terrace derived from Water Canyon. Radiocarbon analyses of charcoal from similar deposits in nearby pit TP2 yielded ages of 8000 to 9500 ^{14}C yrs from depths of 0.5 to 1.0 m (Wong et al., 1995), and the TP1 deposit is probably similar in age.

Site 3. TA-16 South

The sample site south of Water Canyon is a roadcut exposure of an old alluvial fan along West Jemez Road and along the southwest side of TA-16 (Figure 5: location map), that was mapped as part of the Pogona series by Nyhan et al. (1978). The alluvium includes clasts of Tschicoma Formation dacite eroded from the Sierra de los Valles, and the strong soil development indicates that this may be one of the oldest deposits exposed along West Jemez Road, although its age is unknown.

Site 4. Mesita del Buey, TA-51

The Mesita del Buey sample site was a trench excavated by EES-15 as part of hydrological investigations on mesa tops at the Laboratory (Figure 6).

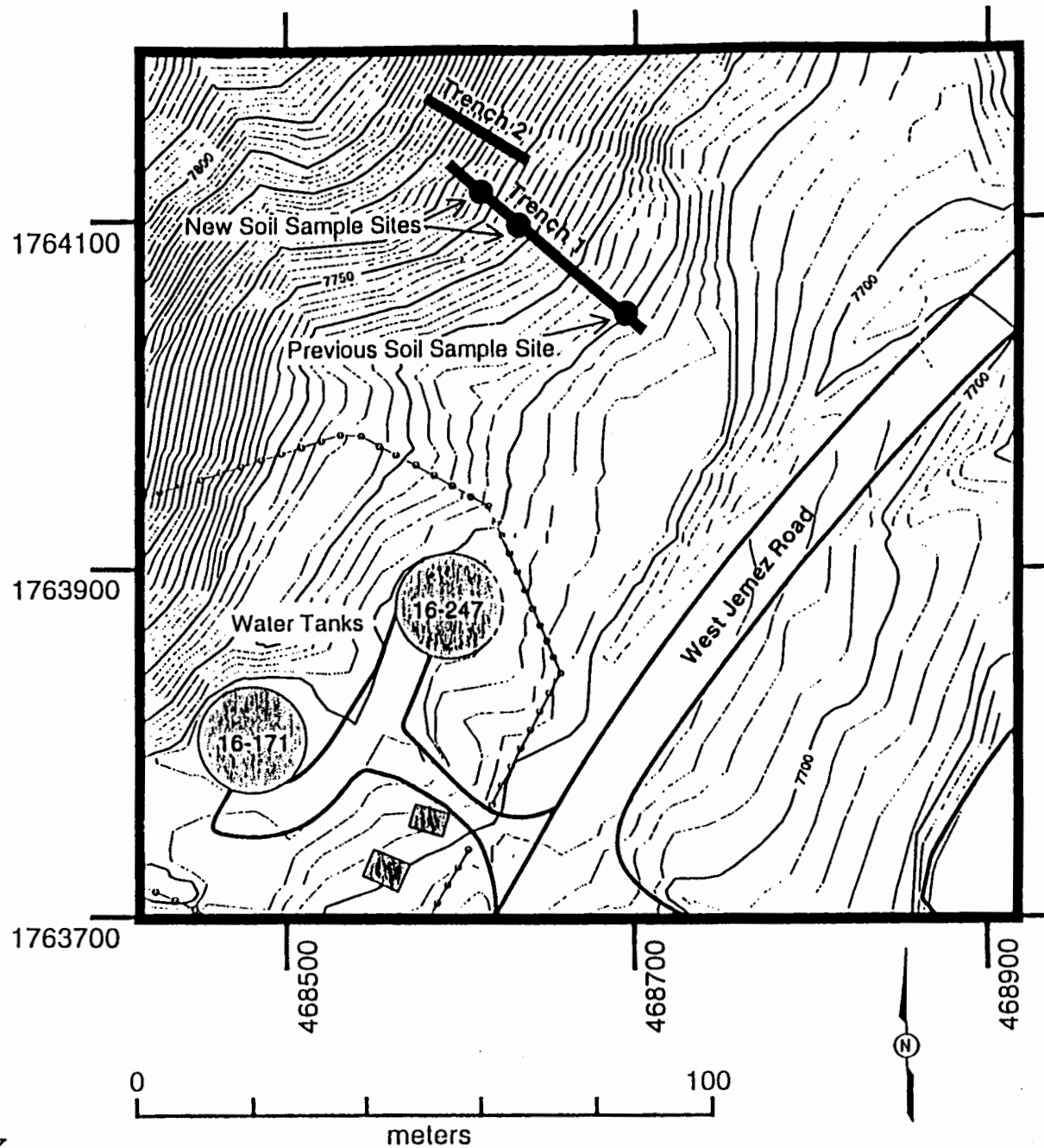


Fig. 3. Sketch of Water Tanks trench at sample sites. Horizontal axis indicates trench distance (m). Modified from Wong et al. (1995).

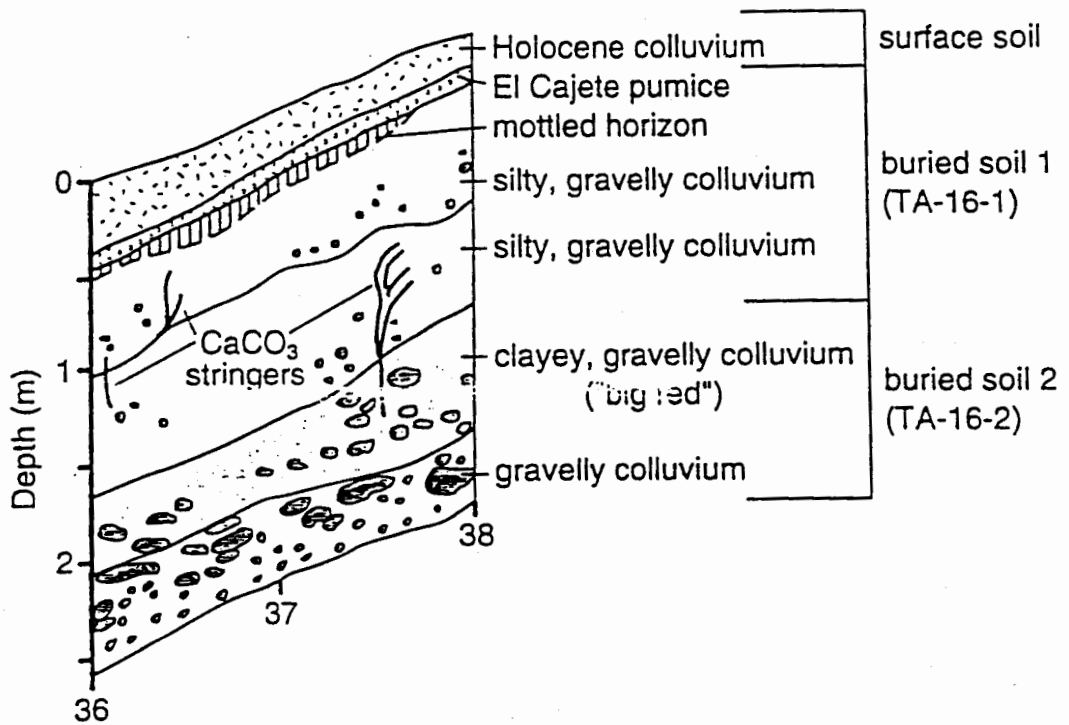


Fig. 4. Map showing location of Water Tanks trenches and sample sites of this report and of Longmire et al. (1995). Topographic base, with 2-foot contours, from FIMAD.

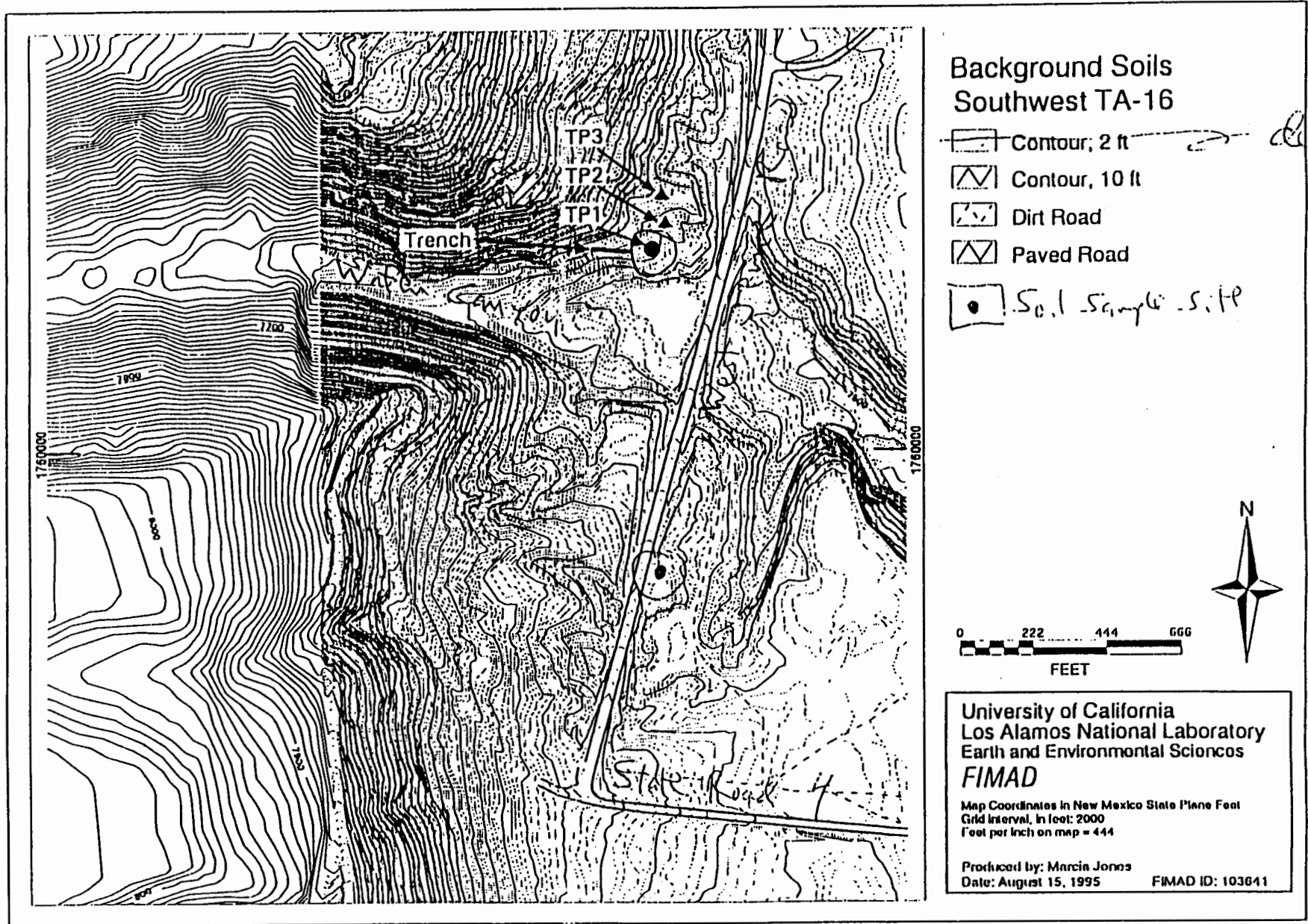


Fig. 5. Map showing location of Water Canyon (TA-16 south) sample sites.

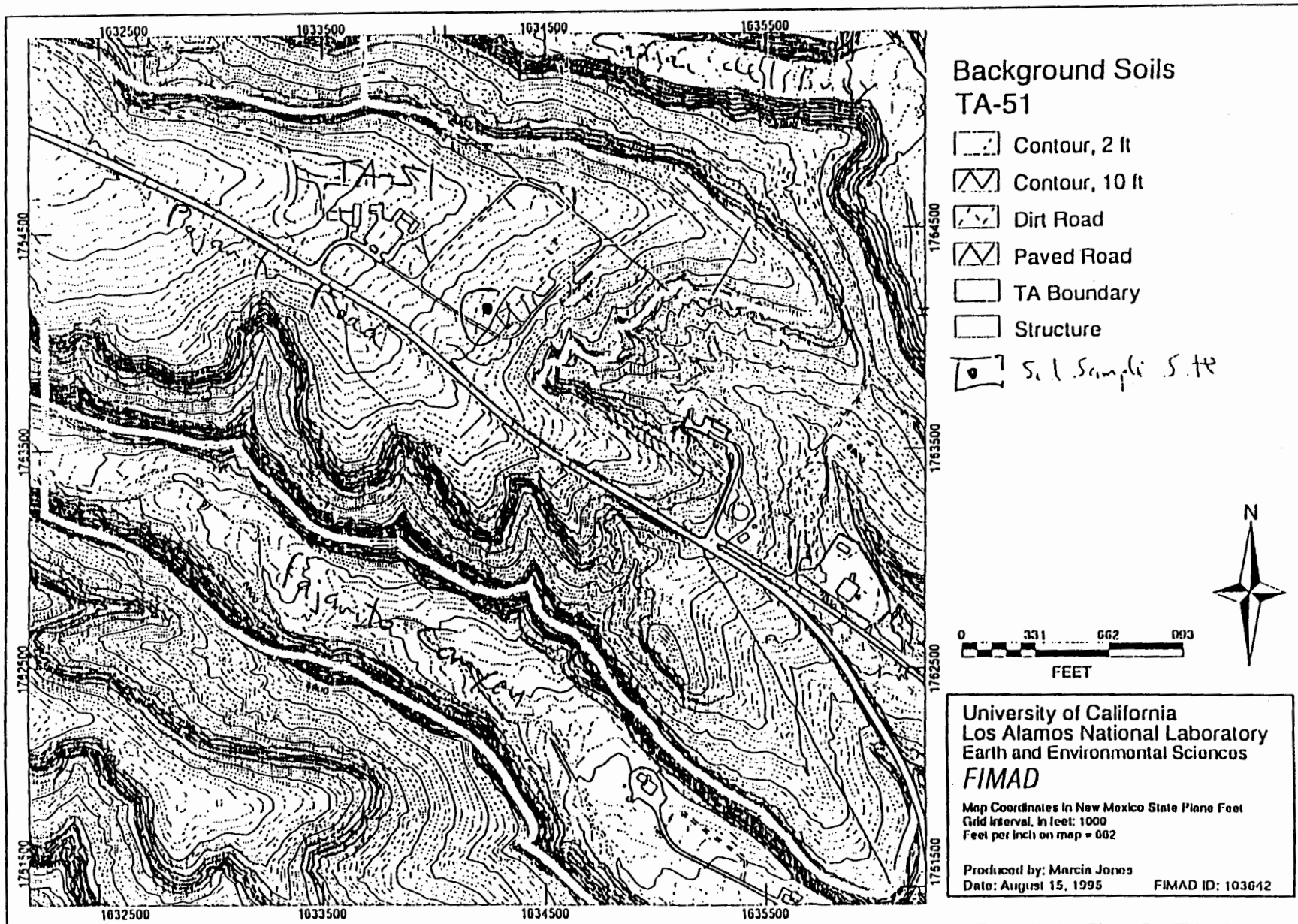


Fig. 6. Map showing location of soil sample site on Mesita del Buey at TA-51.

DRAFT DOCUMENT

The soils on the mesa were mapped as part of the Hackroy series by Nyhan et al. (1978). The sampled soil is relatively thin, (* m thick), and may include deposits that both pre-date and post-date the El Cajete pumice.

Site 5. Pajarito Road, TA-63

Four soil profiles were sampled on the mesa top at TA-63 and vicinity near Pajarito Road from a series of trenches excavated to evaluate potential faulting (Figure 7: location map; Kolbe et al., 1995). Sampled soils on the mesa top were mapped as either the Nyjack series (trench 1) or the Hackroy series (trench 5) by Nyhan et al. (1978). The soils and stratigraphy at the Pajarito Road sites are distinctly different from that on Pajarito Mesa, only about 1 km to the south, particularly in the absence of the El Cajete pumice. Soils at TA-63 are generally thinner (0.5-0.7 m thick), and may in general represent Holocene deposits, although a lower clay-rich horizon is usually present that may indicate remnants of Pleistocene soils. One of the sample sites in trench 1 is from a 2.3 m thick deposit that filled a shallow mesa-top drainage, and includes an older, buried deposit that is inferred to pre-date the El Cajete pumice (Kolbe et al., 1995). The range in soil characteristics and soil chemistry present in the TA-63 samples, in combination with the other mesa top sites in this study and in Longmire et al. (1995), may encompass most of the variability that exists on mesa tops in the central part of the Laboratory.

Site 6. Pajarito Mesa, TA-67

Five soil profiles were sampled on Pajarito Mesa in the central part of the Laboratory from a series of trenches excavated to evaluate potential faulting (Figure 8: location map; Kolbe et al., 1994; Reneau et al., 1995). Sampled soils on the mesa top were mapped as mostly the Nyjack series by Nyhan et al. (1978), although a small area of the Frijoles series was also mapped. Sample sites were chosen to include a range of stratigraphic units and soil characteristics as exposed in the trenches, and the sampled soils range from 1.3 to 2.3 m thick. The general stratigraphic units present include old soils that were buried by the El Cajete pumice, a typically disrupted (bioturbated) pumice layer, and overlying deposits that range in age from at least 30,000 yrs to less than 1000 yrs old (Figure 9: sketch of stratigraphy; Kolbe et al., 1994; Reneau et al., 1995). The fine-grained texture of much of the material overlying the pumice indicates that it includes a substantial component of wind-blown sediment, and the soils underlying the pumice probably represent some mixture of locally weathered tuff and wind-blown sediment. The trench W1 sample site is in an area of relatively thin and poorly-developed soils; the trench E3 sample site is in an area where relatively strong soil development is present below the El Cajete pumice; and the trench E1 sample site is at the site where pre-El Cajete soils

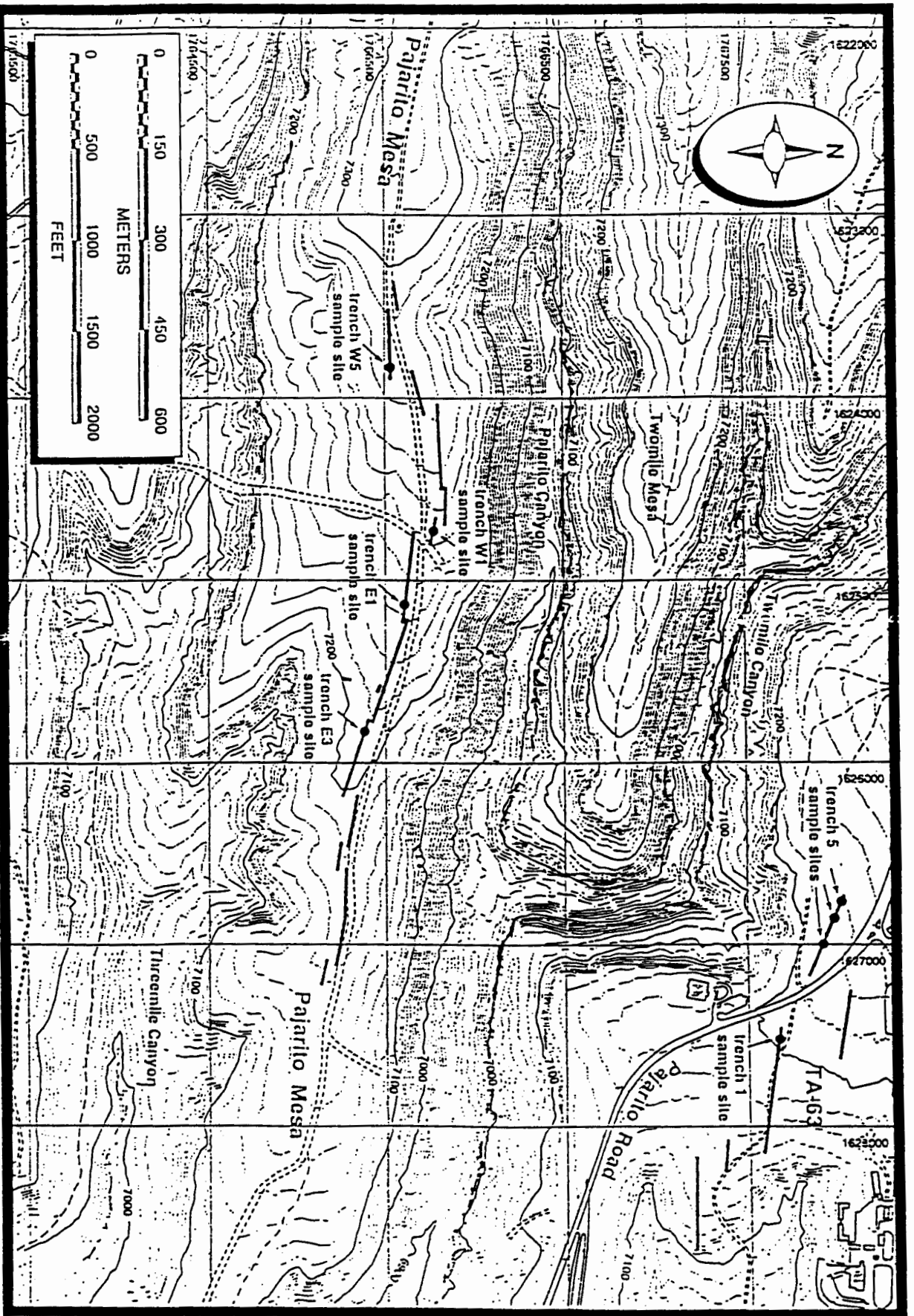


Fig. 7. Sketches of Pajarito Road (TA-63) trenches at sample sites. Horizontal axis indicates trench distance (m). Modified from Kolb et al (1995).

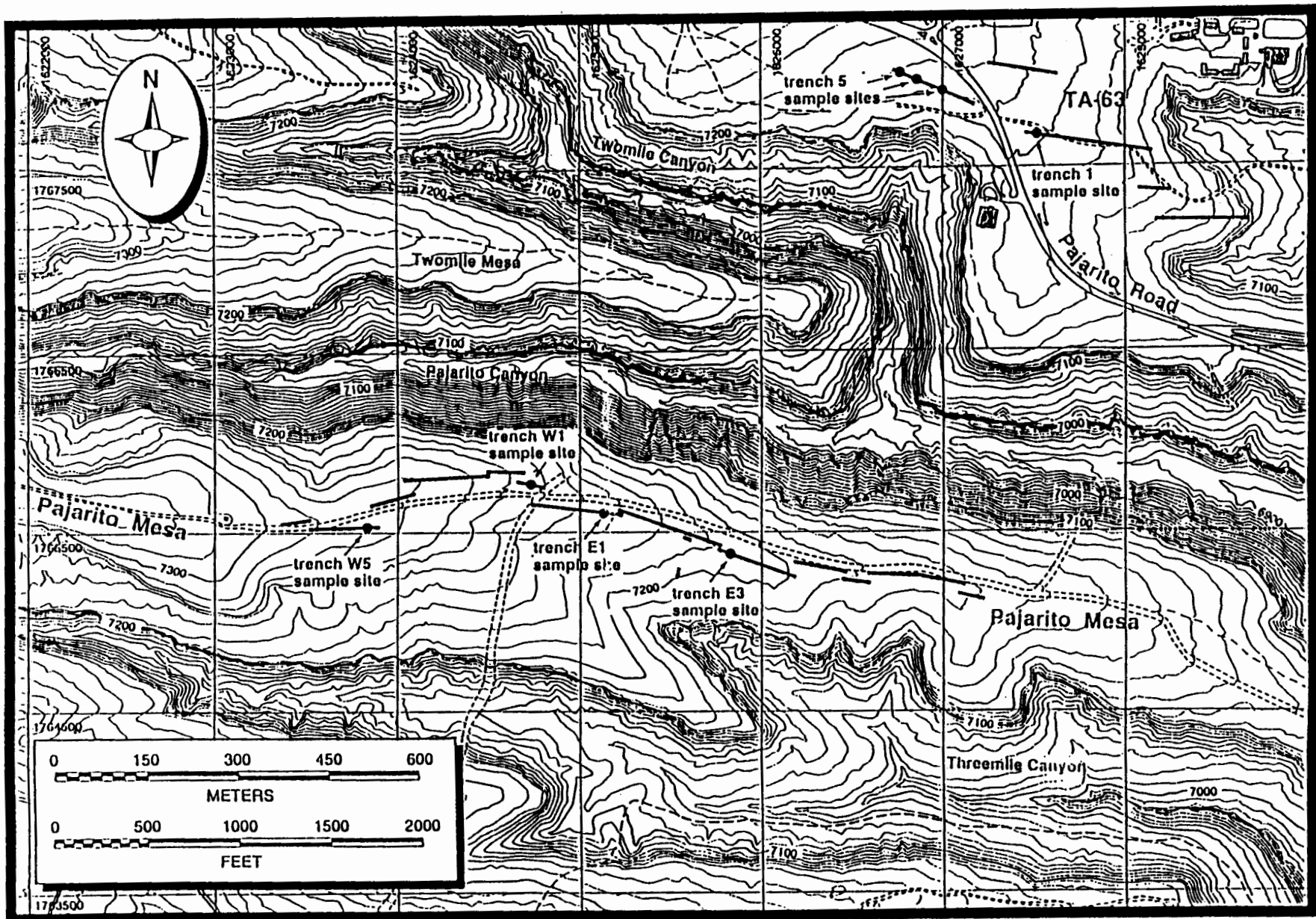


Fig. 8. Sketches of Pajarito Mesa (TA-67) trenches at sample sites. Horizontal axis indicates trench distance (m). Modified from Kolbe et al. (1994).

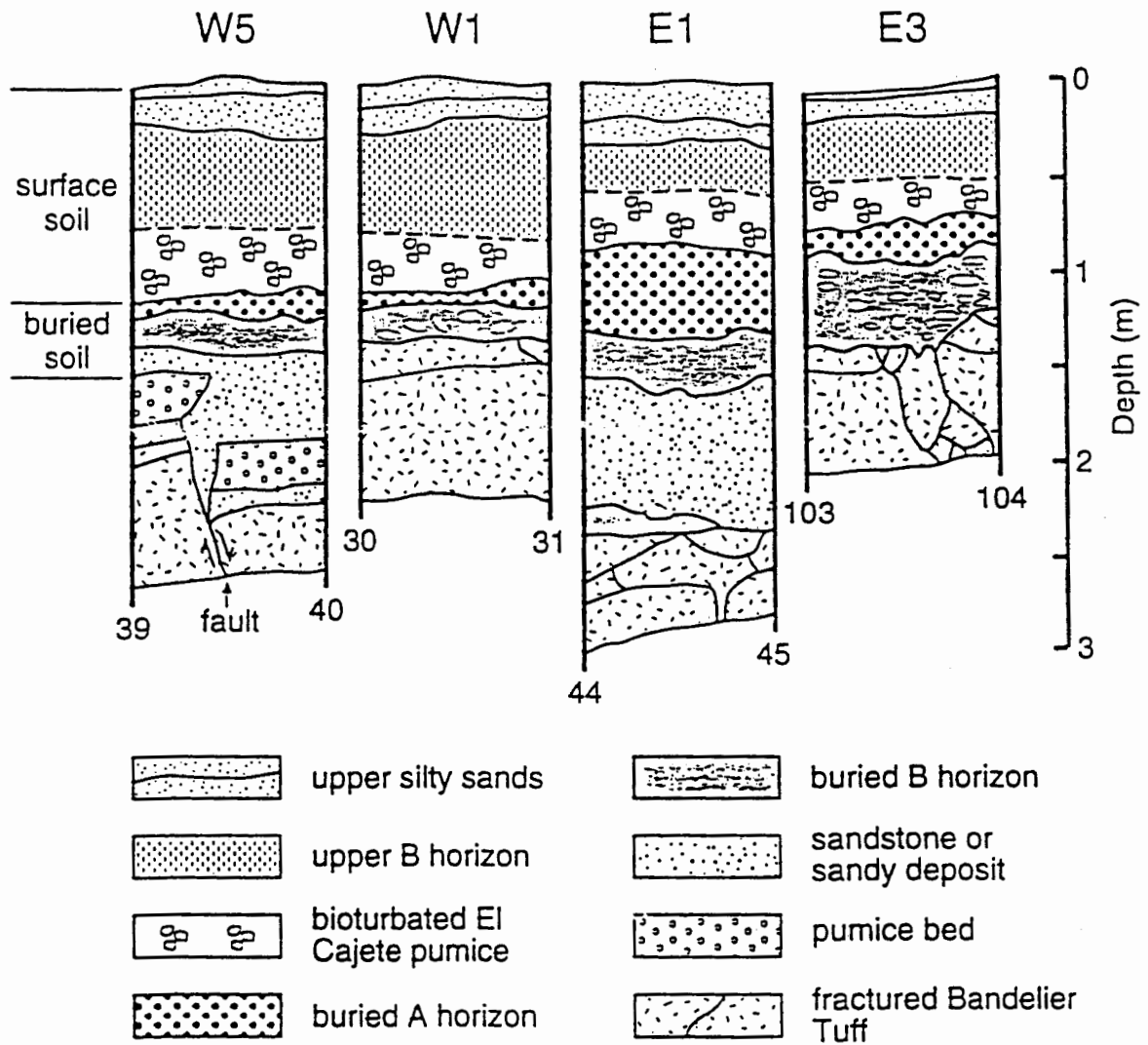


Fig. 9. Map showing stratigraphy at Pajarito Mesa and at TA-67. Modified from Kolbe et al. (1994).

DRAFT DOCUMENT

are thickest, including multiple buried soils. At the remaining site, in trench W5, old pre-El Cajete pumice-rich alluvial beds underlie the sampled soil.

Site 7. Virgin Mesa, Sandoval County

One soil profile was sampled on Virgin Mesa southwest of Jemez Springs and west of the Jemez River and Rio Guadalupe confluence. This area was selected as a regional background site for the Jemez Mountains consisting of soil forming on the Tshirege Member of the Bandelier Tuff. Soils at this site have not been mapped by Nyhan et al. (1978). Analytical results from Virgin Mesa are used in this report as are data collected from the other sites within and adjacent to the Laboratory.

CHARACTERIZATION OF BACKGROUND SOILS

General Soil Parameters

This section presents a summary and discussion of soil characterization results reported by Watt (1995). Results of this and other studies (Longmire et al., 1995) show that Laboratory soils have extreme diversity and spatial variability in their physical and chemical properties and in vertical stratification. A summary of these soil parameters is presented in this report (Table 4) and in Watt (1995).

Soil Horizons

Soil consists of layers or horizons of mineral and/or organic matter of variable thicknesses that parallel the land surface and which differ from the parent material in their morphological, physical, chemical, and mineralogical properties and their biological characteristics (Joffe, 1949; Birkeland, 1984; Soil Survey Staff, 1975). In general, soils form nearly ubiquitous cover across the land surface and their formation largely results from physical, chemical, and biological transformations that occur over time along the boundary between the atmosphere, biosphere, and lithosphere. The general characteristics of a soil at any given point in the landscape will primarily reflect the five major factors that control soil formation: parent material (i.e. substrate soil has formed in), vegetation, topographic position (i.e. slope and aspect), climate, and time. Soils across the Laboratory are spatially highly variable and complex due to the diversity of topography, the complex history of landscape evolution, and variation in the ages of soil parent material.

Soil horizons at the Laboratory generally are unconsolidated and largely consist of O, A, B, E, and C horizons. An O horizon is characterized by surface

Table 4. Summary of physical and chemical soil characterization properties.

Soil Number	Horizon	Depth (cm)	Sand (% wt.)	Silt (% wt.)	Clay (%wt.)	Gravel (% wt.)	Bulk Density (g/cm ³)	Organic Carbon (% wt.)	CEC (meq/100g)	Carbonate (% wt.)	pH	Dithionite Fe ₂ O ₃ (%wt.)	Oxalolate Fe ₂ O ₃ (%wt.)
AC-1	A1	0 - 4	75.1	17.5	7.4	4.30		1.75	5.44		5.5	0.44	0.42
	A2	4 -- 12	88.4	8.5	3.1	6.50		0.47	2.70		5.7	0.48	0.31
	Bw1	12 -- 27	47.5	43.2	9.3	9.10	1.12	2.00	11.56		5.4	0.60	0.35
	Bw2	27 -- 56	65.9	26.0	8.1	13.00		0.83	9.82		6.9	0.53	0.38
	Bw3	56 -- 69	88.3	8.4	3.3	4.60		0.46	3.68		6.8	0.47	0.22
	C	69 -- 90	92.9	4.8	2.3	7.80		0.61	3.19	1.1	6.8	0.32	0.34
	Ckq	90 -- 109	93.7	5.0	1.3	40.60		0.74	3.03	0.47	6.6	0.28	0.32
	C'	109 -- 130	95.3	4.0	0.7	11.00		0.56	2.88		6.8	0.26	0.17
	Bwb	130 -- 151	66.1	23.6	10.3	21.30		1.05	9.73		7.0	0.49	0.43
Blb	151 -- 175	63.6	27.0	9.4	27.10		0.71	12.35		7.0	0.44	0.44	
TA-16-S-1	Bl4b	94 -- 110	22.2	41.0	36.9	9.70	1.68	0.52	27.45		6.3	0.85	0.18
	Bl5b	110 -- 134	25.2	55.7	19.1	12.10	1.62	0.23	19.56		6.5	0.82	0.22
	Bl6b	134 -- 186	29.1	56.7	14.2	11.00	1.62	0.41	19.49		6.5	0.76	0.19
	Bl7b	186 -- 234	30.2	45.7	24.1	28.90	1.65	0.18	17.02		6.6	0.84	0.19
	Bl8b	234 -- 264	32.4	51.8	15.8	11.40	1.60	0.18	14.11		6.5	0.79	0.19
	Bl9b	264 -- 354	21.1	64.5	14.4	4.60	1.59	0.22	13.39		6.3	0.81	0.20
	BCb	354 -- 281+	25.7	58.0	16.4	2.10		1.12	9.33		6.7	0.78	0.25
TA-51	A	0 -- 3	26.0	56.5	17.6	2.90		17.30	43.04		6.4	0.80	0.41
	BA	3 -- 6	13.8	66.6	19.6	0.60		6.97	27.30		6.0	0.86	0.51
	Bw	6 -- 18	18.6	49.8	31.6	3.70		4.86	25.20		6.0	0.96	0.64
	BC	18 -- 25	31.7	45.1	23.2	21.80		8.13	28.95		6.2	1.01	0.60
TA-63a	A	6 -- 12	26.5	57.9	15.6	2.40	1.33	1.79	9.85		5.7	1.08	0.26
	Bw1	12 -- 25	27.4	54.9	17.7	1.10	1.50		10.86		5.7	1.09	0.32
	Bw2	25 -- 35	26.2	53.6	20.2	3.50	1.53	1.21	11.05		5.8	0.99	0.26
	CB	35 -- 47											
	FF	110 -- 111											
TA-63c	A1	0 -- 10	22.1	66.9	11.1	2.10		5.22	14.35		6.1	0.96	0.23
	A2	10 -- 14	22.4	60.3	17.3	0.50	1.45	2.59	12.24		6.1	1.02	0.27
	Bw1	14 -- 36	25.5	62.6	12.0	0.30	1.42	1.60	8.57		6.0	1.00	0.29
	Bw2	36 -- 49	34.5	54.1	11.4	0.60	1.40	1.95	7.66		5.9	0.99	0.27
	Bw3	49 -- 57	38.0	46.0	16.0	1.70	1.48	2.62	8.92		6.0	0.96	0.27
	FF	80 -- 81										1.41	0.27
	FF	110 -- 111										0.83	0.19

Table 4. Summary of physical and chemical soil characterization properties.

Soil Number	Horizon	Depth (cm)	Sand (% wt.)	Silt (% wt.)	Clay (% wt.)	Gravel (% wt.)	Bulk Density (g/cm ³)	Organic Carbon (% wt.)	CEC (meq/100g)	Carbonate (% wt.)	pH	Dithionite Fe ₂ O ₃ (% wt.)	Oxalolate Fe ₂ O ₃ (% wt.)
TA-63-1A	A1	0 - 5	17.7	68.8	13.5	1.00	1.28	3.00	10.94		5.8	0.92	0.55
	A2	5 - 19	15.2	65.4	19.4	2.20	1.38	1.24	10.93		6.2	1.09	0.71
	Bw	19 - 40	14.0	62.9	23.2	3.60	1.58	0.77	13.40		6.8	1.00	0.77
	B1h	40 - 66	19.8	51.7	28.5	9.20	1.63	0.41	19.00		6.8	0.89	0.67
	B1k1	66 - 72	21.3	56.8	21.9	1.90	1.65	0.45	21.26	6.09	7.0	0.72	0.47
	B1k2	72 - 77	16.6	54.2	29.2	2.00	1.65	0.45		6.59	7.1	0.81	0.38
	B1b	77 - 87+	8.4	49.0	42.6	2.30		0.75		3.93	7.1	0.95	
TA-63-2	Bw	8 - 26	14.7	55.0	30.3	0.00		1.02	11.24		6.1	1.17	0.37
	B1h	26 - 40	17.8	56.9	25.3	10.90		0.34	16.34		6.5	1.19	0.37
	B1hk	40 - 53	20.6	59.0	20.3	5.50		0.49	22.05	0.34	7.2	1.09	0.43
	B1k1	53 - 60	23.9	59.3	16.8	2.30	1.58	0.44	19.66	4.4	7.3	0.95	0.27
	B1k2	60 - 65	22.4	49.4	28.2	1.70		0.41	15.45		7.3	1.02	0.22
	B1kb1	65 - 88	11.0	53.0	36.0	4.30		0.37	21.90		7.2	1.19	0.30
	B1kb2	88 - 118	9.3	59.9	30.8	7.10		0.42	20.40		7.0	1.06	0.34
	B1b1	118 - 150	15.7	59.8	24.5	8.80	1.61	0.39	22.68		7.0	1.19	0.49
B1b2	150 - 174	26.4	45.3	28.3	8.10		0.30	15.55		7.1	0.98	0.33	
TA-16-WT-1	C1b1a	100 - 111	36.5	54.9	8.6	75.06		0.85	6.46		7.0	0.58	0.16
	C2b1a	111 - 116						0.46	8.38		6.7	1.41	0.47
	C3b1a	116 - 153	35.8	50.3	14.0		1.83	0.58	6.44		6.6	0.92	0.11
	B1b1b	153 - 170	33.5	41.5	25.0	25.00	1.72	0.03	15.15		6.6	1.03	0.12
	B1b2b	170 - 199	39.9	36.6	23.5		1.70	0.31	13.81		6.6	0.93	0.10
	B1b1c	199 - 210	40.3	34.9	24.8			0.15	11.35		6.6	0.96	0.09
	B1b2c	210 - 235	43.1	31.3	25.6	62.0		0.52	2.17		6.5	0.89	0.13
	B1b3c	235 - 256	42.8	31.3	25.8	44.2		1.00	13.22		6.5	0.85	0.13
TA-16-WT-2	B1b2	256 - 269	32.6	28.5	38.9	61.8	1.74	1.55	22.66		6.9	0.99	0.13
	B1b2	269 - 304	23.2	26.7	50.1	45.2	1.65	0.59	15.35		7.2	1.13	0.16
	B1b2	304 - 331	37.8	27.0	35.3		1.72	0.42	29.46		7.2	0.92	0.13
	B1b2	331 - 364	43.7	15.5	40.8	63.5	1.79	0.85	19.92		7.0	0.89	0.15
	B1b2	364 - 394	45.4	12.5	42.1			0.43	24.92		7.1	0.91	0.08
TA-16-S-2	Ap	0 - 8	34.0	54.3	11.7	23.0		1.37	6.47		5.0	0.65	0.24
	B1	8 - 21	20.7	40.9	38.4	35.8		0.92	17.54		5.7	0.93	0.20
	B1	21 - 39	22.7	67.3	10.1	2.7		0.73	17.19		6.9	1.05	0.32
	B1	39 - 70	22.2	58.3	19.5	5.30		0.47	18.03		7.1	0.89	0.26
	B1	70 - 107	21.1	60.5	18.4	5.10		0.40	20.83		7.1	0.91	0.25
	BC	107 - 159	27.8	46.2	26.0	9.7		0.18	23.38		6.8	0.81	0.19

Table 4. Summary of physical and chemical soil characterization properties.

Soil Number	Horizon	Depth (cm)	Sand (% wt.)	Silt (% wt.)	Clay (% wt.)	Gravel (% wt.)	Bulk Density (g/cm ³)	Organic Carbon (% wt.)	CEC (meq/100g)	Carbonate (% wt.)	pH	Dithionite Fe ₂ O ₃ (% wt.)	Oxalolate Fe ₂ O ₃ (% wt.)
	2C	159 -- 187	76.3	15.3	8.4	56.0		0.22	8.65		7.0	0.35	0.24
TA-67-E1-1	A	0 -- 7	25.6	61.0	13.4	4.6		1.89	9.73		5.8	0.84	0.20
	BA	7 -- 15	28.4	57.9	13.7	5.8	1.25	1.79	9.29		5.7	0.84	0.18
	Bw	15 -- 38	23.7	56.8	19.6	2.3	1.18	1.28			6.0	0.95	0.20
	Bl1	38 -- 50	16.0	63.4	20.7	1.4	1.49	1.82	11.09		6.2	0.99	0.24
	Bl2	50 -- 62	19.7	60.3	20.1	1.5	1.54	0.64	15.74		6.5	1.05	0.21
	2Bwb	62 -- 98	23.5	57.3	19.2	5.4		0.97	15.71		6.9	0.98	0.19
	2BCb	98 -- 108	33.9	52.4	13.7	9.0	1.11	1.39	13.02		6.7	0.84	0.15
TA-67-E-2-1	E/Blb1	108 -- 117	32.8	58.2	9.0	1.30		1.78	11.86		7.4	0.94	0.15
	E/Bl2b1	117 -- 124	30.7	52.1	17.2	4.20		0.21	13.32		7.5	0.80	0.17
	Bl1b1	124 -- 139	27.6	48.8	23.7	0.90		0.41	15.59		7.2	1.11	0.16
	Bl2b1	139 -- 165	30.5	49.2	20.3	1.70		0.49	13.39		7.2	1.26	0.19
	Blkb1	165 -- 195	41.6	43.0	15.5	6.30		1.08	10.65		7.3	0.98	0.22
	Blk1b2	195 -- 222	39.6	23.8	36.6	1.40		0.49	14.54		7.3	0.89	0.17
	Blk2b2	222 -- 252	40.3	39.9	19.8	10.50		0.31	14.82		7.3	0.91	0.17
	Bl3b2	252 -- 272	55.8	26.2	18.0	7.50		0.23			7.3	1.07	0.15
	CR	272+	74.6	20.0	5.4	7.90		0.97			7.1	0.50	0.22
TA-67 E3	A	0 -- 14	20.3	52.2	27.5	4.00	1.36	0.86	7.79		6.1	0.91	0.28
	2BAb1	14 -- 22	15.2	55.7	29.1	4.90	1.55	1.27	17.06		6.1	1.12	0.31
	2Bl1b1	22 -- 40	16.1	59.5	24.5	16.30	1.56	0.73	19.85		6.5	1.17	0.34
	2Bl2b1	40 -- 50	28.1	54.3	17.6	11.10	1.25	0.42	17.90		7.1	0.98	0.28
	2BC1b1	50 -- 57	30.2	57.0	12.8	10.0	1.19	0.94	15.47		6.9	0.90	0.30
	2BC2b1	57 -- 67	35.0	52.6	12.4	10.40	1.23	0.20	18.15		7.0	0.94	0.29
	3Bl1b2	67 -- 76	34.0	55.0	10.9	5.90	1.24	0.47	36.35	1.67	7.2	0.84	0.24
	3Bl2b2	76 -- 87	33.1	51.4	15.6	2.20	1.76	0.03	32.53	1.4	7.5	1.02	0.22
	3Bl3b2	87 -- 101	34.0	43.8	22.3	8.50	1.75	0.27	24.41		7.2	1.08	0.30
TA-67 W1	A1	0 -- 6	35.5	51.8	12.7	6.80		3.37	11.04		5.3	0.83	0.15
	A2	6 -- 13	26.7	60.4	12.9	10.30		2.00	11.94		5.9	0.85	0.16
	A3	13 -- 23	27.4	56.7	15.9	11.20		1.65	12.45		6.2	0.89	0.18
	BA	23 -- 39	24.6	57.9	17.5	10.50	1.16	0.99	12.18		6.3	0.92	0.17
	Bw1	39 -- 65	19.8	47.3	32.9	14.00	1.12		11.31		6.4	0.97	0.23
	Bl1	65 -- 86	19.8	67.1	13.1	4.60	1.27	0.87	12.46		6.6	1.09	0.21
	Bl2	86 -- 109	28.7	55.4	16.0	18.10	1.25	1.16	12.58		6.7	0.99	0.16
	E/Bb	109 -- 120	33.6	59.7	6.8	4.90		0.23		0.71	7.3	0.93	0.11
	Blkb	120 -- 142	58.7	0.0	41.5	1.20		0.88	10.30	1.11	7.1	0.82	0.18
	B/Cr	142 -- 163	63.4	25.6	11.0	0.80		0.58	16.78		7.3	0.92	0.13

Table 4. Summary of physical and chemical soil characterization properties.

Soil Number	Horzon	Depth (cm)	Sand (% wt.)	Silt (% wt.)	Clay (%wt.)	Gravel (% wt.)	Bulk Density (g/cm ³)	Organic Carbon (% wt.)	CEC (meq/100g)	Carbonate (% wt.)	pH	Dithionite Fe ₂ O ₃ (%wt.)	Oxalolate Fe ₂ O ₃ (%wt.)
TA-67 W5	A	0 - 8	28.6	58.2	13.2	6.60	1.19	1.97	13.81		6.2	0.75	0.18
	BA	8 - 26	21.0	59.5	19.5	1.60	1.28	1.10	11.84		6.7	0.88	0.19
	2Bt1b1	26 - 44	18.2	59.2	22.5	3.30	1.32	1.10	14.33		7.0	1.01	0.25
	2Bt2b1	44 - 59	18.7	60.8	20.4	32.10	1.41	0.87	17.65		6.7	1.07	0.22
	2Bt3b1	59 - 79	32.4	51.9	15.7	22.10	1.27	1.05	21.94		7.6	0.89	0.19
	2BC1sb1	79 - 107	39.2	30.7	30.1	18.40	1.04	0.37	30.18	0.9	7.3	0.84	0.19
	2BC2sb1	107 - 124	45.3	41.1	13.7	35.70	1.09	0.43	30.08	1.23	7.4	0.77	0.21
	3BAb2	124 - 136	34.9	57.1	8.0	4.30	1.73	0.43	15.13		7.6	0.63	0.16
	3Btb2	136 - 145	32.3	46.1	21.6	14.40	1.61	0.31	32.00		7.2	0.61	0.14
	4CBt1b3	145 - 168	70.1	14.5	15.4	0.10	1.38	0.42	17.26		7.4	0.42	0.09
	4CBt2b3	168 - 186	72.6	12.7	14.7	23.10		0.51	22.76		7.6	0.42	0.11
	4C1b3	186 - 194	73.6	11.5	15.0	46.80		0.37	25.31		7.3	0.59	0.13
	4C2b3	194 - 211	72.0	11.9	16.1	66.30		0.93	37.88		7.7	0.63	0.15

DRAFT DOCUMENT

accumulation of organic material overlying a mineral soil (Birkeland, 1984). O horizons in Laboratory soils are generally thin (~1-3 cm) and largely consist of poorly decomposed pines needles, leaves, twigs, and other forest litter. An A horizon accumulates humified organic matter mixed with a much larger fraction of minerals. A horizons occur at the surface or below an O horizon. A horizons can also occur as thin disturbed soils horizons with minimal amounts of humified organic matter. Such horizons are common where surface activity (i.e. grazing, overland traffic) has compacted upper soil horizons or resulted in partial stripping of the original A horizon.

The B horizon underlies an A horizon and shows little or no evidence of the original rock structure or sediment (Birkeland, 1984). The B horizon will often contain increases in phyllosilicate clay minerals, iron oxyhydroxides, organic coatings. These geochemically reactive phases may concentrate major and trace elements. The development of the B horizons is strongly influenced by illuvial processes relative to A or C horizons and primarily reflects the downward translocation of organic compounds, clay minerals, clay- and silt-sized particles, and other physical and chemical substances that have leached through and/or from the O and A horizons. B horizons in soils at the laboratory display a wide range of features and degrees of development. B horizons largely display characteristics resulting from several primary soil forming processes and types of illuvial material. Laboratory soils consists of (1) weakly developed B horizons ('w' subscript, Table 4) that have minimal changes in physical and chemical properties relative to the parent material, (2) Clay-rich B horizons that have resulted in an increase in clay-sized material over time ('t' subscript, Table 4), and (3) B horizons that have been influence by the accumulation of calcium carbonate ('k' subscript, Table 4). B horizons can also form as transitional horizons (ie. BA, BC, Table 4) sharing physical and chemical attributes common to either A or C horizons.

Incipient E horizons are found in some Laboratory soils. E horizons are soil horizons that have been primarily influenced by strong leaching conditions where downward and/or lateral translocation of soil water has resulted in the partial removal of clay-sized material and coatings of iron oxides.

The C horizon is a subsurface horizon lacking properties of A and B horizons but may include minimal alteration of the parent material such as accumulation of silica and calcium carbonate, mineral alteration through oxidation and reduction processes, and gleying (Birkeland, 1984). C horizons are wide spread at the Laboratory consisting of slightly altered- and non-altered parent materials. Several soils across the Laboratory have R horizons. The R horizon consists of consolidated bedrock underlying soil horizons and is usually highly fractured but has undergone minimal chemical alteration.

DRAFT DOCUMENT

Soil Stratigraphy

An important characteristic of many of the soils reported here, as well as across the Laboratory, is the complex soil stratigraphy that has resulted from one or more soils profiles that have been superimposed upon pre-existing (ie older) soil profiles. Complex soil profiles consists of a surface soil that may partially overlap underlying and now buried soils. Buried soils, when recognized, are described in a similar fashion to surface soils, but are denoted by the subscript "b" (Table 4). These types of soils are common in geomorphic environments where landscapes are episodically unstable over long periods of time, and in environments where episodic additions of new sediment can be deposited across an existing soil and landscape.

The common occurrence of buried soils across the laboratory (Figures 2, 4 and 9) is particularly relevant to spatial variability of background geochemistry and to the transport and fate of numerous contaminants found at the Laboratory. First, B horizons of buried soils typically have the strongest degree of horizon development, including the highest concentrations of iron oxides and clay-sized material (Table 4). As a result, the proximity of these buried soil B horizons will directly influence the fate and transport of any surface and subsurface contaminants. In addition, where these horizons have been re-exposed at the surface due to recent erosion or excavations the degree of B horizon development may influence local background geochemistry.

Primary and Secondary Solid Phases and Parent Material

Variations in soil-elemental concentrations are related both to chemical characteristics of a particular soil horizon and to parent material. Primary major minerals and solid phases found in the Bandelier Tuff include tridymite, quartz, feldspar, and glass (Broxton et al., 1995). Minor and trace minerals consist of smectite, hornblende, mica, hematite, magnetite, kaolinite, allanite, chevkinite, and gypsum. Primary major minerals, secondary soil minerals, and solid organic matter occur within soil profiles sampled and characterized during this investigation. Secondary soil minerals include aluminum oxides, iron oxides, smectite, illite, kaolinite, calcite, gypsum, and manganese oxides. Some of the more important secondary soil phases with their associated trace elements include: Fe and Al oxides (Be, B, P, V, Mn, Ni, Zn, Mo, As, Se, U); Mn oxides (P, Fe, Co, Ni, Zn, Mo, As, Se, Pb); calcium carbonates (As, Se, P, V, Mn, Fe, Co, Cd, U); illites (B, V, Ni, Co, Cr, Cu, Zn, Mo, As, Se, Pb); smectites (B, Ti, V, Cr, Mn, Fe, Co, Ni, Cu, Zn, Pb, U); and organic matter (Al, V, Cr, Mn, Fe, Ni, Cu, Zn, Cd, Pb, U) (Sposito, 1989). These trace elements are chemically associated with solid phases through adsorption and coprecipitation reactions.

The Bandelier Tuff contains varying amounts of glass (0-88 wt%) (Broxton et al., 1995), which is the most soluble silicate phase and is of great

DRAFT DOCUMENT

importance as a parent material. The fine size and glassy nature of the particles, as well as the high porosity and permeability of the Bandelier Tuff and related sedimentary deposits, enhance weathering and physicochemical and biological interactions in soils. Detailed mineralogical characterization of the soils found on the Pajarito Plateau will provide useful information regarding the stability of these trace minerals.

Clay-Size Material

The occurrence of clay-rich horizons are particularly relevant to the transport and fate of numerous inorganic and organic contaminants found at the Laboratory. Variation in clay-sized material (less than 2 micrometers) is significant within the soils (Figure 10) and subsequently, the extent of contaminant mobility varies depending on the presence of geochemically reactive phases, including clay minerals, iron oxides, solid organic matter, and carbonate minerals. Clay-rich horizons typically alter the local hydrologic environment by providing low permeability and low hydraulic conductivity zones, increasing the water-holding capacity of the horizon and contributing to an overall increase in the degree of chemical weathering (Sposito, 1989; McBride, 1994).

Clay-size material in all the soil samples ranges from 0.7 weight percent (wt%) (AC-1) within a C horizon to 50 wt% (TA-16-2) within a Bt horizon (Table 4). The content of clay-size material can also vary significantly throughout any one soil profile (Table 4; Figures 11-14). This size fraction, however, is heterogeneous in mineralogy and does not entirely consist of phyllosilicate clay minerals. The clay-size fraction is characterized by the smallest particle diameters having relatively large surface areas, which is an important factor in controlling the extent of adsorption of trace elements (Sposito, 1994).

Heterogeneity in the clay-size material (either vertically within one soil or spatially among different soils) can reflect variations in parent material, age, topography, eolian input, and degree of chemical weathering (Longmire et al., 1995; Birkeland, 1984; Sposito, 1989; and McBride, 1994). Clay minerals may be concentrated in B horizons resulting in an increase in clay content relative to the original parent material by downward translocation of material from overlying horizons and by *in situ* formation of clay minerals due to mineral weathering and transformations occurring within the soil environment. Clay minerals may form in Laboratory soils from the enrichment of Al_2O_3 and depletion of SiO_2 from hydrolysis reactions involving glass and framework silicates. Authigenic and translocated kaolinite and smectite are observed in soils and fracture fill material at the Laboratory (Davenport, 1993). The clay mineralogy may be related to original composition or stratification of the parent material. Clay-sized material (as well as sand- and silt-size material) can be added to the soils from atmospheric additions of dust. Spatial variability in the content of clay-sized material can also

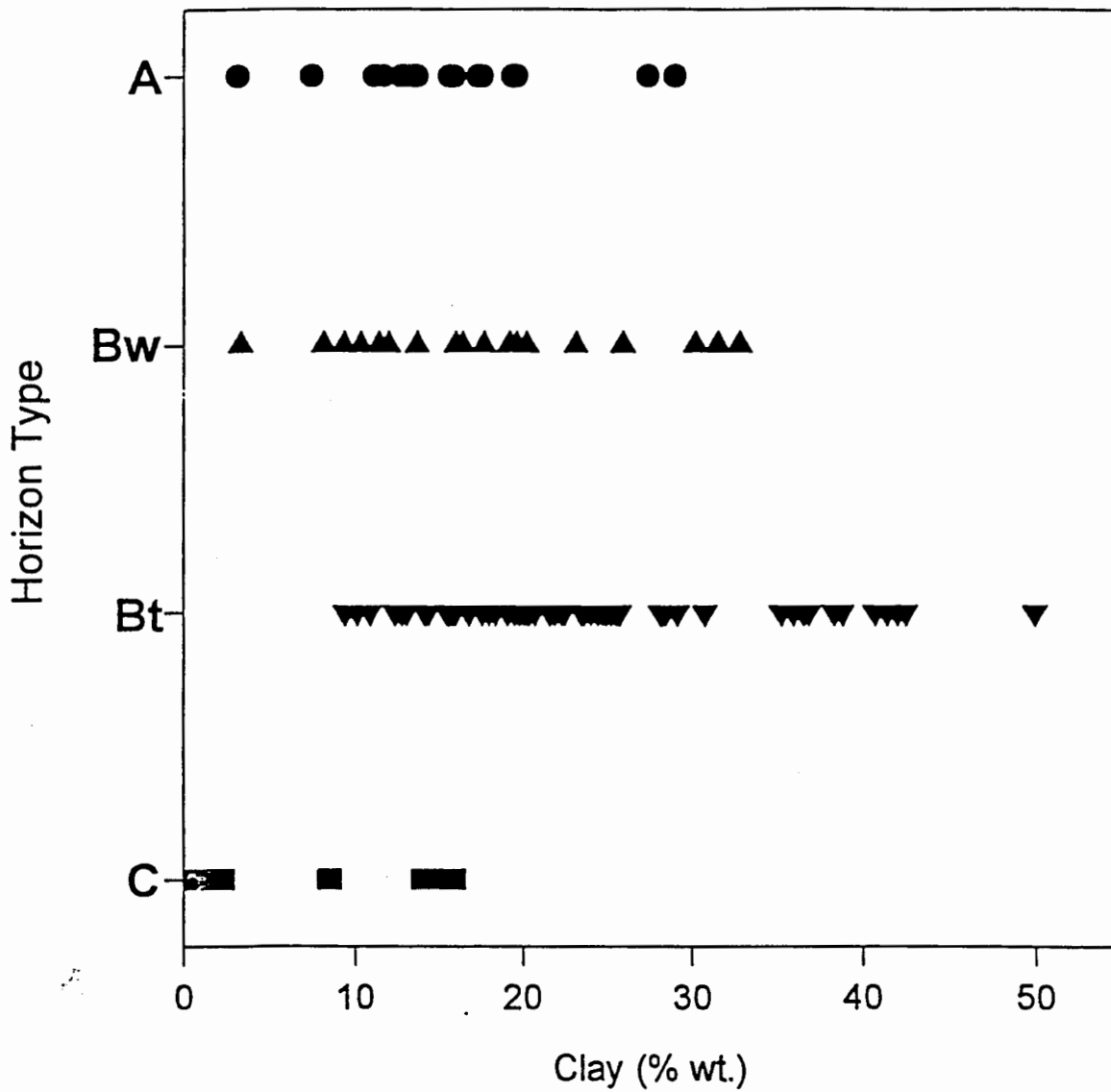
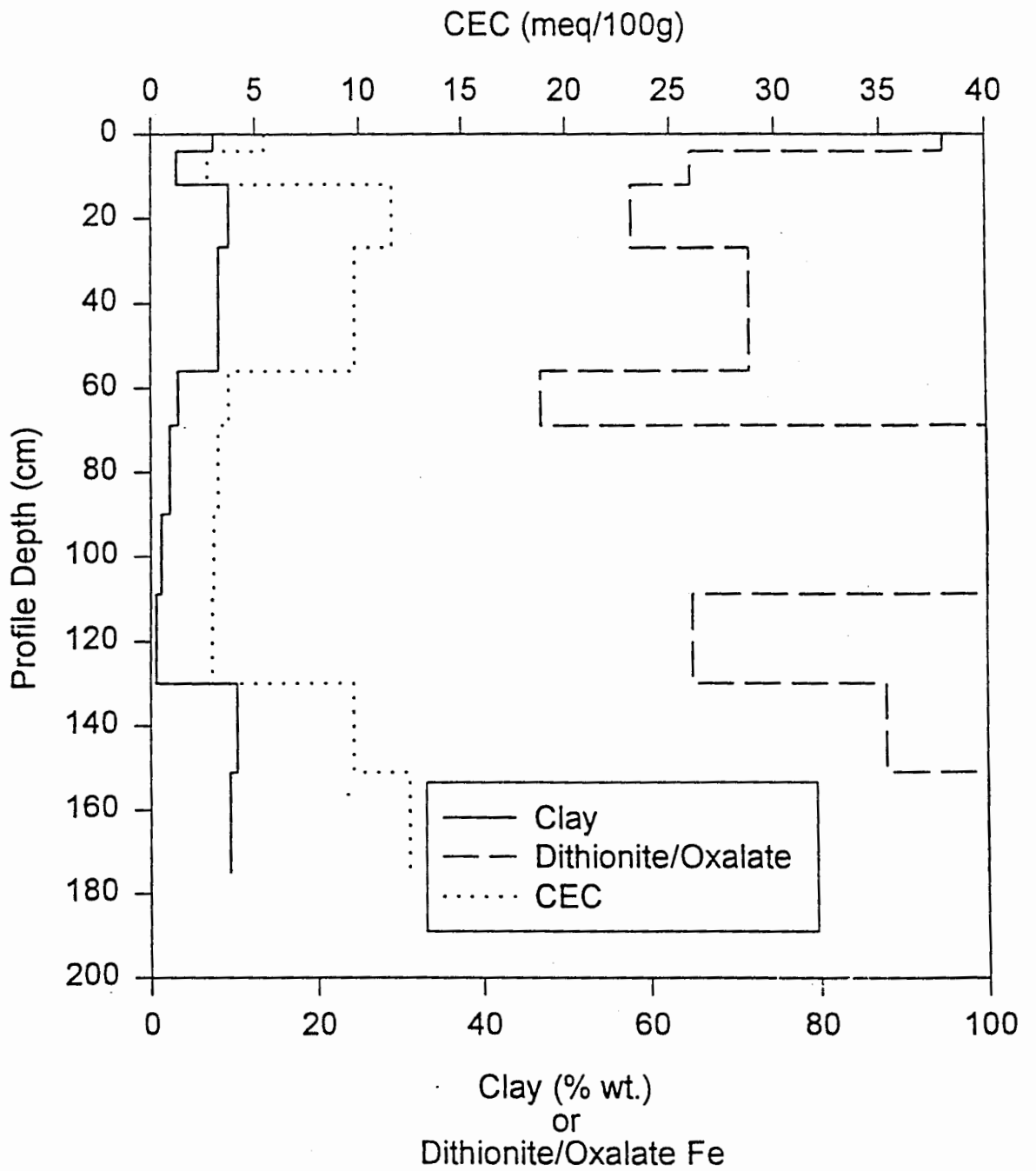


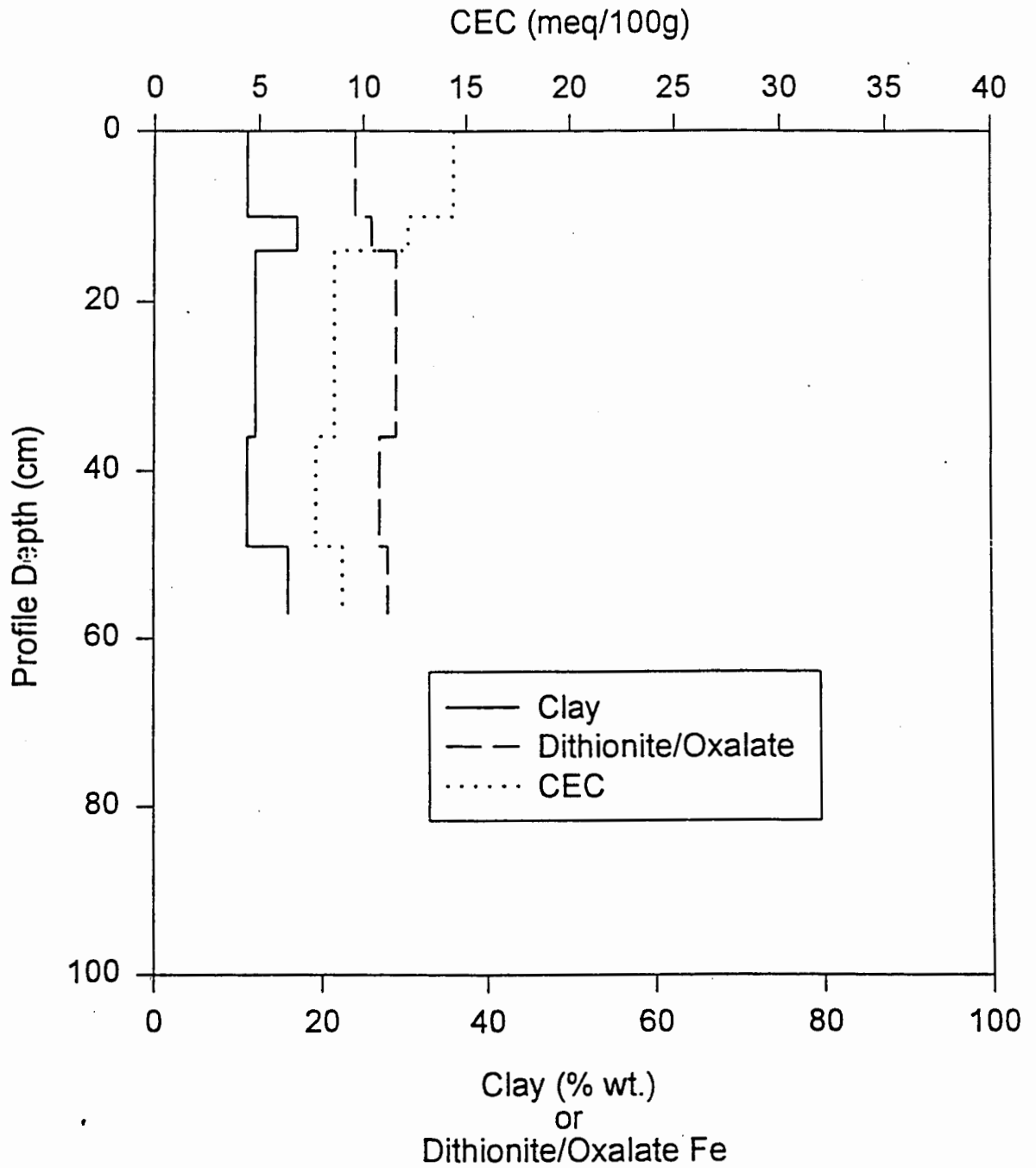
Figure 10. Variation in % wt. clay contents for dominant genetic soil horizons.

AC-1



Figure//. Profile distribution of cation exchange capacity (CEC), % wt clay, and ratio of oxalate to dithionite extractable Fe oxides.

TA-63c



Figure/2. Profile distribution of cation exchange capacity (CEC), % wt clay, and ration of oxalate to dithionite extractable Fe oxides.

TA-67 W5

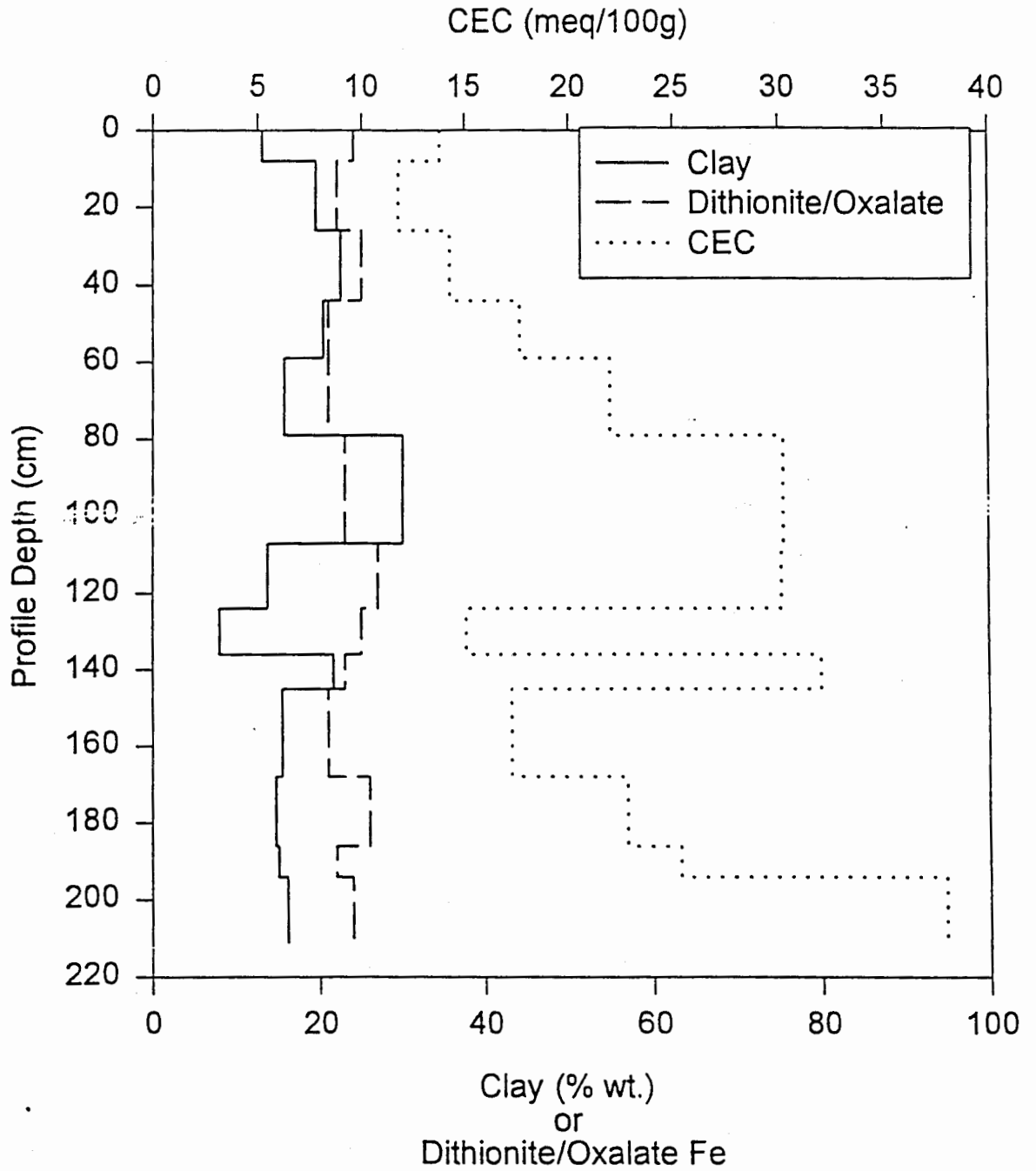


Figure B. Profile distribution of cation exchange capacity (CEC), % wt clay, and ratio of oxalate to dithionite extractable Fe oxides.

TA-16- WT- 1 and 2

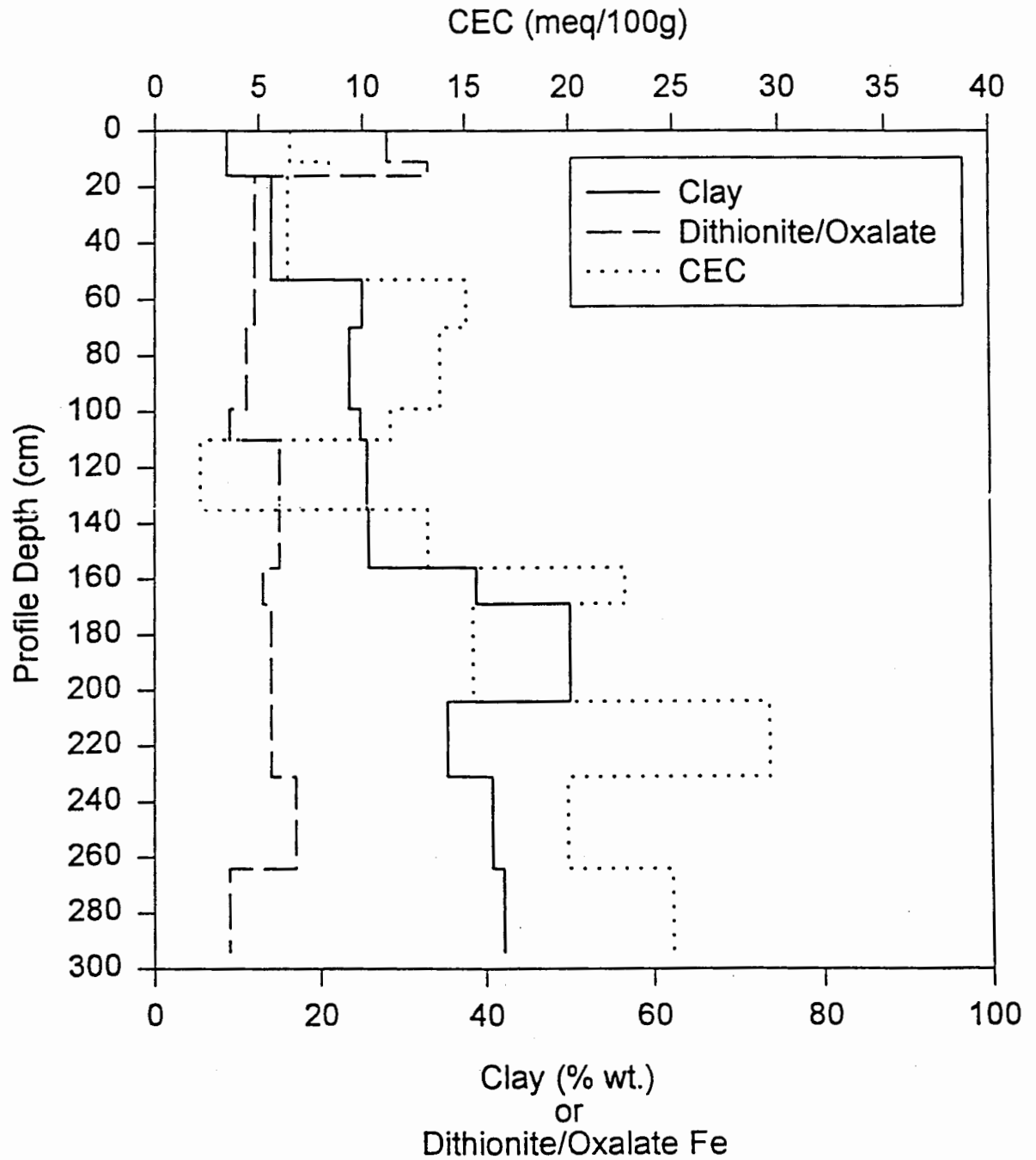


Figure 4. Profile distribution of cation exchange capacity (CEC), % wt clay, and ration of oxalate to dithionite extractable Fe oxides.

DRAFT DOCUMENT

be due to variations in the clay content of the parent material. Such variations in clay content frequently occur in soils derived from colluvial or alluvial deposits.

Soil pH

Laboratory-determined soil pH values range from 5.0, for a sample obtained from an A horizon (WC-1) to 7.6 for two samples collected from B and C horizons at (TA-67 W1; Table 4). Solid organic carbon, possibly present as humic and fulvic acids, is concentrated in A horizons containing carboxylic acids that deprotonate under moderately acidic (4.5) conditions (Thurman, 1985; Stevenson, 1994). Other organic acids with pka ($-\log_{10}$ dissociation K for the acid) values ranging from 3 to 7 may also control soil pH within the A horizons. This deprotonation results in acidic pH conditions within A horizons. In addition, enhanced biological activity in A horizons produces a high partial pressure of CO₂ gas, which reacts with soil-pore water and thereby decreases soil pH (Drever, 1988). Soils that have higher pH values (7.0-8.2) can be primarily attributed to the presence of calcium carbonate (Bk) horizons (Table 4). Soil pH is an important parameter that controls precipitation-dissolution (Lindsay, 1979) and adsorption-desorption reactions (Sposito, 1984), which is addressed in the section on trace element geochemistry.

Calcium-Carbonate Content

Calcium carbonate content of the soils is variable, ranging from 0.1 wt% in a Bt2b1 horizon at TA-67 W5 to 6.6 wt% in a Btk2 horizon at TA-63-1A (Table 4). Most soil horizons have no measurable calcium carbonate. Most of the calcium carbonate found in soils in the southwestern US and on the Pajarito Plateau probably originates from wind-blown or atmospheric sources (Gile et al., 1966; Watt and McFadden, 1992). Carbonate chemistry is important in controlling soil pH; in providing active adsorption sites for anionic and cationic adsorbates; providing ligands for metal complexing, especially for uranyl (U(VI)) (Langmuir, 1978; Brookins, 1988); in enhancing the stability of smectite characterized by a high cation exchange capacity (CEC); and in controlling hydraulic conductivity. Calcium carbonate is an important adsorbent for cations (Cd²⁺, Zn²⁺, Mn²⁺, Co²⁺, Ni²⁺, Ba²⁺) and anions (PO₄³⁻, SeO₃²⁻, and possibly UO₂(CO₃)₂²⁻), where solution pH and calcium carbonate concentration are the most important factors controlling adsorption processes (Zachara et al., 1993).

DRAFT DOCUMENT

Cation Exchange Capacity

Cation exchange capacity (CEC) in the sampled soils ranges from 2 to 43 milliequivalents/100 grams soil (meq/100 g) (Table 4), which is reflective of the different types and amounts of clay minerals and variations in organic matter content in these soils. Because B horizons generally have the highest clay mineral content, they also generally have the highest CEC (Figures 11-14). Higher CEC values are associated with 2:1 (octahedral:tetrahedral layers) clay minerals such as smectite or mixed-layer smectite, whereas the lower CEC values are representative of 1:1 clay minerals including kaolinite (Sposito, 1989; McBride, 1994). Clay minerals with higher CEC values are geochemically more reactive (larger surface area) than those with lower CEC values. Clay minerals and other adsorbents with larger surface areas have higher adsorption capacities compared to clay minerals with smaller surface areas (Sposito, 1984, 1989; McBride, 1994).

Solid Organic Carbon

Solid organic carbon (SOC) content ranges from 0.03 to 17.3 wt% for soil samples characterized during this investigation (Table 4). Values greater than about 1.5-2 wt% are unlikely in soils formed in semi-arid environments and under forest conditions (Sposito, 1989; Soil Survey Staff, 1981). High values of SOC reported here and in Watt (1995) are probably a result of laboratory error. The measured SOC content typically is highest in the A horizons where accumulation of humified organic matter is a dominant soil process. In general, soil profiles described on mesa tops at higher elevations with cooler temperatures tend to have higher SOC content than soil profiles described in Ancho and Water Canyons at lower elevations.

Bulk Density

Measured soil bulk density ranges from 1.04 g/cm³ (TA-67 W5) to 1.79 g/cm³ (TA-16-2; Table 4). Bulk density is generally higher for Bt horizons and gravel-rich horizons and lowest for weakly developed Bw horizons and A horizons.

Extractable Iron Oxyhydroxides

Results of oxalate and dithionite Fe extractions performed on soil samples collected during this investigation are provided in Table 4. Dithionite extraction largely removes all iron oxide coatings (Fe(OH)₃) including well developed crystalline forms (α -FeOOH, Fe₂O₃) whereas the oxalate extraction

DRAFT DOCUMENT

largely removes amorphous forms of iron oxides, including amorphous $\text{Fe}(\text{OH})_3$ and magnetite (Fe_3O_4) largely associated with poorly crystalline forms of iron oxide (i.e. ferrihydrite) (Schwertmann and Taylor, 1989).

Iron removed from Laboratory soils during the oxalate extraction (reported as mean wt% Fe_2O_3) ranges from 0.09 wt% in a Bt2b1b horizon at TA-16-2 to 0.77 wt% in a Bw horizon at TA-63-1A (Table 4). Iron removed from Laboratory soils during the dithionite extraction (reported as mean wt% Fe_2O_3) ranges from 0.26 wt% in a C' horizon (AC-1) to 1.41 wt% in a C2b1a horizon (WC-2; Table 5). Several fracture fillings sampled at TA-63 contained 0.83 to 1.41 wt% Fe_2O_3 using the dithionite extraction method (Table 4).

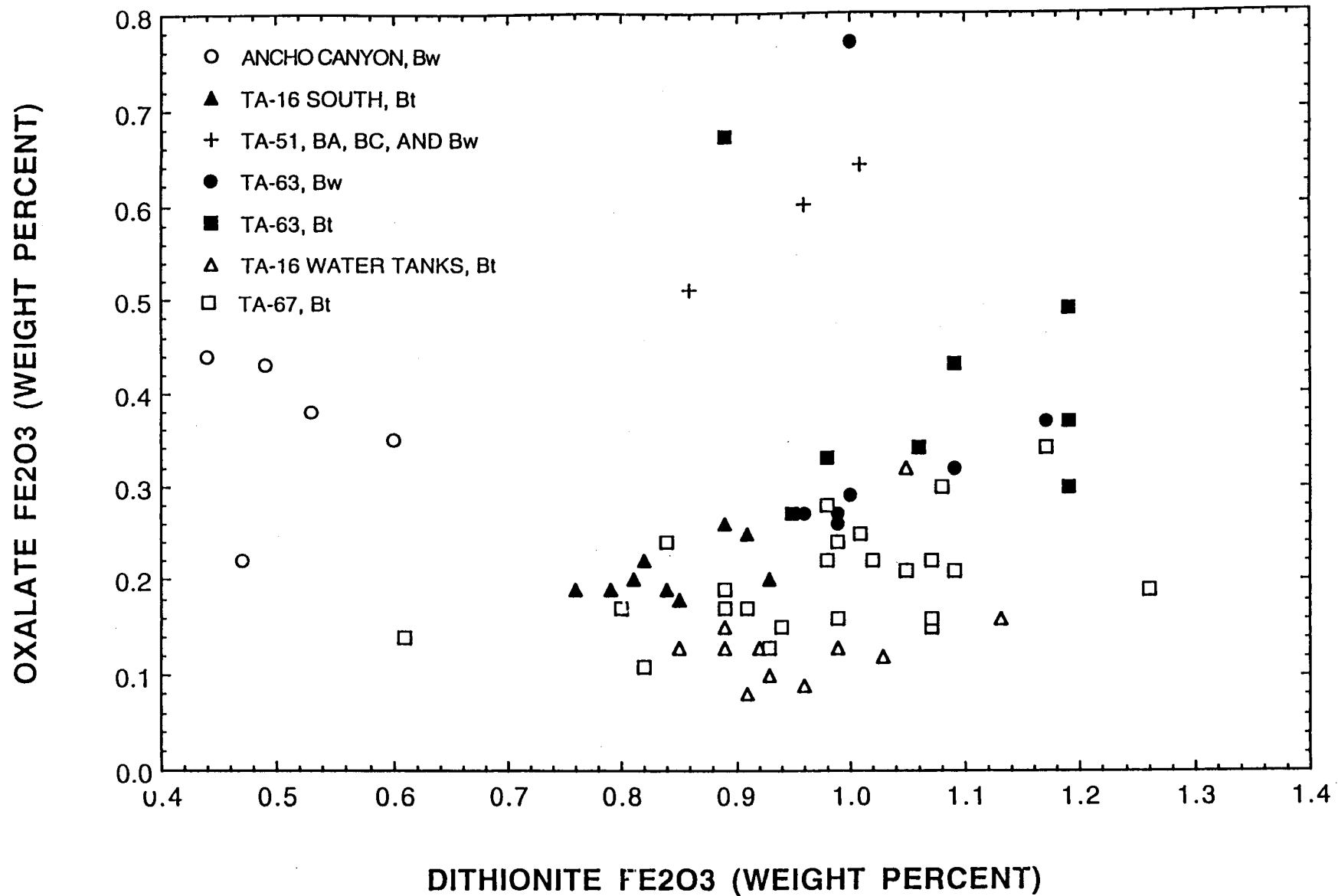
Oxalate- and dithionite-extracted Fe makes up varying percentages of the total Fe in soil samples collected during this investigation. Higher percentages of Fe were extracted from well-developed soil profiles containing one or more B horizons than from the less developed-soils (Table 4), indicating a greater abundances of iron oxides and iron oxyhydroxides in the well-developed soils. The ratio of dithionite/oxalate extractable iron oxides generally represents the relative proportions of amorphous forms of iron oxides with better developed, crystalline forms of iron oxides. With time and increased degrees of soil formation, poorly crystalline forms of Fe oxides are transformed into more developed crystalline forms. In general, weakly developed soil Bw horizons have higher quantities of amorphous forms of iron oxides relative to more developed soil Bt horizons (Figures 11-14).

Figure 15 shows distributions of dithionite- and oxalate-extracted Fe (reported as Fe_2O_3) for different B horizons characterized during this investigation. Soil samples collected from Ancho Canyon are chemically distinct from the mesa top soils. The Ancho Canyon soils have a greater percentage of oxalate-extracted Fe, mainly consisting of amorphous $\text{Fe}(\text{OH})_3$, with lower concentrations of dithionite-extracted Fe relative to the mesa top soils. The mesa top soils, however, contain higher amounts of dithionite-extracted Fe, suggesting that higher concentrations of crystalline Fe oxide (Fe_2O_3) and Fe oxyhydroxide ($\alpha\text{-FeOOH}$) occur in these more developed soils. In general, samples collected from the Bt horizons contain lower percentages of oxalate-extracted Fe than do samples collected from the Bw horizons.

GEOCHEMISTRY OF SELECTED TRACE ELEMENTS

Trace-element geochemistry of each soil profile (associated with the < 2mm soil fraction) varies as a function of soil age, mineralogy of soil and parent material, the amount and composition of eolian dust and other forms of aerosols, degree of chemical weathering, and hydrology. General discussions of the geochemical characteristics of trace elements are provided by Longmire

FIGURE 15. B HORIZONS, BACKGROUND SOILS, LOS ALAMOS.



DRAFT DOCUMENT

et al. (1995). This section focuses on geochemical distributions of As, Be, Fe, U, and Th within A, B, and C horizons.

Concentration distributions, including minimum, arithmetic mean, and maximum, for several analytes (elements) within A, B, C horizons are shown in Figures 16, 17, and 18, respectively. Analytical results of soil samples digested by HNO_3 prior to chemical analyses, using EPA-SW846 analytical methods (3050), are shown in these figures. Concentration units are ppm for the elements shown in Figures 16, 17, and 18 excluding Al and Fe, which are reported as wt%. The number of samples collected from each horizon varies and most samples were collected from B horizons ($n=111$) during this investigation, which are geochemically important because of element enrichment. Smaller numbers of samples were collected from the A ($n=17$) and C horizons ($n=16$). Concentrations of most of the elements are log-normally distributed in the soil horizons and the log-normal mean is greater than the arithmetic mean. Ranges in element distribution can exceed a factor of ten for most of the elements plotted on Figures 16, 17, and 18. These figures can be used to compare element concentration ranges with site-specific soil data, provided that the local soil horizon(s) is known.

Figure 19 shows mean-element concentrations (HNO_3 digestion) within A, B, and C horizons for Laboratory soils. In general, the B horizons contain higher concentrations of most trace elements (Al, As, Ba, Be, Cr, Fe, Ni, Th, Tl, and V) relative to A and C horizons. This trace-element enrichment within B horizons is most likely due to the presence of geochemically-reactive phases, primarily clay minerals and iron oxides. The A horizons sampled during this investigation contain higher concentrations of Co, Pb, and U (anthropogenic) relative to the B and C horizons, and the C horizons have higher concentrations of Tl relative to the A and B horizons.

Arithmetic mean and ranges for analyte concentrations (HF and HNO_3 digestions) within A, B, and C horizons are provided in Table 5. Generally, these data agree well with soil data reported from other sources summarized in Tables 6 and 7, including Longmire et al. (1995), Ferenbaugh et al. (1990) for Sigma Mesa on the Pajarito Plateau, and Schacklette and Boerngen (1984) for many different locations in the United States. Laboratory soils contain higher concentrations of Th and U (Table 6) relative to other soils listed in Tables 6 and 7, which is a result of local parent material at the Laboratory derived from U- and Th-rich volcanic rock. Anthropogenic sources of U from firing sites, however, apparently contribute to elevated U concentrations within A and several B horizons at TA-51, TA-63, and TA-67 (Table 5). Laboratory soils generally fall within the range of elemental concentrations reported elsewhere in the United States (Schacklette and Boerngen, 1984, Table 7), although the mean values for Laboratory soils are higher for some elements.

FIGURE 16. A HORIZONS, BACKGROUND SOILS, LOS ALAMOS.

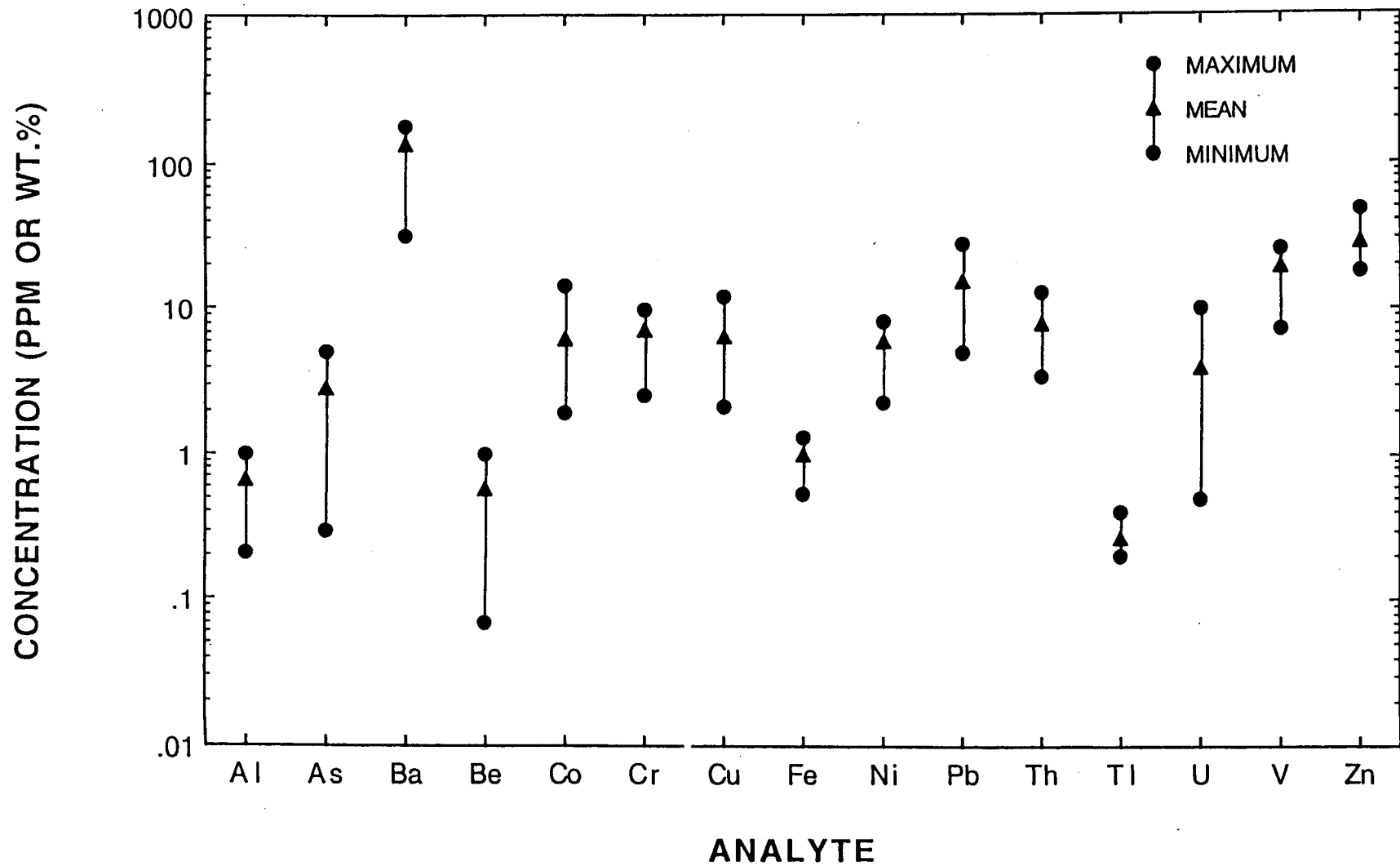


FIGURE 17. B HORIZONS, BACKGROUND SOILS, LOS ALAMOS.

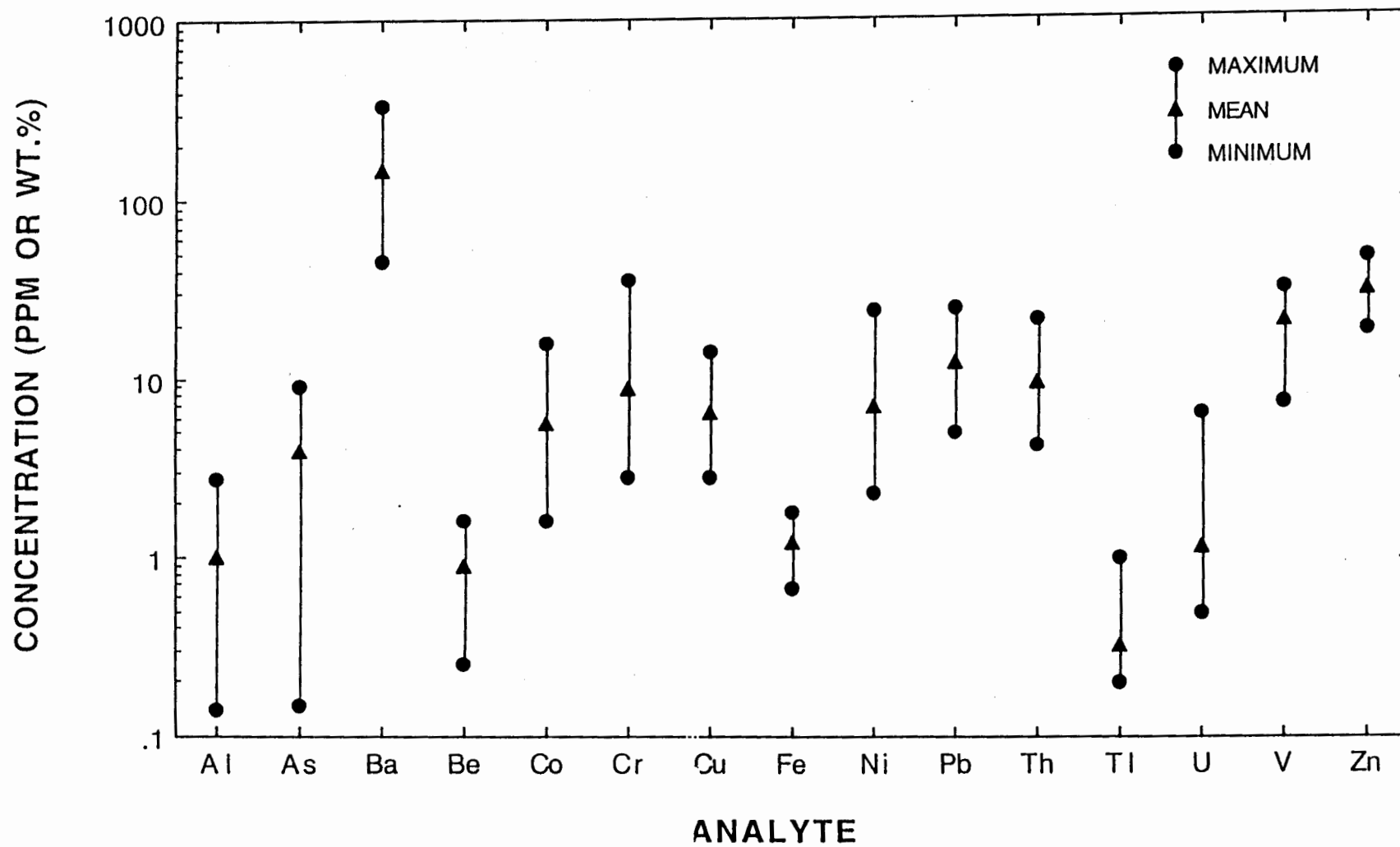


FIGURE 18. C HORIZONS, BACKGROUND SOILS, LOS ALAMOS.

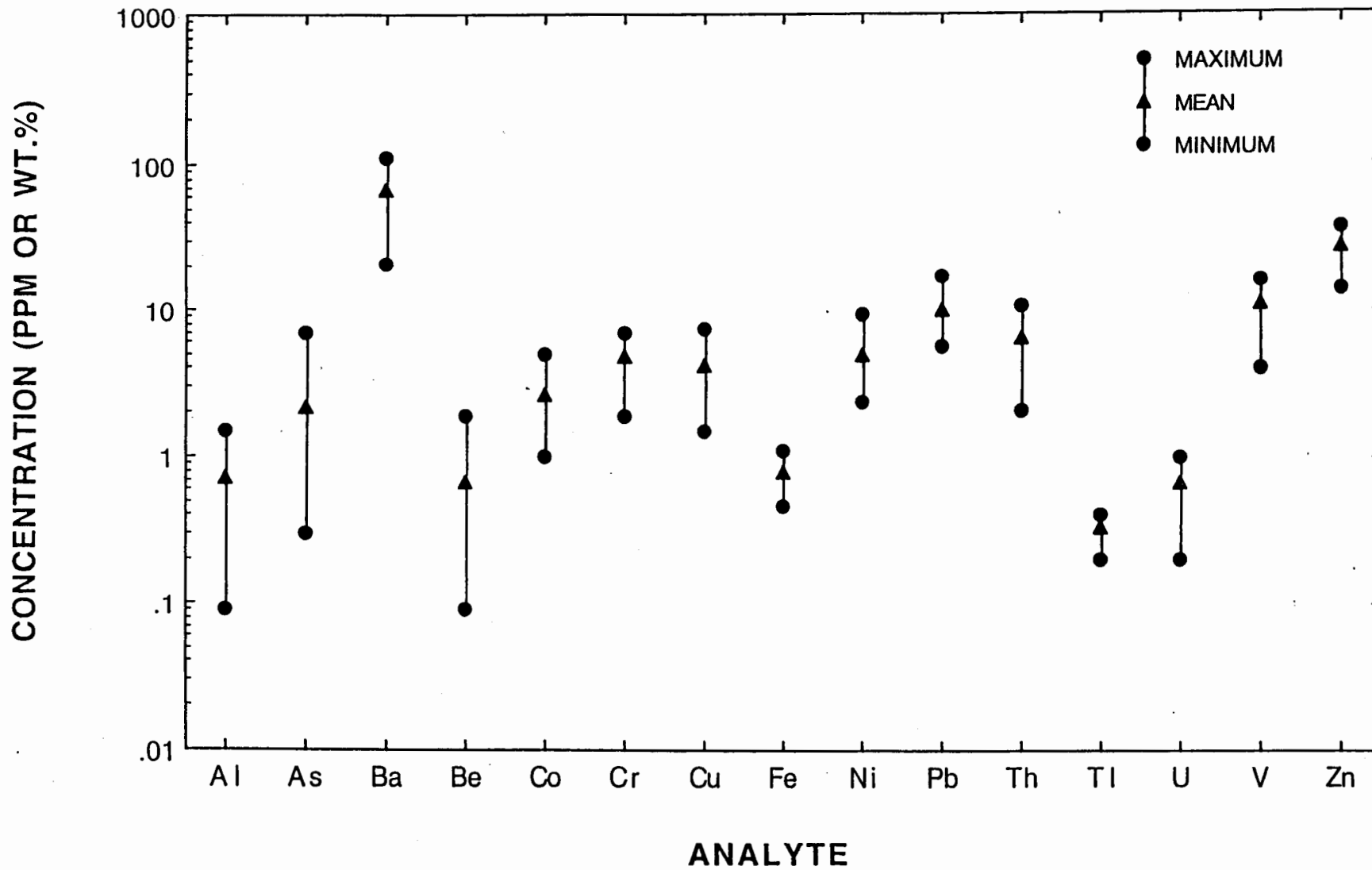


FIGURE 19. MEAN CONCENTRATIONS, BACKGROUND SOILS, LOS ALAMOS.

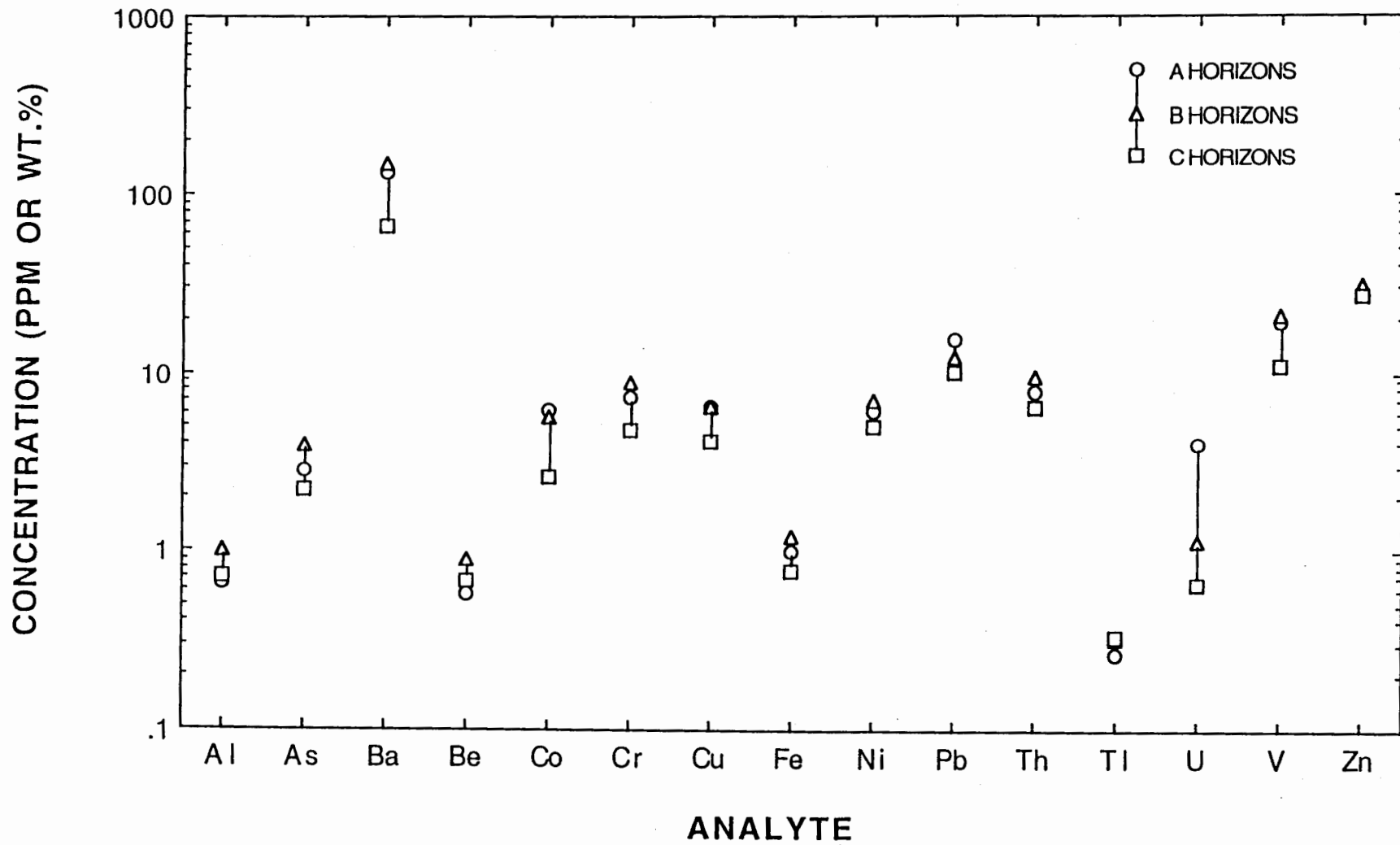


TABLE 5. Background Elemental Concentrations in A Horizons at Los Alamos, NM.

Nitric Acid Dissolution (EPA-SW846)				Hydrofluoric Acid Dissolution		
Element ^a	Number of Samples	Mean	Range	Number of Samples	Mean	Range
Al (wt.%)	16	0.65	0.21 - 1.00	14	4.92	2.10 - 6.30
Sb	3	0.37	0.20 - 0.50	16	0.92	0.50 - 0.92
As	14	2.76	0.30 - 5.00	14	8.20	0.90 - 18.0
Ba	16	134	32.0 - 180	14	549	200 - 650
Be	16	0.59	0.07 - 1.00	14	2.02	1.40 - 2.40
Cr	16	7.22	2.50 - 9.80	14	23.1	5.50 - 31.0
Co	16	6.16	1.90 - 14.0	14	10.1	0.79 - 13.0
Cu	16	6.44	2.10 - 12.0	14	9.83	1.90 - 17.0
Fe (wt.%)	16	0.99	0.54 - 1.30	14	1.76	1.30 - 2.30
Pb	16	15.3	5.00 - 37.0	14	24.6	7.50 - 37.0
Mn	16	439	240 - 950	14	523	370 - 680
Ni	13	6.06	2.30 - 8.30	13	9.56	4.40 - 13.0
Tl	12	0.27	0.20 - 0.80	16	0.69	0.20 - 0.80
Th	16	7.83	3.50 - 12.8	17	14.5	8.50 - 22.6
U	17	3.97	0.50 - 9.90	15	8.11	3.00 - 17.7
V	16	19.1	7.40 - 26.0	14	47.4	15.0 - 62.0
Zn	16	28.1	18.0 - 47.0	14	49.4	41.0 - 58.0

^aData are reported in parts per million (ppm) unless otherwise noted.

TABLE 5. Background Elemental Concentrations in B Horizons at Los Alamos, NM.

Nitric Acid Dissolution (EPA-SW846)				Hydrofluoric Acid Dissolution		
Element ^a	Number of Samples	Mean	Range	Number of Samples	Mean	Range
Al (wt.%)	111	0.98	0.14- 2.70	107	5.70	2.00 - 8.10
Sb	16	0.41	0.20 - 1.00	111	0.97	0.30 - 2.60
As	94	3.87	0.30 - 9.00	105	10.1	0.50 - 25.0
Ba	111	148	46.0 - 340	106	519	220 - 810
Be	111	0.89	0.25 - 1.60	105	2.32	1.30 - 2.32
Cr	106	8.90	2.80 - 36.0	106	24.8	11.0 - 46.0
Co	111	5.64	1.60 - 16.0	106	9.14	2.30 - 25.0
Cu	111	6.54	2.80 - 14.0	106	9.90	3.00 - 20.0
Fe (wt.%)	111	1.20	0.68 - 1.80	106	2.09	1.40 - 3.60
Pb	110	12.3	5.00 - 25.0	106	22.4	7.60 - 47.0
Mn	110	362	150 - 1,000	107	489	260 - 1,600
Ni	108	6.95	2.30 - 24.0	104	12.4	4.00 - 43.0
Tl	72	0.32	0.20 - 1.00	112	0.76	0.50 - 1.30
Th	112	9.53	4.20 - 21.6	111	16.5	10.0 - 27.6
U	112	1.13	0.50 - 6.40	112	4.01	1.00 - 11.9
V	111	20.8	7.40 - 32.0	106	50.4	23.0 - 69.0
Zn	110	31.3	19.0 - 47.0	107	60.0	26.0 - 130

^aData are reported in parts per million (ppm) unless otherwise noted.

TABLE 5. Background Elemental Concentrations in C Horizons at Los Alamos, NM.

Nitric Acid Dissolution (EPA-SW846)				Hydrofluoric Acid Dissolution		
Element ^a	Number of Samples	Mean	Range	Number of Samples	Mean	Range
Al (wt.%)	14	0.71	0.09-1.50	13	5.02	2.60 - 7.40
Sb	0	-	-	15	0.63	0.30 - 1.20
As	13	2.17	0.30 - 7.00	13	8.92	3.00 - 14.0
Ba	14	66.7	21.0 - 110	13	278	150 - 620
Be	12	0.67	0.09 - 1.90	13	2.67	1.00 - 4.40
Cr	14	4.79	1.90 - 6.90	13	13.9	4.90 - 31.0
Co	14	2.60	1.00 - 4.90	13	5.12	1.90 - 12.0
Cu	14	4.19	1.50 - 7.30	13	4.56	1.00 - 8.80
Fe (wt.%)	14	0.78	0.47 - 1.10	13	1.45	0.91 - 2.20
Pb	9	10.1	5.60 - 17.0	13	20.1	4.40 - 30.0
Mn	14	194	82.0 - 440	13	348	200 - 550
Ni	7	4.99	2.40 - 9.20	13	7.61	2.30 - 17.0
Tl	3	0.33	0.20 - 0.40	15	0.64	0.30 - 1.00
Th	14	6.55	2.10 - 10.3	15	14.4	7.80 - 19.0
U	14	0.66	0.20 - 1.00	15	3.77	1.70 - 4.90
V	14	10.9	4.00 - 16.0	13	26.2	9.00 - 44.0
Zn	14	26.8	14.0 - 37.0	13	57.8	33.0 - 76.0

^aData are reported in parts per million (ppm) unless otherwise noted.

TABLE 6. Background Elemental Concentrations in Soils at Los Alamos, NM (Longmire et al., 1995).

Element ^a	Nitric Acid Dissolution (EPA-SW846)			INAA or DNAA (Uranium Only)		
	Number of Samples	Mean	Range	Number of Samples	Mean	Range
As	72	4.9	0.5 - 13.6	67	5.04	1.20 - 10.81
Ba	72	176	24 - 730	75	459	125 - 829
Be	72	1.23	0.18 - 4.00		-	-
	75	^b 2.37	1.00 - 4.40			
Co	72	15.2	5.5 - 34	75	7.14	0.44 - 23.35
Cr	72	12.2	1.9 - 37.0	74	34.74	2.03 - 71.07
Cu	67	6.6	0.6 - 16.0		-	-
Fe (wt.%)	72	1.51	0.33 - 3.60	75	2.37	1.09 - 4.86
Ni	70	10.3	2.0 - 28.0		-	-
Pb	69	16.7	4.0 - 37.0		-	-
		^b 28.36	18.00 - 56.00			
Se	41	0.75	0.30 - 2.40		-	-
Th	72	7.1	0.6 - 15.0	75	16.06	10.09 - 27.30
Tl	40	0.42	0.20 - 0.90		-	-
U	72	0.94	0.20 - 2.40	75	3.41	1.54 - 6.73
V	72	26.6	4.0 - 56.0	72	48.95	11.54 - 113.10

^aData are reported in parts per million (ppm) unless otherwise noted.

^bHydrofluoric acid used in sample dissolution.

TABLE 7. Elemental Concentrations in Soil.

Element ^a	Farenbaugh et al. (1990)		Schacklette and Boerngen (1984)	
	Mean	Range	Mean	Range
	Sigma Mesa, Los Alamos		Random Locations, USA	
Al (%)	5.8	5.3 - 6.7	5.8	0.5 - >10
As	3.9	1.3 - 6.7	5.5	<0.1 - 97
Ba	410	120 - 810	580	70 - 5,000
Be	1.9	1.1 - 3.3	0.68	<1 - 15
Br	1.9	0.40 - 5.7	0.52	<0.5 - 11
Cd (ppb)	170	30 - 520	-	-
Cl	<100	-	-	-
Cr	27	4.2 - 136	41	3 - 2,000
Cu	10	2.0 - 18	21	2 - 300
F	240	50 - 390	280	<10 - 1,900
Fe (%)	1.7	1.0 - 2.6	2.1	0.1 - >10
Hg (ppb)	18	7.0 - 29	46	<10 - 4,600
Mn	510	330 - 840	380	30 - 5,000
Ni	8.9	1.6 - 19	15	<5 - 700
Pb	24	8.0 - 98	17	<10 - 700
Rb	120	90 - 160	69	<20 - 210
Th	-	-	9.1	2.4 - 31
Ti (%)	0.26	0.079 - 0.49	0.22	0.05 - 2.0
U	-	-	2.5	0.68 - 7.9
Zn	54	38 - 71	55	10 - 2,100

^aData are reported in parts per million (ppm) unless otherwise noted.

DRAFT DOCUMENT

Element concentration distributions resulting from HF and HNO₃ digestions, including minimum, arithmetic mean, and maximum, for several analytes (elements) within A, B, and C horizons are shown in Figures 20, 21, and 22, respectively. Total sample digestion using HF generally results in higher elemental concentrations (maximum, mean, and minimum values) than partial digestion using HNO₃. Concentration ranges for As, Cr, Pb, U, and other analytes in the B horizons using the two digestion procedures overlap to a greater extent than other analytes collected within the A and C horizons. This suggests that these elements have been redistributed within the B horizons, possibly through translocation, precipitation, and adsorption processes, and concentrated in acid-soluble (pH 1) phases such as surface coatings.

Mean concentration ratios (HF/HNO₃ digestion) for several analytes (elements) of soil samples collected from A, B, and C horizons are shown in Figure 23. A higher concentration ratio for a given analyte suggests lesser amounts of leaching with HNO₃ and that an element, for example Al, is primarily concentrated within a silicate phase(s) that does not completely dissolve at pH 1. These phases include feldspars, glass, and other silicate and oxide minerals. Lower concentration ratios for certain elements (Fe, Ni, V) suggest that these elements are concentrated in one or more acid soluble phases such as clay minerals, calcium carbonate, and ferric hydroxide. Lower concentration ratios are observed for Al, Be, As, Ba, Cr and Th within the B horizons relative to the A and C horizons. This suggests that these elements may have been redistributed within the B horizons. Other elements including Pb, U, and Zn have lower concentration ratios within the A horizons relative to the B and C horizons, whereas Cu, Ni, and Tl have the lower concentration ratios in the C horizons. Iron and V are distributed evenly between the A, B, and C horizons and these elements are distributed at a ratio of 2:1.

Different trace elements shown in Figures 16 through 23 are distributed in B horizons possibly by the following processes (Longmire et al., 1995; Sposito, 1984, 1989): (1) trace elements that are concentrated primarily on surfaces of soil particles through chemical weathering, for example As and Be; (2) trace elements that remain concentrated within soil particle matrices consisting of primary minerals (silicates) and glass, for example Ni, Pb, Th, Tl, V, and Zn; and (3) trace elements that are distributed as a combination of processes (1) and (2), for example Ba, Co, Cr, Cu, Pb, and U. Process (1) is due mainly to adsorption of trace elements onto surfaces of clay minerals, iron oxides, solid organic matter, and calcium carbonate, whereas process (2) is dominated by incorporation within primary minerals and volcanic glass (Longmire et al., 1995; Sposito, 1984, 1989). Enrichment of As in soil correlates with soil development, specifically with the formation of B horizons containing iron oxides, clay minerals, and solid organic matter as possible dominant adsorbents (Longmire et al., 1995). Factors controlling extent of element

FIGURE 20. COMPARISON OF SAMPLE DIGESTION USING HF (TOTAL) OR HNO₃ WITH ANALYTICAL TECHNIQUES (ICPES (Be, Cr, Pb), AA (As), AND ICPMS (Th, U)), A HORIZONS, LOS ALAMOS.

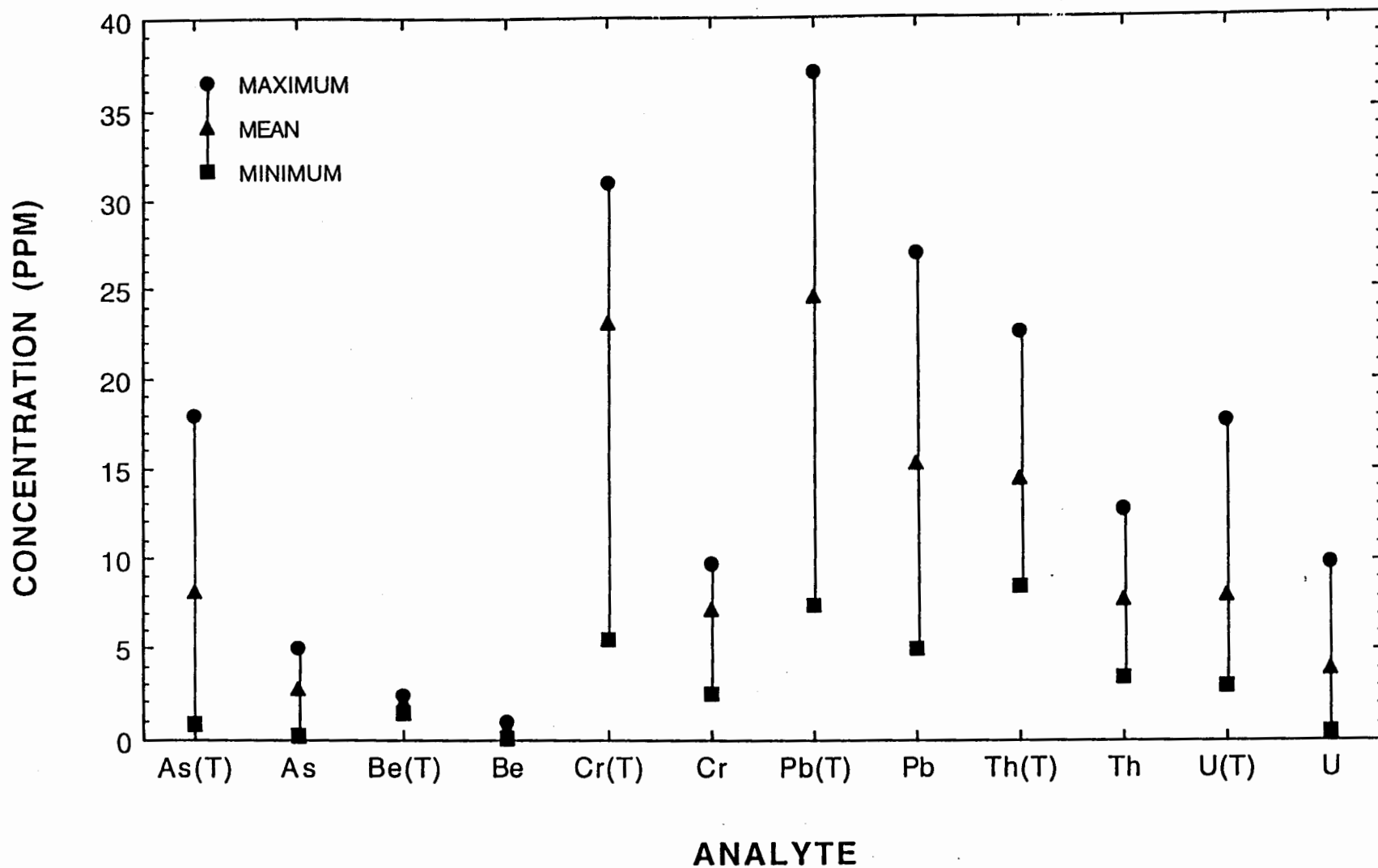


FIGURE 21. COMPARISON OF SAMPLE DIGESTION USING HF (TOTAL) OR HNO₃ WITH ANALYTICAL TECHNIQUES (ICPES (Be, Cr, Pb), AA (As), AND ICPMS (Th, U)), B HORIZONS, LOS ALAMOS.

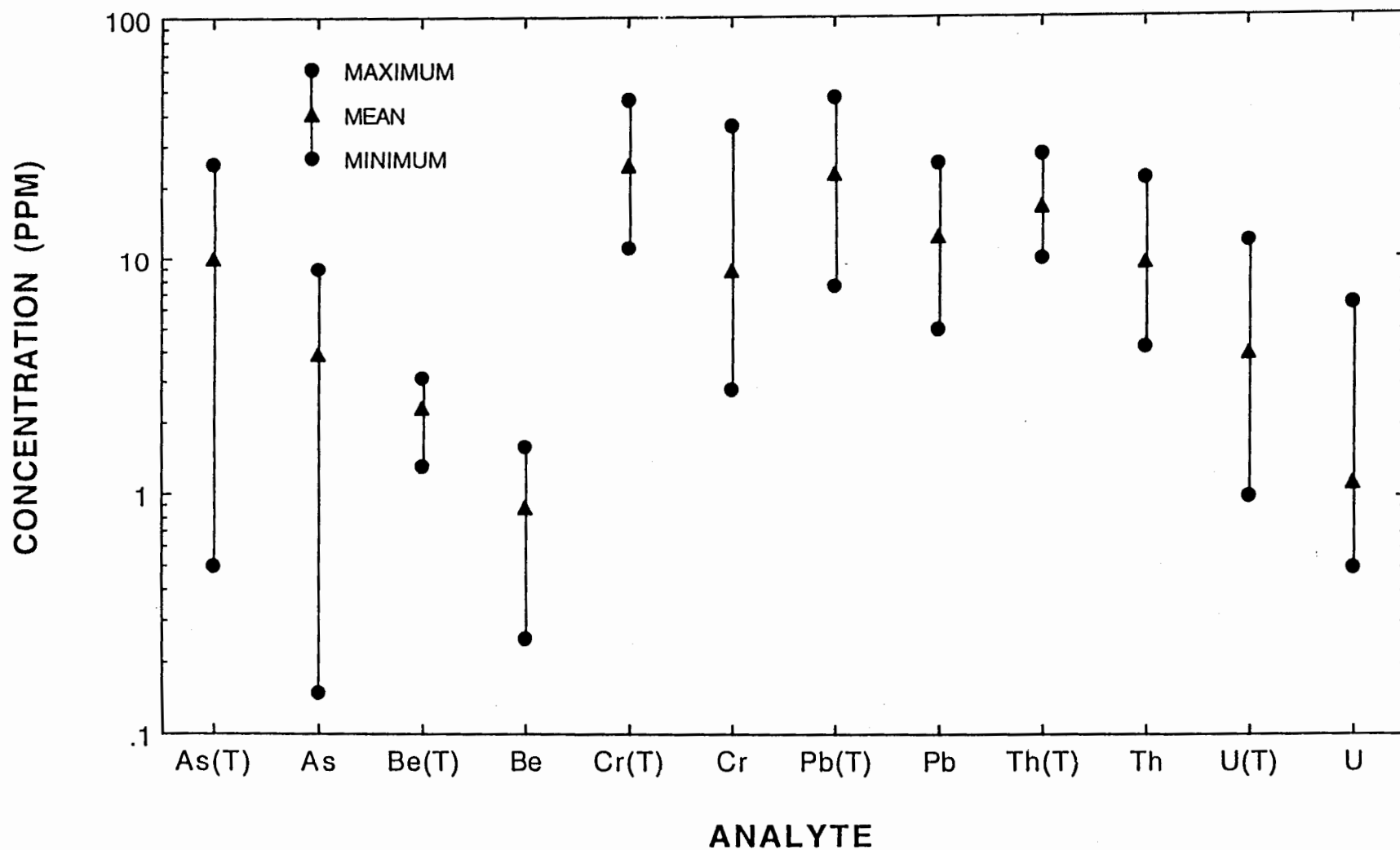


FIGURE 22. COMPARISON OF SAMPLE DIGESTION USING HF (TOTAL) OR HNO₃ WITH ANALYTICAL TECHNIQUES (ICPES (Be, Cr, Pb), AA (As), AND ICPMS (Th, U)), C HORIZONS, LOS ALAMOS.

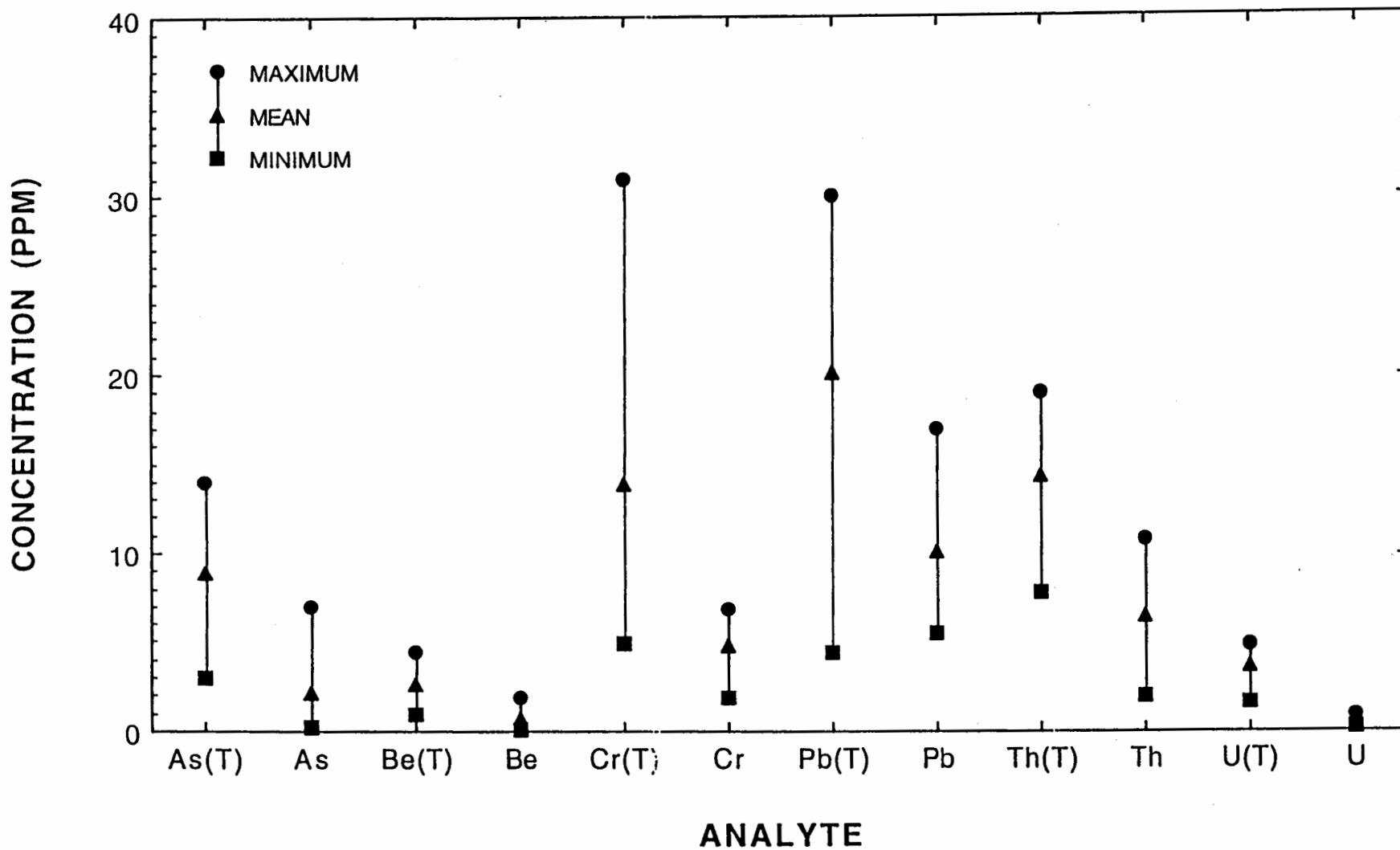
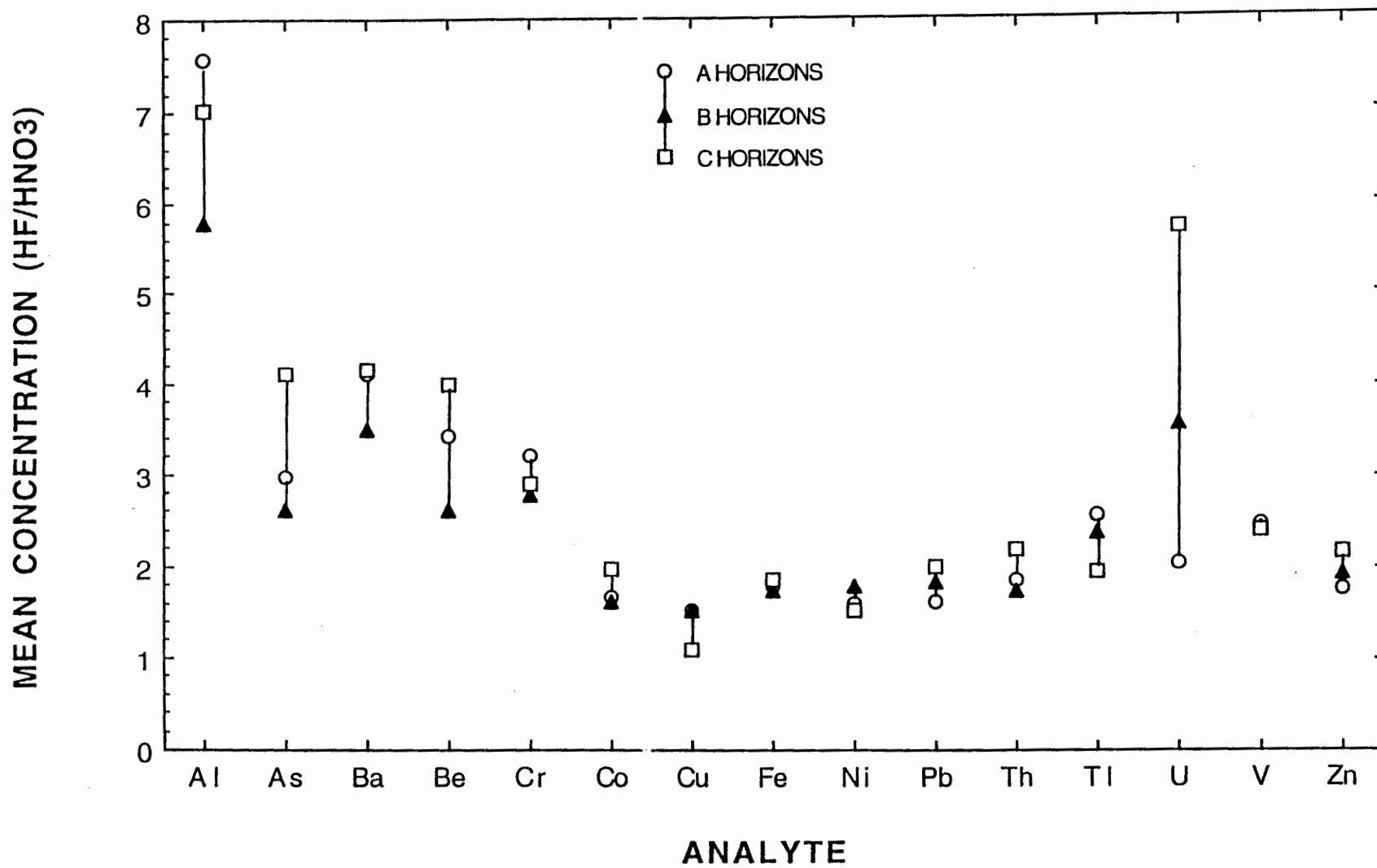


FIGURE 23. A, B, C HORIZONS, BACKGROUND SOILS, LOS ALAMOS.



DRAFT DOCUMENT

leaching from primary soil phases include solid-state diffusion, solubility of the host phase, dissolution kinetics, solution flux, pH, Eh, and speciation of the trace element.

Arsenic, Beryllium, and Iron

Figures 24 and 25 are bivariate plots of Fe versus As and Fe versus Be, respectively, within several different types of B horizons characterized during this investigation. Overall, there is a strong correlation between Fe and As and Fe and Be and this correlation is discussed in the statistics section of this report. Soil profiles containing well developed B (Bt) horizons contain higher concentrations of As, Be, and Fe than do weakly developed B (Bw) horizons for mesa top and canyon bottom soils. The soil profile in Ancho Canyon is characterized by lower concentrations of these elements because this soil is less developed relative to the mesa top soils (Watt, 1995). Iron, in the forms of iron oxide, amorphous ferric hydroxide, and ferric oxyhydroxide, is an important soil constituent. In addition to As and Be, other trace elements including Cr, Mn, Ni, and other trace elements correlate well with Fe in the soil profiles characterized in this investigation and soil profiles described by Watt and McFadden (1992) and Longmire et al. (1995). Iron forms several sparingly soluble phases in soil, including $\text{Fe}_3(\text{OH})_8$, amorphous $\text{Fe}(\text{OH})_3$, and goethite ($\alpha\text{-FeOOH}$), under different oxidation-reduction conditions. These solids are important adsorbents for many metals found at the Laboratory and elsewhere (Leckie et al., 1980; Hsi and Langmuir, 1985; Rai and Zackara, 1984).

Beryllium is an important element at the Laboratory because of its use in detonation of ballistics. Beryllium forms hydroxo complexes (BeOH^+ , $\text{Be}(\text{OH})_2^0$, and $\text{Be}(\text{OH})_3^-$) above pH 6 (Rai and Zachara, 1984). There are very little data available on adsorption and precipitation/dissolution reactions of Be at low temperatures. Available thermochemical data suggest that $\beta\text{-Be}(\text{OH})_2$ is moderately insoluble and this phase precipitates rapidly from solution (Rai and Zachara, 1984). There is some evidence that Be adsorption onto soil surfaces (iron oxides and clay minerals) is pH dependent. Column experiments conducted by Alesii et al. (1980) and Korte et al. (1976) show that Be was more strongly attenuated than were Zn, Cd, Ni, and Hg. Korte et al. (1976) suggest that calcareous soils high in clay minerals appear to be effective in Be retention.

Distributions of oxalate- and dithionite extracted Fe versus Be, in B horizons for two geomorphic settings (canyon bottom and mesa tops), are shown in Figures 26 and 27, respectively. Figure 26 shows an overlap of Ancho Canyon and mesa top samples with respect to oxalate-extracted Fe and Be, suggesting that amorphous $\text{Fe}(\text{OH})_3$ is present in various concentrations in all soil samples. The correlation of Be with oxalate-extracted Fe is not obvious in

FIGURE 24. B HORIZONS, BACKGROUND SOILS, LOS ALAMOS.

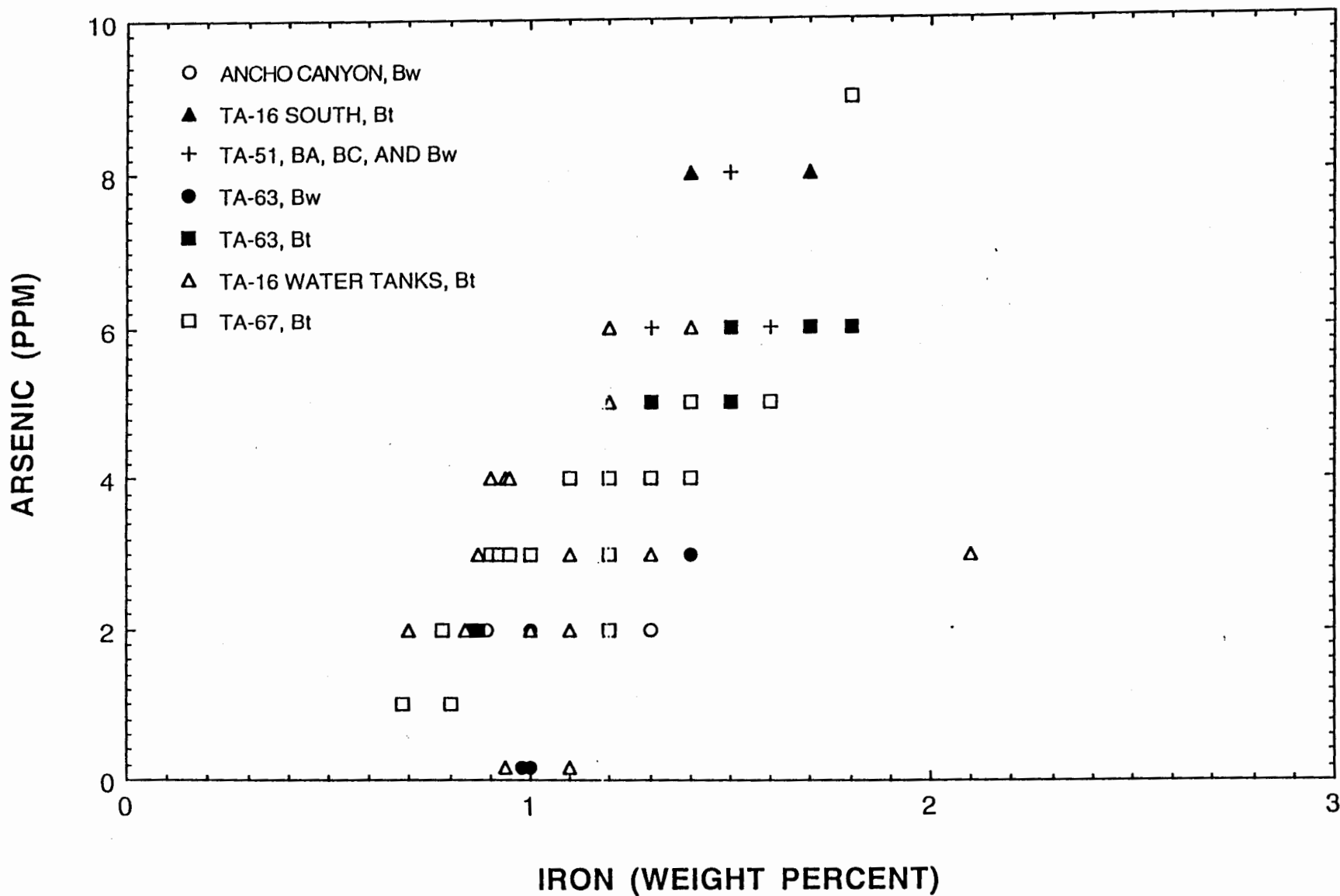


FIGURE 25. B HORIZONS, BACKGROUND SOILS, LOS ALAMOS.

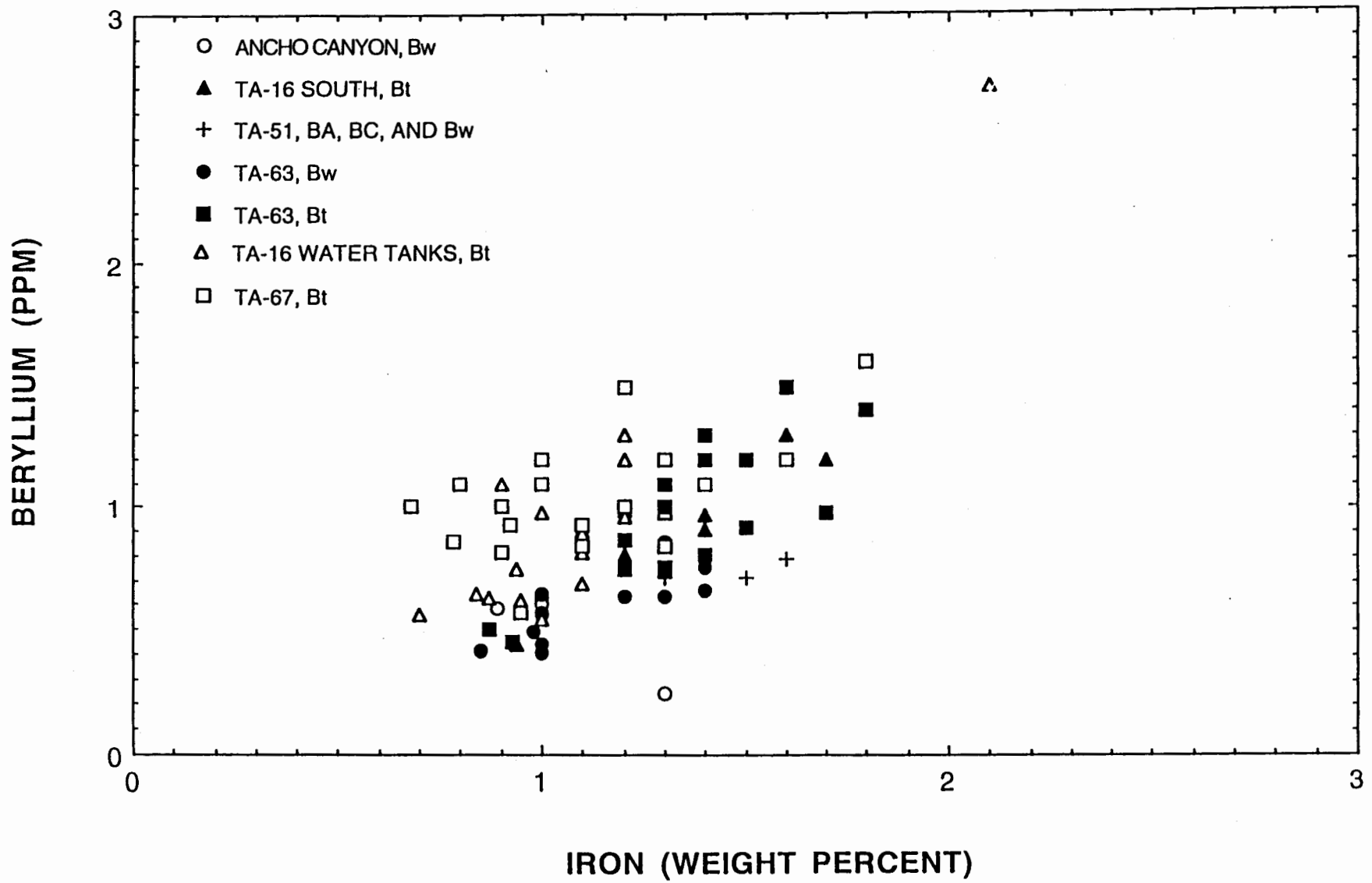


FIGURE 26. B HORIZONS, BACKGROUND SOILS, LOS ALAMOS.

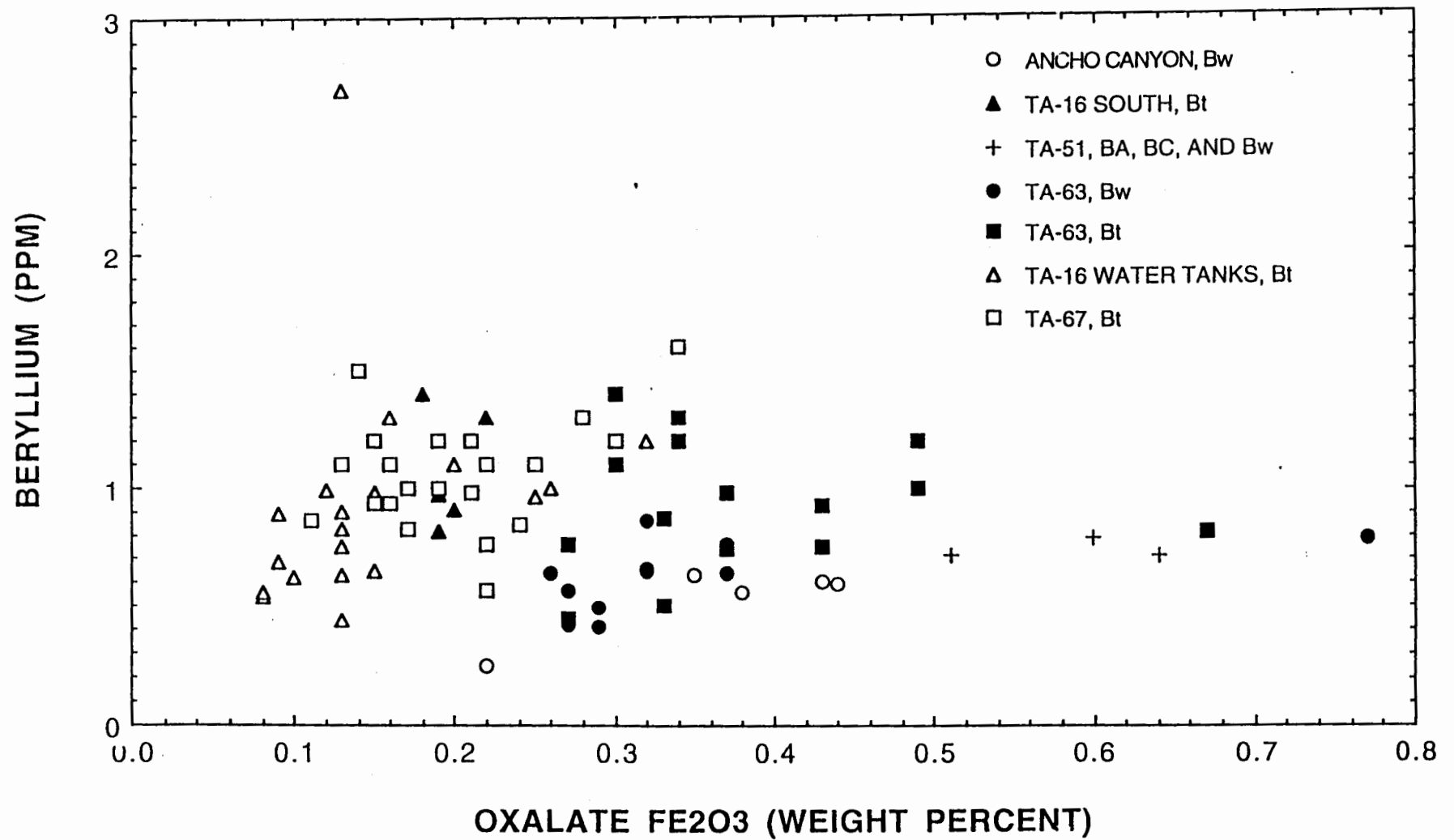
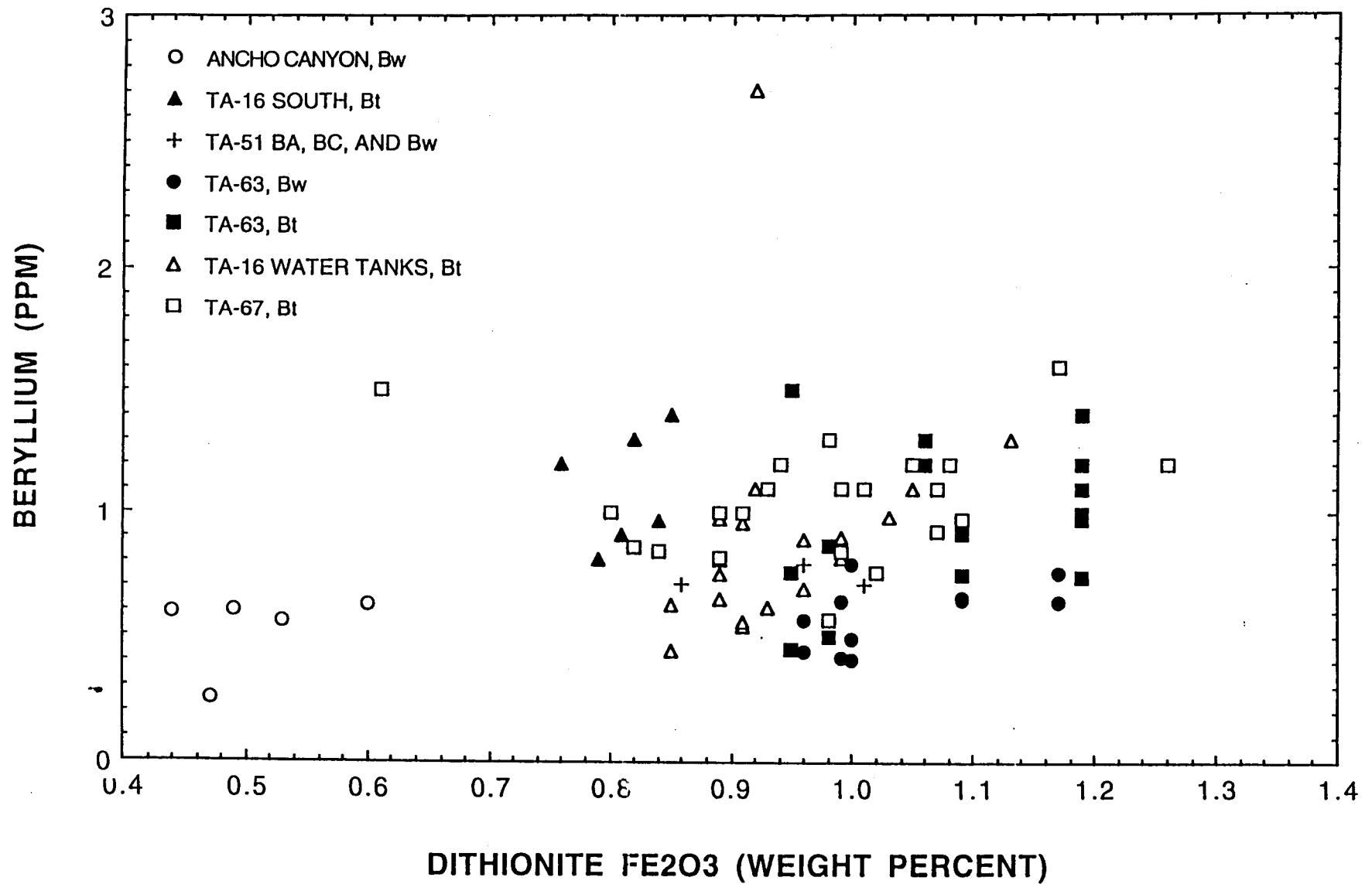


FIGURE 27. B HORIZONS, BACKGROUND SOILS, LOS ALAMOS.



DRAFT DOCUMENT

Figure 26 due to complex nature and distribution of amorphous $\text{Fe}(\text{OH})_3$. A better correlation of dithionite-extracted Fe with Be for the two different geomorphic environments is shown in Figure 27. Soil samples collected in Ancho Canyon have lower concentrations of Be and dithionite-extracted Fe than do the mesa top samples (Figure 27). This suggests that Be probably is more associated (chemisorption) with goethite and hematite rather than amorphous $\text{Fe}(\text{OH})_3$.

Thorium and Uranium

Thorium and U are important actinide elements that occur naturally in the Bandelier Tuff and soils on the Pajarito Plateau, and these elements may also occur above background concentrations resulting from Laboratory activities. An understanding of background elemental distributions of Th and U will provide constraints on the fate and transport of anthropogenic actinides. Thorium is stable in the 4+ valence state and forms hydroxo complexes ($\text{Th}(\text{OH})_3^+$ and $\text{Th}(\text{OH})_4^0$) above pH 4 in organic-free solution (Langmuir and Herman, 1980). Thorium hydroxo species strongly adsorbed onto iron oxides and clay minerals. Thorium is considered to be less leachable than U in these soils based on thermodynamic considerations and results of experimental data cited in Brookins (1988) and Langmuir and Herman (1980). Under relatively oxidizing conditions, U(VI) forms stable carbonato complexes (UO_2CO_3^0 , $\text{UO}_2(\text{CO}_3)_2^{2-}$, and $\text{UO}_2(\text{CO}_3)_3^{4-}$) in aqueous solutions above pH 6 (Langmuir, 1978; Brookins, 1988). These carbonato complexes adsorb onto surfaces of iron oxides and clay minerals; however, desorption of these complexes under alkaline pH conditions has been demonstrated by Tripathy (1984) and Hsi and Langmuir (1985).

Figure 28 shows the total distributions (HF digestion) of Th and U in the Bandelier Tuff (Longmire et al., 1995) and in soils characterized during this investigation. Total Th and U concentrations in soil samples collected from the B and C horizons generally fall within the distribution for the Tshirege Member of the Bandelier Tuff, where tuff mapping unit 1 has the highest concentrations of Th and U followed by mapping units 2 and 3 (Longmire et al., 1995). Concentrations of total Th and U in the soils, excluding the A horizons, overlap with the ranges of these two elements in mapping units 2 and 3 of the Bandelier Tuff.

Several soil samples collected from A and B horizons at TA-63 and TA-67 contain elevated concentrations of U, which may represent aerosol dispersion of U from Laboratory firing sites within TA-67 and TA-15 (Figures 28 and 29). These apparently biased data have been excluded from the background-elemental database for the Laboratory for purposes of calculating

FIGURE 28. BANDELIER TUFF AND BACKGROUND SOILS, LOS ALAMOS.

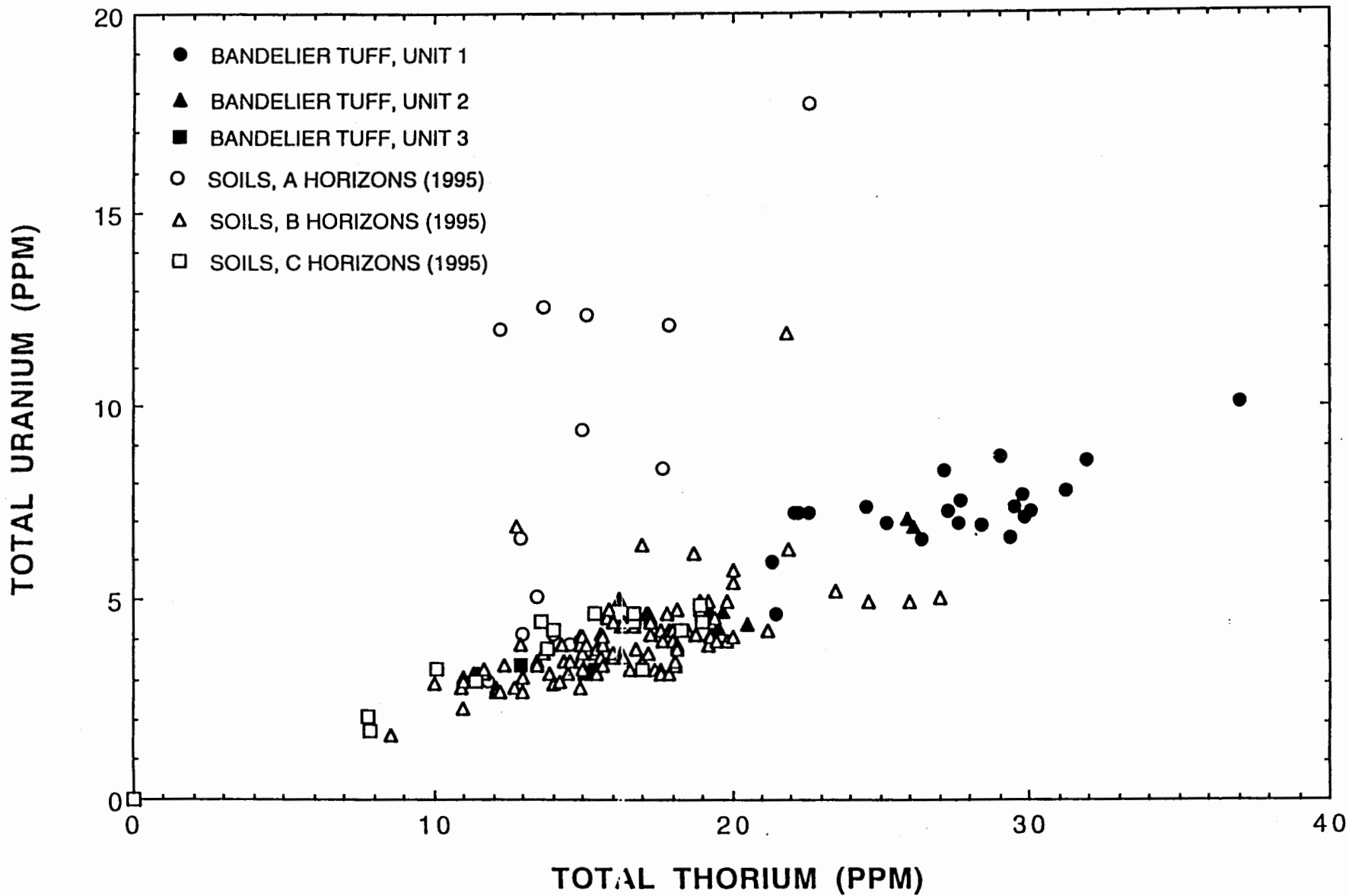
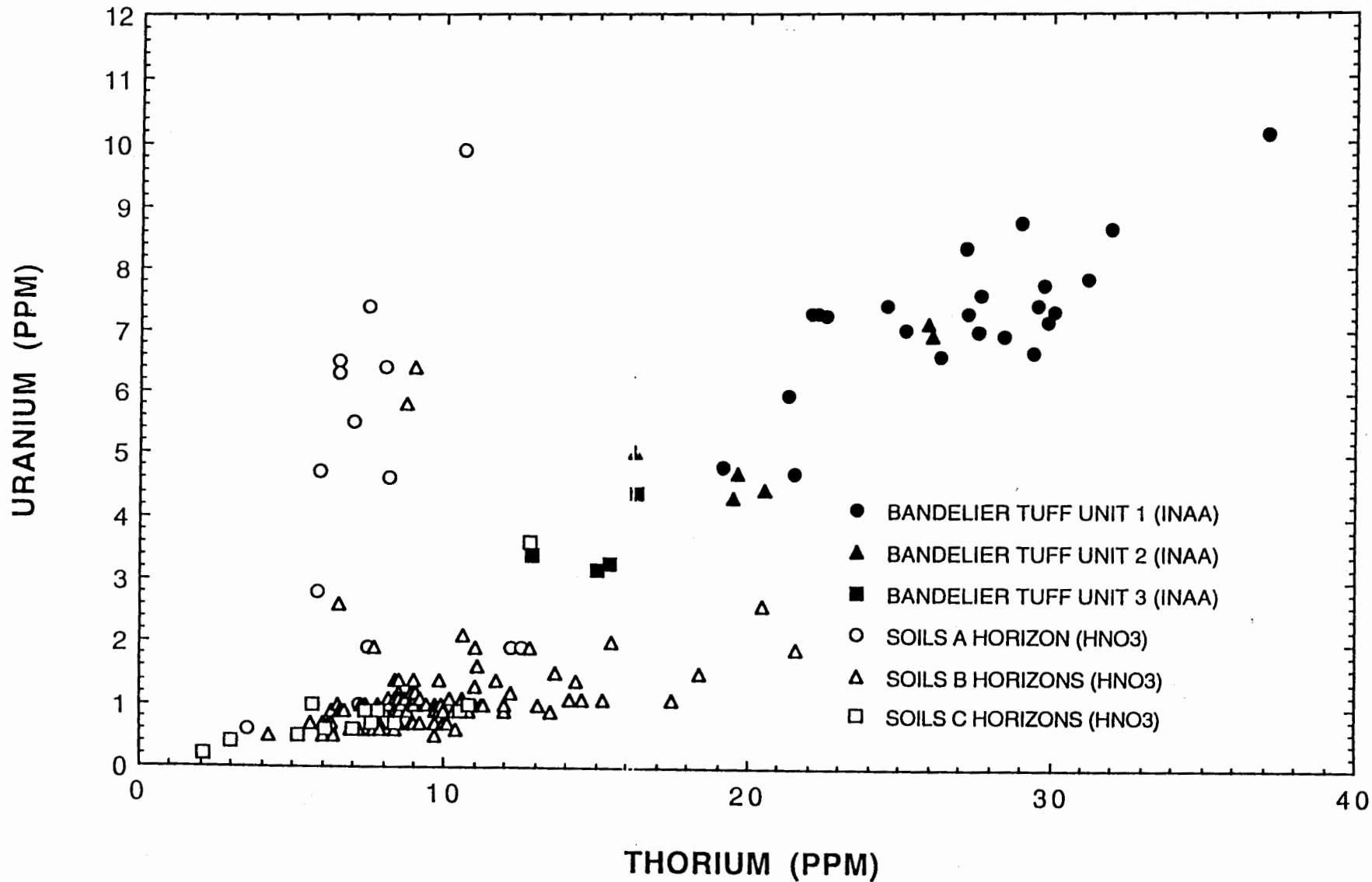


FIGURE 29. BANDELIER TUFF AND BACKGROUND SOILS, LOS ALAMOS.



DRAFT DOCUMENT

UTLs; however, they may be useful for determining U concentrations within TA-63, TA-67, and other sites down-wind from firing sites.

Most of the soil samples collected from the B horizons are characterized by significantly higher concentration ratios of total U (Figures 23 and 28) to HNO₃-digested or soluble U (Figures 23 and 29) relative to the A and C horizons. Differences in mass balance between total and soluble U suggest that up to 30% of the soluble U has been mobilized from the primary minerals and possibly redistributed in secondary phases (clay minerals, carbonate minerals, and Fe oxides and hydroxides) within some of the B horizons. Redistribution of soluble U is based on the assumption that Th is not as mobile as U under oxidizing and near neutral pH conditions based on results of geochemical data presented by Langmuir and Herman (1980) and Figure 23 in which Th concentration ratios (HF/HNO₃) within the soil horizons are fairly consistent relative to U. This redistribution also assumes that Th and U are not significantly concentrated in dust.

Figure 30 shows the distribution of total U versus HNO₃-digested U for the A and C horizons. The total U ratio : HNO₃-digested U (projected through the origin on Figure 30) generally is 5:1 (total U ≤ 5 ppm; HNO₃-digested U ≤ 1 ppm) or less for soil samples collected from the C horizons, which may represent natural background U distributions in soils. This ratio decreases to approximately 2:1 (projected through the origin shown on Figure 30) for samples collected from most the A horizons at TA-63 and TA-67, which suggests that soluble U is present, possibly as anthropogenic U. Anthropogenic U may occur in several redox states over time, including 0, IV, and VI. Prior to U leaching in the soils, U(IV) probably is the dominant valence state within primary phases present in the soils. Uranium (VI) minerals generally are characterized by higher solubilities relative to U(IV) minerals. Increased dissolution of U solids occur as the oxidation state of U increases, which decreases the total U:HNO₃-digested U ratio. Oxidation of U metal to U(VI) minerals is observed at firing sites across the DOE complex. Ebinger et al. (1990) report that schoepite (UO₃·2H₂O) has been identified on depleted U at the Yuma Proving Ground, Arizona. Studies conducted on the oxidation state and mineralogy of depleted U, using x-ray diffraction on Laboratory soil samples collected from TA-33, also show that schoepite is the dominant U(VI) mineral forming from the oxidation of U metal (personal communication with Pam Gordan, CST-7 on July 25, 1995). Schoepite may be an alteration (oxidation) product of U metal at TA-67 based on these previous studies.

Distributions of U and sulfate within the A and C horizons are shown in Figure 31. Concentrations of sulfate, in which this anion may be derived from dust and subsequently translocated through the soil horizons, range from 11 to 90 ppm within the C horizons. Within the A horizons, sulfate concentrations show a smaller range (6 to 25 ppm) than in the C horizons. Higher

FIGURE 30. A AND C HORIZONS, BACKGROUND SOILS, LOS ALAMOS.

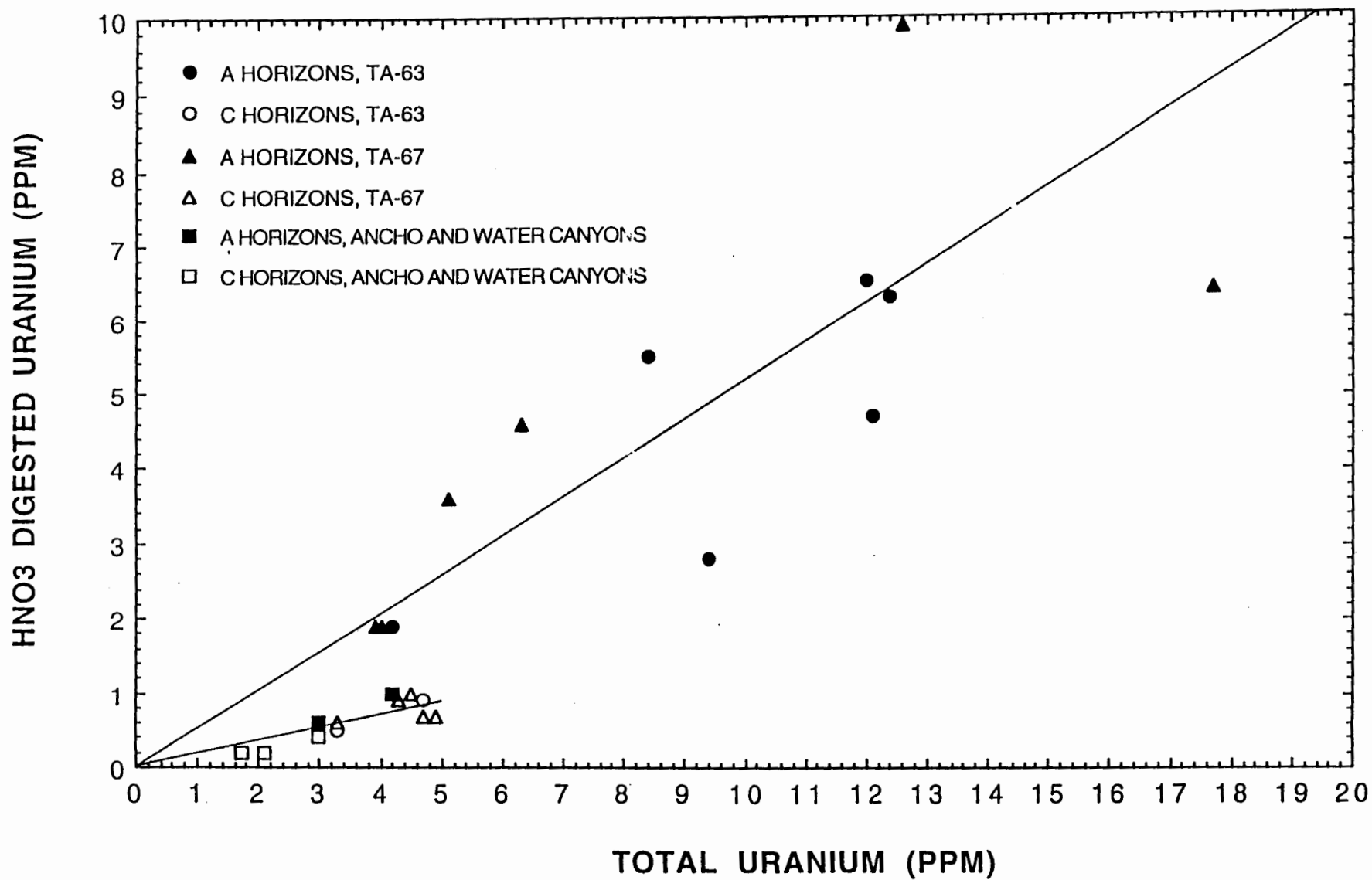
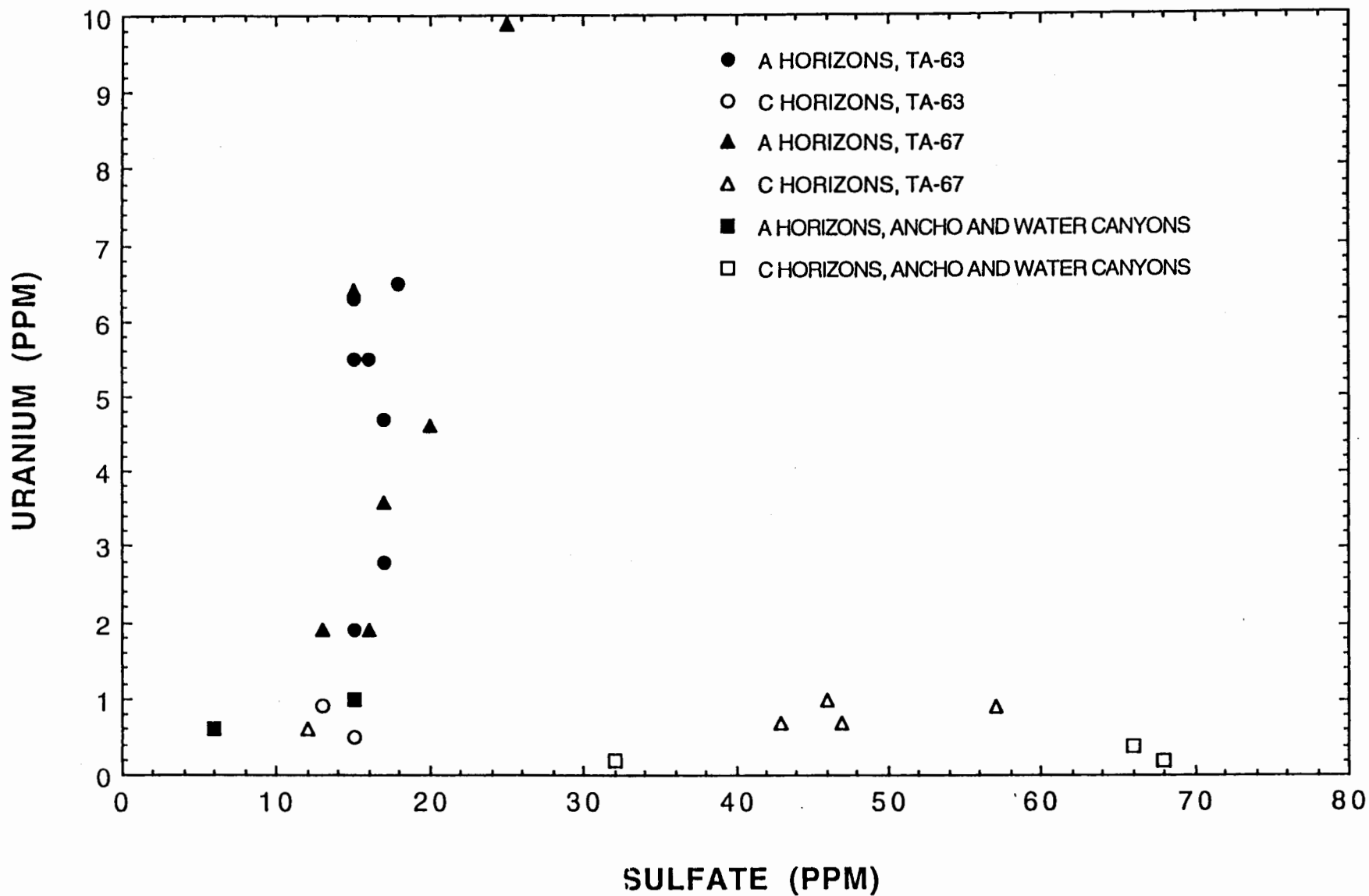


FIGURE 31. A AND C HORIZONS, BACKGROUND SOILS, LOS ALAMOS.



DRAFT DOCUMENT

concentrations of U (0.6 to 9.9 ppm) occur in the A horizons than U than in the C horizons (0.1 to 3.6 ppm). Distributions of U and sulfate shown in Figure 31 suggest that these two species do not correlate well with each other and that soluble U is not significantly bound to sulfate minerals such as gypsum ($\text{CaSO}_4 \cdot 2\text{H}_2\text{O}$).

Figure 32 shows the distributions of Fe and U within the A and C horizons. Within the A horizons, these two elements are widely distributed, whereas in the C horizons they are independent of one another. Concentrations of Fe within the C horizons show a smaller range (0.45 to 1.1 wt%) than in the A horizons (0.54 to 1.34 wt%). Solid phases of Fe, possibly consisting of ferrihydrite, amorphous $\text{Fe}(\text{OH})_3$, and $\alpha\text{-FeOOH}$, may provide active adsorption sites for soluble U(VI) which may account for the correlation observed between these two elements. Adsorption of U(VI) species onto surfaces of Fe oxides is significant at near neutral pH conditions (Hsi and Langmuir, 1985). Within the A horizons, U may be adsorbed onto solid organic matter, which is more abundant within the A horizons.

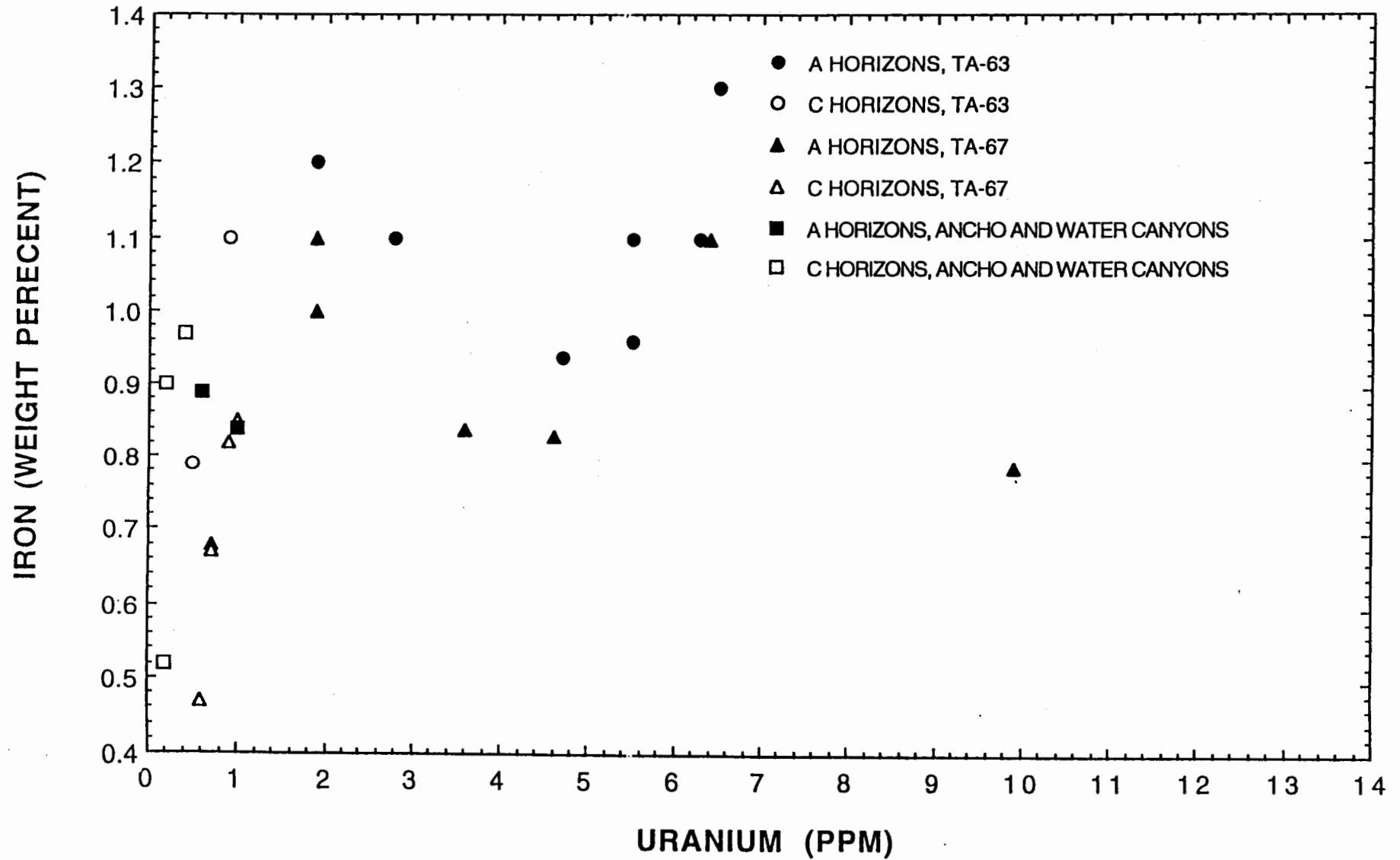
RESULTS AND STATISTICAL ANALYSIS OF BACKGROUND-SOIL DATA

The goal of the statistical analysis of the background soil data is to develop a technically-defensible set of data for ER Project decision-making. The key to technical defensibility is ensuring that the soils represent the natural variation found within the Laboratory's A, B and C soil horizons¹ found in a variety of geomorphic settings. Thus, the background soil samples should not have been impacted by Laboratory operations. The soil samples presented in this report have been collected at sampling locations both within the interior of the Laboratory and along the margins. These new samples are first compared in this study to the original background data presented by Longmire et al. (1995). All data that are statistically and geochemically comparable to the original background soil data are then included in a combined LANL-wide soil background data set.

The primary use of the background data is as a part of the RCRA Facility Investigation screening process ("Screening Assessment Methodology at Los Alamos National Laboratory", LANL ER Project, January 1995, draft). As a part of the RFI process, data for most sites are compared to natural background concentration of inorganics. The background screening value for inorganic analytes is the 95th percentile upper tolerance limit (UTL), which is the 95% upper confidence limit of the 95th percentile of the data distribution. The type of data distribution for each inorganic analyte must be estimated to calculate these UTLs. Thus, the second part of the statistical analysis of the soil data presented

¹ We do not consider background samples collected from calcium carbonate zones or fine fractions due to the small number of samples for these data groups.

FIGURE 32. A AND C HORIZONS, BACKGROUND SOILS, LOS ALAMOS.



DRAFT DOCUMENT

in this report is an estimate of the type of data distribution for each inorganic analyte. The last part of the statistical analysis will be to calculate background screening values for each analyte (either UTLs or maximum reported values for infrequently detected analytes). Elements that fail background screening are compared to risk-based screening action levels (SALs) or ecotoxicological screening action levels (ESALs). For most inorganics, the SAL comparison step represents the definitive screening assessment step, which then is the basis for proposing no further action for LANL potential release sites.

The ER Project background assessment team has identified several key elements based on either the potential risk posed by background concentrations or the geochemical properties of the elements. Background concentrations of Al, As, Be, Mn, and U may pose a significant background risk. Aluminum, Fe, and Th are of interest due to their geochemical properties. For these key elements, this report will consider differences in background concentrations correlated to subdivisions of the B soil horizon, and variation between background sampling locations. This information will assist in the technical assessment of the need for site-specific background data for these key elements, and provide the geochemical and statistical basis for the design of site-specific background assessments.

This section considers the data reported by the standard EPA digestion and analysis of inorganics (extraction method 3050 and analysis methods 6010, 7060, and 300.0 [ion chromatography]). Total elemental concentration data are not analyzed, with the exception of K, Th, and U because these data will be used to estimate the abundance of naturally-occurring isotopes of these inorganics. The 3050 digestion is the standard digestion procedure used in target analyte list (TAL) inorganic analyses in support of RFI characterization.

Initial Data Analysis Steps

Some of the inorganic results in the combined background soil data set are reported as less than the detection level (<DL). Table 8 summarizes all values (including laboratory replicates) that were reported for all inorganic analytes in the combined data set. The full data set is presented in Appendix A. To facilitate statistical analysis of the data, all values reported as <DL were replaced by one-half of the detection limit. This replacement approach is recommended in the EPA risk assessment guidance (EPA 1992, 1166). Low detection frequencies analytes (Sb, Cd, Hg, Se, Ta, and Tl) are excluded from the analyses presented in the next two sections of this report.

DRAFT DOCUMENT

Table 8. Summary of combined data sets by soil horizons (values in ppm).

Analyte	A Horizon						Average
	Non-detects			Detects			
	Count	Min	Max	Count	Min	Max	
Aluminum	0			25	2100	23000	8332.00
Antimony	22	0.6	5	3	0.2	0.5	0.37
Arsenic	0			23	0.3	5.4	3.12
Barium	0			25	27	190	125.28
Beryllium	0			25	0.07	1.2	0.66
Cadmium	8	0.4	2	1	1.4	1.4	1.40
Calcium	0			25	610	4500	1812.40
Chloride	0			24	8	24	13.33
Chromium	0			25	1.9	16	8.02
Cobalt	0			25	1.9	29	10.10
Copper	1	0.5	0.5	24	1.7	12	5.88
Iron	0			25	3300	16000	10296.00
Lead	1	4	4	24	5	37	16.13
Magnesium	0			25	440	2800	1582.00
Manganese	0			25	140	1100	440.00
Mercury	9	0.1	0.1	0			
Nickel	4	2	2	21	2.3	12	6.64
Potassium	0			25	410	2900	1533.60
Potassium-TOTAL	0			14	20000	26000	22285.71
Selenium	8	0.2	0.3	1	0.7	0.7	0.70
Sodium	0			25	64	660	174.24
Sulfate	1	12	12	23	13	44	22.09
Tantalum	25	0.2	0.9	0			
Thallium	8	0.2	1	17	0.2	0.4	0.25
Thorium	0			25	2	12.8	7.21
Thorium-TOTAL	0			17	8.5	22.6	14.46
Uranium	0			26	0.2	9.9	2.92
Uranium-TOTAL	0			15	3	17.7	8.11
Vanadium	0			25	4.6	35	20.33
Zinc	0			25	14	58	28.64

DRAFT DOCUMENT

Table 8 (continued). Summary of combined data sets of soil horizons.

Analyte	B Horizon						
	Non-detects			Detects			Average
	Count	Min	Max	Count	Min	Max	
Aluminum	0			132	1400	62000	12852.27
Antimony	118	0.1	5	16	0.2	1	0.41
Arsenic	5	0.3	0.3	116	0	11.2	4.33
Barium	0			132	46	730	160.04
Beryllium	0			132	0.25	4	1.01
Cadmium	18	0.4	2	3	0.6	2.7	1.93
Calcium	0			132	1100	14000	2989.39
Chloride	0			126	8	246	27.81
Chromium	0			132	2.8	46	10.20
Cobalt	0			132	1.6	22	6.65
Copper	0			132	2.7	16	6.62
Iron	0			132	6800	36000	13237.12
Lead	1	4	4	131	5	30	13.19
Magnesium	0			132	800	10000	2385.61
Manganese	0			131	76	1000	348.15
Mercury	19	0.1	0.1	1	0.1	0.1	0.10
Nickel	3	2	2	129	2.3	30	8.00
Potassium	0			132	680	6900	1855.23
Potassium-TOTAL	0			106	11000	36000	24188.68
Selenium	3	0.2	0.3	19	0.3	1.3	0.74
Sodium	0			132	58	1800	296.32
Sulfate	0			126	9	722	58.79
Tantalum	134	0.2	0.9	0			
Thallium	44	0.2	1	90	0.2	1	0.35
Thorium	0			134	4.2	21.6	9.35
Thorium-TOTAL	0			111	10	27.6	16.53
Uranium	0			134	0.5	6.4	1.10
Uranium-TOTAL	0			112	1	11.9	4.01
Vanadium	0			132	7.4	57	23.05
Zinc	0			131	14	76	33.21

DRAFT DOCUMENT

Table 8 (continued). Summary of combined data sets of soil horizons.

Analyte	C Horizon						
	Non-detects			Detects			
	Count	Min	Max	Count	Min	Max	Average
Aluminum	0			24	900	33000	10083.33
Antimony	23	0.2	5	0			
Arsenic	1	0.2	0.2	23	0.3	7	2.63
Barium	0			24	21	410	90.33
Beryllium	2	0.08	0.08	22	0.09	1.9	0.78
Cadmium	10	0.4	0.4	0			
Calcium	0			24	500	87000	5401.67
Chloride	0			24	9	303	44.18
Chromium	0			24	1.9	15	6.10
Cobalt	0			24	1	34	8.32
Copper	1	0.5	0.5	23	0.6	7.3	3.90
Iron	0			24	3300	17000	9020.83
Lead	7	4	4	17	4	24	11.04
Magnesium	0			24	420	7400	1772.50
Manganese	0			24	76	440	193.63
Mercury	9	0.1	0.1	15	0.1	0.1	0.10
Nickel	8	2	2	16	2.4	15	6.68
Potassium	0			24	410	4200	1536.25
Potassium-TOTAL	0			13	26000	35000	29538.46
Selenium	7	0.2	0.3	3	0.3	1.7	0.87
Sodium	0			24	90	1700	523.63
Sulfate	0			24	12	1200	122.83
Tantalum	24	0.12	0.9	0			
Thallium	19	0.125	1	4	0.2	0.6	0.40
Thorium	0			24	2.1	10.8	6.19
Thorium-TOTAL	0			15	7.8	19	14.37
Uranium	0			24	0.2	1.5	0.69
Uranium-TOTAL	0			15	1.7	4.9	3.77
Vanadium	0			24	4	32	13.18
Zinc	0			24	14	57	29.00

DRAFT DOCUMENT

Table 8 (continued). Summary of combined data sets of soil horizons.

Analyte	All Data						
	Non-detects			Detects			Average
	Count	Min	Max	Count	Min	Max	
Aluminum	0			181	900	62000	11860.77
Antimony	163	0.1	5	19	0.2	1	0.40
Arsenic	6	0.2	0.3	162	0	11.2	3.91
Barium	0			181	21	730	145.99
Beryllium	2	0.08	0.08	179	0.07	4	0.93
Cadmium	36	0.4	2	4	0.6	2.7	1.80
Calcium	0			181	500	87000	3146.69
Chloride	0			174	8	303	28.07
Chromium	0			181	1.9	46	9.35
Cobalt	0			181	1	34	7.35
Copper	2	0.5	0.5	179	0.6	16	6.17
Iron	0			181	3300	36000	12271.82
Lead	9	4	4	172	4	37	13.39
Magnesium	0			181	420	10000	2193.31
Manganese	0			180	76	1100	340.30
Mercury	37	0.1	0.1	2	0.1	0.1	0.10
Nickel	15	2	2	166	2.3	30	7.70
Potassium	0			181	410	6900	1768.51
Potassium-TOTAL	0			133	11000	36000	24511.28
Selenium	18	0.2	0.3	23	0.3	1.7	0.76
Sodium	0			181	58	1800	309.60
Sulfate	1	12	12	173	9	1200	62.79
Tantalum	183	0.12	0.9	0			
Thallium	71	0.125	1	111	0.2	1	0.34
Thorium	0			183	2	21.6	8.64
Thorium-TOTAL	0			143	7.8	27.6	16.06
Uranium	0			184	0.2	9.9	1.30
Uranium-TOTAL	0			142	1	17.7	4.42
Vanadium	0			181	4	57	21.37
Zinc	0			180	14	76	32.02

DRAFT DOCUMENT

The background data set includes samples that have been designated as "collocated" samples, and there are also laboratory replicates included in the combined background soil data set. Collocated samples are a type a field duplicate sample. In this case, the collocated samples were collected from the same trenches next to original sampling for a given soil horizon. Thus, collocated samples may be used to estimate to local sampling variability for inorganic analytes. The duplicate analyses provide an estimate of the analytical measurement variability. The collocated samples have about 1.8 times the variability as the duplicate measurements (based ratio of average normalized variances for the two data groups for both HNO₃ digested and total analyses). Because the duplicate analyses are to some extent providing "redundant" information², all laboratory duplicate analyses were averaged to estimate a single value for each sampling location. The duplicate analysis average is used in the statistical analyses. Given the variability observed for collocated samples, these samples are treated as another value for that soil horizon and are retained as separate samples in the statistical analyses.

Graphical Display of Background Data

Two types of plots are presented for graphical display of the background data. "Box plots" (Figures 33-39, 41, 43, 45, 47, 49, 51, 53, and 55) are used to show data differences as a function of grouping variables. "Scatter plots" (Figures 40, 42, 44, 46, 48, 50, 52, and 54) are used to show correlations between pairs of variables (concentrations of inorganic analytes). Either sampling location or the soil horizon is used as a grouping variable in the box plots. The box plots show the actual values (as filled circles) for each soil horizon. The ends of the box represent the "inter-quartile" range of the data distribution. The inter-quartile range is specified by the 25th percentile and 75th percentile of the data distribution. The line within the box plot is the median (50th percentile) of the data distribution and the 10th and 90th percentiles are outside the box plots. Thus the box indicates concentration values for the central half of the data, and concentration shifts can be readily assessed by comparing the boxes. If the majority of the data is represented by a single concentration value (usually the detection limit), the box is reduced to a single line. The dotted line across all of the boxes is the overall average of all data groups represented by the box plots.

²For example, potassium duplicates have a coefficient of variation (CV) of 8%, the collected samples have a CV of 25%, and the CV of all B soil horizon analyses is 49%.

DRAFT DOCUMENT

Analysis of Key Inorganics by Soil Subhorizons and Background Sampling Locations

Because the background sampling locations do not have equal (in proportion) representation of the soil subhorizons, a simplistic one-way analysis of location and subhorizon may be misleading. For example, the upper LA Canyon samples (Longmire et al., 1995) do include any A or C horizons (Table 9), and these results should not be directly compared to AC sampling locations, which include one A horizon sample and three C horizon samples. A linear statistical model can be built to determine if there is a significant interaction term between location and soil horizon, but this is beyond the current scope of this report. One simple solution to the location-horizon interaction is to compare the locations that are most similar in the distribution of soil subhorizons. Technical Area-16, TA-63, and TA-67 are the three most similar background sampling locations in the number of samples collected from each horizon. The results for these background sampling locations is presented graphically below.

Similarly, the analysis of soil horizons is also confounded by a possible location-horizon interaction term. As a crude measure of the difference between horizons, a Wilcoxon rank sum test was used to determine if there were statistically significant distribution shifts between the soil subhorizons. The set of six soil subhorizons (A, BA, BC, Bt, Bw, and C) were significantly different for six of the seven key inorganics (Table 10). Aluminum exhibited a marginally significant distribution shift ($p=0.052$, or slightly greater than a significant probability of 0.05). In general, the major elements did not exhibit significant distribution shifts for comparisons among B subhorizons, but the minor elements were significantly different between soil subhorizons (Table 10). The statistical differences of the key inorganics by horizon and location is discussed in more detail below.

Thus, there is a rationale to evaluate soil subhorizons in planning for site-specific background of certain key minor elements. However, it is also important that the key major elements do not exhibit significant differences between soil subhorizons. This observation supports our use of the major element to trace element correlations to assist in evaluating the inclusion of samples into a LANL-wide background data base. These correlations are discussed in the following section of this report.

DRAFT DOCUMENT

Table 9. Distribution of the number of samples by soil subhorizon and background sampling location.

Subhorizon	Location						Subhorizon total
	AC	LA	TA-16	TA-63	TA-67	TA-69	
A	1	0	2	7	6	2	18
BA	0	0	0	0	5	0	5
BC	0	1	1	0	5	1	8
Bb	0	0	0	0	1	0	1
BR	0	0	0	0	0	1	1
Bt	1	6	25	16	23	7	78
Bw	4	0	1	12	3	1	21
C	3	0	4	2	5	3	17
Location total	9	7	33	37	48	15	149

Table 10. Summary of the results of the Wilcoxon rank sum test comparison of soil subhorizons.

Analyte	Data groups compared		
	A, BA, BC, Bt, Bw, C	BA, BC, Bt, Bw	Bt, Bw
Aluminum	0.052	0.126	0.765
Arsenic	0.002 *	0.160	0.025 *
Beryllium	<0.001 *	0.005 *	0.001 *
Iron	<0.001 *	0.890	0.860
Manganese	<0.001 *	<0.001 *	<0.001 *
Thorium-total	0.009 *	0.073	0.164
Uranium-total	0.001 *	0.019 *	0.005 *

* These probabilities indicate a statistically significant difference between soil subhorizons. Probabilities less than 0.05 indicate that there is a statistically significant difference between the horizons, and a probability greater than 0.05 indicates that there is no statistically significant difference between the soil horizons. Bb and BR were excluded from the analysis because they were represented by one sample each.

Aluminum by subhorizon and location

Aluminum concentrations are not significantly different between six soil subhorizons (Table 10, Figure 33). There is no significant difference between the B subhorizons. There is little difference in the Al concentration range between TA-16 and TA-67, and the median concentration for TA-63 and TA-67 are similar (Figure 33). Thus, there is little evidence for significant differences between mesa top background sampling locations for Al.

DRAFT DOCUMENT

Arsenic by subhorizon and location

The median percentiles (25th to 75th percentile) of the As concentrations are similar for all soil subhorizons except the C horizon (Figure 34). The concentration range for the Bt subhorizon is greater than the other subhorizons, but this could be due to the larger number of samples representing the Bt horizon. There is little difference in the location of the median percentiles of the TA-16, TA-63, and TA-67 background sampling locations (Figure 34). Thus, there is little evidence for significant differences in As concentrations between mesa top background sampling locations.

Beryllium by subhorizon and location

There are statistically significant distribution shifts for Be between groups of soil subhorizons (Table 10, Figure 35). However, the differences in the median percentiles for soil subhorizons are modest, and exhibit slight distribution shifts. There is little difference in the Be median percentiles between TA-16 and TA-63, and the median percentiles of TA-67 are modestly elevated compared to TA-16 and TA-63 (Figure 35). Thus, some Be variation can be attributed to differences between sampling locations.

Iron by subhorizon and location

The median percentiles of the A and C soil horizons for Fe are lower than the median percentiles for the B subhorizons (Figure 36). There is no statistical difference between the B subhorizons (Figure 36, Table 10). There is little difference in the location of the median percentiles of the TA-16, TA-63, and TA-67 background sampling locations (Figure 36). Thus, there is little evidence for significant differences in Fe concentrations between mesa top background sampling locations.

Manganese by subhorizon and location

Although there is considerable overlap in the Mn concentrations represented by the median percentiles of the soil subhorizons (Figure 37), there are statistically significant differences between the major horizon groups (Table 10). There is little difference in the Mn median percentiles between TA-16 and TA-67, and the median percentiles of TA-63 are elevated compared to TA-16 and TA-67 (Figure 37). Thus, there is some variation in Mn concentrations that can be attributed to differences in Mn concentrations between sample locations.

DRAFT DOCUMENT

Total thorium by subhorizon and location

The Th median percentiles of the B subhorizons and the C horizon are similar (Figure 38), and there is no statistical difference between the B subhorizons (Table 10). The median percentiles of the background sampling locations are similar, and median values of the mesa top sampling locations (TA-16, TA-63, and TA-67) vary within a narrow range between 15.6 mg/kg and 17 mg/kg (Figure 38). Thus, there is little evidence for significant differences in Th concentrations between mesa top background sampling locations.

Total uranium by subhorizon and location

Uranium median percentile values show that the A and BA horizons are elevated relative to other horizons (Figure 39), and there are statistically significant differences between soil horizons (Table 10). The median percentiles of the BC, Bt, Bw and C horizons are similar (Figure 39). The median percentiles of the mesa top sampling locations are similar, although the 90th percentile of TA-63 and TA-67 are significantly elevated relative to other sampling locations (Figure 39). It may be that the A and BA horizons sampling locations in TA-63 and TA-67 have been impacted by airborne releases from weapons testing in that portion of the laboratory. These data are evaluated in more detail in the following section of the report, to determine if this new background data collected from TA-63 and TA-67 can be added to the existing background data reported in Longmire et al. (1995).

Summary of results by subhorizon and location

The differences between soil horizons tend to be statistically significant, where the B horizon data is typically elevated relative to the A or C soil horizons. If site-specific background data are needed, it may be necessary to consider pedological and chemical differences between B subhorizons for some analytes (Be, Mn, and U). Differences between background sampling locations tend to be less significant when comparing mesa top locations, but there are significant differences between canyon and mesa top sampling locations. In summary, we recommend that the results presented in this section of the report should be considered when assessing the need to collect site-specific background to support risk assessment or a corrective measures study (CMS), but that the LANL-wide data base is expected to be adequate for most screening level decisions.

DRAFT DOCUMENT

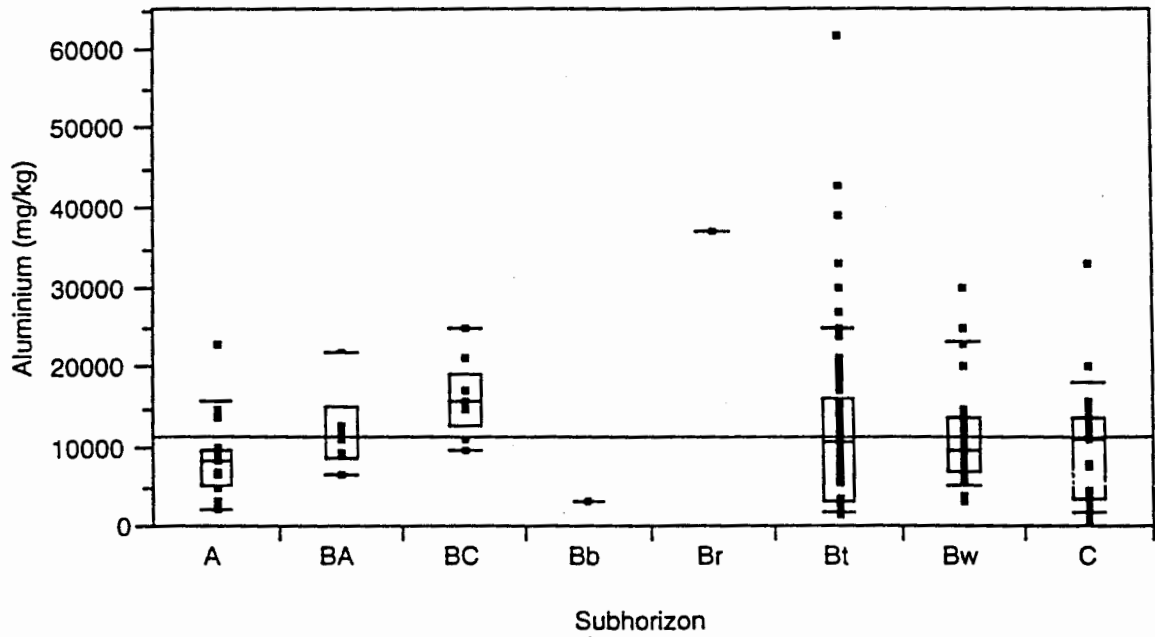
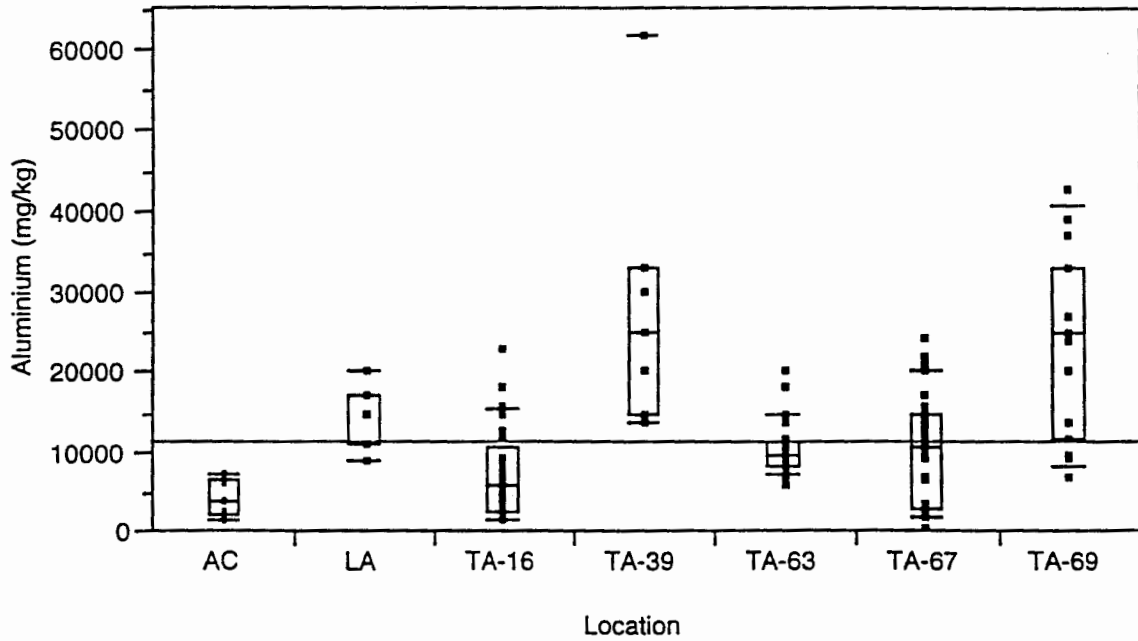


Figure 33. Summary of Al results by soil subhorizon and location.

DRAFT DOCUMENT

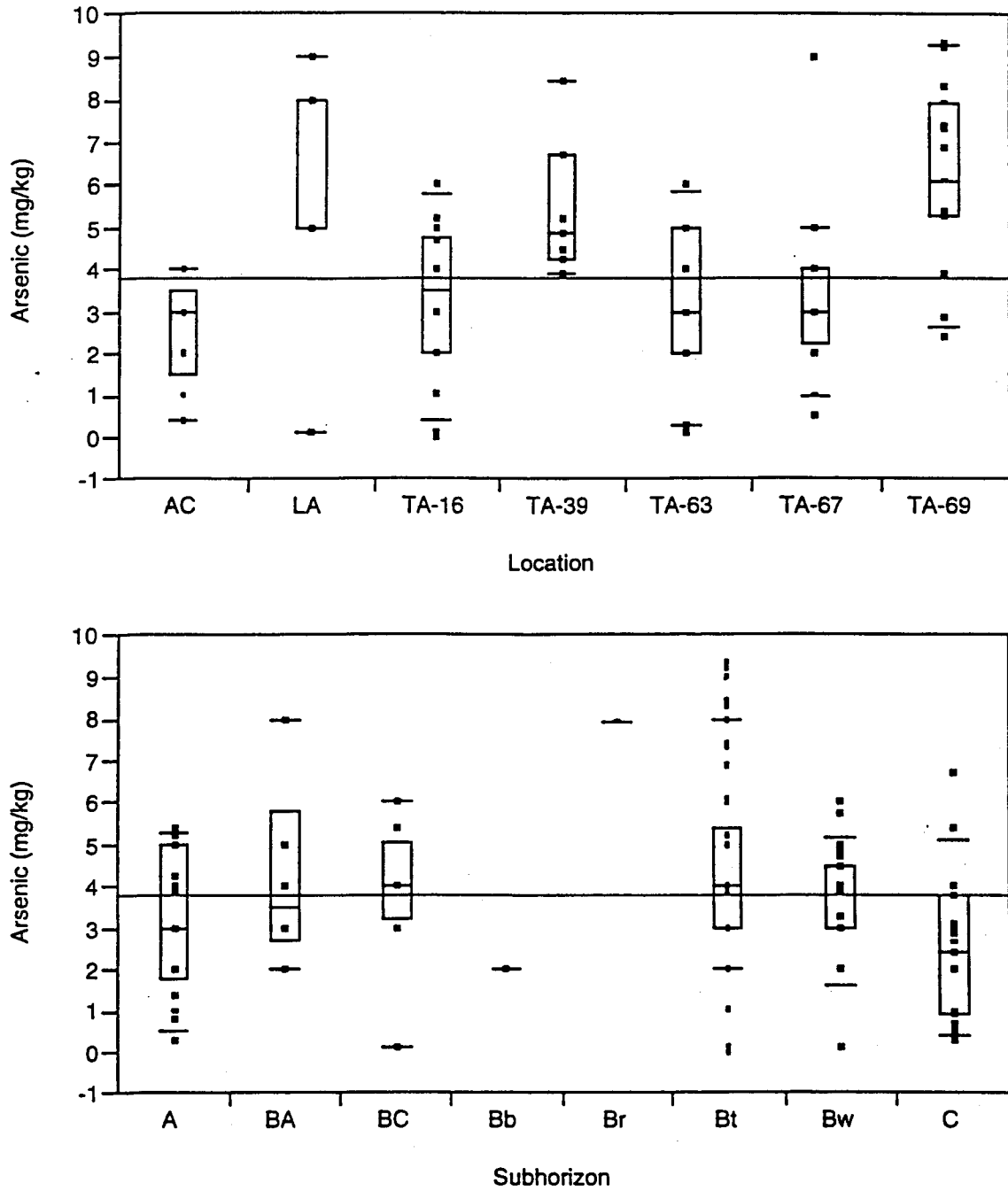


Figure 34. Summary of As results by soil subhorizon and location.

DRAFT DOCUMENT

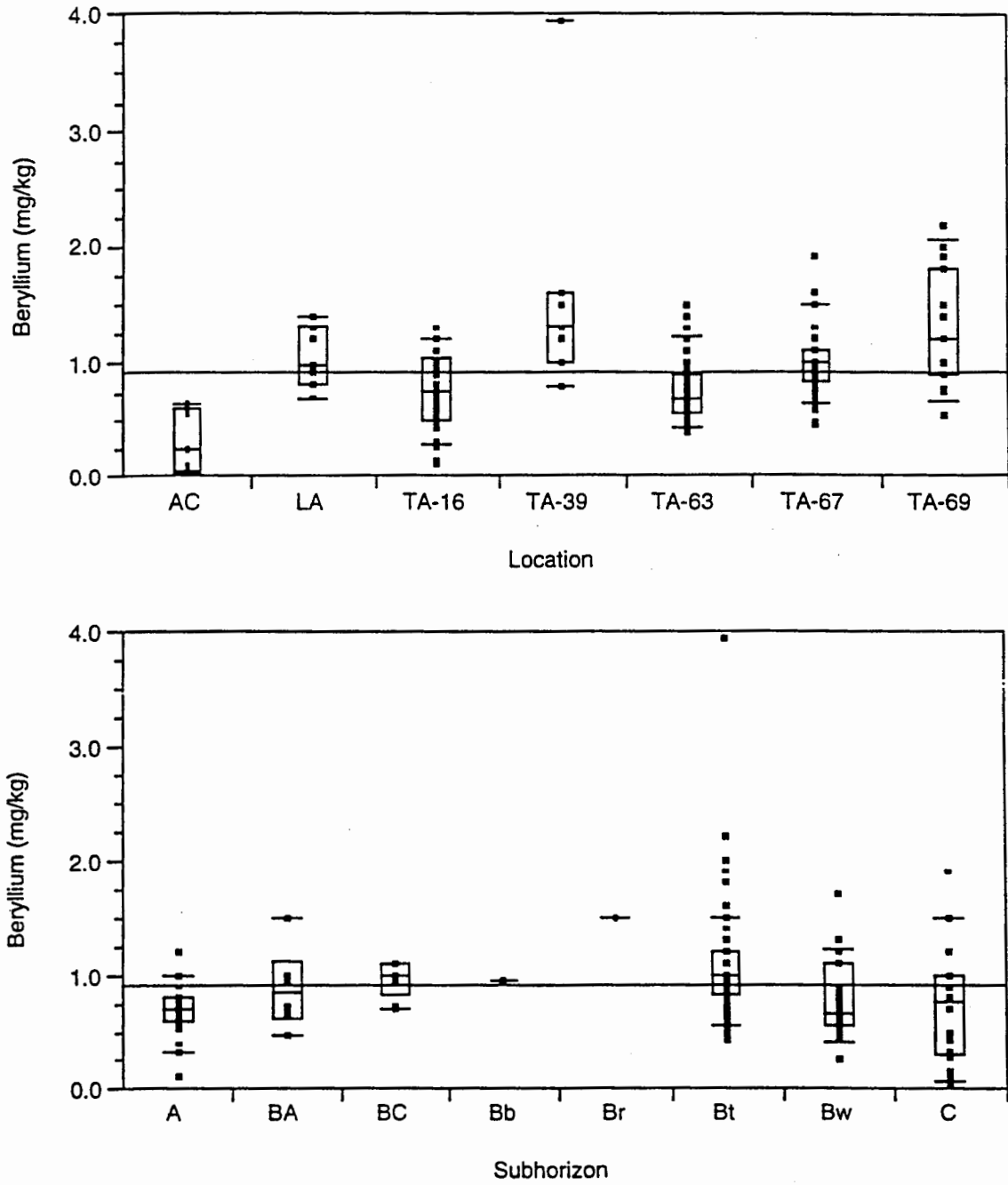


Figure 35. Summary of Be results by soil subhorizon and location.

DRAFT DOCUMENT

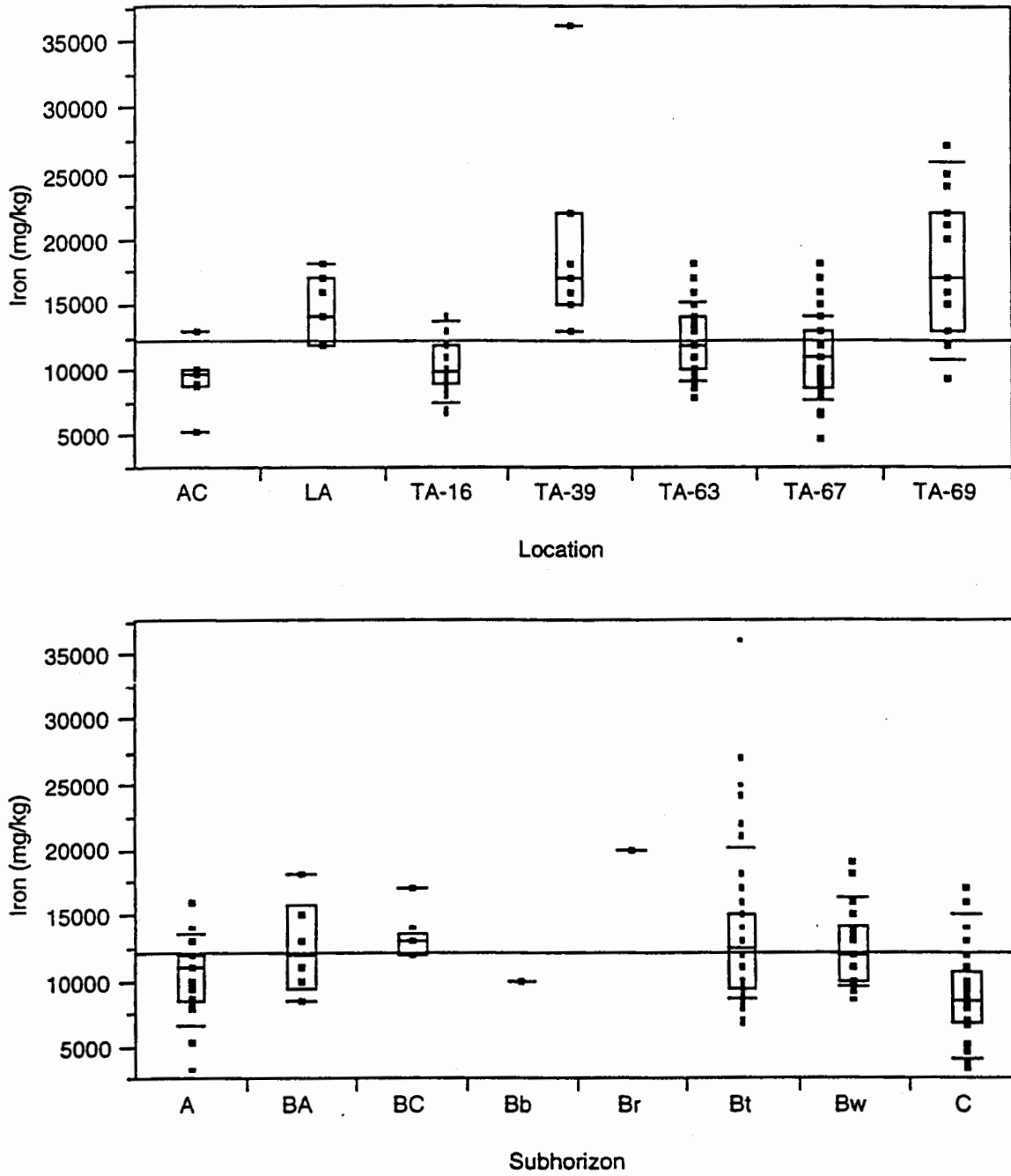


Figure 36. Summary of Fe results by soil subhorizon and location.

DRAFT DOCUMENT

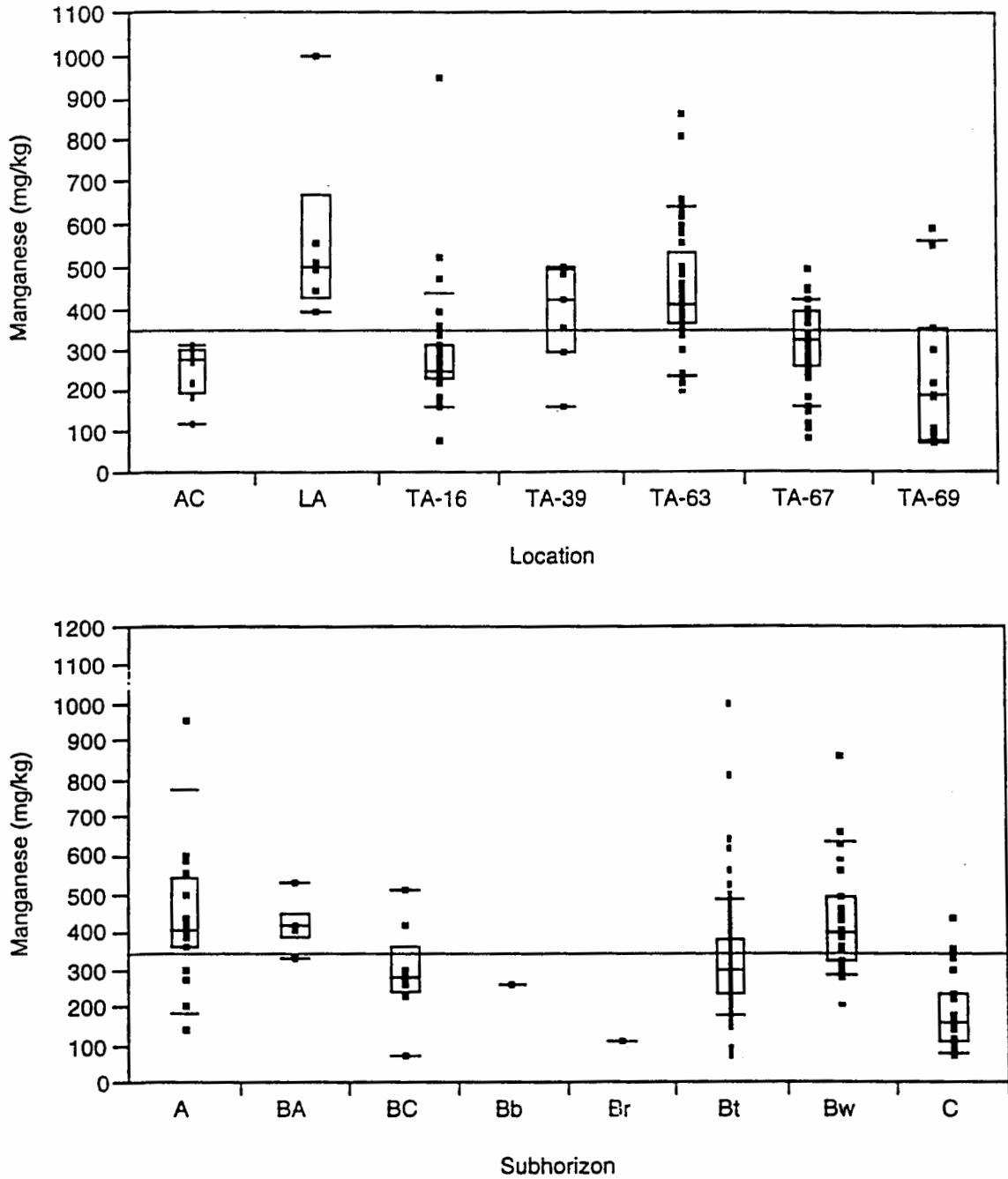


Figure 37. Summary of Mn results by soil subhorizon and location.

DRAFT DOCUMENT

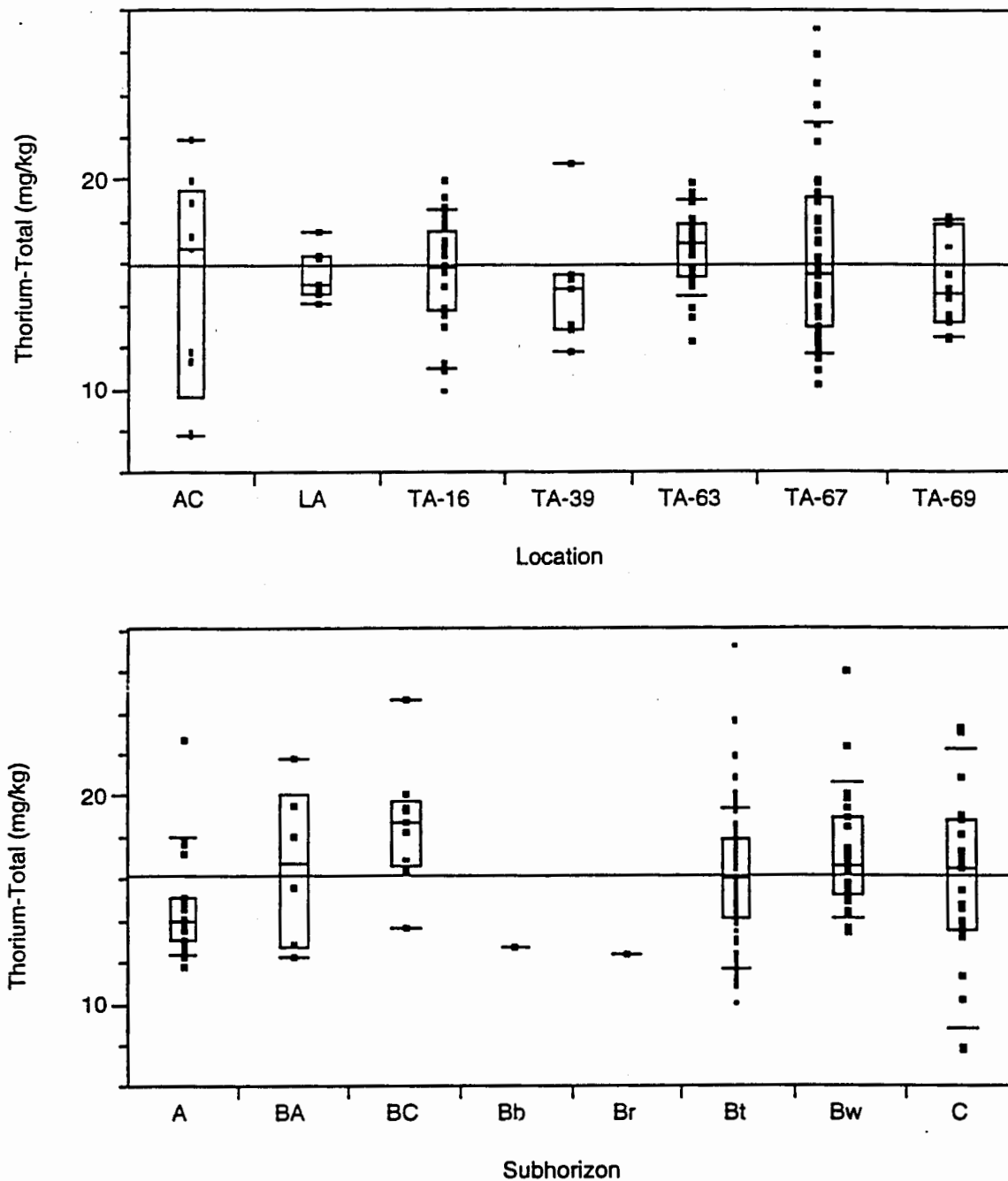


Figure 38. Summary of total Th results by soil subhorizon and location.

DRAFT DOCUMENT

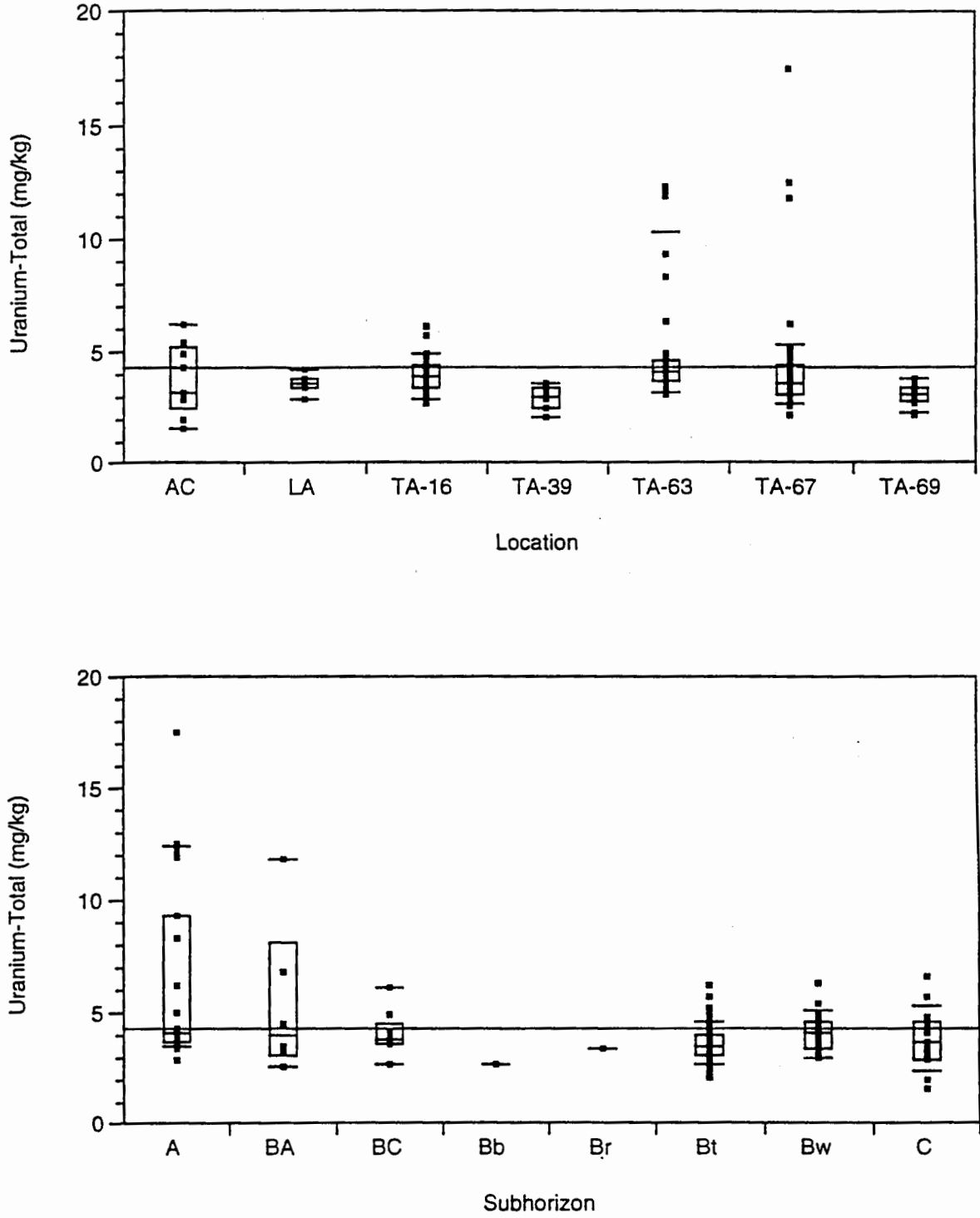


Figure 39. Summary of total U results by soil subhorizon and location.

DRAFT DOCUMENT

Comparison of New Background Data to Existing LANL-wide Background Data

The new background soil data set differs in two primary respects from the original LANL-wide background data. First, the new data were mostly sampled at locations within the interior of the Laboratory. Second, the frequency of samples from the A, B and C horizons differed between the two data sets. Many more soils horizons were sampled in this investigation. These factors make a simple distribution or mean comparison of the data sets non-informative. In lieu of sophisticated multivariate or generalized linear model approaches, we decided to use an approach that combined statistics, geochemistry, and risk-based screening values to eliminate "outliers" from the combined data distributions that we inferred to contain contamination from Laboratory activities (i.e., widely dispersed fallout from explosive testing).

The key to this approach is the presence of a significant correlation between the major elements (Al, Fe, and K) and most of the other trace elements in LANL soils. These correlations are summarized in Table 11. The U data were screened for outliers in a different way, and this approach is discussed below. The geochemical basis for this correlation is discussed by Longmire et al. (1995). The first step in our outlier screening process is to calculate the statistical residual from a regression analysis of the trace elements and the minor elements. The regression analysis is performed on the combined data set, where the < detection limit (DL) and laboratory duplicate values are treated as discussed above. Residuals that differ significantly from the distribution of residuals are tentatively classified as outliers. These regression residual outliers are excluded from the combined data set if they meet one or more of the following conditions:

- 1) The value is also an outlier in its soil horizon group. Preference is given to eliminating outliers from the A horizon, because these outliers may logically be associated with a release associated with Laboratory activities and do not represent natural background concentrations.
- 2) The HNO₃ digestion result is inconsistent with the total analysis of the same sample. These outliers most likely represent laboratory artifacts, and should not be included in the background data base. Both usually low results and unusually high (i.e., where the HNO₃ results is greater than the total result) may be excluded for this reason.
- 3) The value would have an unacceptable impact on the estimation of the statistical distribution. For example, an outlier may be an order of magnitude greater than the next largest value, and using this value

DRAFT DOCUMENT

would inflate the estimated UTL. Some of these values may represent an undersampled part of the background distribution, but it beyond the scope of this report to estimate statistical properties of every possible background soil type. For example the calcium carbonate horizon has been excluded from these analyses, and only the more broadly distributed soil horizons (A, B, and C) are evaluated.

- 4) The residual represents a significant fraction of the SAL. Because the SAL comparison represents the step that follows the background comparison in the screening assessment process, this condition helps to place the outlier into a decision-making context. Outliers with residuals that represent a significant fraction of the SAL may be excluded from the LANL-wide background data base.

Our goal in this report is not to definitively determine whether each sample value represents background, but to use a weight-of-evidence approach, described above, to eliminate results that are inconsistent with the majority of the LANL-wide background data. We cannot be certain that some values excluded in this process represent legitimate natural background conditions, but this process is intended to increase the defensibility, and therefore usability, of the LANL-wide background data.

Detection of Uranium Outliers

Uranium outliers were identified in a process similar to other inorganics, with the exception that we used Th as a correlate of uranium. As discussed in trace geochemistry section of this report, the common correlation of Th and U in both the soil and the Bandelier Tuff indicates that most of the B and C soil horizons have been ultimately derived from the Bandelier Tuff. Given this assumption, the Th-U relationship for the Bandelier Tuff can be viewed as a limiting case for relationship between the Th-U for the soils. The correlation plot of Th-U (Figure 40) shows the statistical outliers. Figure 41 shows the data distributions for the A, B, C soil horizons and the Bandelier Tuff. These data distributions show some apparent outliers in the soil data, which are primarily in A horizons soils. All of the values identified on these plots were judged to be true outliers from the background U soil concentration distribution and have been eliminated from the combined LANL-wide background data set. All A horizon samples are from mesa tops in the central part of the Laboratory and indicate widespread, low-level contamination from explosives testing. These excluded U samples are summarized in Table 12.

DRAFT DOCUMENT

Table 11. Summary of correlation analysis between "trace" elements and major soil elements of the combined soil background data sets.

Element	Correlation with		
	Aluminum	Iron	Potassium
Aluminum	1	0.870	0.859
Antimony (4)	0.583	0.424	0.538
Arsenic (2)	0.634	0.775	0.568
Barium	0.543	0.535	0.559
Beryllium	0.772	0.777	0.843
Cadmium (1)	0.427	0.487	0.447
Calcium	0.345	0.241	0.400
Chlorine	0.197	0.063	0.195
Chromium	0.742	0.801	0.695
Cobalt	0.268	0.167	0.270
Copper	0.401	0.599	0.412
Iron	0.870	1	0.783
Lead	0.499	0.525	0.482
Magnesium	0.893	0.854	0.906
Manganese (4)	-0.055	0.158	-0.055
Mercury (1)	0.281	0.122	0.322
Nickel	0.703	0.777	0.716
Potassium	0.859	0.783	1
Potassium-TOTAL (3)	-0.393	-0.503	-0.326
Selenium (1)	0.714	0.631	0.548
Sodium	0.545	0.322	0.609
Sulfate	0.305	0.148	0.338
Tantalum	0.017	-0.047	-0.050
Thallium (4)	0.527	0.559	0.425
Thorium	0.263	0.288	0.318
Thorium-TOTAL (3)	0.373	0.219	0.268
Uranium	-0.037	0.006	0.045
Uranium-TOTAL (3)	-0.138	-0.170	-0.096
Vanadium	0.753	0.901	0.673
Zinc (4)	0.614	0.689	0.616

Sample size is 174 with the exception of (1) 39, (2) 157, (3) 171, (4) 173

DRAFT DOCUMENT

Table 12. Summary of uranium values excluded from the combined background data set.

Sample ID	Sample location	Soil Horizon	Residual	Excluded	Rationale
FS2100	TA-63	A	5.32	Yes	Greater than tuff regression, A horizon outlier
FS2114	TA-63	A	6.15	Yes	Greater than tuff regression, A horizon outlier
FS2118	TA-63	A	5.11	Yes	Greater than tuff regression, A horizon outlier
FS2119	TA-63	A	1.65	Yes	Greater than tuff regression, A horizon outlier
FS2150	TA-63	A	4.28	Yes	Greater than tuff regression, A horizon outlier
FS2154	TA-63	A	3.54	Yes	Greater than tuff regression, A horizon outlier
FS2159	TA-67	A	5.12	Yes	Greater than tuff regression, A horizon outlier
FS2186	TA-67	A	8.47	Yes	Greater than tuff regression, A horizon outlier
FS2219	TA-67	A	3.31	Yes	Greater than tuff regression, A horizon outlier
FS2096	TA-51	BA	4.48	Yes	Greater than tuff regression, BA horizon outlier
FS2149	TA-63	B	1.41	Yes	Greater than tuff regression
FS2160	TA-67	BA	5.06	Yes	Greater than tuff regression, BA horizon outlier

Detection of Arsenic Outliers

Seven low values were identified by the regression analysis of As (Figure 42). These values are primarily from the B soil horizon (Figure 43). These values are summarized in Table 13, and all were excluded from the combined background data set.

Table 13. Summary of arsenic values excluded from the combined background data set.

Sample ID	Sample location	Soil Horizon	Residual	Excluded	Rationale
FS2089	LA	B	-3.51	Yes	Inconsistent with total result (0.15 vs 16), A horizon outlier
FS2123	TA-16	B	-3.15	Yes	Inconsistent with total result (0.15 vs 17), A horizon outlier
FS2130	TA-16	B	-2.70	Yes	Inconsistent with total result (0 vs 16), A horizon outlier
FS2115	TA-63	B	-2.79	Yes	Inconsistent with total result (0.15 vs 15), A horizon outlier
FS2120	TA-63	B	-2.72	Yes	Inconsistent with total result (0.15 vs 12), A horizon outlier
FS2114	TA-63	A	-3.00	Yes	Large residual, A horizon outlier
FS2118	TA-63	A	-3.00	Yes	Inconsistent with total result (0.3 vs 13), A horizon outlier

Detection of Barium Outliers

One high outlier was identified in the Ba-K correlation plot (Figure 44). This value was a B soil horizon outlier (Figure 45), the HNO₃ digestion result was greater than the total result, and the residual of this outlier represented about 10% of the SAL (532 ppm divided by 5300 ppm). This outlier was excluded from the combined background data set (Table 14).

Table 14. Summary of barium values excluded from the combined background data set.

Sample ID	Sample location	Soil Horizon	Residual	Excluded	Rationale
FS2040	TA-69	B	532	Yes	B horizon outlier, Nitric acid result of 730 > total result of 558.7, Large fraction of SAL

DRAFT DOCUMENT

Detection of Beryllium Outliers

No outliers were detected in the Be-K regression analysis.

Detection of Calcium Outliers

One high outlier was identified in the Ca-K correlation plot (Figure 46). This value was a C soil horizon outlier (Figure 47), the HNO₃ digestion result was greater than the total result, and it was nearly an order of magnitude larger than the next highest Ca result (Figure 47). This outlier was excluded from the combined background data set (Table 15). It is interesting to note that this Ca value was two to three times greater than Ca values reported for the CaCO₃ soil horizons.

Table 15. Summary of calcium values excluded from the combined background data set.

Sample ID	Sample location	Soil Horizon	Residual	Excluded	Rationale
FS2060	TA-39	C	75 600	Yes	Outlier in C horizon, Nitric acid result of 730 > total result of 558.7, Including the value in the statistical analysis would significantly inflate the UTL

Detection of Chlorine Outliers

No outliers were detected due to a low correlation with the major elements.

Detection of Chromium Outliers

One high outlier was identified in the Cr-Fe correlation plot (Figure 48). This value was a B soil horizon outlier (Figure 49), the HNO₃ digestion result was greater than the total result, and the residual of this outlier represented about 15% of the SAL (36.9 ppm divided by 210 ppm). This outlier was excluded from the combined background data set (Table 16).

DRAFT DOCUMENT

Table 16. Summary of chromium values excluded from the combined background data set.

Sample ID	Sample location	Soil Horizon	Residual	Excluded	Rationale
FS2170	TA-67	B	36.9	Yes	Outlier in B horizon, Nitric acid result of 46 > total result of 25, Residual is a large fraction of SAL

Detection of Cobalt Outliers

No outliers were detected in the regression analyses.

Detection of Copper Outliers

No outliers were detected in the regression analyses.

Detection of Lead Outliers

Three high values were identified by the regression analysis of Pb (Figure 50). These values were collected from the A and B soil horizons (Figure 51), and only one value represents a significant fraction of the SAL (22.9 ppm of 400 ppm) and represents an outlier in the A soil horizon group. The C soil horizon outlier was excluded, because it was not viewed that this value could reasonably represent an impact from Laboratory operations or airborne deposition of leaded gas exhaust. These values are summarized in Table 17, which presents the rationale for excluding one of the three outliers from the combined background data set.

DRAFT DOCUMENT

Table 17. Summary of lead values excluded from the combined background data set.

Sample ID	Sample location	Soil Horizon	Residual	Excluded	Rationale
FS2054	TA-16	A	22.9	Yes	A horizon outlier, Residual is a large fraction of SAL
FS2079	Tsk.	C	16.9	No	Not a significant C horizon outlier, Residual is a small fraction of SAL
FS2118	TA-63	A	13.7	No	Not a significant A horizon outlier, Residual is a small fraction of SAL

Detection of Magnesium Outliers

No outliers were detected in the regression analyses.

Detection of Manganese Outliers

No outliers were detected in the regression analyses.

Detection of Nickel Outliers

One high value was identified by the regression analysis of Ni (Figure 52). This value was collected from the B soil horizon (Figure 53), and does not represent a significant fraction of the SAL (12.6 ppm of 1500 ppm). This value is summarized in Table 18, and presents the rationale for not excluding this value from the combined background data set.

Table 18 Summary of nickel outlier, and rationale for not excluding from the combined background data set.

Sample ID	Sample location	Soil Horizon	Residual	Excluded	Rationale
FS2090	LA	B	12.6	No	Small fraction of SAL, not an outlier in the B soil horizon

DRAFT DOCUMENT

Detection of Sodium Outliers

No outliers were detected in the regression analyses.

Detection of Sulfate Outliers

No outliers were detected in the regression analyses.

Detection of Vanadium Outliers

No outliers were detected in the regression analyses.

Detection of Zinc Outliers

One high value was identified by the regression analysis of Zn (Figure 54). This value was in the A soil horizon (Figure 55), and the HNO₃ digestion result was greater than the total results. This value is summarized in Table 19, and presents the rationale for excluding this value from the combined background data set.

Table 19. Summary of zinc outlier, and rationale for not excluding from the combined background data set.

Sample ID	Sample location	Soil Horizon	Residual	Excluded	Rationale
FS2000	ULAC	A	30.5	Yes	Significant A horizon outlier, Nitric acid result of 58 > the total result of 54.57

Estimating Data Distributions for Updated LANL-wide Background Soil Data

Table 20 summarizes the distributional properties of the inorganic analytes in the combined background data set. Distributions were either normally distributed or were transformed to approach normality with either a log- or square root transformation. The purpose of estimating the statistical distribution that best models the data is to use this estimated statistical distribution to calculate the UTLs.

DRAFT DOCUMENT

Calculation of Background Screening Values for Updated LANL-wide Background Soil Data

Upper tolerance limits are calculated for all inorganics elements, except for chloride, where enough values were detected to allow estimation of the statistical distribution. Chloride has an unusual distribution, which does not allow the use of a simple statistical distribution model. We propose to use the maximum detected value for chloride and the rarely detected elements (Sb, Cd, Hg, Se, Ta, and Tl).

For the elements that are normally distributed without any data transformation and the elements that are normally distributed after a square root transformation, parametric tolerance limits were calculated by using the following equation:

$$UTL_{0.95,0.95} = \text{mean} + \text{standard deviation} * k_{0.95,0.95} \quad (1)$$

The k-factor depends on the number of background samples; complete tables of k-factors are published in the RCRA groundwater statistical analysis document (EPA 1989) and Gilbert (1987). Readers are referred to the LANL ER Project policy paper on background comparisons for example k-factors.

The UTLs for log normally distributed elements were estimated by a simulation process. These simulations were run in the S-plus statistical programming environment. The S-plus code is presented in Appendix A. These simulations were run for 10,000 trials, which were sufficient to estimate these UTLs to two or three significant digits.

After calculating the UTLs, these values were screened to ensure that some UTL values were not artificially inflated due to a small sample size. The raw calculated UTLs are presented in Table 21. The relative value of the median, mean, and calculated UTLs for the soil horizon subgroups and the overall combined background data set were also compared. If the mean and the median for a soil horizon were less than the combined data set mean and median and the UTL for the subset were greater than the combined data set, the overall data UTL was substituted for the soil horizon UTL. These trimmed UTL values for inorganics and naturally occurring radionuclides are presented in Tables 22 and 23, respectively, and it is proposed that these values, which include the sample maximum for the analytes discussed above, be used as the LANL-wide background screening values for LANL ER Project decision-making.

Guidance for ER Project Background Data Users

ER Project background data users are advised to compare their site data to the relevant soil horizon (or geologic strata) that best represent the locations where samples were collected. In some cases, the soil horizon is either not

DRAFT DOCUMENT

known or is irrelevant, because the sampled material is fill material of unknown origin. Where the soil horizon is not known, data users are advised to use the combined A, B, and C soil horizon background screening values.

The background screening process for RFI screening assessments consists of the following steps:

- 1) Use LANL-wide background data, which are presented in this report. These data include:
 - a) soil data by horizon,
 - b) geological data by stratigraphic layer, and
 - c) sediment data from Ancho, Indio, and Water Canyons
- 2) Data analysts will use the appropriate subset of the LANL-wide data, except where soil horizon is neither known nor relevant (e.g., fill of unknown origin was sampled).
- 3) The initial comparison for all analytes will be to background screening values for all inorganics and naturally-occurring radionuclides (by background data subsets as described above). Background screening values are based on the following sources:
 - a) maximum reported value for fallout-related radionuclides from the LANL environmental surveillance reports,
 - b) maximum reported value for inorganics with more than 20% non-detects,
 - c) maximum reported value for inorganics where the statistical distribution could not be estimated, and
 - d) UTLs calculated for normal, lognormal, or square root-transformed distributions based on a 99th percentile and 95% confidence. NOTE - UTLs for data subsets are checked for consistency with the data group to make sure that inflated UTLs are not used.
- 4) Additional background analyses are required for the following cases:
 - a) background screening values are exceeded AND SALs are exceeded,
 - b) ecological risk is determined to be primary decision point, or
 - c) aluminum, arsenic, beryllium, or manganese are known (or suspected) to have been released at the PRS.
- 5) Additional analyses include:
 - a) graphical comparisons of background and PRS data,
 - b) statistical "distribution shift" tests,
 - c) regression analysis of trace elements and major elements (soil and sediment only), or
 - d) regression analysis of Th and U (any solid media)

DRAFT DOCUMENT

Table 20. Statistical distribution of the combined background data set inorganic analytes. These data are for the nitric acid digestion extraction method (EPA method 3050) unless noted otherwise.

Analyte	Statistical Distribution
Aluminum	Log transformed data are approximately normally distributed.
Antimony	Only 19 of 182 total values are detects; no distribution was estimated.
Arsenic	Data are approximately normally distributed.
Barium	Square root transformed data are approximately normally distributed.
Beryllium	Square root transformed data are approximately normally distributed.
Cadmium	Only 4 of 40 total values are detects; no distribution was estimated.
Calcium	Log transformed data are approximately normally distributed.
Chlorine	Log transformation does not significantly improve fit to a normal distribution; data may be best modeled by a mixture distribution; recommend using the maximum detected value as a background screening value.
Chromium	Log transformed data are normally distributed.
Cobalt	Log transformed data are approximately normally distributed.
Copper	Square root transformed data are approximately normally distributed.
Iron	Square root transformed data are normally distributed.
Lead	Data are approximately normally distributed.
Magnesium	Log transformed data are approximately normally distributed.
Manganese	Square root transformed data are normally distributed.
Mercury	Only 2 of 39 total values are detects; no distribution was estimated.
Nickel	Data transformations do not improve fit to normality; untransformed data were used to estimate parameters of the normal distribution.
Potassium	Square root transformed data are more normally distributed.
Potassium-total	Data are approximately normally distributed.
Selenium	Only 23 of 41 total values are detects, no distribution was estimated.
Sodium	Log transformed data are approximately normally distributed.
Sulfate	Log transformed data are normally distributed.
Tantalum	Zero of 183 total values are detects, no distribution was estimated.
Thallium	Only 111 of 182 total values are detects; no distribution was estimated.
Thorium	Data are approximately normally distributed.
Thorium-total	Data are approximately normally distributed.
Uranium	Data are approximately normally distributed.
Uranium-total	Data are approximately normally distributed.
Vanadium	Square root transformed data are approximately normally distributed.
Zinc	Square root transformed data are approximately normally distributed.

DRAFT DOCUMENT

Table 21. Summary of calculated UTLs and maximum concentrations by soil horizons.

Aluminum								
Data Group	Count	minimum	median	maximum	Mean	Std Dev	Prob>ChiSq (1)	UTL _{95th} by sim
A	24	2350	8500	23000	8581	4875	0.107	26642
B	126	1400	11000	61500	12574	9498		43594
C	24	900	11000	33000	10083	7265		46090
All Horizons	174	900	10000	61500	11680	8810		38691

Antimony								
Data Group	Count	minimum	median	maximum	Mean	Std Dev	Prob>ChiSq (1)	Max. detect
A	24	0.2	0.7	2.5	1.248	1.000	0.0267	0.5
B	126	0.2	0.55	2.5	0.818	0.752		1
C	23	0.1	0.7	2.5	1.307	0.988		ND
All Horizons	173	0.1	0.6	2.5	0.943	0.844		1

Arsenic								
Data Group	Count	minimum	median	maximum	Mean	Std Dev	Prob>ChiSq (1)	UTL _{95th}
A	21	0.8	3.8	5.4	3.33	1.52	0.0001	6.99
B	108	1	4	9.3	4.34	1.87		8.12
C	21	0.3	2.4	6.7	2.50	1.72		6.58
All Horizons	150	0.3	4	9.3	3.95	1.92		7.82

Barium								
Data Group	Count	minimum	median	maximum	Mean	Std Dev	Prob>ChiSq (1)	UTL _{95th} (sqrt)
A	24	27	135	190	128.9	42.9	0	263
B	125	46	140	370	155.4	72.8		321
C	24	21	75	410	90.3	81.7		286
All Horizons	173	21	130	410	142.7	74.1		315

Beryllium								
Data Group	Count	minimum	median	maximum	Mean	Std Dev	Prob>ChiSq (1)	UTL _{95th}
A	24	0.105	0.695	1.2	0.681	0.239	0.0001	1.41
B	126	0.25	0.965	3.95	0.992	0.442		1.91
C	24	0.04	0.745	1.9	0.715	0.505		2.38
All Horizons	174	0.04	0.895	3.95	0.911	0.447		1.95

Cadmium								
Data Group	Count	minimum	median	maximum	Mean	Std Dev	Prob>ChiSq (1)	Max. detect
A	9	0.2	0.2	1.4	0.422	0.452	0.3002	1.4
B	20	0.2	0.2	2.6	0.420	0.573		2.7
C	10	0.2	0.2	0.2	0.2	0		ND
All Horizons	39	0.2	0.2	2.6	0.364	0.465		2.7

DRAFT DOCUMENT

Table 21 (cont.). Summary of calculated UTLs and maximum concentrations by soil horizons.

Calcium

Data Group	Count	minimum	median	maximum	Mean	Std Dev	Prob>ChiSq (1)	UTL _{95th} by sim
A	24	670	1800	4500	1860	774	0.0001	4033
B	126	1100	2300	14000	2937	1919		6479
C	23	500	1700	4100	1854	1066		5930
All Horizons	173	500	2100	14000	2644	1771		6115

Chlorine

Data Group	Count	minimum	median	maximum	Mean	Std Dev	Prob>ChiSq (1)	UTL _{95th} by sim
A	24	8	12.45	24	13.33	4.22	0.0037	25.0
B	126	8	14	246	27.81	40.74		78.2
C	24	9	23	303	44.18	64.36		170.4
All Horizons	174	8	14.45	303	28.07	42.64		75.9

Chromium

Data Group	Count	minimum	median	maximum	Mean	Std Dev	Prob>ChiSq (1)	UTL _{95th} by sim
A	24	1.9	8.15	16	8.20	3.25	0	20.5
B	125	2.8	9.3	36.5	9.76	4.49		19.0
C	24	1.9	5.6	15	6.10	3.24		17.0
Chromium	173	1.9	8.6	36.5	9.04	4.36		19.3

Cobalt

Data Group	Count	minimum	median	maximum	Mean	Std Dev	Prob>ChiSq (1)	UTL _{95th} by sim
A	24	2.8	7.3	29	10.41	7.05	0.0147	31.0
B	126	1.6	6	22	6.67	3.61		14.8
C	24	1	4	34	8.32	8.74		41.2
All Horizons	174	1	6	34	7.41	5.28		19.2

Copper

Data Group	Count	minimum	median	maximum	Mean	Std Dev	Prob>ChiSq (1)	UTL _{95th} by sim
A	24	0.25	5.7	12	5.80	2.88	0	42.3
B	126	2.7	6	16	6.55	2.39		29.2
C	24	0.25	3.9	7.3	3.75	1.99		22.2
All Horizons	174	0.25	5.75	16	6.06	2.59		30.7

DRAFT DOCUMENT

Table 21 (cont.). Summary of calculated UTLs and maximum concentrations by soil horizons.

Iron

Data Group	Count	minimum	median	maximum	Mean	Std Dev	Prob>ChiSq (1)	UTL _{95th} (sqrt)
A	24	3300	11000	16000	10363	2751	0	18116
B	126	6800	13000	36000	13085	4246		21760
C	24	3300	8450	17000	9021	3513		18499
All Horizons	174	3300	12000	36000	12149	4256		21294

Magnesium

Data Group	Count	minimum	median	maximum	Mean	Std Dev	Prob>ChiSq (1)	UTL _{95th} by sim
A	24	485	1650	2800	1628	534	0	3460
B	126	800	2100	10000	2335	1138		4484
C	24	420	1550	7400	1773	1416		5962
All Horizons	174	420	1975	10000	2160	1150		4613

Manganese

Data Group	Count	minimum	median	maximum	Mean	Std Dev	Prob>ChiSq (1)	UTL _{95th} (sqrt)
A	24	140	405	1100	446.9	216.0	0	1003
B	125	76	330	1000	348.3	146.6		673
C	24	76	160	440	193.6	99.4		463
All Horizons	173	76	320	1100	340.5	166.4		714

Mercury

Data Group	Count	minimum	median	maximum	Mean	Std Dev	Prob>ChiSq (1)	Max. detect
A	9	0.05	0.05	0.05	0.05	0	0.6219	ND
B	20	0.05	0.05	0.1	0.0525	0.0112		0.1
C	10	0.05	0.05	0.1	0.0550	0.0158		0.1
All Horizons	39	0.05	0.05	0.1	0.0526	0.0112		0.1

Nickel

Data Group	Count	minimum	median	maximum	Mean	Std Dev	Prob>ChiSq (1)	UTL _{95th}
A	24	1	6	12	5.93	2.73	0.0017	12.2
B	126	1	7	29	7.73	4.08		16.0
C	24	1	4.45	15	4.79	3.70		13.3
All Horizons	174	1	7	29	7.07	4.01		15.2

DRAFT DOCUMENT

Table 21 (cont.). Summary of calculated UTLs and maximum concentrations by soil horizons.

Potassium-

TOTAL

Data Group	Count	minimum	median	maximum	Mean	Std Dev	Prob>ChiSq (1)	UTL _{95th}
A	23	20000	23090	32050	24016	3960	0	33239
B	125	11000	23000	36000	24065	4604		33374
C	23	16270	30000	42000	30194	4982		41796
All Horizons	171	11000	24000	42000	24882	5011		35015

Selenium

Data Group	Count	minimum	median	maximum	Mean	Std Dev	Prob>ChiSq (1)	Max. detect
A	9	0.1	0.1	0.7	0.172	0.199	0.0005	0.7
B	20	0.1	0.5	1.3	0.625	0.369		1.3
C	10	0.1	0.125	1.7	0.340	0.503		1.7
All Horizons	39	0.1	0.3	1.7	0.447	0.417		1.7

Sodium

Data Group	Count	minimum	median	maximum	Mean	Std Dev	Prob>ChiSq (1)	UTL _{95th} by sim
A	24	64	105	660	179	166	0.0004	602
B	126	58	235	1800	286	239		798
C	24	90	365	1700	524	484		2682
All Horizons	174	58	225	1800	304	292		915

Sulfate

Data Group	Count	minimum	median	maximum	Mean	Std Dev	Prob>ChiSq (1)	UTL _{95th}
A	24	6	17.5	44	21.42	9.22	0.0039	42.7
B	126	9	30	722	58.79	94.06		249.0
C	24	12	44.5	1200	122.83	254.99		711.6
All Horizons	174	6	28.5	1200	62.47	125.69		316.6

Tantalum

Data Group	Count	minimum	median	maximum	Mean	Std Dev	Prob>ChiSq (1)	Max. detect
A	24	0.1	0.1	0.45	0.160	0.117	0.803	ND
B	126	0.1	0.1	0.45	0.182	0.130		ND
C	24	0.06	0.1	0.45	0.199	0.155		ND
All Horizons	174	0.06	0.1	0.45	0.182	0.132		ND

DRAFT DOCUMENT

Table 21 (cont.). Summary of calculated UTLs and maximum concentrations by soil horizons.

Thallium

Data Group	Count	minimum	median	maximum	Mean	Std Dev	Prob>ChiSq (1)	Max. detect
A	24	0.1	0.2	0.5	0.242	0.125	0.0002	0.4
B	126	0.1	0.2	1	0.302	0.194		1
C	23	0.0625	0.1	0.6	0.168	0.150		0.6
All Horizons	173	0.0625	0.2	1	0.276	0.186		1

Thorium-TOTAL

Data Group	Count	minimum	median	maximum	Mean	Std Dev	Prob>ChiSq (1)	UTL _{95th}
A	23	11.8	14	22.6	14.8	2.49	0.0193	20.5
B	125	10	16.4	27.15	16.4	3.09		22.7
C	23	7.8	16.46	23.23	15.8	4.11		25.3
All Horizons	171	7.8	16	27.15	16.1	3.21		22.6

Uranium

Data Group	Count	minimum	median	maximum	Mean	Std Dev	Prob>ChiSq (1)	UTL _{95th}
A	15	0.2	1	3.6	1.316	0.835	0	3.46
B	123	0.5	0.9	2.4	1.003	0.353		1.72
C	24	0.2	0.7	1.5	0.688	0.289		1.36
All Horizons	162	0.2	0.9	3.6	0.985	0.436		1.87

Uranium-TOTAL

Data Group	Count	minimum	median	maximum	Mean	Std Dev	Prob>ChiSq (1)	UTL _{95th}
A	15	3	3.851	5.1	3.907	0.465	0.5	5.10
B	122	2.182	3.7	6.3	3.766	0.781		5.34
C	23	1.7	3.8	6.728	3.911	1.148		6.58
All Horizons	160	1.7	3.7	6.728	3.800	0.818		5.45

Vanadium

Data Group	Count	minimum	median	maximum	Mean	Std Dev	Prob>ChiSq (1)	UTL _{95th} (sqrt)
A	24	4.6	21	35	20.7	7.62	0	42.8
B	126	7.4	22.5	56.5	22.9	8.69		42.0
C	24	4	14	32	13.2	6.89		32.0
All Horizons	174	4	21	56.5	21.3	8.92		41.9

DRAFT DOCUMENT

Table 21 (cont.). Summary of calculated UTLs and maximum concentrations by soil horizons.

Zinc								
Data Group	Count	minimum	median	maximum	Mean	Std Dev	Prob>ChiSq (1)	UTL _{95th} (sqrt)
A	23	14	28	40	27.1	7.45	0.008	47.1
B	125	14	31	75.5	32.8	8.91		51.5
C	24	14	29	57	29.0	9.27		52.5
All Horizons	172	14	30.75	75.5	31.5	9.00		50.8

UTL_{95th} - 95% upper tolerance limit of the 95th percentile calculated using normal theory.

UTL_{95th} (sqrt) - 95% upper tolerance limit of the 95th percentile calculated using normal theory on square root transformed data.

UTL_{95th} by sim - 95% upper tolerance limit of the 95th percentile calculated using log-transformed data and computer simulation.

Max. detect. - maximum detected value is proposed as a background screening value due to a small number of detects.

ND - Not detected

(1) Probability that the A, B and C horizon data are drawn from the same distribution, or are statistically not different, as measured the Kruskal-Wallis test. The Kruskal-Wallis is a three or more data group extension of the Wilcoxon rank sum test. Probabilities less than 0.05 indicate that there is a statistically significant difference between the horizons, and a probability greater than 0.05 indicates that there is no statistically significant difference between the soil horizons.

DRAFT DOCUMENT

Table 22. Summary of proposed background soil screening values.

Analyte	Soil Horizon			All Data
	A	B	C	
Aluminum	26600	43600	38700 *	38700
Antimony	0.5	1	ND	1
Arsenic	6.99	8.12	6.58	7.82
Barium	263	321	286	315
Beryllium	1.41	1.91	1.95 *	1.95
Cadmium	1.4	2.7	ND	2.7
Calcium	4030	6480	5930	6120
Chlorine	25.0	78.2	170	75.9
Chromium	19.3 *	19.0	17.0	19.3
Cobalt	31.0	14.8	41.2	19.2
Copper	30.7 *	29.2	22.2	30.7
Iron	18100	21800	18500	21300
Lead	28.4	22.3	21.9	23.3
Magnesium	3460	4480	4610 *	4610
Manganese	1000	673	463	714
Mercury	ND	0.1	0.1	0.1
Nickel	12.2	16.0	13.3	15.2
Potassium-TOTAL	33200	33400	41800	35000
Potassium	3070	3420	3410 *	3410
Selenium	0.7	1.3	1.7	1.7
Sodium	602	798	2680	915
Sulfate	42.7	249	712	317
Tantalum	ND	ND	ND	ND
Thallium	0.4	1	0.6	1
Thorium	13.3	15.0	12.3	14.6
Thorium-TOTAL	20.5	22.7	25.3	22.6
Uranium	1.87 *	1.72	1.36	1.87
Uranium-TOTAL	5.10	5.34	6.58	5.45
Vanadium	42.8	42.0	32.0	41.9
Zinc	47.1	51.5	50.8 *	50.8

* Values were trimmed to the all data UTL to eliminate inflated UTLs.

ND = Not detected.

Units are mg/kg.

DRAFT DOCUMENT

Table 23. Computed background screening values for naturally occurring radionuclides compiled by soil horizon.

Analyte	Soil Horizon			All Data
	A	B	C	
Total Potassium (mg/kg)	33200	33400	41800	35000
Potassium-40 (pCi/g)	27.2	27.3	34.2	28.6
Total Thorium (mg/kg)	20.5	22.7	25.3	22.6
Thorium-232 (pCi/g)	2.24	2.48	2.77	2.47
Total Uranium (mg/kg)	5.10	5.34	6.58	5.45
Uranium-234 (pCi/g)	1.81	1.90	2.33	1.94
Uranium-235 (pCi/g)	0.078	0.082	0.101	0.084
Uranium-238 (pCi/g)	1.70	1.78	2.20	1.82
Total Uranium (pCi/g)	3.59	3.76	4.64	3.84

DRAFT DOCUMENT

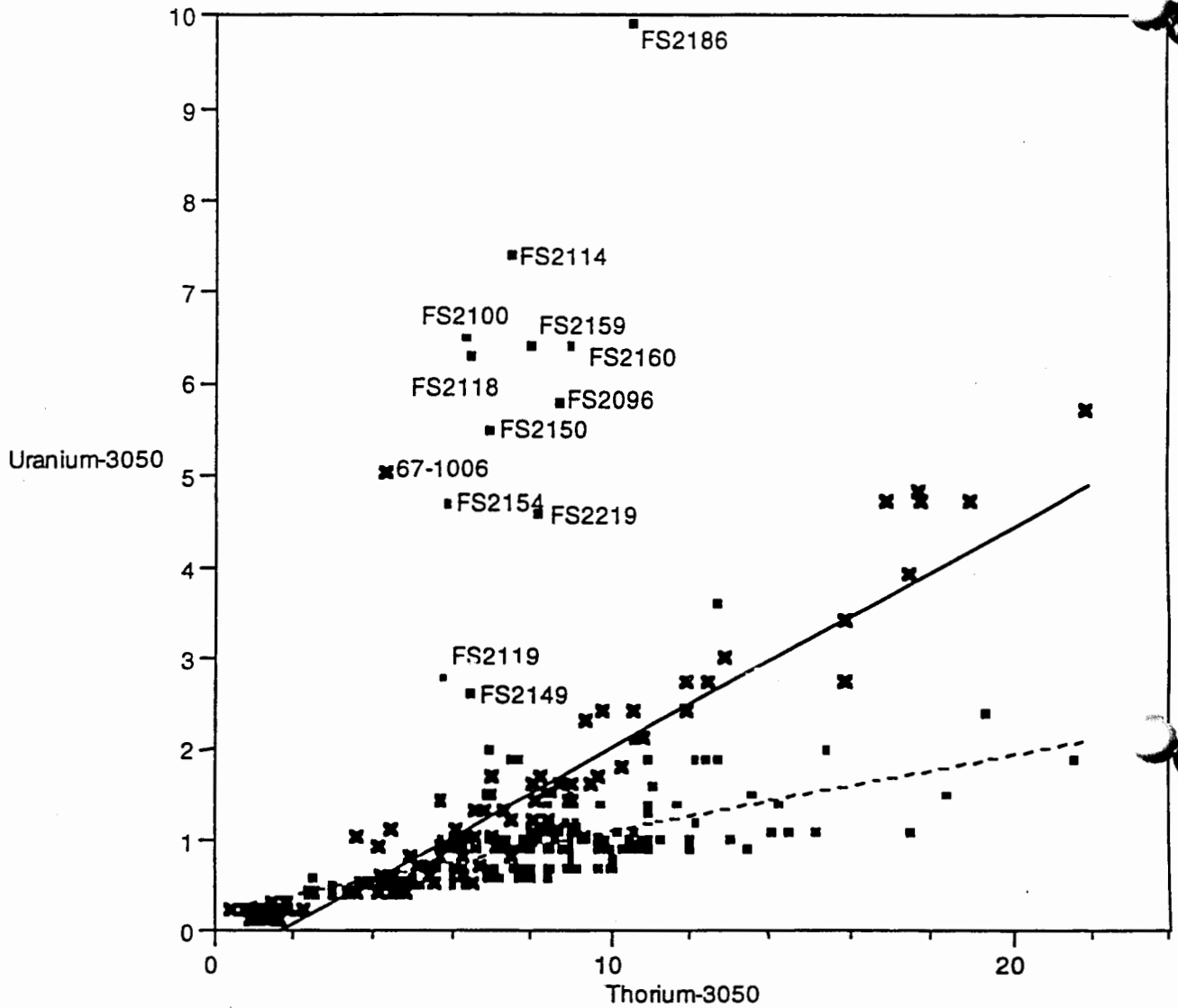


Figure 40. Correlation between Th and U results (both extracted by method 3050). Labeled values are outliers in the Th-U regression analysis. Solid line is the linear regression between Th and U for the Bandelier tuff data (Longmire et al., 1995) ($y = -0.403 + 0.241x$, $r^2 = 0.907$, where the one outlier was excluded from the analysis). Dashed line is the linear regression between Th and U for the A, B and C soil horizon data ($0.233 + 0.0867x$, $r^2 = 0.367$, where the 11 outliers were excluded from the analysis).

DRAFT DOCUMENT

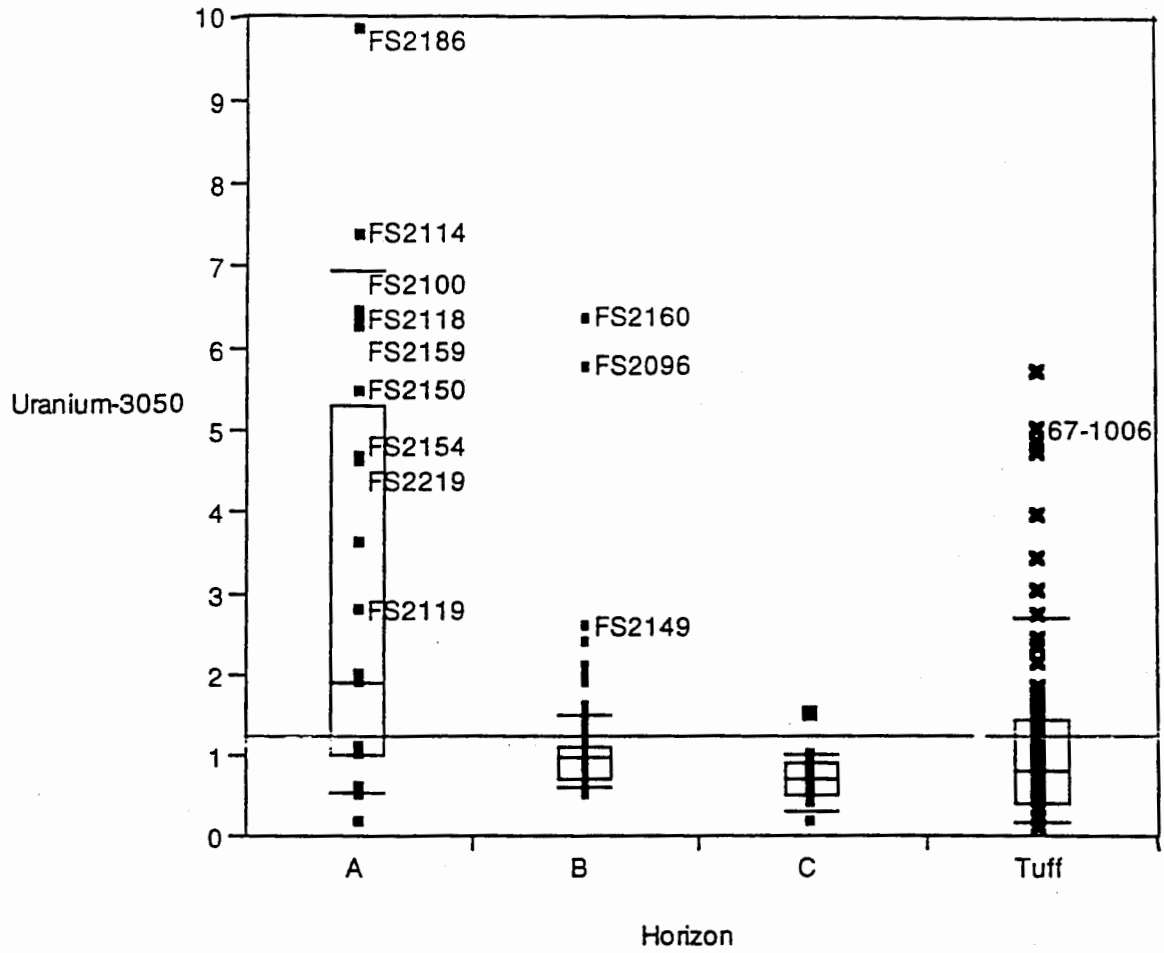


Figure 41. Uranium (3050 extraction method) results by soil horizon. Labeled values are outliers in the U-Th regression analysis.

DRAFT DOCUMENT

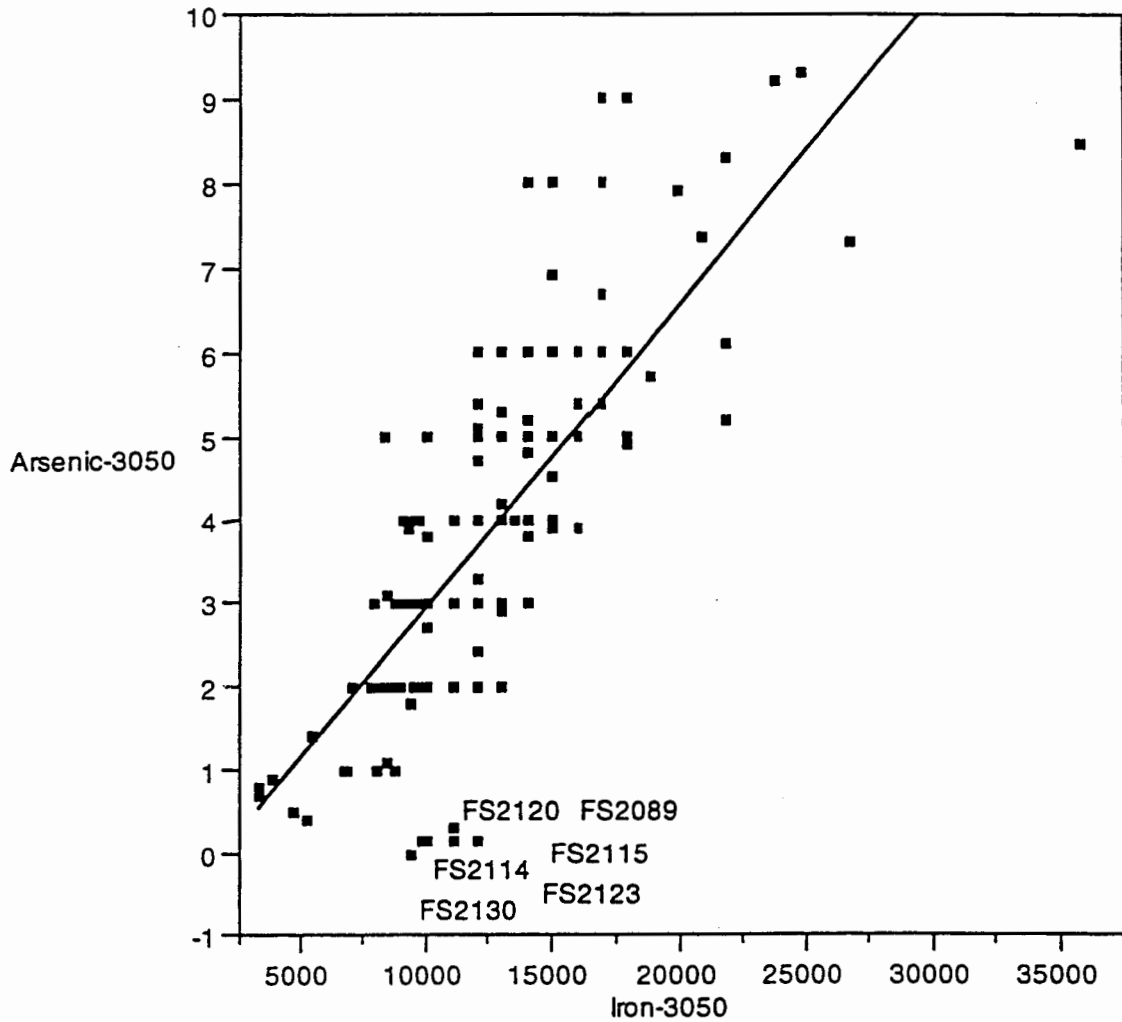


Figure 42. Correlation of As to Fe results (both extracted by method 3050). Labeled values are outliers in the As-Fe regression analysis. The solid line is the linear regression between As and Fe for the A, B and C soil horizons data ($-0.654+0.000359x$, $r^2=0.600$), where the six outliers were included in the analysis).

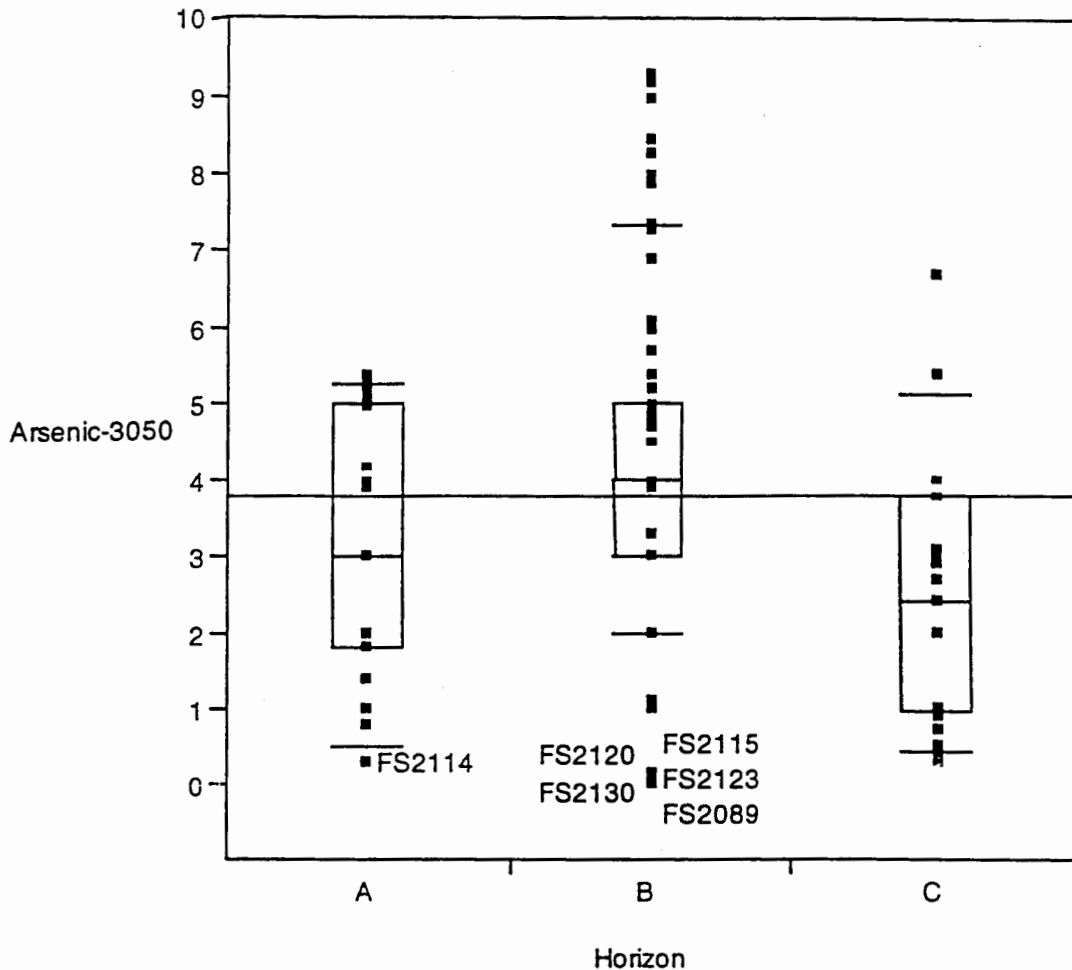


Figure 43. Arsenic (3050 extraction method) results by soil horizon. Labeled values are outliers in the As-Fe regression analysis.

DRAFT DOCUMENT

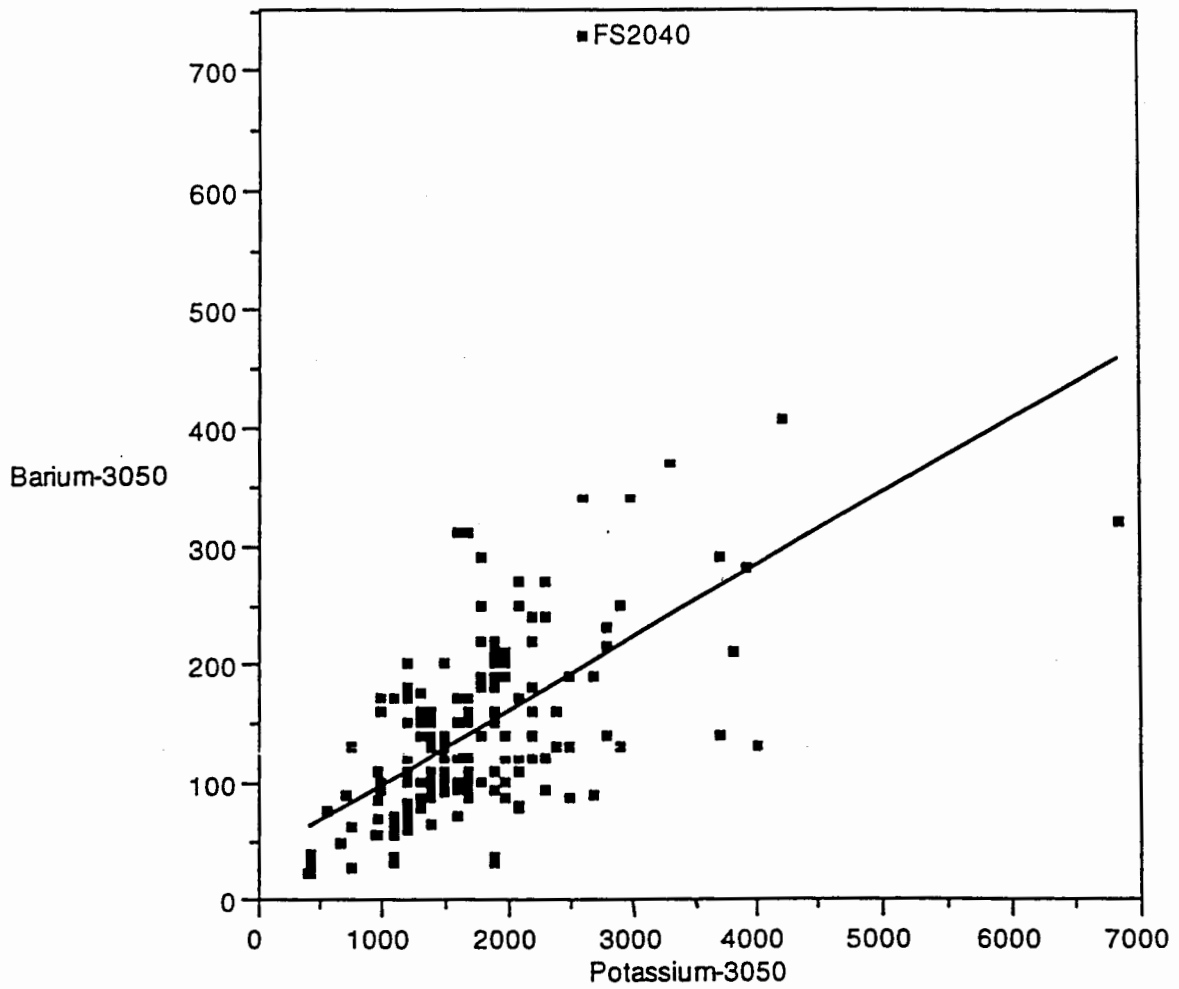


Figure 44. Correlation of Ba to K results (both extracted by method 3050). The labeled value is an outlier in the Ba-K regression analysis. Solid line is the linear regression between Ba and K for the A, B and C soil horizon data ($38.9+0.0613x$, $r^2=0.312$, where the one outlier was included in the analysis).

DRAFT DOCUMENT

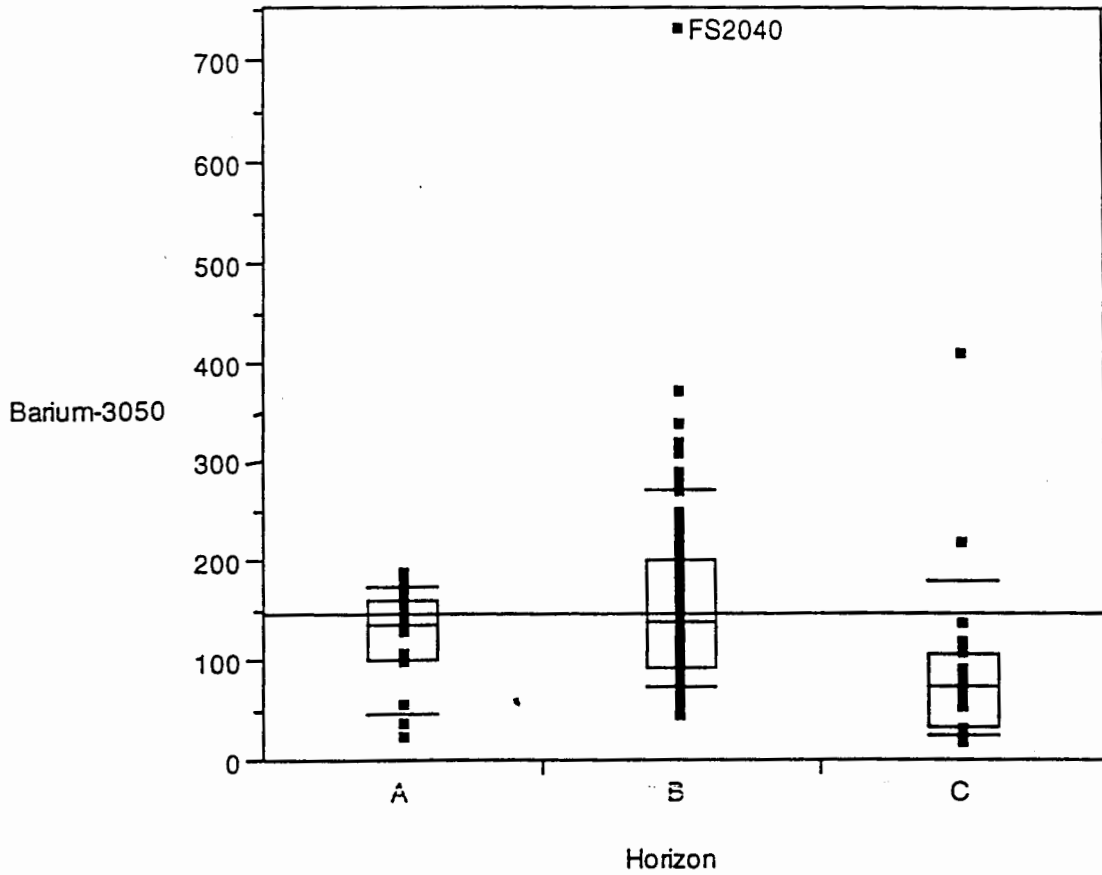


Figure 45. Barium (3050 extraction method) results by soil horizon. The labeled value is an outlier in the Ba-K regression analysis.

DRAFT DOCUMENT

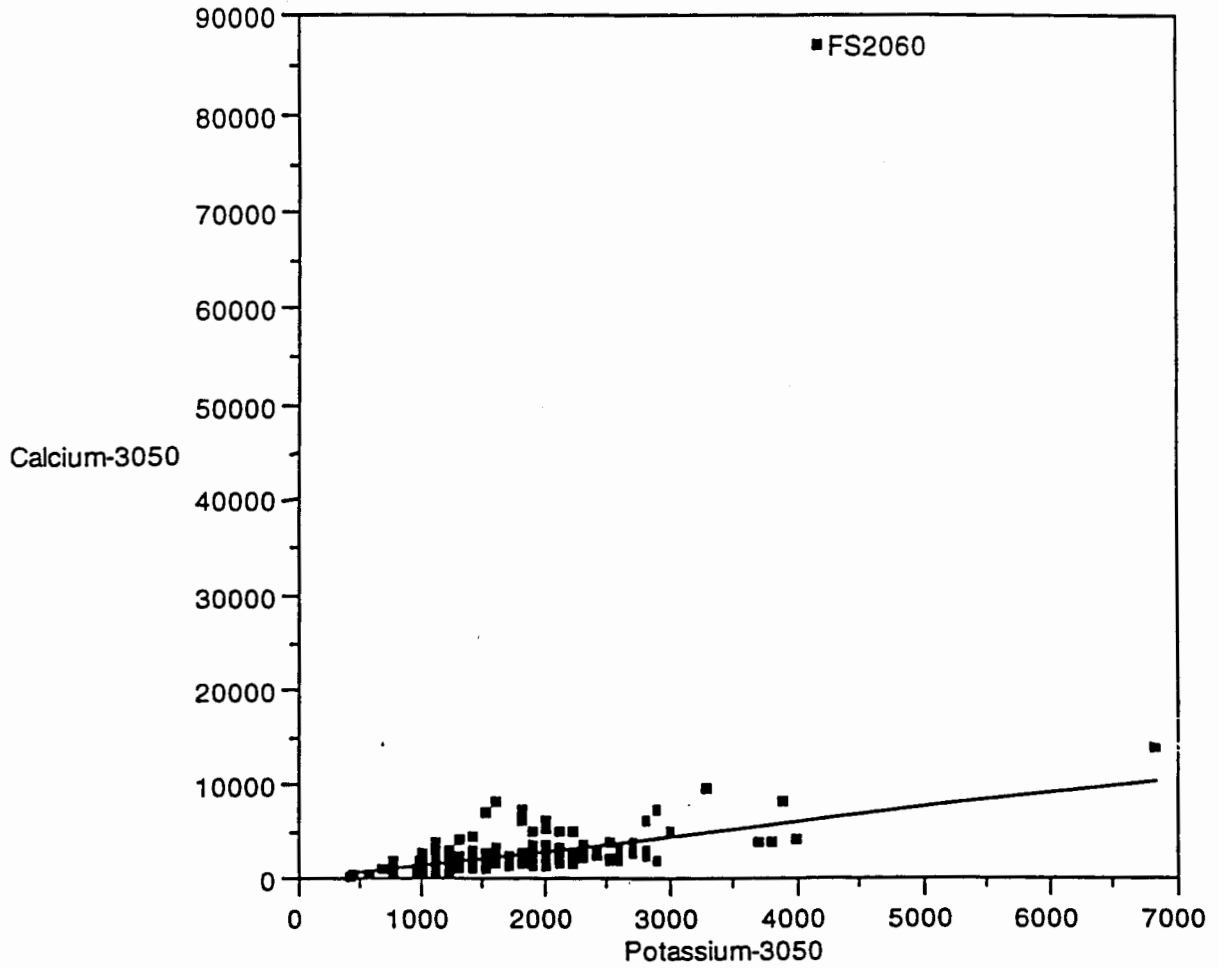


Figure 46. Correlation of Ca to K results (both extracted by method 3050). The labeled value is an outlier in the calcium-potassium regression analysis. Solid line is the linear regression between Ca and K for the A, B and C soil horizon data ($-4.61+1.53x$, $r^2=0.436$, where the one statistical outlier was excluded from the analysis).

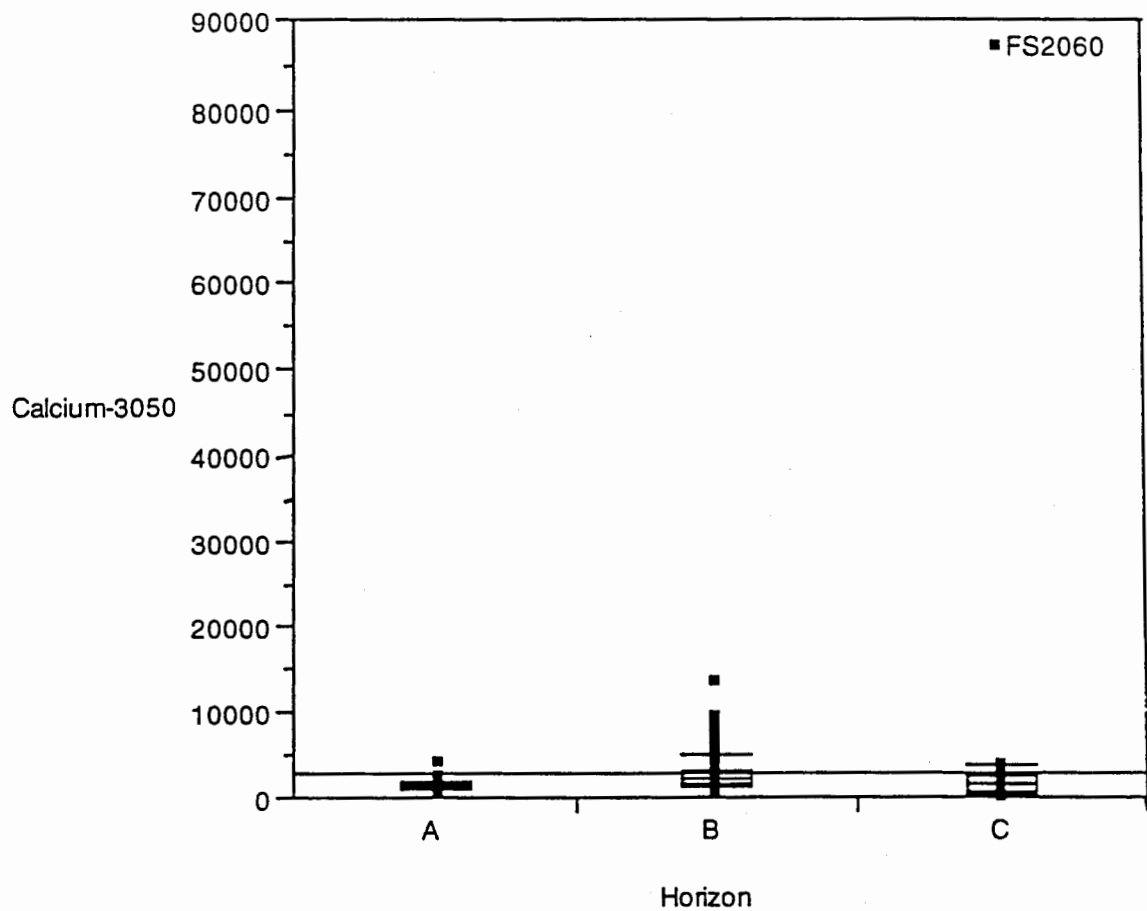


Figure 47. Calcium (3050 extraction method) results by soil horizon. The labeled value is an outlier in the Ca-K regression analysis.

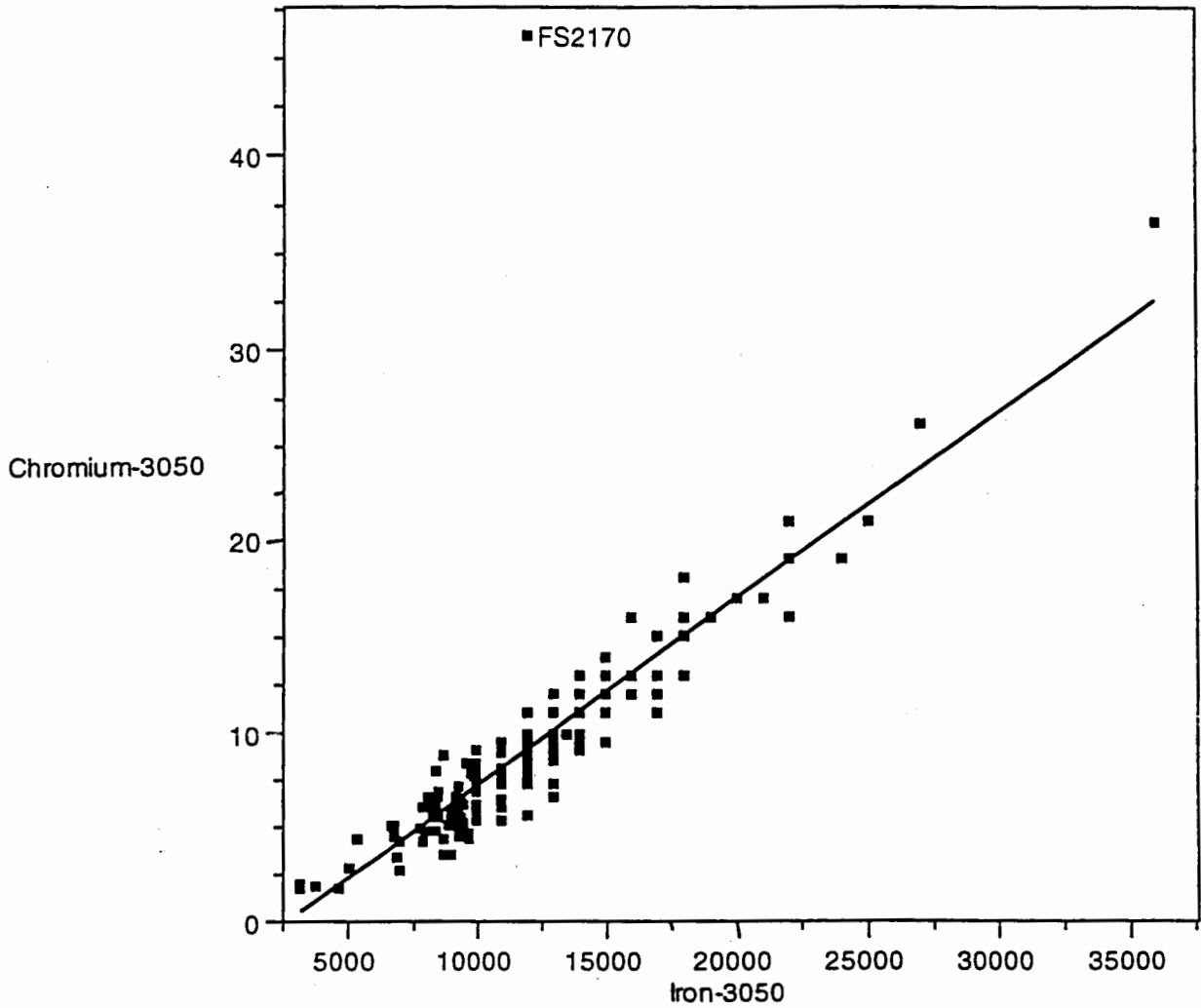


Figure 48. Correlation of Cr to Fe results (both extracted by method 3050). The labeled value is an outlier in the Cr-Fe regression analysis. Solid line is the linear regression between Cr and Fe for the A, B and C soil horizon data ($-2.58+0.000974x$, $r^2=0.641$, where the one outlier was included in the analysis).

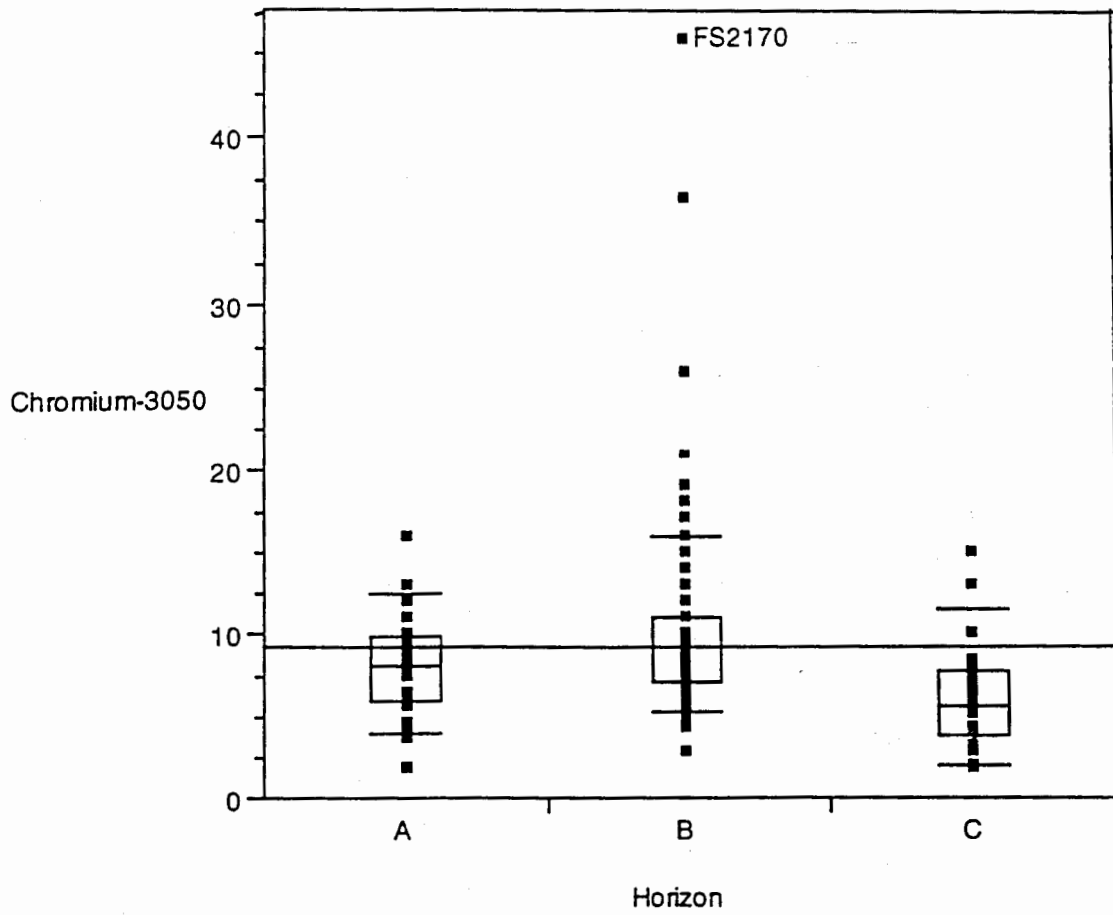


Figure 49. Chromium (3050 extraction method) results by soil horizon. The labeled value is an outlier in the Cr-Fe regression analysis.

DRAFT DOCUMENT

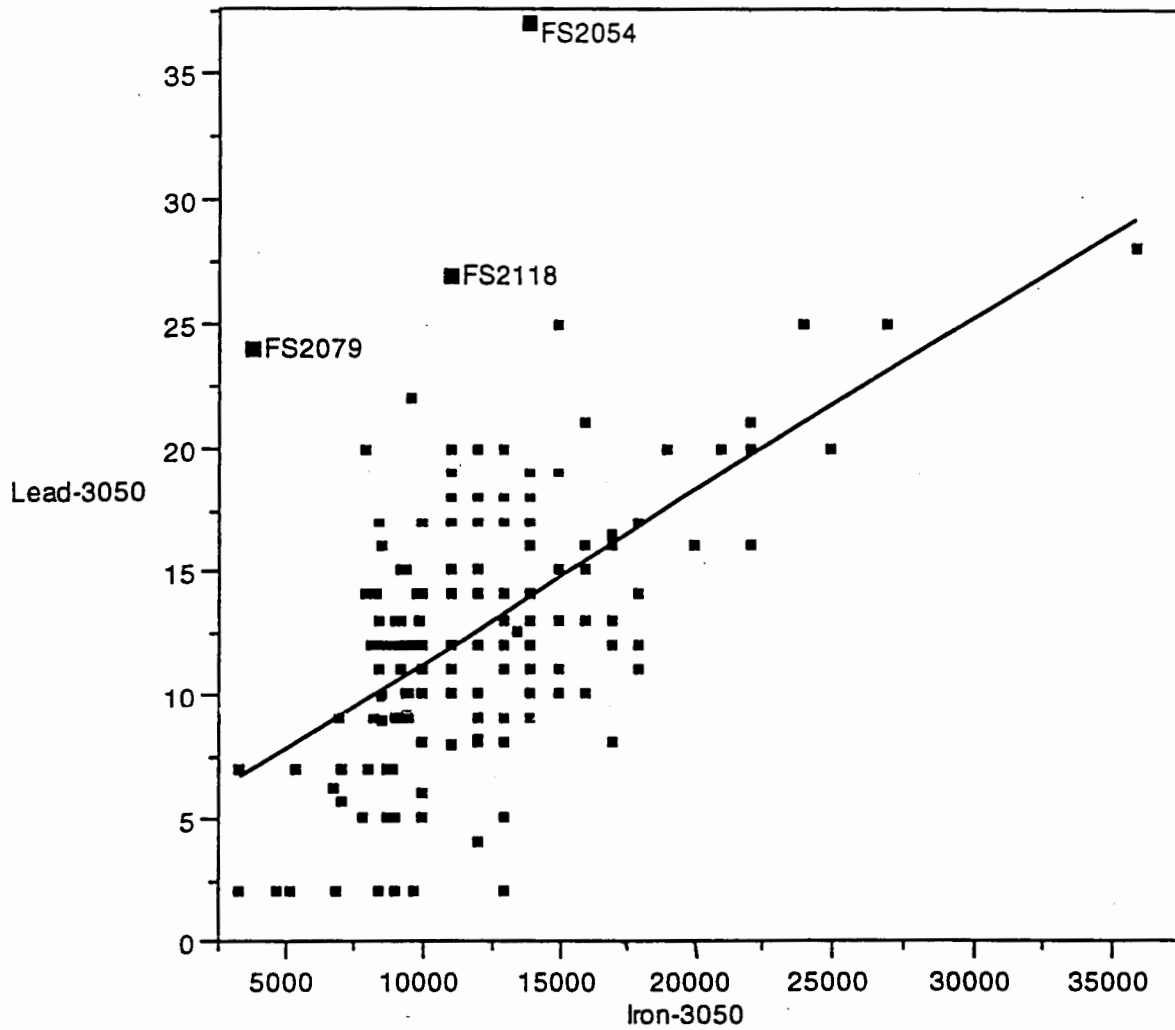


Figure 50. Correlation of Pb to Fe results (both extracted by method 3050). The labeled values are outliers in the Pb-Fe regression analysis. Solid line is the linear regression between Pb and Fe for the A, B and C soil horizon data ($4.47+0.000685x$, $r^2=0.276$, where the outliers were included in the analysis).

DRAFT DOCUMENT

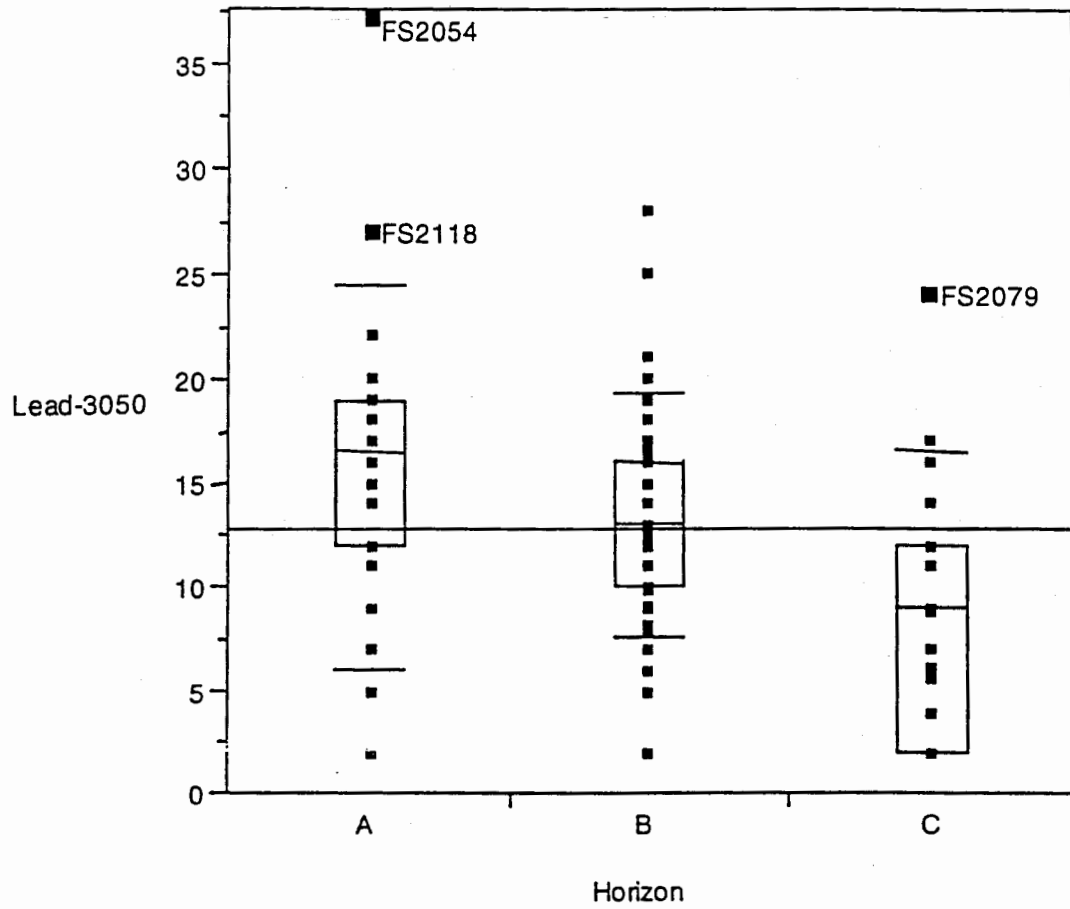


Figure 51. Lead (3050 extraction method) results by soil horizon. The labeled values are outliers in the Pb-Fe regression analysis.

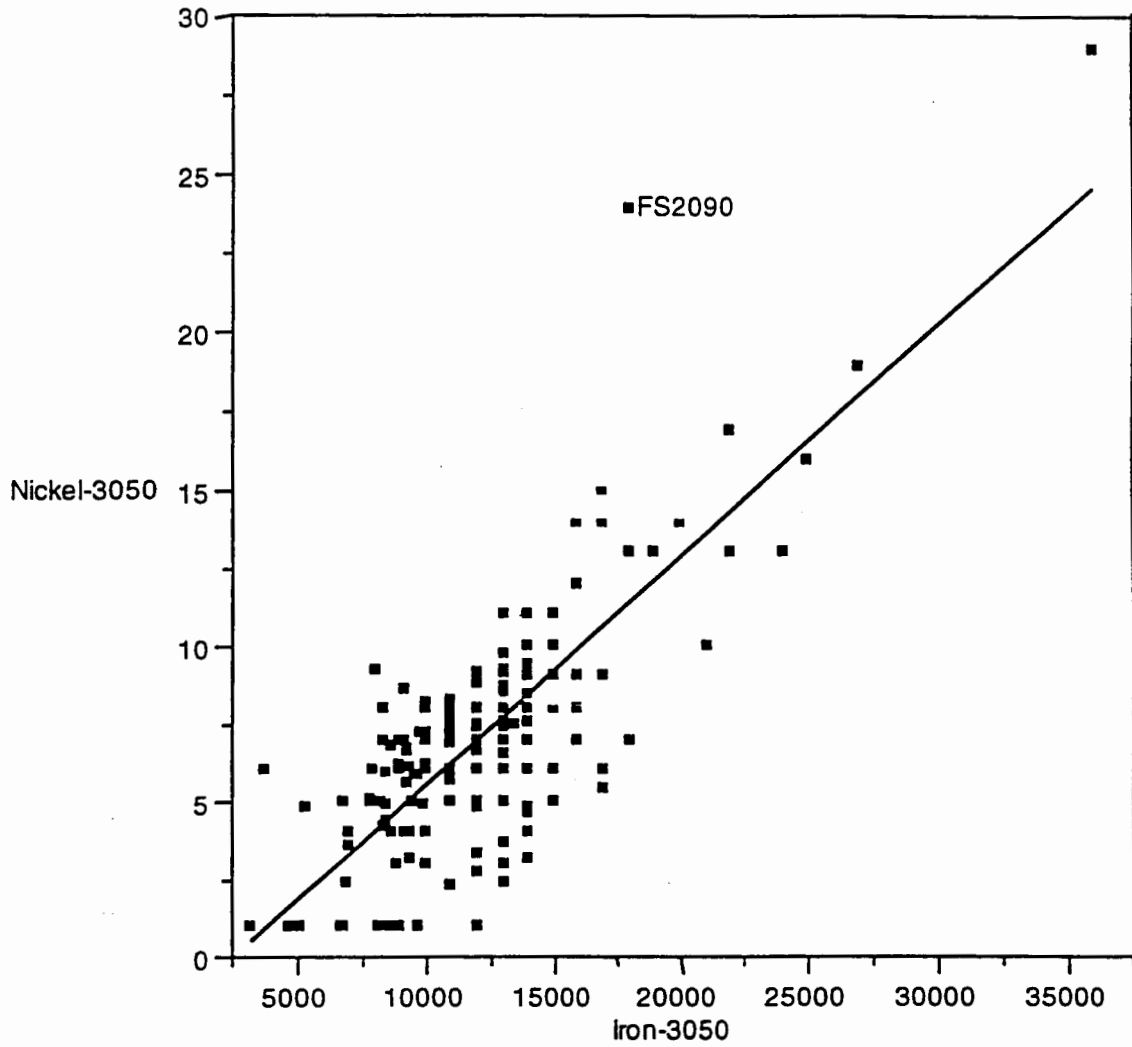


Figure 52. Correlation of Ni to Fe results (both extracted by method 3050). The labeled value is an outlier in the Ni-Fe regression analysis. Solid line is the linear regression between Ni and Fe for the A, B and C soil horizon data ($-1.81+0.000731x$, $r^2=0.604$, where the one outlier was included in the analysis).

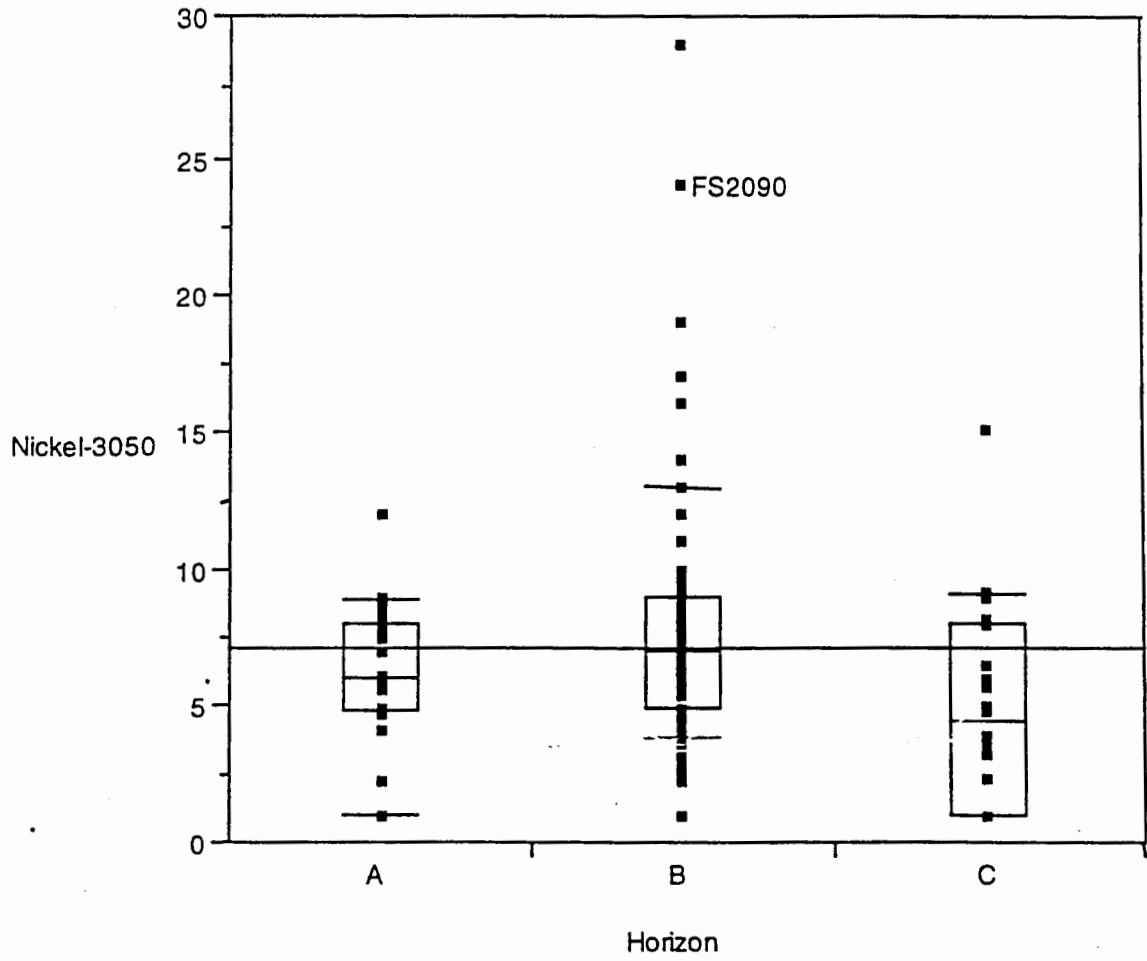


Figure 53. Nickel (3050 extraction method) results by soil horizon. The labeled value is an outlier in the Ni-Fe regression analysis.

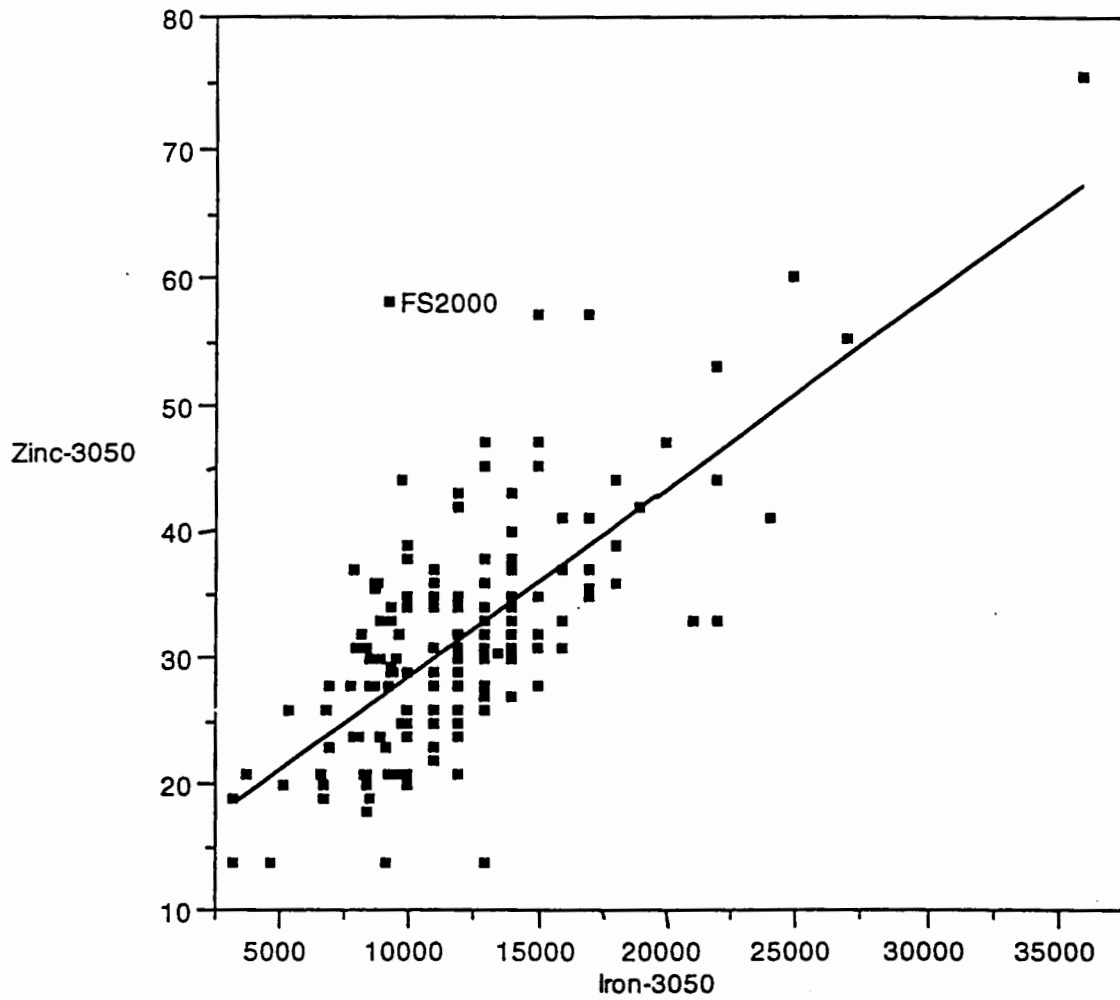


Figure 54. Correlation of Zn to Fe results (both extracted by method 3050). The labeled value is an outlier in the Zn-iFe regression analysis. Solid line is the linear regression between Zn and Fe for the A, B and C soil horizon data ($13.631802+0.0014864x$, $r^2=0.475104$, where the one outlier was included in the analysis).

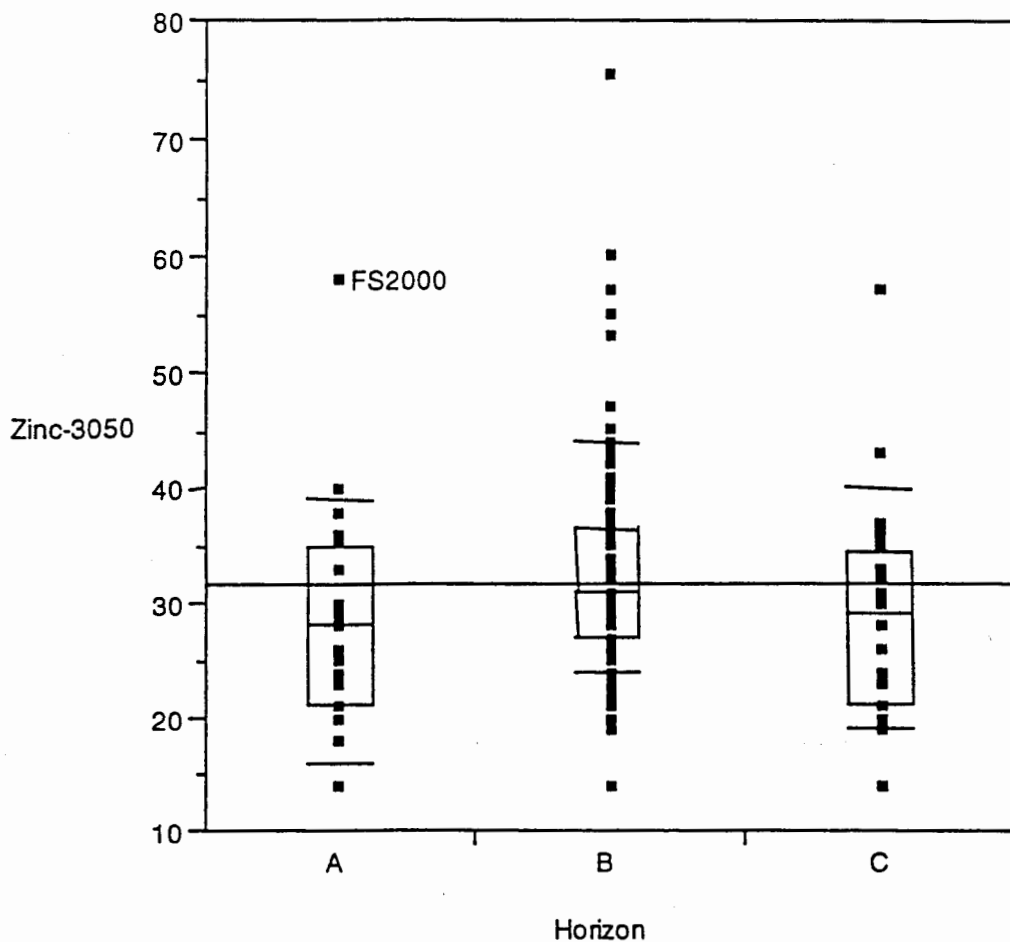


Figure 55. Zinc (3050 extraction method) results by soil horizon. The labeled value is an outlier in the Zn-Fe regression analysis.

DRAFT DOCUMENT

SUMMARY AND RECOMMENDATIONS

Background elemental concentrations were determined for RCRA metals and other elements within fourteen soil profiles at six different geographic locations around the Laboratory. These background characterization studies supplement the previous eight soil profiles reported by Longmire et al. (1995). Background concentrations of analytes do not exceed their respective SALs except for As, Be, and Mn. Because of the dependence of As, Be, Th, U, and other elements on soil development, the selection of appropriate background samples for a specific site should include a consideration of appropriate LANL soil characteristics.

Two types of sample digestion techniques, consisting of HNO_3 and HF, were used prior to chemical analyses. Leachable (HNO_3 digestion) background elemental concentrations in soils provide information relevant to the bioavailability of elements for risk calculations. The leachable elemental concentrations are statistically treated and are the primary focus of this report, whereas the total element concentrations (HF digestion) provide geochemical and pedological information. EPA SW846 methods recommend that nitric acid and other reagents are suitable for digesting solid samples.

Field, analytical, and statistical methods used in this investigation are sufficient for defining background elemental concentrations in soils for inorganic contaminants of concern, excluding radionuclides. This database for background soils enlarges the Laboratory-wide database provided by Longmire et al. (1995). This database primarily consists of mesa top soils, with only three sites within Los Alamos and Ancho Canyons. The UTLs for elements are calculated for the A, B, and C soil horizons in which the greatest number of samples have been collected from the B horizons. Additional sampling and characterization of the A and C horizons is required because few samples (< 30) have been collected from each of these horizons, including samples collected by Longmire et al. (1995). The A horizons are important because they are the surface horizon of many soils found on the Pajarito Plateau underlying potential release sites. Additional soil samples need to be collected on side slopes and within the canyons, because these soils are chemically very different from mesa top soils. There are very few chemical and pedological data and information on canyon soils at the Laboratory.

Longmire et al. (1995) concluded that soils present on the Pajarito Plateau are extremely variable in physical and chemical properties, including particle size, percent calcium carbonate, clay mineralogy, iron oxides, and trace-element chemistry. Results of this investigation support their conclusions and this investigation provides additional information on the local variations of chemical data and different soil parameters at several adjacent soil profiles on mesa tops.

DRAFT DOCUMENT

Well-developed soils on mesa tops have higher concentrations of trace elements relative to weakly developed soils found in canyons. The B horizons generally are higher in trace elements relative to A and C horizons, excluding anthropogenic U found at TA-63 and TA-67. High abundances of clay minerals and iron oxides, characterized by relatively high surface areas, within B horizons control trace-element concentrations in soils. Well developed B (Bt) horizons typically found on mesa tops contain higher concentrations of trace elements than do weakly developed B (Bw) horizons found on mesa tops and in canyon bottoms. In addition, variations in soil-elemental concentrations are related to chemical characteristics of a particular soil horizon and to the parent material. Iron is a useful element to include as part of the analyte list for site characterization investigations because As, Be, and other trace elements correlate well with it.

Several soil samples collected from A and B horizons at TA-63 and TA-67 contain elevated concentrations of U, which may represent aerosol dispersion of U from Laboratory firing sites within TA-67 and TA-15. These apparently biased data have been excluded from the background-elemental database for the Laboratory for purposes of calculating UTLs; however, they may be useful for determining local contamination within TA-63, TA-67, and other sites down-wind from firing sites.

1. We recommend that Characterization of Laboratory-wide and site-specific background element distributions in soils requires use of a multidisciplinary approach involving the Decision Support Council, Earth Sciences Council, and Field Units.
2. We recommend standardizing field sampling procedures and requiring better field descriptions of sampling sites.
3. We recommend using consistent sample digestion (HNO_3) procedures (EPA 3050) prior to chemical analyses to compare background soil samples to SWMU samples.
4. We recommend expanding the background-elemental database for canyon soils to refine calculations of the mean, standard deviation, and UTLs for different RCRA metals and other relevant elements.
5. We recommend that additional sampling and characterization of the A and C horizons because few samples (< 30) have been collected from each of these horizons, including samples collected by Longmire et al. (1995).

DRAFT DOCUMENT

6. We recommend utilizing results of Laboratory-wide background characterization investigations to the fullest extent to enhance maximal success and benefits of remediation strategies at contaminated sites.
7. We recommend a background screening process for RFI screening assessments consists of the following steps:
 - 1) Use LANL-wide background data, which are presented in this report. These data include:
 - a) soil data by horizon,
 - b) geological data by stratigraphic layer, and
 - c) sediment data from Ancho, Indio, and Water Canyons
 - 2) Data analysts will use the appropriate subset of the LANL-wide data, except where soil horizon is neither known nor relevant (e.g., fill of unknown origin was sampled).
 - 3) The initial comparison for all analytes will be to background screening values for all inorganics and naturally-occurring radionuclides (by background data subsets as described above). Background screening values are based on the following sources:
 - a) maximum reported value for fallout-related radionuclides from the LANL environmental surveillance reports,
 - b) maximum reported value for inorganics with more than 20% non-detects,
 - c) maximum reported value for inorganics where the statistical distribution could not be estimated, and
 - d) UTLs calculated for normal, lognormal, or square root-transformed distributions based on a 99th percentile and 95% confidence. NOTE - UTLs for data subsets are checked for consistency with the data group to make sure that inflated UTLs are not used.
 - 4) Additional background analyses are required for the following cases:
 - a) background screening values are exceeded AND SALs are exceeded,
 - b) ecological risk is determined to be primary decision point, or
 - c) aluminum, arsenic, beryllium, or manganese are known (or suspected) to have been released at the PRS.
 - 5) Additional analyses include:
 - a) graphical comparisons of background and PRS data,
 - b) statistical "distribution shift" tests,
 - c) regression analysis of trace elements and major elements (soil and sediment only), or
 - d) regression analysis of Th and U (any solid media)

DRAFT DOCUMENT

Acknowledgments

This work was conducted as part of the Environmental Restoration Project of Los Alamos National Laboratory, supported by the Earth Science Technical Team (Framework Studies) and the Earth Science Technical Council. The authors thank David Broxton, Jamie Gardner, Everett Springer, and Les McFadden for their support; Dan Gerth, Evangeline Hodge, Cynthia Mahan, and Kitty Roberts for analytical chemistry support; Andy Adams, John Carney, and Antonio Garcia, for field and office assistance; and Anthony Garcia for drafting support and Deb Carlson for Splus statistical programming support. Constructive reviews of this report were provided by Andy Adams, David Broxton, Florie Caporuscio, Alison Dorries, Bonnie Koch, Robert Simeone, and Everett Springer.

DRAFT DOCUMENT

REFERENCES

- Alesii, B.A., Fuller, W.H., and Bozle, M.V., 1980, Effect of leachate flow-rate in metal migration through soil, *Jour. Environ. Qual.*, Vol. 9, pp. 115-126.
- American Society of Agronomy, 1986, *Methods of Soil Analysis, Part 1. Physical and Mineralogical Methods*, No. 9, Part 1. American Society of Agronomy, 1188 p.
- Birkeland, P.W., 1984, *Soils and Geomorphology*, Oxford University Press, New York, 372 p.
- Brookins, D.G., 1988, *Eh-pH Diagrams for Geochemistry*, Springer-Verlag, New York, 176 p.
- Broxton, D.E., Heiken, G., Chipera, S.J., and Byers, F.M.Jr., 1995, *Stratigraphy, petrography, and mineralogy of tuffs at technical area 21, Los Alamos National Laboratory, New Mexico: in Phase Report 1A, TA-21 Operable unit RCRA Facility Investigation, Los Alamos National Laboratory Report LAUR 93-2028*, pp. A1-A18.
- Davenport, D.W., 1993, *Micromorphology, mineralogy, and genesis of soils and fracture fills on the Pajarito Plateau, New Mexico*, Ph.D. Dissertation, Texas Tech University, Lubbock, 109 p.
- Drever, J.I., 1988, *The Geochemistry of Natural Waters, Second Edition*, Prentice Hall, Inc., New Jersey, 437 p.
- Dixon, J.B. and Weed, S.B., 1990, editors, *Minerals in Soil Environments, Second Edition*, Soil Science Society of America, Madison, Wisconsin, 1244 p.
- Ebinger, M. H., Essington, E. H., Gladney, E. S., Newman, B. D., and Reynolds, C. L., 1990, *Long-Term Fate of Deplete Uranium at Aberdeen and Yuma Proving Grounds Final Report, Phase I: Geochemical Transport and Modeling*, Los Alamos National Laboratory Report LA-11790-MS, 37 p.
- EPA (US Environmental Protection Agency), April 1992. *Guidance for Data Useability in Risk Assessment (Part A)*, Office of Emergency Remedial Response, US Environmental Protection Agency, Washington DC.
- EPA (US Environmental Protection Agency), April 1989. *Statistical Analysis of Ground-Water Monitoring Data at RCRA Facilities. Interim Final*

DRAFT DOCUMENT

Guidance, Office of Solid Waste, Waste Management Division, US Environmental Protection Agency, Washington DC.

EPA (US Environmental Protection Agency), 1989, Statistical Analysis of Ground-Water Monitoring Data at RCRA Facilities, Interim Final Guidance, Office of Solid Waste Management Division, Washington D.C.

EPA (US Environmental Protection Agency), 1987, EPA Contract Laboratory Program, statement of work for for inorganic analysis, multi-media, multi-concentrations (SOW No. 787), Waste Management Division, US Environmental Protection Agency, Washington DC.

EPA (US Environmental Protection Agency), November 1986, Test Methods for Evaluating Solid Waste. Volume 1A: Laboratory Manual Physical/Chemical Methods Office of Solid Waste, Waste Management Division, US Environmental Protection Agency, Washington DC.

Environmental Restoration Project Assessments Council, March 28, 1995. Statistical Comparisons to Background, Part I," Los Alamos National Laboratory Report LA-UR-95-1217, Los Alamos, New Mexico. (Environmental Restoratiog Project Assessments Council 1995)

Ferenbaugh, R. W., Gladney, E. S., and Brooks, G. H., 1990, Sigma Mesa: Background elemental concentrations in soil and vegetation, 1979, Los Alamos National Laboratory, report LA-11941-MS. 22 p.

Gautier, M. A. and Gladney, E.S., 1986, Health and environmental data management, and quality assurance, editors: Los Alamos National Laboratory report LA-10300-M, Vols. I and II.

Gilbert, R.O., 1987, Statistical Methods for Environmental Pollution Monitoring, Von Nostrand Reinhold Company Inc. New York. 320 p.

Gile, L.H., Peterson, F.F., and Grossman, R.B., 1966, Morphological and genetic sequences of carbonate accumulation in desert soils, Soil Science, Vol. 101, pp. 347-360.

Gladney, E.S., Curtis, D.B., Perrin, D.R., Owens, J.W., and Goode, W.E., 1980, Nuclear techniques for the chemical analysis of environmental materials: Los Alamos Scientific Laboratory report LA-8192-MS.

DRAFT DOCUMENT

- Gladney, E.S., Owens, J.W., Gunderson, T.C., and Goode, W.E., 1981, Quality assurance for environmental analytical chemistry: 1976-1979, Los Alamos National Laboratory report LA-8730-MS.
- Hsi, C.K.D. and Langmuir, D., 1985, Adsorption of uranyl onto ferric oxyhydroxides: Application of the surface complexation site-binding model, *Geochim. et Cosmochim. Acta*, Vol. 49, pp. 1931-1941.
- Joffe, J.S., 1949, *Pedology*: Pedology Publ., New Brunswick, New Jersey, 662 p.
- Kolbe, T., Sawyer, J., Gorton, A., Olig, S., Simpson, D., Fenton, C., Reneau, S., Carney, J., Bott, J., and Wong, I., 1994, Evaluation of the Potential for Surface Faulting at the Proposed Mixed Waste Disposal Facility, TA-67: unpublished report for Los Alamos National Laboratory, Woodward-Clyde Federal Services, Oakland, California, August 1994, 3 volumes.
- Kolbe, T., Sawyer, J., Springer, J., Olig, S., Reneau, S., Hemphill-Haley, M., and Wong, I., 1995, Evaluation of the Potential for Surface Faulting at TA-63: unpublished report for Los Alamos National Laboratory, Woodward-Clyde Federal Services, Oakland, California, January 1995.
- Korte, N.E., Skopp, J., Fuller, W.H., Nieble, E.E., and Alesii, B.A., 1976, Trace element movement in soils: Influence of soil physical and chemical properties, *Soil Sci.*, Vol. 122, pp. 350-359.
- Langmuir, D., 1978, Uranium solution-mineral equilibria at low temperatures with applications to sedimentary ore deposits, *Geochim. et Cosmochim. Acta*, Vol. 42, pp. 547-570.
- Langmuir, D. and Herman, J.S., 1980, The mobility of thorium in natural waters at low temperatures, *Geochim. et Cosmochim. Acta*, Vol. 44, pp. 1753-1766.
- Leckie, J.O., Benjamin, M.M., Hayes, K., Kaufman, G., and Altman, S., 1980, Adsorption/coprecipitation of trace elements from water with iron oxyhydroxide, Electric Power Research Institute, RP-910, various pagination.
- Lindsay, W. L., 1979, *Chemical Equilibria in Soils*, Wiley-Interscience, New York, 449 p.
- Longmire, P., Reneau, S., Watt, P., McFadden, L., Gardner, J., Duffy, C., and Rytli, R., 1995, Natural Background Geochemistry, Geomorphology, and

DRAFT DOCUMENT

Pedogenesis of Selected Soil Profiles and Bandelier Tuff, Los Alamos, New Mexico, 1995: Los Alamos National Laboratory Report LA-12913-MS, Los Alamos, New Mexico (in press).

McBride, M., 1994, Environmental Chemistry of Soils, Oxford University Press, New York, 406 p.

Nyhan, J. W., Hacker, L. W., Calhoun, T. E., and Young, D. L., 1978, Soil Survey of Los Alamos County, New Mexico: Los Alamos Scientific Laboratory Informal Report LA-6779-MS, 102 p.

Rai, D. and Zachara, J.M., 1984, Chemical attenuation rates, coefficients, and constants in leachate migration, Vol. 1: A critical review, Electric Power Research Institute, EA-3356, various pagination.

Reneau, S.L., Kolbe, T.R., Simpson, D.T., Carney, J.S., Gardner, J.M., and Vaniman, D.T., 1994, Surficial materials and structure at Pajarito Mesa, Los Alamos National Laboratory, New Mexico: report prepared for the Los Alamos National Laboratory Mixed Waste Disposal Facility team, 66 p.

Reneau, S.L., Kolbe, T., Simpson, D., Carney, J.S., Gardner, J.N., Olig, S.S., and Vaniman, D.T., 1995, Surficial materials and structure at Pajarito Mesa: *in* Reneau, S. L., and Raymond, R., Jr., eds., Geological Site Characterization For the Proposed Mixed Waste Disposal Facility, Los Alamos National Laboratory: Los Alamos National Laboratory Report, Los Alamos, New Mexico (in press).

Ryti, R.T., 1995, Guidance on making comparisons to natural background concentrations of metals for the Los Alamos National Laboratory Environmental Restoration Project, External review draft, 11 p.

Schacklette, H. T. and Soerngen, J. G., 1984, Element concentrations in soils and other surficial materials of the conterminous United States: United States Geological Survey Professional Paper 1270.

Schwertmann, U., and Taylor, R.M., 1989, Iron oxides: In J.B. Dixon and S.B. Weed (eds.), Minerals in Soil Environments, Soil Science of America Book Series, no. 1, pp. 379-438.

Soil Survey Staff, 1981, Examination and Description of Soils in the Field: in Soil Survey Manual (USDA-ARS) U.S. Government Printing Office, Washington D.C.

DRAFT DOCUMENT

- Soil Survey Staff, 1975, Soil Taxonomy, U.S. Dept. Agri. Handbook No. 436, 754 p.
- Sposito, G, 1989, The Chemistry of Soils, Oxford University Press, New York, 277 p.
- Sposito, G, 1984, The Surface Chemistry of Soils, Oxford University Press, New York, 234 p.
- Stevenson, F.J., 1994, Humus Chemistry, Second Edition, John Wiley and Sons, New York, 496 p.
- Stuiver, M., and Reimer, P.J., 1993, Extended ^{14}C data base and revised CALIB 3.0 ^{14}C age calibration: Radiocarbon, v. 35, pp. 215-230.
- Thurman, E.M., 1985, Organic Geochemistry of Natural Waters, Martinus Nijhoff/Dr W. Junk Publishers, 497 p.
- Watt, 1995, Preliminary report on uncontaminated soil profiles, Los Alamos National Laboratory, New Mexico: Department of Earth and Planetary Sciences, University of New Mexico Albuquerque, New Mexico 93 p.
- Watt, P. M. and McFadden, L., 1992, Preliminary soils analyses from Los Alamos County: Department of Earth and Planetary Sciences, University of New Mexico Albuquerque, New Mexico 90 p.
- Wong, I., Kelson, K., Olig, S., Kolbe, T., Hemphill-Haley, M., Bott, J., Green, R., Kanakari, H., Sawyer, J., Silva, W., Stark, C., Haraden, C., Fenton, C., Unruh, J., Gardner, J., Reneau, S., and House, L., 1995, Seismic Hazards Evaluation of the Los Alamos National Laboratory: unpublished report, Woodward-Clyde Federal Services, Oakland, California, January 1995, 3 volumes.
- Wong, I., Hemphill-Haley, M., Kelson, K., Kolbe, T., Green, R., Kanakari, H., Bott, J., Silva, W., Haraden, C., Gardner, J., House, L., and Reneau, S., 1993, Seismic Hazard Evaluation of the Los Alamos National Laboratory, Draft Final Report: unpublished report, Woodward-Clyde Federal Services, Oakland, California.
- Zachara, J.M., Cowan, C.E., and Resch, C.T., 1993, Metal cation/anion adsorption on calcium carbonate: Implications to metal ion concentrations in groundwater: *in* Metals in Groundwater, Allen, H.E., Perdue, E.M., and Brown, D.S. editors, Lewis Publishers, Michigan, pp. 37-71.

Appendix A

S-Plus Code Used to Calculate Lognormal UTLs

DRAFT DOCUMENT

File: Inorm_utl1.s

```
function(q,p,n,ave,sd,nt)
{
# Inorm_utl1.s is used as function LUTL1 in Splus
# This function is used to estimate the upper 95% CI of the 99th
# percentile for a lognormal distribution. Uses Gilbert's MBE of LN.
# q = the quantile to estimate
# p = the confidence limit of q
# n = number of values sampled
# ave = mean of logtransformed data
# sd = st. dev. of logtransformed data
# nt = number of simulation trials
#.....

# Calculate the qth quantile of the normal distribution
q1_qnorm(q)

# Initialize arrays
t1_rep(-1,n)
t2_rep(-1,nt)

i_0

repeat

{ i_i+1

# Get the "n" lognormal samples
t1_rlnorm(n,ave,sd)

# Calculate the mean and sd the hard "Swanson" way
dummy_InormUMV.s(t1)
ave1_dummy$mu
sd1_sqrt(dummy$s2)

# Calculate an estimate of the 99th percentile
t2[i]_exp(ave1+q1*sd1)
if(i>=nt) break
}

# Find the upper p*100% of the qth percentile
quantile(t2,p)
}
```

DRAFT DOCUMENT

File: InormUMV.s

```
function(x)
{
# InormUMV.s (Splus function)
# Calls: psi.s
# Min Variance Unbiased ests of parameters of lognormal(mu,var=s2) distn
# for X~lognorm(mu,s2), Y=log(X)~normal(mu,s2)
# returns:E=mean(X), V=var(X)
#      mu=mean(Y),s2=var(Y)
# ref:Gilbert('87),Stat Methods for Env Pollution Mon, pp165-166
  n <- length(x)
  y <- log(x)
  ymu <- mean(y)
  vy <- var(y)
  psi1 <- psi.s(vy/2, n)
  psi2 <- psi.s(2 * vy, n)
  psi3 <- psi.s((vy * (n - 2))/(n - 1), n)
  E <- exp(ymu) * psi1
  V <- exp(2 * ymu) * (psi2 - psi3)
  mu <- log(E^2/(V + E^2)^0.5)
  s2 <- log(V/E^2 + 1)
  return(E, V, mu, s2)
}
```

DRAFT DOCUMENT

File: psi.s

```
function(t, n)
{
# psi.s (Splus function)
# called by InormUMV.s
# psi function in Gilbert('87) Stat. Meth. Env. Pollution. Mon, pp 165
# for Min Variance Unbiased ests of parameters of lognormal(mu,var=s2) distn
  psi <- 0
  psi[1] <- ((n - 1) * t)/n
  for(i in 1:25) {
    psi[i + 1] <- (psi[i] * (n - 1)^2 * t)/((i + 1) * n * (n + (2 *
      i - 1)))
    if(abs((psi[i + 1] - psi[i])/psi[i]) < 1e-09)
      break
  }
  psi <- 1 + sum(psi)
  psi
}
```

Geochemistry of Background Sediment Samples at Technical Area 39

Steven Reneau, EES-1, Patrick Longmire, CST-7, Katherine Campbell, EES-5, and Eric McDonald, EES-1

Draft

September 26, 1995

Summary

This report presents results of chemical analyses of 24 analytes in 16 background sediment samples collected from Ancho Canyon and Indio Canyon at Technical Area (TA) 39. Systematic variations in the background chemistry of sediments at TA-39 occur between different geomorphic settings and different particle sizes. These differences indicate that the best comparison of potentially contaminated sediments to background should utilize the most comparable subset of the background data set. The lowest concentrations of most analytes occur within coarse, well-sorted sands in active stream channels (which are dominated by quartz and sanidine crystals), and the concentrations of most analytes generally increase with decreasing sediment particle size. The concentration of U within a sample of black sand (dominated by high density magnetite grains) was within the range of other background samples. This relationship is important because the presence of higher concentrations of U in black sand deposits would thus indicate anthropogenic U that was concentrated by density as in a placer deposit.

Analyte concentrations in sediments are generally lower than those associated with B horizons in soils, but are comparable to elemental concentrations within the A and C horizons. Concentrations of elements in the sediments are strongly influenced by the total surface area available for adsorption, and concentrations of trace elements are minimal within the medium- and coarse-grained sediments with low surface areas relative to silt and clay. Different minerals concentrated in the sediments, such as magnetite, however, are higher in trace elements resulting

mainly from ionic substitution within the mineral lattice. For example, magnetite-rich black sands are higher in As, Be, Cr, Mn, Ni, Pb, Th, U, V, and Zn relative to silicate-rich sediments.

Correlations exist between concentrations of different metals in the sediment samples (i.e., Fe and As, Fe and Be) that are similar to those present in soils at the Laboratory, although the concentrations of metals in the sediments are generally less than in the soils. Relationships between Fe and other metals of concern can be used to evaluate whether anomalously high values in a data set are within background ranges or instead reflect contamination.

Concentrations of many analytes from sampled prehistoric channel and floodplain sediments are higher than their concentrations in recent deposits, probably caused by post-depositional additions of solutes associated with shallow groundwater flow within the alluvium. The processes that increased concentrations of some trace elements within the prehistoric deposits may be similar to the processes affecting old sediments beneath the valley floor penetrated in core holes, suggesting that higher concentrations of many trace elements might be encountered in the subsurface than in surface sediment samples.

Principal components analysis (PCA) indicates that 91% of the variability in the background sediment data set can be accounted for by a single component, which is due to the strong correlations that occur between many major and trace elements. The remaining 9% is almost entirely accounted for by a second component that separates the two sample areas in Ancho and Indio Canyons. These results are similar to those obtained by PCA of the background soil data set of Longmire et al. (1995), for which overall variability is dominated by strongly correlated variation of several major and trace elements, and variation between sample sites is the second most important source of variability. Preliminary upper tolerance limits (UTLs) exceed the maximum values by up to 50%, and will require revision as more background sediment data are obtained.

Introduction

Sixteen sediment samples were collected from Ancho and Indio Canyons, TA-39 (Fig. 1), in August 1994 to provide background chemical concentrations from deposits comparable to those

collected as part of Field Unit 2 (OU 1132) site characterization activities in Ancho Canyon. TA-39 has been used as a high-explosives firing site since 1953, and contaminants of potential concern that may have dispersed during experiments include Ba, Be, Cr, Pb, Tl, and U (LANL, 1993).

Two primary sample areas were chosen to increase the chance that the range of variability in natural sediment deposits were included and that any unanticipated contamination would be detected. The main sample areas are Indio Canyon, the largest drainage basin in the Laboratory entirely within Bandelier Tuff that has had no Laboratory facilities, and a small tributary to Ancho Canyon near State Road 4 that also has no upstream Laboratory activities (Fig. 2). An additional sample site is a stream bank along Ancho Canyon that exposes prehistoric (1000-3000 year old) sediments, which was chosen to evaluate whether such old deposits could also be used to provide valid background values. Sampled deposits were chosen to maximize the natural variability that exists within these sediments, and to evaluate systematic variations in chemistry that may exist between different geomorphic settings (i.e., channel vs. floodplain; Fig. 3) and between different size fractions. Descriptions of the samples analyzed in this study are presented in Table 1.

One limitation of this sampling program is the small size of the sample set from any specific geomorphic setting or type of deposit (i.e., coarse sands in active channel), at most two per sample set. These data, therefore, may not encompass the full range of variability that exist in sediments at TA-39. However, there is generally an internal consistency in this data set and systematic variations exist between settings and size fractions, suggesting that this limited data set may be generally representative of similar settings in drainage basins underlain entirely by Bandelier Tuff.

Laboratory Methods

Sediment samples were dried at low temperature in a laboratory oven and sieved to remove gravel (> 2 mm) and roots. Splits of two large floodplain samples were dry sieved to separate the samples into three different size fractions: 0.25-2 mm (coarse and medium sand), 0.25-0.075 mm (fine sand), and < 0.075 mm (very fine sand, silt, and clay). Clumps of sediment were manually crushed, but no chemical dispersants were used and the larger size fractions may therefore contain small portions of finer particle sizes.

Sample splits of all sediment samples were subject to three laboratory pretreatment procedures: partial digestion using nitric acid (HNO₃) at pH 1 (following EPA procedure 3050), which simulates the bioavailability of elements by humans through ingestion; leaching with deionized water, for analysis of easily dissolved Cl and SO₄; and complete digestion using hydrofluoric acid (HF), to provide total elemental concentrations. Analysis of As was by electrothermal vapor atomic absorption (ETVAA); of Cl and SO₄ by ion chromatography (IC); of Ta, Th, Tl, and U by inductively coupled plasma mass spectroscopy (ICPMS); and the remainder by inductively coupled plasma emission spectroscopy (ICPES). Results of the chemical analyses are presented in Tables 2, 3, and 4.

Quality Assurance Checks

Sample splits of two bulk floodplain samples were submitted for analysis to provide an independent quality assurance (QA) check of the reproducibility of the analyses. For the combined 92 duplicate analyses of 24 analytes from the two sets of paired samples and two sample digestion procedures, 87 of the duplicate analyses (95%) were within the reported uncertainty, and three of the remainder (3%) were within twice the reported uncertainty (analyses of Al, Be, and Ni for one of the sample pairs). Only two sets of analyses (2%) were not consistent within twice the reported uncertainty, As and Ta for the paired samples FS2229 and FS2232. Overall, these results therefore indicate that the laboratory analyses can be considered reproducible within normal statistical limits.

Comparison of Channel Samples and Floodplain Samples

Significant differences in analyte concentrations are present between the samples of coarse channel sands and the bulk floodplain samples, as summarized in Tables 5 and 6. For nearly all analytes, concentrations are higher in the floodplain deposits than in the channel deposits, as shown for As, Be, and U in Figure 4. This is consistent with the dominance of quartz and sanidine phenocrysts derived from the Bandelier Tuff within the channel deposits, and with the higher concentrations of fine-grained sediment in the floodplain deposits that could both have

greater mineralogical variability (including higher abundances of clay minerals and ferric oxyhydroxides) and larger amounts of adsorbed trace elements. These differences indicate that the most precise evaluation of the presence or absence of contaminants within sediment samples and their possible concentrations should consider the geomorphic setting of the sediment samples. Specifically, lower natural concentrations of U, Be, and other analytes should be expected in the channel sands than in the floodplain deposits, and concentrations of these elements within potentially contaminated channel sediments should be compared to the coarser-grained background samples and not the full data set.

Analyses of Black (Magnetite-Rich) Sands

One sample of relatively clean black (primarily magnetite, Fe_3O_4) sand from Indio Canyon was analyzed to examine the natural elemental concentrations within these heavy mineral deposits. Field measurements of one black sand deposit near a TA-39 firing site had indicated above background radioactivity, and laboratory X-ray fluorescence (XRF) analyses of a sample from this site confirmed high concentrations of U (217 ppm; Ed Essington, unpublished data, 1994). It was thus hypothesized that such black sands may concentrate some anthropogenic heavy metals such as U as a "placer" deposit, and that selective sampling of black sands could provide an additional tool to examine the transport of high-density contaminants away from firing sites.

The sampled black sands from Indio Canyon (FS 2225, Tables 2 and 3) have very high concentrations of many elemental species, including the highest concentrations of Fe, Mn, Sb, Th, V, and Zn from the HNO_3 digestion and Cr, Mn, Ni, Sb, Th, V, and Zn from the HF digestion (the low reported value of Fe in the HF digestion is believed to be due to laboratory error). Notably, although the concentration of U in the black sands was higher than in the typical channel sands, it was within the range of analyses from the floodplain samples. This indicates that where concentrations of U in black sands exceed the range of background floodplain samples, anthropogenic U may be present, and supports the hypothesis that depleted uranium particles from firing sites can be concentrated downstream in black sands due to sorting of sediment particles by their respective densities during transport by surface water.

In addition to U, many other analytes are also present in higher concentrations in the black sands than in other sediments in these canyons. As an example, Figure 5 shows the elemental concentrations for the black sands and the bulk sediment samples collected within the active channel deposits in Indio Canyon. These differences in elemental concentrations indicate the importance of mineralogy in influencing trace element distributions in heterogeneous sediments. The ratio of the elemental concentration in the black sands to the concentration in nearby channel deposits varies greatly between elements, and these ratios (HNO_3 digestion) in decreasing order are: V (47) > Zn (33) > Mn (23) > Be (17) > Cr (12) > Th (10) > Ni (9) > U (5) > As (4) > Pb (3) > Sb (1). The higher concentrations in the magnetite-rich sands occur as a result of ionic substitution of the trace elements with one or more major elements within the mineral lattice (Bloss, 1971) and/or adsorption onto alteration products such as ferric oxyhydroxides (Rai and Zachara, 1984).

Comparison of Different Size Fractions Within Floodplain Samples

Two large samples of floodplain deposits, one each from Ancho and Indio Canyons, were separated into three different size fractions to further examine the relation of particle size to elemental variability. A comparison of the elemental concentrations in these separates with the coarse channel sands (Tables 7 and 8), reveal several notable points.

Concentrations of most analytes progressively increase from the coarse channel sands to the fine sand separate, although element concentrations in the fine sands are generally indistinguishable from the very fine sand, silt, and clay fraction. These variations support the general increase in trace element concentration with decreasing grain size as indicated by the comparison of the channel sands with the bulk floodplain deposits. The similarity of the two finer size separates, however, suggests either that they are mineralogically similar or that they have similar adsorptive properties. Specifically, the percentage of clay minerals in these samples is unknown, and it is possible that they have very low clay contents, being dominated by very fine sands and silts that are geochemically similar to the fine sand fractions. For example, grain size analysis of a texturally-similar floodplain deposit overlying the sampled prehistoric channel sands

in Ancho Canyon indicate the presence of only 8-9% clay-sized particles, compared with 26-44% silt and 47-66% sand (Bw1 and Bw2 horizons of Longmire et al., this report, Ancho Canyon site). Alternatively, because chemical dispersants were not used to disaggregate clays, it is possible that the coarse size fractions include aggregates of silt and clay or thin clay coatings on larger sediment particles. The higher analyte concentrations in the coarse and medium sand separates than in the channel sands suggest that the latter are perhaps better sorted, containing a higher percentage of quartz and sanidine crystals from the Bandelier Tuff, and also suggest that the coarse and medium sand separates may provide an analog with relatively "dirty" or less well sorted channel deposits.

Mud Deposit

One sample of a one-day old mud deposit from a flood in Indio Canyon (FS 2226, flood of August 24, 1994) was collected as a possible fine-grained end member of natural sedimentary deposits in this environment. This deposit has the highest concentrations analyzed for several elements, including Al, Ba, Be, Ca, Mg, Na, Pb, and U for the HNO₃ digestion and Ta, Tl, and U for the HF digestion (Tables 2 and 3). Comparisons of concentrations of As, Be, and U in the mud deposits with channel and floodplain deposits are shown in Figure 4. For several analytes, the mud deposit exceeded element concentrations in the fine floodplain fractions taking into account the analytical uncertainties. These analytes are Be, Cu, Pb, and U for both the HNO₃ and HF digestion and also Na for the HNO₃ digestion. The difference between the dominance of certain elements in the partial (HNO₃) and total (HF) digestions of samples from this deposit may be due to the presence of dissolved components that had been deposited at this site by evaporation, followed by precipitation and/or adsorption of solutes onto silt- and clay-sized sediments. Another possible complication with this deposit is that the proximity of State Road 4 may be responsible for the anomalous presence of certain elements derived from automobile exhaust, such as Pb. The high concentrations of other elements, such as U, may be more likely due to their adsorption onto silt- and clay-sized particles, although part of the U and other elements may be anthropogenic, dispersed from the TA-39 firing sites (see discussion in Longmire et al., this report, concerning possible anthropogenic U in surface horizons of some mesa-top soils).

Comparison of Modern Sediment Samples and Prehistoric Samples

Samples of prehistoric sediments exposed in a stream bank along the main fork of Ancho Canyon were analyzed to test the hypothesis that prehistoric sediments could provide a reasonable local background in areas where adequate local background samples could not otherwise be obtained from active channels and floodplains because of the possibility of contamination. Alternatively, these samples may be more comparable to sediments penetrated at depth in a core hole than to surface samples because of post-depositional geochemical changes associated with shallow groundwater flow or vadose zone transport over long periods of time. Erosion of the sampled stream bank along the main drainage of Ancho Canyon exposed a section of coarse channel sands and gravels overlying an older floodplain deposit, shown schematically in Figure 3. Radiocarbon dating of charcoal contained within these sediments provided ages of about 1200 yrs for the channel sands and about 3200 yrs for the underlying floodplain deposit, demonstrating their prehistoric age.

Analyses from the prehistoric sediment deposits (FS2227 and FS2228) were compared to both the bulk channel and floodplain deposits and to appropriate size fractions from the separated floodplain deposits to ensure that possible natural variability within the modern deposits was being considered (Tables 9 and 10). The prehistoric channel sands were thus compared with the medium and coarse sand fractions of the floodplain deposits, and the prehistoric floodplain deposits were compared with the fine sand to clay fractions of the modern floodplain deposits.

This comparison indicated that for most elements the modern and prehistoric samples could not be distinguished, but that for some elements significant differences exist that suggest post-depositional elemental mobility over the last 1000 to 3000 years. The old channel sand deposit in particular differed from both the modern channel deposits and also the medium and coarse sand fraction of the floodplain deposits with higher concentrations of Co, Cr, Fe Mn, V, and Zn in both the HNO₃ and the HF digestions, Ba, Ca, Mg, and Ni in only the HF digestion, and Cl and SO₄ in the deionized water leachate. As compared to the finer fractions of the recent floodplain

deposits, the old floodplain deposits had higher concentrations of Na in the HNO₃ digested fraction and Cl and SO₄ in the deionized water leachate.

The differences seen between the modern and the prehistoric deposits suggest which elements may be naturally higher in subsurface samples penetrated in boreholes due to solute transport, mineral precipitation, and adsorption processes. Notably, some contaminants of concern at TA-39, such as Be and U, are similar between the recent and the old deposits, suggesting that natural concentrations of Be and U in the subsurface may be similar to those in young deposits.

Arsenic and Beryllium in Sediments

Arsenic and Be are of special concern at the Laboratory in evaluations of possible contamination because their concentrations in soils routinely exceed action levels established by the Environmental Protection Agency (EPA) (0.4 ppm for As and 0.16 ppm for Be, using HNO₃ digestion) (Longmire et al., 1995). As a result, the evaluation of As and Be in soils currently is based on a comparison with background values, and not to action levels, and background values thus play a key role in the decision making process. The analytical data obtained in this study similarly show that concentrations of As and Be in the sediment samples exceed the previously established action levels, although their concentrations are generally less than observed in soils.

The concentrations of As and Be are generally strongly correlated with Fe concentration in soils at the Laboratory (Longmire et al., 1995, this report), and these elemental relationships are also present in the sediments collected within Ancho and Indio Canyons. Figures 6 and 7 are bivariate plots of As versus Fe and Be versus Fe for these sediments, showing high regression coefficients (r^2) of 0.84 and 0.95, respectively. These plots are useful in defining the natural distribution field for As and Be as they relate to Fe concentration, and in recognizing which values may indicate contamination as opposed to natural variations in background concentrations of these analytes.

Comparison With Background Soils

The background sediment samples from Ancho and Indio Canyons were compared with background soils data from the Laboratory (Longmire et al., 1995) to evaluate if the sediment chemistry was similar to certain parts of the soil data set. In general, elemental concentrations in the sediments are most similar to soil samples that contained low concentrations of Fe. In the soils, Fe concentration is generally correlated with the percentage of clay-sized particles in each sample (Longmire et al., 1995), and the lower elemental concentrations present in the TA-39 sediments are consistent with their relatively low Fe content. For example, bivariate plots of As versus Fe and Be versus Fe for background soils and sediments collected at the Laboratory are shown in Figures 8 and 9. Arsenic, Be, and Fe concentrations in the sediments are most similar to concentrations within A and C horizons or within weakly developed B horizons in soils. We thus infer that either the dominant source for the sediments is erosion of soils containing low concentrations of Fe, or that much of the fine-grained Fe-rich component of the soils is winnowed out of the sediments during transport in floods, being carried downstream towards the Rio Grande.

Principal Components Analysis

The variability within the background chemical data set was examined statistically using a principal components analysis (PCA). The concentrations of 21 major and trace elements that are generally observed above detection levels in each sample can be represented by a vector in a 21-dimensional space. PCA is a rotation of these natural coordinates that allows us to capture most of the variability among the samples in far fewer than 21 dimensions, however, because concentrations of the various elements are in general highly correlated (Everitt and Dunn, 1991). In brief, PCA describes the dispersion of an array of m observations in n -dimensional space (here, the concentrations of n elements in m samples of soil and/or sediments) in terms of a set of orthogonal coordinates (called the principal components) that are ordered as follows. The first principal component is in the direction of greatest variation. If we consider the observations as a cloud of points in a n -dimensional space, the first principal component is the direction parallel to which this cloud has its greatest length. The second principal component is constrained to be orthogonal to the first and oriented in the direction in which the cloud has the largest width, and so

forth. Typically a cloud of multivariate observations is elongated, with significant variation in far fewer than n dimensions, so that PCA allows for the reduction of the dimensionality of the problem of evaluating multidimensional data. In this section we use PCA to further evaluate, both qualitatively and quantitatively, the differences and similarities between the background soil data of Longmire et al. (1995) and the background sediment samples of this report.

Principal components analysis of the background soil samples of Longmire et al. (1995) (21 analytes in 44 samples assigned to A, B, or C horizons, using a HNO_3 digestion) shows that 68% of the total variance among these samples is accounted for by the first principal component, and 92% by the first three principal components (out of 21).

Large values of the first principal component correspond to high concentrations of many elements and correlations that exist between elements. In particular, the major elements Al, Fe, Mg, and K are highly correlated with this first principal component (and with each other), as are several minor and trace elements: As, Be, Cr, Cu, Ni, Th, and V. Sulfate, Cl, Mn, Na, U, and Zn are poorly correlated with this component and with the elements listed above. Samples above median total enrichment for soils (as measured by the first principal component) are predominantly from B horizons (Fig. 10), suggesting that the most important control on variability in these data is the degree of soil development (most likely due to increases in clay and iron oxyhydroxides), as postulated by Longmire et al. (1995).

Variations in the concentrations of Ca, Zn, Mn, Na, and sulfate dominate the second and third principal components. These components serve primarily to separate the discrete locations sampled by Longmire et al. (1995). For example, soil samples collected in upper Los Alamos Canyon (exceptionally high in organic matter) are strung out at the upper end of the second component (towards the top of Fig. 10). Samples collected in TA-69 from a well-developed, clay-rich soil, cluster at lower end of this component but are high relative to the third component, with a couple of exceptions. The samples collected from a poorly developed soil in lower Los Alamos Canyon near the Tsankawi ruins are grouped at the low end of the third component.

Exploiting the reduction in dimensionality obtained by PCA allows us to visualize the large multivariate data set in two or three dimensions, and further, to see where the sediment samples

that are the subject of this report fall with respect to the soil samples. The floodplain sediment samples from Ancho and Indio Canyons generally occur well within the cloud defined by the background soil samples (Fig. 10). Relative to the soil samples, the floodplain samples have low concentrations of many elements, that is they occur at the low end relative to the first principal component. With respect to the next two principal components they generally occur near the middle of the distributions. The recent mud deposit sample is similar to the finer-grained separates of the floodplain samples (Fig. 10).

The channel sands lie on the edge of the cloud formed by the soil samples (Fig. 10). The modern channel sands are typically lowest in concentrations of most analytes, and they also fall at the low end of the third component. By contrast, the old channel sand sample is higher in many analytes compared to the floodplain samples but has a larger third component than any soil sample.

The power of the PCA method for detecting outliers is best seen in the case of the unique black magnetite-rich sand sample. With respect to the first principal component, it is only slightly above the average for the soil samples. With respect to the next two components, however, it is well outside the range covered not only by the other sediment samples but also by all the samples discussed by Longmire et al. (1995). That is, although not extraordinarily high compared to B-horizon samples in general, the proportions of the elements in this sample are such as to place it far outside the "cloud" of other observations in the 21-dimensional space.

Among the modern floodplain samples, segregation of analyte concentration by grain size is pronounced. The coarse fraction (0.25 to 2 mm) varies from 5223 to 6174 in the first principal component, while the medium and fine fractions vary from 10388 to 11475. The bulk samples are intermediate, at 7148 to 11534.

Similar results are observed when the sediment samples are analyzed by themselves using PCA. Specifically, a first principal component is highly correlated with general enrichment in almost all elements, induced largely by the different grain sizes among the available samples (Fig. 11). This first principal component accounts for 91% of the variability among the modern floodplain and channel samples. The remaining 9% is almost entirely accounted for by a second

component that separates the two sample areas, Ancho and Indio Canyons, indicating minor chemical differences between sediments from these sites.

Summary Statistics For Background Sediment Samples

Summary statistics for the sediment data are presented in Table 11. In view of the fact that for both the soil data and the sediment data, sample location is the second most important explanatory factor for the variation in observed concentrations, as shown by the principal components analysis, the sediment data discussed in this report should be considered strictly preliminary. Two sample areas are almost certainly insufficient to represent the scope of variability that will be encountered when more background sediment locations from other parts of the Pajarito Plateau are added.

This caveat should be borne in mind when using the statistics shown in Table 11, which include medians, means, standard deviations, minima, maxima and (.95,.95) UTLs based on the 16 sediment samples. The statistics were calculated based on values from all samples, excluding outliers in the data set that would inflate the estimate of the mean by more than 10%. These outliers are presented in Table 12, and include values for the black magnetite-rich sands, the recent mud deposit, and the prehistoric channel and floodplain deposits. The UTLs in Table 11 are calculated following procedures discussed in EPA (1989), and indicate values that we are 95% confident exceed the 95th percentiles of the true distributions. These UTLs are up to 50% larger than the maximum values observed, as a result of the small sample size, and will require revision as more background sediment samples are obtained.

Implications for Sampling and Interpretation of Data

The data set discussed in this report is limited by its small sample size, and thus may not be representative of the full range of background sediment chemistry present at TA-39. In addition, this data set is not intended to be representative of all sediments on the Pajarito Plateau as the sampled canyons entirely drain areas underlain by the Bandelier Tuff. For example, additional variation will undoubtedly occur in the canyons that head in the Sierra de los Valles and thus drain

areas underlain by Tschicoma Formation dacite. However, the results of this study suggest several implications for the collection of samples and the interpretation of analytical data that should allow improved evaluations of potential contamination in sediments at the Laboratory.

First, because of the dependence of sediment geochemistry on grain size and mineralogy, field notes on the characteristics of each sample (such as the general grain size or the presence of black sands) can be valuable in understanding variations in the analytical data. Second, the correlations that are present between Fe and other metals can be used as an additional test for possible deviations from background, such as for high values that may lie beyond the background data set but still be consistent with the natural elemental trends. Third, selective sampling of certain types of deposits (such as black magnetite-rich sands where dense particles like depleted U may be concentrated) may be useful in examining the distributions of contaminants. Finally, sediments in the subsurface sampled in core holes may have significantly higher concentrations of certain elements than surface sediment due to post-depositional alteration associated with migrating water, and selection of appropriate background samples for comparison needs to be made accordingly.

Acknowledgments

This work was supported by the Framework Studies Program and the Earth Science Technical Council of the Environmental Restoration Project, in close coordination with the OU 1132 (FU 2) field team. We thank Jamie Gardner, EES-1, and Everett Springer, EES-15, for their support, and Ed Essington, EES-15, for discussions concerning OU 1132 sediment sampling efforts. Lara Heister, EES-1, assisted with the field work and laboratory sample preparation, and CST-3 performed the chemical analyses.

References

Bloss, F. D., 1971, *Crystallography and Crystal Chemistry*: New York, Holt, Rinehart and Winston, 545 p.

Everitt, B. S., and Dunn, G., 1991, Applied Multivariate Data Analysis: New York, Halsted Press.

EPA (U.S. Environmental Protection Agency), 1989, Statistical Analysis of Ground-water Monitoring Data at RCRA Facilities. Interim Final Guidance: Office of Solid Waste, Waste Management Division, U.S. Environmental Protection Agency, Washington, D.C., April 1989.

LANL, 1993, RFI Work Plan for Operable Unit 1132: unpublished report, Los Alamos National Laboratory.

Longmire, P., Reneau, S., Watt, P., McFadden, L., Gardner, J., Duffy, C., and Ryti, R., 1995, Natural background geochemistry, geomorphology, and pedogenesis of selected soil profiles and Bandelier Tuff, Los Alamos, New Mexico, 1995: Los Alamos National Laboratory Report LA-12913-MS (in press).

Longmire, P., McDonald, E., Ryti, R., Reneau, S., and Watt, P., Natural background geochemistry of selected soil profiles, Los Alamos, New Mexico: (this report).

Rai, D., and Zachara, J. M. 1984, Chemical attenuation rates, coefficients, and constants in leachate migration, Volume 1: A critical review: Electric Power Research Institute Report EA-3356, Richland, Washington.

Figure Captions

Figure 1. Location map of TA-39.

Figure 2. Location map of background sediment sample sites in Ancho and Indio Canyons.

Figure 3. Schematic sketch showing geomorphic setting of background sediment samples.

Approximate ages of sediments are from radiocarbon analyses of charcoal collected from Ancho Canyon sample site.

Figure 4. Comparison of the concentrations of As, Be, and U between floodplain deposits (sample FS 2220), active channel deposits (sample FS 2224), and mud deposits (sample FS 2226) in Indio Canyon, using HNO₃ digestion.

Figure 5. Comparison of the concentrations of selected elements in black, magnetite-rich sands (sample FS 2225) and active channel sands (sample FS 2224) in Indio Canyon, using HNO₃ digestion.

Figure 6. Plot of As vs. Fe for background sediment samples in Ancho and Indio Canyons (excluding samples FS 2223, 2225, 2228, and 2232), using HNO₃ digestion.

Figure 7. Plot of Be vs. Fe for background sediment samples in Ancho and Indio Canyons (excluding samples FS 2223, 2225, 2228, and 2232), using HNO₃ digestion.

Figure 8. Plot of As vs. Fe for background sediment samples in Ancho and Indio Canyons (excluding samples FS 2223, 2225, 2228, and 2232), and the A, B, and C horizons of background soils at the Laboratory (Longmire et al., 1995), using HNO₃ digestion.

Figure 9. Plot of Be vs. Fe for background sediment samples (from active channels and floodplains) in Ancho and Indio Canyons (excluding samples FS 2223, 2225, 2228, and 2232), and the A, B, and C horizons of background soils at the Laboratory (Longmire et al., 1995), using HNO₃ digestion.

Figure 10. Background soil samples of Longmire et al. (1995) and sediment samples of this report displayed in a coordinate system defined by the first two principal components of the background soil data set. The black sand sample lies outside of this plot. See text for discussion.

Figure 11. Sediment samples from Ancho and Indio Canyons displayed in a coordinate system defined by their first two principal components. The black sand sample and the prehistoric channel sample from Ancho Canyon lie outside of this plot.

List of Tables

Table 1. Location of sample sites and description of samples, TA-39.

Table 2. Chemical data for samples, TA-39, HNO₃ digestion.

Table 3. Chemical data for samples, TA-39, HF digestion.

Table 4. Chemical data for samples, TA-39, deionized water leachate.

Table 5. Summary of background sediment analyses, TA-39, HNO₃ and deionized water digestion.

Table 6. Summary of background sediment analyses, TA-39, HF digestion.

Table 7. Summary of different size fractions, TA-39, HNO₃ and deionized water digestion.

Table 8. Summary of different size fractions, TA-39, HF digestion.

Table 9. Comparison of modern and old deposits, TA-39, HNO₃ and deionized water digestion.

Table 10. Comparison of modern and old deposits, TA-39, HF digestion.

Table 11. Summary statistics for background sediment samples.

Table 12. Outliers in background sediment data set.

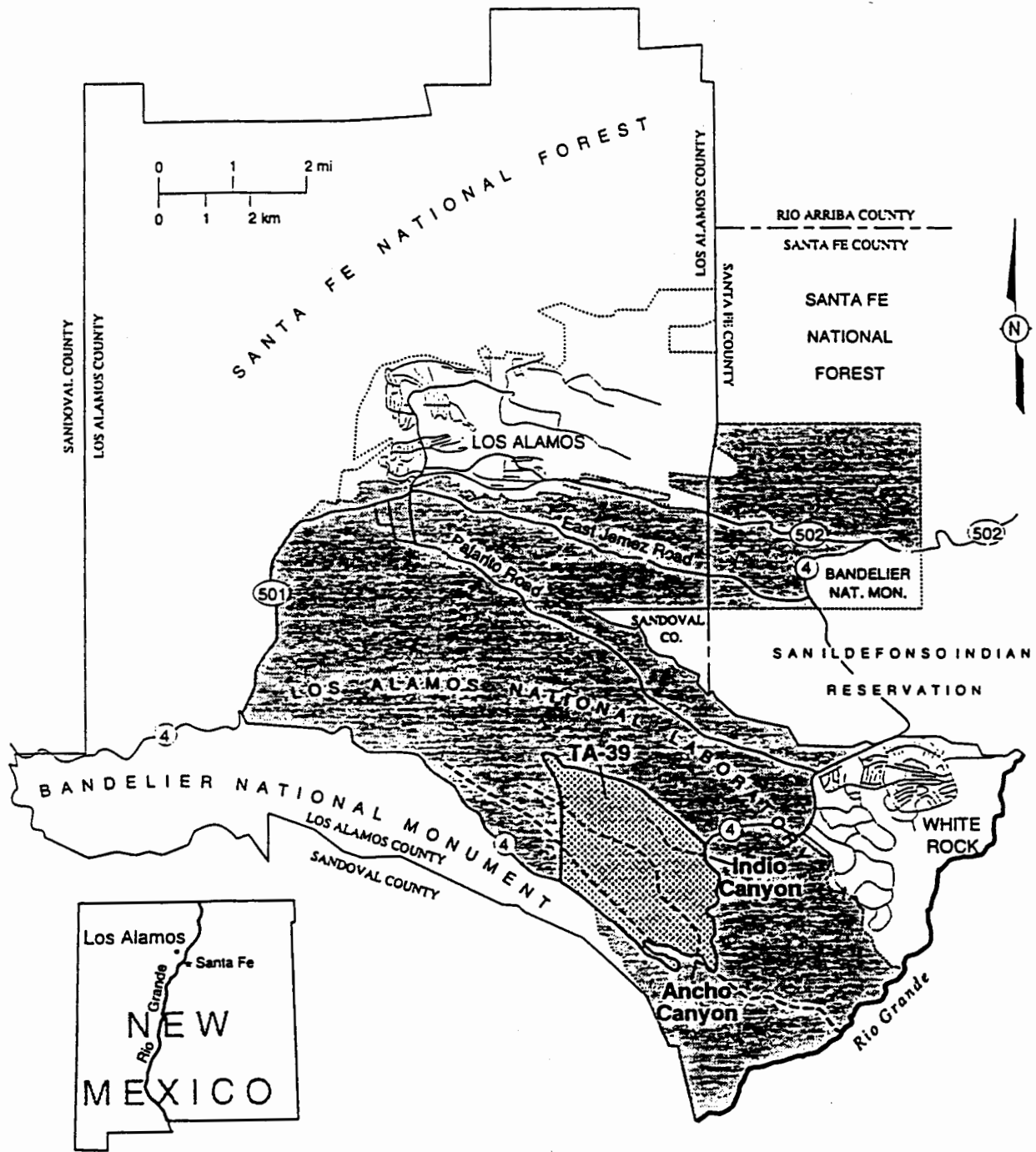
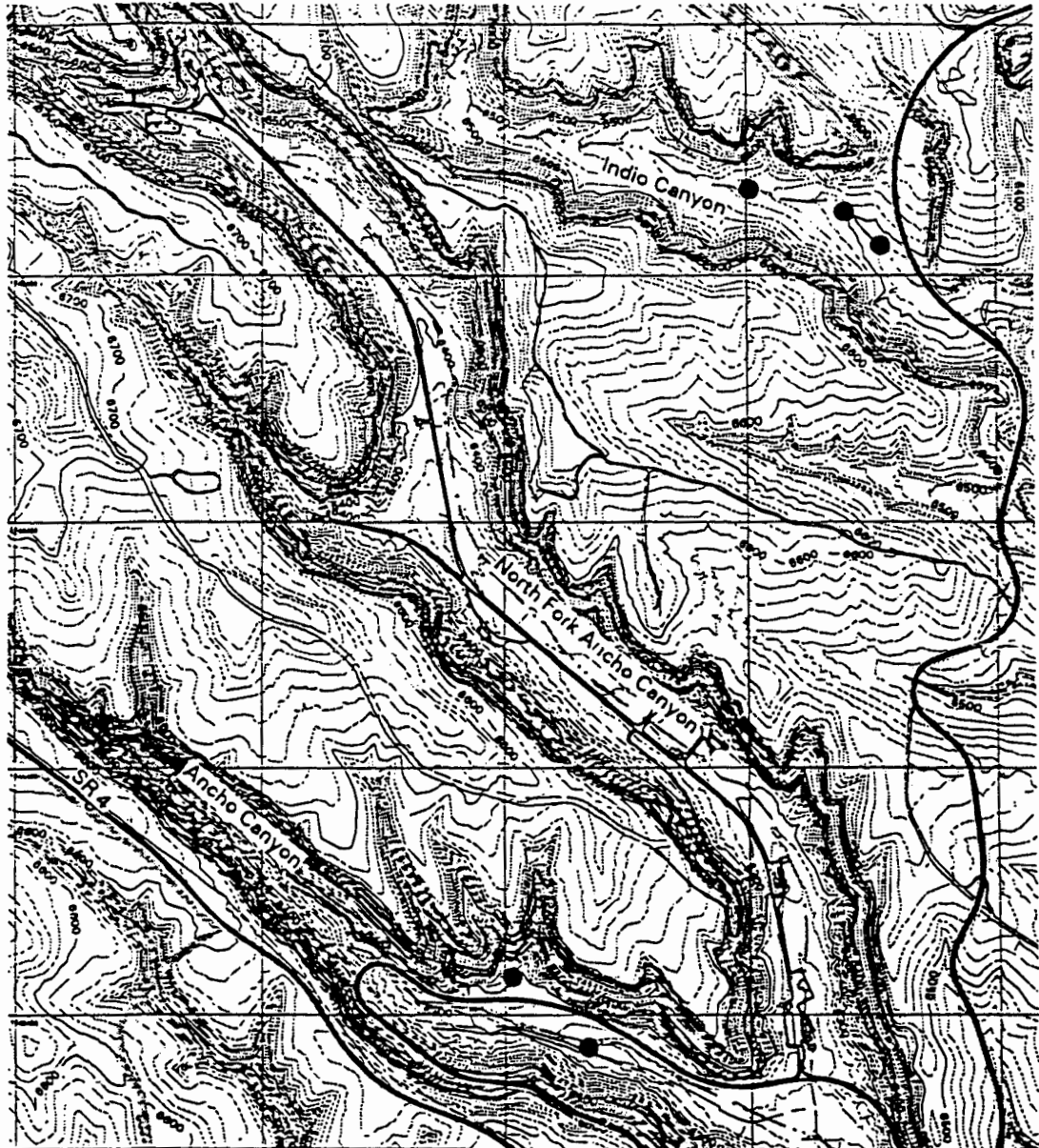


Fig. 1



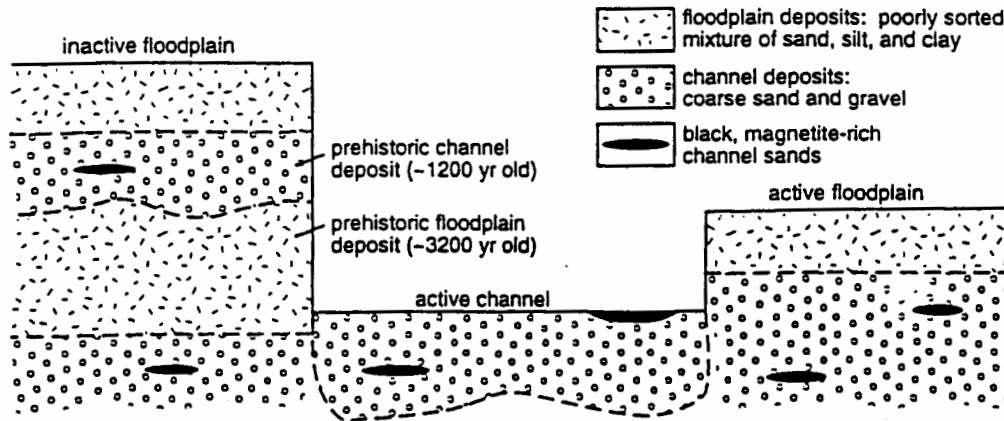
	Structure
	Contour, 10 ft
	Contour, 100 ft
	Dirt Road
	Paved Road
	TA Boundary
	Background Sediment Site

FEET

1983 North American Datum
 Projection and Grid Ticks:
 New Mexico State Plane Coordinate System,
 Central Zone (Transverse Mercator)
 Grid Interval: 2000 feet

Notice: Information on this map is provisional
 and has not been checked for accuracy.

FIMAD G103466 31 May 95



11:30

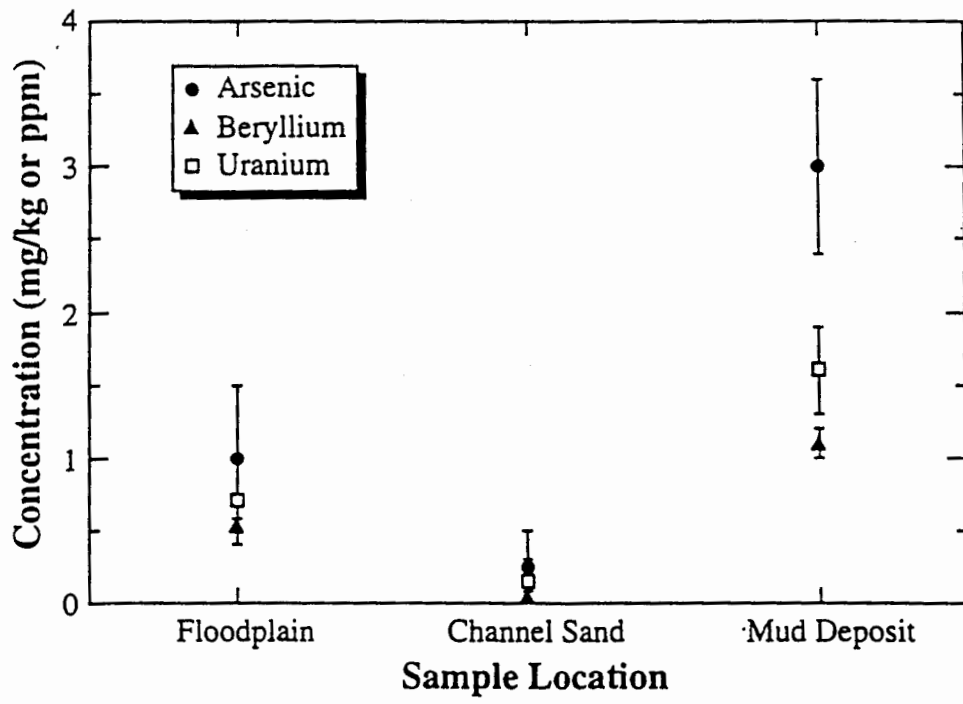


Fig. 4

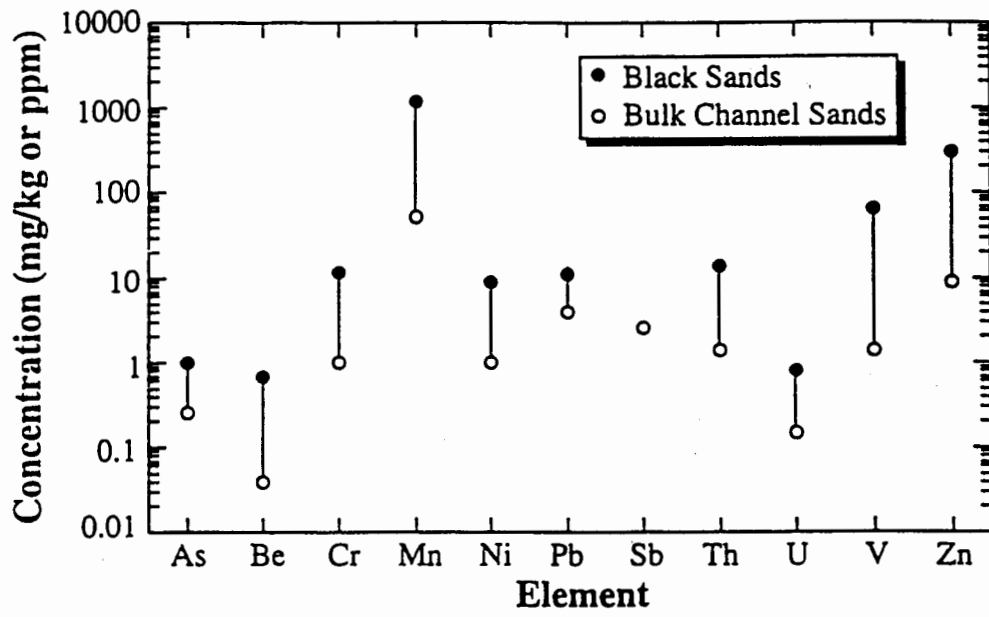


Fig. 5

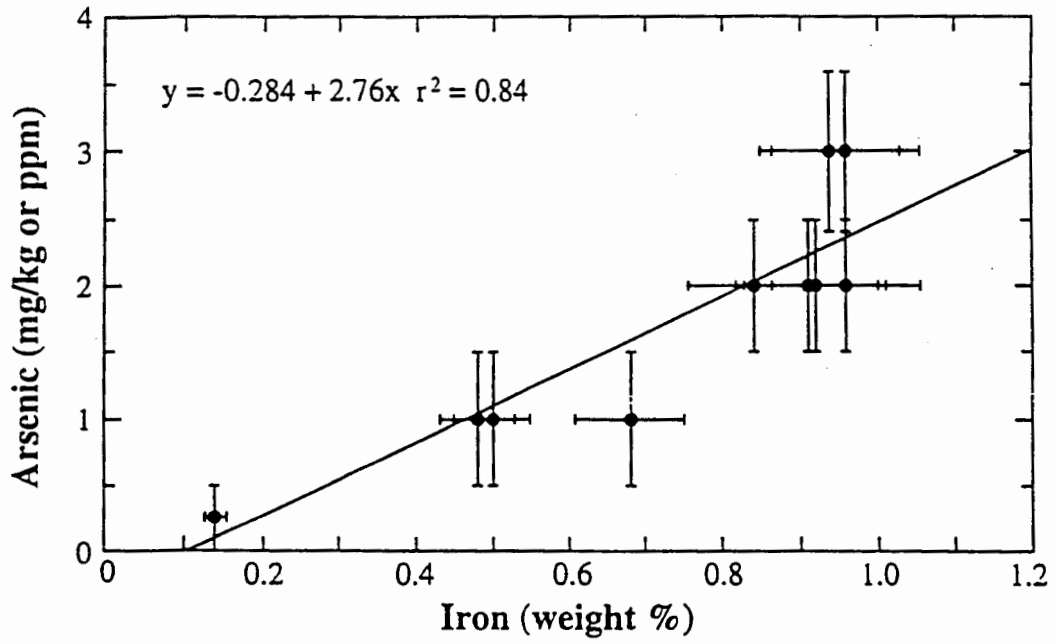


Fig. 6

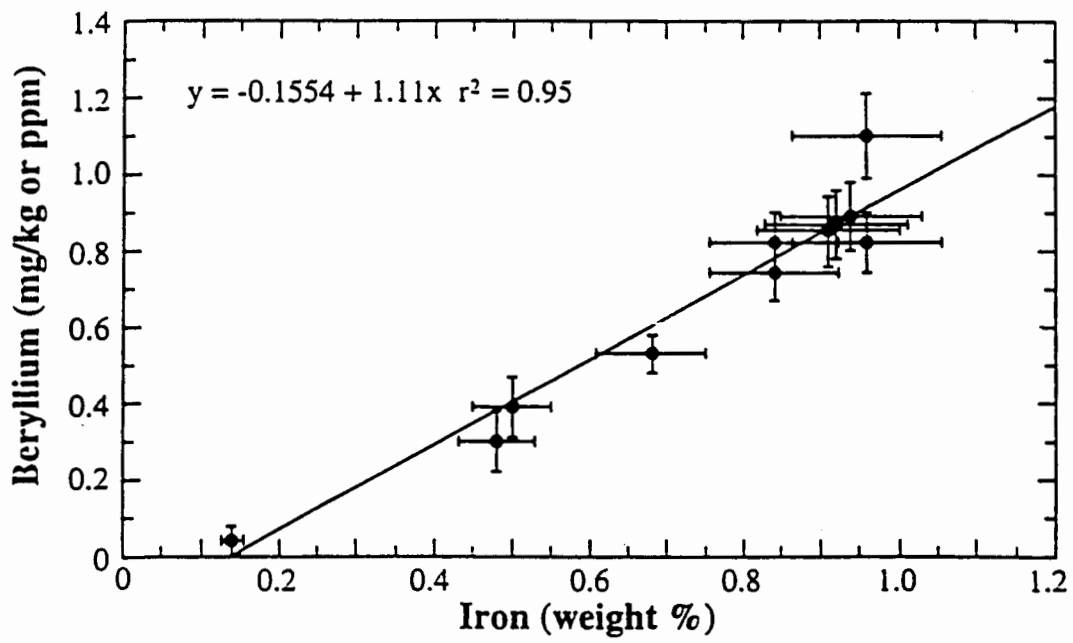


Fig. 7

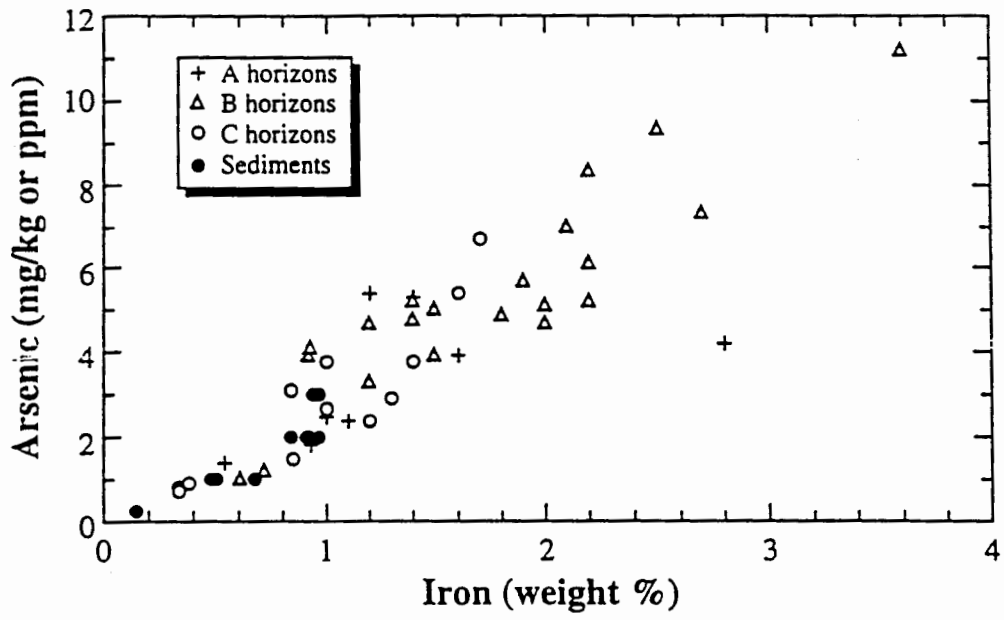


Fig. 8

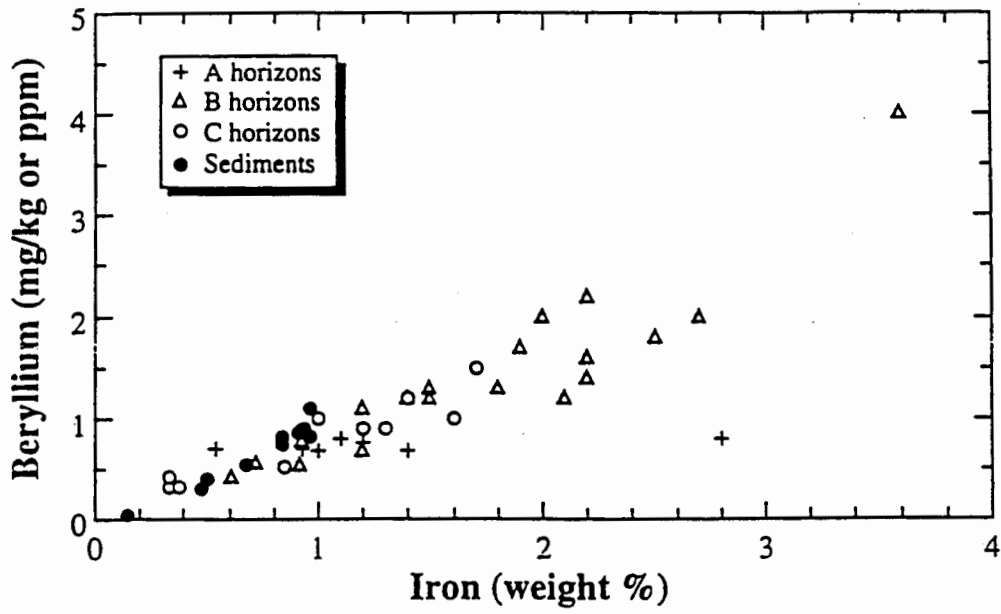


Fig. 9

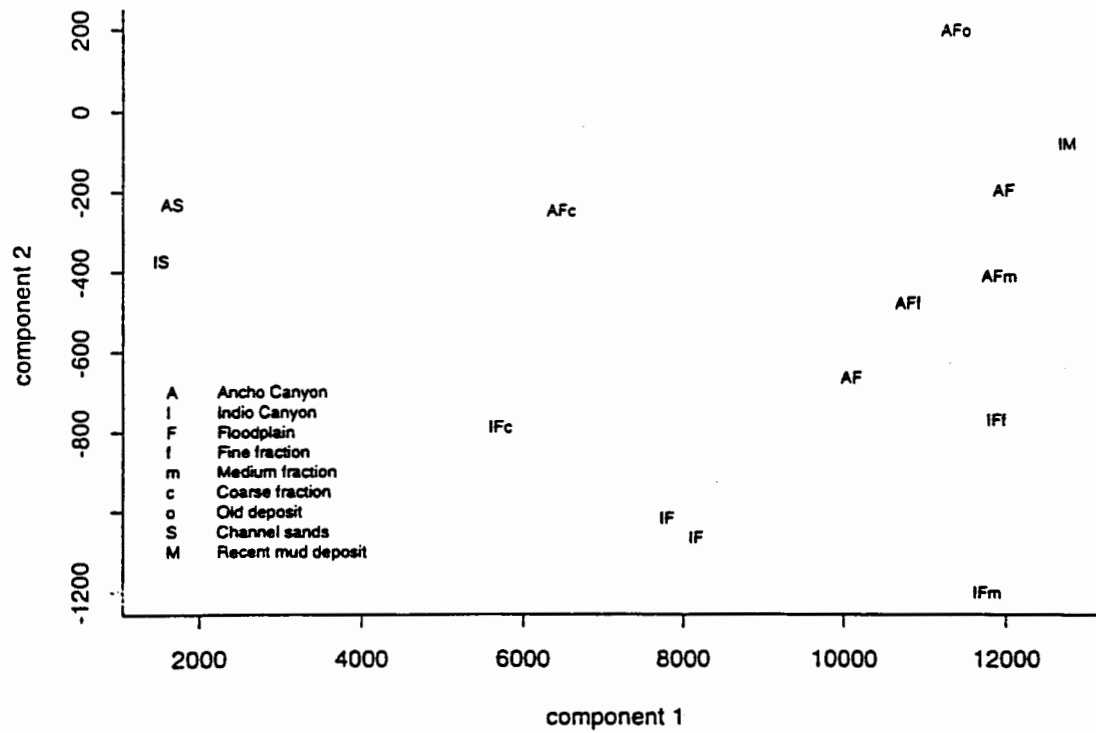


Fig. 11

Table 1
Location of Sample Sites and Description of Samples, TA-39

Sample Number	Sample Location	Type of Deposit	Sample Depth	Particle Size	Notes
FS 2220	Indio Cyn, 6425'	floodplain	0-18"	< 2 mm (sand, silt, clay)	bulk sample, gravel removed
FS 2221	Indio Cyn, 6425'	floodplain	0-18"	< 0.075 mm (very fine sand, silt, clay)	sample split, sieved
FS 2222	Indio Cyn, 6425'	floodplain	0-18"	0.25-0.075 mm (fine sand)	sample split, sieved
FS 2223	Indio Cyn, 6425'	floodplain	0-18"	< 2 mm (sand, silt, clay)	duplicate of FS 2220
FS 2224	Indio Cyn, 6425'	channel sands	0-6"	< 2 mm (mainly coarse sand)	bulk sample, gravel removed
FS 2225	Indio Cyn, 6400'	channel sands	0-1"	< 2 mm (mainly fine sand)	black (magnetite) sands
FS 2226	Indio Cyn, 6387'	mud in channel	0-1"	< 2 mm (mainly fine sand, silt, clay)	mud deposits from recent flood
FS 2227	Ancho Cyn, 6228'	old floodplain	4.1-4.6'	< 2 mm (sand, silt, clay)	bulk sample, gravel removed
FS 2228	Ancho Cyn, 6228'	old channel sands	2.6-3.1'	< 2 mm (mainly coarse sand)	bulk sample, gravel removed
FS 2229	Ancho Cyn, 6295'	floodplain	8-16"	< 2 mm (sand, silt, clay)	bulk sample, gravel removed
FS 2230	Ancho Cyn, 6295'	floodplain	8-16"	< 0.075 mm (very fine sand, silt, clay)	sample split, sieved
FS 2231	Ancho Cyn, 6295'	floodplain	8-16"	0.25-0.075 mm (fine sand)	sample split, sieved
FS 2232	Ancho Cyn, 6295'	floodplain	8-16"	< 2 mm (sand, silt, clay)	duplicate of FS 2229
FS 2233	Ancho Cyn, 6295'	channel sands	0-6"	< 2 mm (mainly medium sand)	bulk sample, gravel removed
FS 2234	Indio Cyn, 6425'	floodplain	0-18"	0.25-2 mm (coarse+medium sand)	sample split, sieved
FS 2235	Ancho Cyn, 6295'	floodplain	8-16"	0.25-2 mm (coarse+medium sand)	sample split, sieved

Table 2. TA-39 Background Sediment Chemistry Data, HNO₃ Digestion

Sample	Al (ppm)	Al (+/-)	As (ppm)	As (+/-)	Ba (ppm)	Ba (+/-)	Be (ppm)	Be (+/-)	Ca (ppm)	Ca (+/-)
FS2220	4600	460	1	0.5	53	5.3	0.53	0.05	1200	120
FS2221	7300	730	3	0.60	99	9.90	0.89	0.09	1900	190
FS2222	6900	690	2	0.50	77	7.70	0.82	0.08	1700	170
FS2223	4400	440	2	0.50	54	5.40	0.56	0.06	1300	130
FS2224	740	74	<0.5		8	0.80	<0.08		180	18
FS2225	1400	140	1	0.50	14	1.40	0.70	0.08	990	99
FS2226	8400	840	3	0.60	100	10	1.10	0.11	2600	260
FS2227	7700	770	2	0.50	71	7.10	0.74	0.07	1500	150
FS2228	2300	230	0.90	0.50	32	3	0.17	0.08	770	77
FS2229	7800	780	2	0.50	90	9	0.85	0.09	2100	210
FS2230	6800	680	2	0.50	90	9	0.82	0.08	2500	250
FS2231	7600	760	3	0.60	95	9.50	0.87	0.09	2400	240
FS2232	6200	620	2	0.50	75	7.50	0.67	0.08	1800	180
FS2233	930	93	<0.5		8.30	0.83	<0.08		230	23
FS2234	3200	320	1	0.50	37	3.70	0.30	0.08	960	96
FS2235	4100	410	1	0.50	49	4.90	0.39	0.08	1100	110

Sample	Co (ppm)	Co (+/-)	Cr (ppm)	Cr (+/-)	Cu (ppm)	Cu (+/-)	Fe (ppm)	Fe (+/-)	K (ppm)	K (+/-)	Mg (ppm)	Mg (+/-)
FS2220	2.2	0.5	3.5	0.5	3.5	0.5	6800	680	970	97	920	92
FS2221	3.50	0.50	5.80	0.60	7.30	0.70	9400	940	1500	150	1500	150
FS2222	3	0.50	4.70	0.50	5.60	0.60	9600	960	1400	140	1300	130
FS2223	2.30	0.50	3.30	0.50	3.50	0.50	6500	650	990	99	870	87
FS2224	0.60	0.50	1	0.50	0.80	0.50	1400	140	180	74	170	17
FS2225	6	0.60	12	1.20	4.40	0.50	57000	5700	220	22	530	53
FS2226	3.50	0.50	5.60	0.60	12	1.20	9600	960	1800	180	1700	170
FS2227	2.70	0.50	5.20	0.50	4.30	0.50	8400	840	1600	160	1400	140
FS2228	3.10	0.50	5.40	0.50	1.80	0.50	13000	1300	540	54	570	57
FS2229	3.50	0.50	5.70	0.60	5.70	0.60	9100	910	1900	190	1500	150
FS2230	3	0.50	5.90	0.60	7.50	0.80	8400	840	1900	190	1500	150
FS2231	3.80	0.50	5.90	0.60	7.30	0.70	9200	920	2200	220	1600	160
FS2232	3.20	0.50	4.70	0.50	4.80	0.50	8000	800	1600	160	1300	130
FS2233	0.70	0.50	0.80	0.50	0.90	0.50	1400	140	200	20	200	20
FS2234	1.50	0.50	2.20	0.50	2.70	0.50	4800	480	650	65	590	59
FS2235	2	0.50	2.50	0.50	3	0.50	5000	500	1100	110	820	82

Table 2. TA-39 Background Sediment Chemistry Data, HNO₃ Digestion (continued)

Sample	Mn (ppm)	Mn (+/-)	Na (ppm)	Na (+/-)	Ni (ppm)	Ni (+/-)	Pb (ppm)	Pb (+/-)	Sb (ppm)	Sb (+/-)
FS2220	240	24	120	14	4	2	5	4	<5	
FS2221	330	33	120	14	7	2	10	4	<5	
FS2222	350	35	120	14	5	2	10	4	<5	
FS2223	240	24	95	14	4	2	8	4	<5	
FS2224	53	5.30	46	14	<2		4	4	<5	
FS2225	1200	120	68	14	9	2	11	4	<5	
FS2226	380	38	190	19	6	2	16	4	5	5
FS2227	220	22	150	15	4	2	7	4	<5	
FS2228	240	24	66	14	4	2	5	4	<5	
FS2229	330	33	100	14	6	2	10	4	<5	
FS2230	230	23	76	14	5	2	7	4	<5	
FS2231	300	30	110	14	7	2	9	4	<5	
FS2232	280	28	91	14	6	2	8	4	<5	
FS2233	46	4.60	34	14	<2		<4		<5	
FS2234	180	18	75	14	4	2	5	4	<5	
FS2235	190	19	80	14	4	2	6	4	<5	

Sample	Ta (ppm)	Ta (+/-)	Th (ppm)	Th (+/-)	Tl (ppm)	Tl (+/-)	U (ppm)	U (+/-)	V (ppm)	V (+/-)	Zn (ppm)	Zn (+/-)
FS2220	<0.3		5.2	0.4	0.5	0.3	0.7	0.3	7.2	0.7	31	3.1
FS2221	<0.3		7.70	0.50	<0.3		0.90	0.30	12	1.20	38	3.80
FS2222	<0.3		7.10	0.50	<0.3		1	0.30	10	1	44	4.40
FS2223	<0.3		5.80	0.40	<0.3		0.90	0.30	7	0.70	31	3
FS2224	<0.3		1.40	0.30	<0.3		<0.3		1.40	0.50	9	1
FS2225	<0.3		14	1	<0.3		0.80	0.30	66	6.60	300	30
FS2226	<0.3		6.60	0.50	<0.3		1.60	0.30	11	1.10	48	4.80
FS2227	<0.3		5.80	0.40	<0.3		0.60	0.30	9	0.90	33	3
FS2228	<0.3		2.20	0.30	<0.3		<0.3		20	2	47	5
FS2229	<0.3		8	0.60	<0.3		0.70	0.30	11	1.10	39	4
FS2230	<0.3		6.90	0.80	<0.3		0.60	0.30	13	1.30	32	3
FS2231	<0.3		7.10	0.80	<0.3		0.60	0.30	12	1.20	37	3.70
FS2232	<0.3		6	0.70	<0.3		0.60	0.30	9	0.90	34	3.40
FS2233	<0.3		0.90	0.30	<0.3		<0.3		1	0.50	9	1
FS2234	<0.3		3.60	0.40	<0.3		0.50	0.30	5	0.50	24	2
FS2235	<0.3		4.30	0.50	1.50	0.30	0.40	0.30	5	0.50	24	2

Table 3. TA-39 Background Sediment Chemistry Data, HF Digestion

Sample	Al (ppm)	Al (+/-)	As (ppm)	As (+/-)	Ba (ppm)	Ba (+/-)	Be (ppm)	Be (+/-)	Ca (ppm)	Ca (+/-)	Co (ppm)	Co (+/-)
FS2220	61000	6100	8.20	1.60	222	22	3.20	0.32	3800	380	2.30	0.50
FS2221	57000	5700	5.30	1	370	37	3.80	0.38	4900	490	4	0.50
FS2222	62000	6200	5.30	1	270	27	4.40	0.44	4300	430	3.80	0.50
FS2223	61000	6100	6.30	1.30	240	24	3.50	0.35	4000	400	2.60	0.50
FS2224	51000	5100	6.20	1.20	130	13	1.10	0.11	2000	200	0.70	0.50
FS2225	11000	1100	4.80	1	32	3.20	1.60	0.16	3400	340	< 0.5	
FS2226	63000	6300	8.60	1.70	300	30	5.30	0.50	4900	490	3.40	0.50
FS2227	69000	6900	10.40	2.10	340	34	4	0.40	6100	610	3.90	0.50
FS2228	63000	6300	7.50	1.50	290	29	1.50	0.15	8100	810	7	0.70
FS2229	60000	6000	8	1.60	330	33	3.60	0.36	4900	490	3.50	0.50
FS2230	56000	5600	9.10	1.80	410	41	3.20	0.32	5800	580	3.80	0.50
FS2231	59000	5900	5.90	1.20	380	38	3.60	0.36	5500	550	3.90	0.50
FS2232	61000	6100	3.60	0.70	310	31	3.40	0.34	4700	470	3.30	0.50
FS2233	48000	4800	2.10	0.40	120	12	0.91	0.09	1800	180	1	0.50
FS2234	61000	6100	3	0.60	180	18	2.40	0.24	3400	340	1.50	0.50
FS2235	59000	5900	2.50	0.50	210	21	2.90	0.29	3500	350	2	0.50

Sample	Cr (ppm)	Cr (+/-)	Cu (ppm)	Cu (+/-)	Fe (ppm)	Fe (+/-)	K (ppm)	K (+/-)	Mg (ppm)	Mg (+/-)	Mn (ppm)	Mn (+/-)
FS2220	8.30	0.80	5.10	0.50	13000	1300	27000	2700	1700	170	420	42
FS2221	18	1.80	12	1.20	17000	1700	23000	2300	2700	270	490	49
FS2222	12	1.20	9.60	1	17000	1700	27000	2700	2500	250	580	58
FS2223	9.90	1	6	0.60	14000	1400	29000	2900	1900	190	430	43
FS2224	1.10	0.50	1	0.50	4900	490	26000	2600	470	47	180	18
FS2225	83	8.30	< 0.5		110	11	3600	360	3000	300	13000	1300
FS2226	14	1.40	15	1.50	16000	1600	26000	2600	2600	260	540	54
FS2227	15	1.50	7.60	0.80	17000	1700	27000	2700	3300	330	450	45
FS2228	23	2.30	2.60	0.50	52000	5200	25000	2500	2500	250	1300	130
FS2229	15	1.50	8.70	0.90	16000	1600	26000	2600	2700	270	460	46
FS2230	23	2.30	13	1.30	19000	1900	22000	2200	3100	310	420	42
FS2231	17	1.70	13	1.30	18000	1800	24000	2400	3100	310	480	48
FS2232	14	1.40	8.10	0.80	15000	1500	24000	2400	2500	250	430	43
FS2233	2.50	0.50	1.20	0.50	4100	410	24000	2400	530	53	130	13
FS2234	4.40	0.50	3.40	0.50	8500	850	25000	2500	1000	100	290	29
FS2235	7.50	0.80	4.80	0.50	11000	1100	26000	2600	1600	160	330	33

Table 3. TA-39 Background Sediment Chemistry Data, HIF Digestion (continued)

Sample	Na (ppm)	Na (+/-)	Ni (ppm)	Ni (+/-)	Pb (ppm)	Pb (+/-)	Sb (ppm)	Sb (+/-)	Ta (ppm)	Ta (+/-)	Th (ppm)	Th (+/-)
FS2220	19000	1900	5	2	11	4	< 5		6	0.40	13	0.30
FS2221	15000	1500	11	2	20	4	< 5		4.70	0.30	17	0.30
FS2222	18000	1800	6	2	16	4	< 5		5.30	0.30	18	0.40
FS2223	20000	2000	7	2	13	4	< 5		4.20	0.30	13	0.30
FS2224	20000	2000	< 2		< 4		< 5		1.20	0.20	3.90	0.20
FS2225	2700	270	47	5	50	5	14	5	15	0.90	130	4
FS2226	18000	1800	7	2	27	4	< 5		5.70	0.30	18	0.40
FS2227	18000	1800	8	2	14	4	< 5		4.40	0.40	15	0.60
FS2228	20000	2000	14	2	< 4		< 5		2.60	0.30	9.40	0.40
FS2229	16000	1600	8	2	12	4	< 5		4.30	0.40	15	0.60
FS2230	14000	1400	10	2	13	4	< 5		4	0.40	16	0.60
FS2231	14000	1400	8	2	13	4	< 5		4.40	0.40	15	0.60
FS2232	16000	1600	14	2	13	4	< 5		4.60	0.50	15	0.60
FS2233	18000	1800	< 2		4	4	< 5		0.90	0.20	3.30	0.20
FS2234	21000	2100	2	2	8	4	< 5		3	0.30	8.80	0.40
FS2235	19000	1900	5	2	10	4	< 5		3.20	0.30	10	0.40

Sample	Tl (ppm)	Tl (+/-)	U (ppm)	U (+/-)	V (ppm)	V (+/-)	Zn (ppm)	Zn (+/-)
FS2220	0.50	0.20	3.90	0.20	16	1.60	64	6.40
FS2221	0.70	0.20	5.70	0.30	33	3.30	70	7
FS2222	0.70	0.20	5.60	0.30	25	2.50	88	8.80
FS2223	0.50	0.20	4	0.20	19	1.90	66	6.60
FS2224	0.20	0.20	1.10	0.20	2.70	0.50	25	2.50
FS2225	0.30	0.20	4	0.20	450	45	2500	250
FS2226	0.90	0.30	7.20	0.40	25	2.50	89	8.90
FS2227	0.80	0.20	4.70	0.40	27	2.70	72	7.20
FS2228	0.40	0.20	1.50	0.20	84	8.40	210	21
FS2229	0.80	0.20	4.30	0.30	27	2.70	69	7
FS2230	0.80	0.20	4.90	0.40	41	4.10	68	6.80
FS2231	0.80	0.20	4.30	0.30	33	3.30	73	7.30
FS2232	0.80	0.20	4.30	0.30	26	2.60	65	6.50
FS2233	0.30	0.20	0.70	0.20	4	0.50	34	3.40
FS2234	0.50	0.20	2.50	0.20	9	0.90	43	4.30
FS2235	0.60	0.20	3	0.20	14	1.40	52	5.20

Table 4
TA-39 Background Sediment Chemistry Data,
Deionized Water Leachate

Sample	Cl (ppm)	Cl (+/-)	SO4 (ppm)	SO4 (+/-)
FS2220	<2.5		<5	
FS2221	<2.5		10	5
FS2222	<2.5		5.9	5
FS2223	<2.5		<5	
FS2224	<2.5		<5	
FS2225	<2.5		<5	
FS2226	<2.5		<5	
FS2227	8.4	2.5	35	5
FS2228	10.3	2.5	26.5	5
FS2229	<2.5		<5	
FS2230	<2.5		<5	
FS2231	<2.5		<5	
FS2232	<2.5		<5	
FS2233	<2.5		<5	
FS2234	<2.5		<5	
FS2235	<2.5		<5	

Table 5
Summary of Background Sediment Analyses, TA-39, HNO₃ and Deionized Water Digestion

Element	Coarse Channel Sands, Average (ppm) *	Bulk Floodplain Deposit, Average (ppm) **	Minimum Value (ppm) ***	Maximum Value (ppm) ***
Al	835 ± 134	5750 ± 1768	740 ± 74 a	8400 ± 840 c
As	< 0.5	1.8 ± 0.4	< 0.5 a	3 ± 0.6 c, e, f
Ba	8.2 ± 0.2	68 ± 21	8 ± 0.8 a	100 ± 10 c
Be	< 0.08	0.65 ± 0.15	< 0.08 a	1.1 c
Ca	205 ± 35	1600 ± 495	180 ± 18 a	2600 ± 260 c
Cl	< 2.5	< 2.5	< 2.5	10.3 ± 2.5 i
Co	0.65 ± 0.07	2.8 ± 0.8	0.6 ± 0.5 a	3.8 ± 0.5 f
Cr	0.9 ± 0.14	4.3 ± 1.3	0.8 ± 0.5 a	5.9 ± 0.6 e, f
Cu	0.85 ± 0.07	4.4 ± 1.2	0.8 ± 0.5 a	7.3 ± 0.7 e
Fe	1400 ± 140	7650 ± 1273	1400 ± 140 a	57000 ± 5700 d
K	190 ± 14	1365 ± 544	180 ± 74 a	2200 ± 220 f
Mg	185 ± 21	1148 ± 357	170 ± 17 a	1700 ± 170 c
Mn	50 ± 5	272 ± 46	46 ± 4.6 a	1200 ± 120 d
Na	40 ± 8	102 ± 8	34 ± 14 a	190 ± 19 c
Ni	< 2	5 ± 1.4	< 2 a	9 ± 2 d
Pb	< 4	7.8 ± 1.8	< 4 a	16 ± 4 c
Sb	< 5	< 5	< 5	5 ± 5 d
SO ₄	< 5	< 5	< 5	26.5 ± 5 i
Ta	< 0.3	< 0.3	< 0.3	< 0.3
Th	1.2 ± 0.4	6.3 ± 1.1	0.9 ± 0.3 a	14 ± 1 d
Tl	< 0.3	< 0.3	< 0.3	1.5 ± 0.3 g
U	< 0.3	0.7 ± 0.1	< 0.3 a	1.6 ± 0.3 c
V	1.2 ± 0.3	8.6 ± 2.1	1 ± 0.5 a	66 ± 6.6 d
Zn	9 ± 1	34 ± 4	9 ± 1 a	300 ± 30 d

Notes

* Samples FS2224 and FS2233.

** Samples FS2220, FS2223 (duplicate), FS2229, and FS2232 (duplicate)

*** a = coarse channel sands; b = bulk floodplain deposit; c = mud deposit; d = black sands; e = very fine sand to clay separate of floodplain sample; f = fine sand separate of floodplain deposit; g = coarse to medium sand separate of floodplain deposit; h = 3000 year old floodplain deposit; i = 1200 year old coarse channel sand.

Table 6
Summary of Background Sediment Analyses, TA-39, HF Digestion

Element	Coarse Channel Sands, Average (ppm) *	Bulk Floodplain Deposit, Average (ppm) **	Minimum Value (ppm) ***	Maximum Value (ppm) ***
Al	49500 ± 2121	60750 ± 354	11000 ± 1100 d	69000 ± 6900 h
As	4.2 ± 2.9	6.8 ± 0.6	2.1 ± 0.4 a	10.4 ± 2.1 h
Ba	125 ± 7	276 ± 63	32 ± 3.2 d	410 ± 41 e
Be	1.0 ± 0.1	3.4 ± 0.1	0.91 ± 0.09 a	5.3 ± 0.5 c
Ca	1900 ± 141	4350 ± 636	1800 ± 180 a	8100 ± 810 i
Co	0.9 ± 0.2	3.0 ± 0.7	< 0.5 d	7 ± 0.7 i
Cr	1.8 ± 1.0	11.8 ± 3.8	1.1 ± 0.5 a	83 ± 8.3 d
Cu	1.1 ± 0.1	7.0 ± 2.0	< 0.5 d	13 ± 1.3 e, f
Fe	4500 ± 566	14500 ± 1414	4100 ± 410 a	? (d?)
K	25000 ± 1414	26550 ± 2121	3600 ± 360 a	29000 ± 2900 b
Mg	500 ± 42	2200 ± 566	470 ± 47 a	3300 ± 330 h
Mn	155 ± 35	435 ± 14	130 ± 13 a	13000 ± 1300 d
Na	19000 ± 1414	17750 ± 2475	2700 ± 270 d	21000 ± 2100 g
Ni	< 2	8.5 ± 3.5	< 2 a	47 ± 5 d
Pb	< 4	12 ± 0.4	< 4 a, i	27 ± 4 c
Sb	< 5	< 5	< 5	14 ± 5 d
Ta	1.1 ± 0.2	4.8 ± 0.5	0.9 ± 0.2 a	6 ± 0.4 b
Th	3.6 ± 0.4	14 ± 1.4	3.3 ± 0.2 a	130 ± 4 d
Tl	0.3 ± 0.1	0.7 ± 0.2	0.2 ± 0.2 a	0.9 ± 0.3 c
U	0.9 ± 0.3	4.1 ± 0.3	0.7 ± 0.2 a	7.2 ± 0.4 c
V	3.4 ± 0.9	22 ± 6	2.7 ± 0.5 a	450 ± 45 d
Zn	30 ± 6	66 ± 1	25 ± 2.5 a	2500 ± 250 d

Notes

* Samples FS2224 and FS2233.

** Samples FS2220, FS2223 (duplicate), FS2229, and FS2232 (duplicate)

*** a = coarse channel sands; b = bulk floodplain deposit; c = mud deposit; d = black sands; e = very fine sand to clay separate of floodplain sample; f = fine sand separate of floodplain deposit; g = coarse to medium sand separate of floodplain deposit; h = 3000 year old floodplain deposit; i = 1200 year old coarse channel sand.

Table 7
Summary of Different Size Fractions, TA-39, HNO₃ and Deionized Water Digestion

Element	Coarse Channel Sands, Average (ppm) *	Coarse and Medium Sand, Average (ppm) **	Fine Sand, Average (ppm) ***	Very Fine Sand, Silt, Clay, Average (ppm) ****
Al	835 ± 134	3650 ± 636	7250 ± 495	7050 ± 354
As	< 0.5	1 ± 0.5	2.5 ± 0.7	2.5 ± 0.7
Ba	8.2 ± 0.2	43 ± 8	86 ± 13	95 ± 6
Be	< 0.08	0.35 ± 0.06	0.85 ± 0.04	0.86 ± 0.05
Ca	205 ± 35	1030 ± 99	2050 ± 495	2200 ± 424
Cl	< 2.5	< 2.5	< 2.5	< 2.5
Co	0.65 ± 0.07	1.8 ± 0.4	3.4 ± 0.6	3.3 ± 0.4
Cr	0.9 ± 0.14	2.4 ± 0.2	5.3 ± 0.9	5.9 ± 0.1
Cu	0.85 ± 0.07	2.9 ± 0.2	6.5 ± 1.2	7.4 ± 0.1
Fe	1400 ± 140	4900 ± 141	9400 ± 283	8900 ± 707
K	190 ± 14	875 ± 318	1800 ± 566	1700 ± 283
Mg	185 ± 21	705 ± 163	1450 ± 212	1500 ± 150
Mn	50 ± 5	185 ± 7	325 ± 35	280 ± 71
Na	40 ± 8	78 ± 4	115 ± 7	98 ± 31
Ni	< 2	4 ± 2	6.0 ± 1.4	6.0 ± 1.4
Pb	< 4	5.5 ± 0.7	9.5 ± 0.7	8.5 ± 2.1
Sb	< 5	< 5	< 5	< 5
SO ₄	< 5	< 5	< 5.5	< 7.5
Ta	< 0.3	< 0.3	< 0.3	< 0.3
Th	1.2 ± 0.4	4.0 ± 0.5	7.1 ± 0.5	7.3 ± 0.6
Tl	< 0.3	< 0.9	< 0.3	< 0.3
U	< 0.3	0.45 ± 0.07	0.80 ± 0.28	0.75 ± 0.21
V	1.2 ± 0.3	5 ± 0.5	11 ± 1	13 ± 1
Zn	9 ± 1	24 ± 2	41 ± 5	35 ± 4

Notes

* Samples FS2224 and FS2233.

** Samples FS2234 and FS2235.

*** Samples FS2222 and FS2231.

*** Samples FS2221 and FS2230.

Table 8
Summary of Different Size Fractions, TA-39, HF Digestion

Element	Coarse Channel Sands, Average (ppm) *	Coarse and Medium Sand, Average (ppm) **	Fine Sand, Average (ppm) ***	Very Fine Sand, Silt, Clay, Average (ppm) ****
Al	49500 ± 2121	60000 ± 1414	60500 ± 2121	56500 ± 707
As	4.2 ± 2.9	2.8 ± 0.4	5.6 ± 0.4	7.2 ± 2.7
Ba	125 ± 7	195 ± 21	325 ± 78	390 ± 28
Be	1.0 ± 0.1	2.7 ± 0.4	4.0 ± 0.6	3.5 ± 0.4
Ca	1900 ± 141	3450 ± 71	4900 ± 849	5350 ± 636
Co	0.9 ± 0.2	1.8 ± 0.4	3.9 ± 0.1	3.9 ± 0.1
Cr	1.8 ± 1.0	6.0 ± 2.2	15 ± 4	21 ± 4
Cu	1.1 ± 0.1	4.1 ± 1.0	11 ± 2	13 ± 1
Fe	4500 ± 566	9750 ± 1768	17500 ± 707	18000 ± 1414
K	25000 ± 1414	25500 ± 707	25500 ± 2121	22500 ± 707
Mg	500 ± 42	1300 ± 424	2800 ± 424	2900 ± 283
Mn	155 ± 35	295 ± 50	530 ± 71	455 ± 50
Na	19000 ± 1414	20000 ± 1414	16000 ± 2828	14500 ± 707
Ni	< 2	3.5 ± 2.1	7.0 ± 1.4	11 ± 1
Pb	< 4	9.0 ± 1.4	15 ± 2	17 ± 5
Sb	< 5	< 5	< 5	< 5
Ta	1.1 ± 0.2	3.1 ± 0.1	4.9 ± 0.6	4.4 ± 0.5
Th	3.6 ± 0.4	9.4 ± 0.9	17 ± 2	17 ± 1
Tl	0.3 ± 0.1	0.6 ± 0.1	0.8 ± 0.1	0.8 ± 0.1
U	0.9 ± 0.3	2.8 ± 0.4	5.0 ± 0.9	5.3 ± 0.6
V	3.4 ± 0.9	12 ± 4	29 ± 6	37 ± 6
Zn	30 ± 6	48 ± 6	81 ± 11	69 ± 1

Notes

- * Samples FS2224 and FS2233.
- ** Samples FS2234 and FS2235.
- *** Samples FS2222 and FS2231.
- *** Samples FS2221 and FS 2230.

Table 9
Comparison of Modern and Old Deposits, TA-39, HNO₃ and Deionized Water Digestion

Element	Coarse Channel Sands, Average (ppm) *	Old Channel Sands (ppm) **	Bulk Floodplain Deposit, Average (ppm) ***	Old Floodplain Deposits (ppm) ****
Al	835 ± 134	2300 ± 230 a	5750 ± 1768	7700 ± 770
As	< 0.5	0.9 ± 0.5	1.8 ± 0.4	2 ± 0.5
Ba	8.2 ± 0.2	32 ± 3 a	68 ± 21	71 ± 7.1
Be	< 0.08	0.17 ± 0.08 a	0.65 ± 0.15	0.74 ± 0.07
Ca	205 ± 35	770 ± 77 a	1600 ± 495	1500 ± 150
Cl	< 2.5	10.3 ± 2.5 b, c	< 2.5	8.4 ± 2.5 b
Co	0.65 ± 0.07	3.1 ± 0.5 b	2.8 ± 0.8	2.7 ± 0.5
Cr	0.9 ± 0.14	5.4 ± 0.5 b	4.3 ± 1.3	5.2 ± 0.5
Cu	0.85 ± 0.07	1.8 ± 0.5 a	4.4 ± 1.2	4.3 ± 0.5
Fe	1400 ± 140	13000 ± 1300 b	7650 ± 1273	8400 ± 840
K	190 ± 14	540 ± 54 a	1365 ± 544	1600 ± 160
Mg	185 ± 21	570 ± 57 a	1148 ± 357	1400 ± 140
Mn	50 ± 5	240 ± 24 b	273 ± 46	220 ± 22
Na	40 ± 8	66 ± 14	102 ± 8	150 ± 15 b
Ni	< 2	4 ± 2	5 ± 1.4	4 ± 2
Pb	< 4	7 ± 4	7.8 ± 1.8	7 ± 4
Sb	< 5	< 5	< 5	< 5
SO ₄	< 5	26.5 ± 0.5 b	< 5	35 ± 5 b, c
Ta	< 0.3	< 0.3	< 0.3	< 0.3
Th	1.2 ± 0.4	2.2 ± 0.3 a	6.3 ± 1.1	5.8 ± 0.4
Tl	< 0.3	< 0.3	< 0.3	< 0.3
U	< 0.3	< 0.3	0.7 ± 0.1	0.6 ± 0.3
V	1.2 ± 0.3	20 ± 2 b	8.6 ± 2.1	9 ± 0.9
Zn	9 ± 1	47 ± 5 b	34 ± 4	33 ± 3

Notes

* Samples FS2224 and FS2233.

** Sample FS2228; a = beyond range of modern channel sands, but within range of medium to coarse sand separate of banks; b = beyond range of medium to coarse sand separate of floodplain deposits; c = maximum value from this data set.

*** Samples FS2220, FS2223 (duplicate), FS2229, and FS2232 (duplicate)

**** Sample FS2227; a = beyond range of modern bulk floodplain deposits, but within range of fine sand to clay separates of floodplain deposits; b = beyond range of fine sand to clay separates of floodplain deposits; c = maximum value from this data set.

Table 10
Comparison of Modern and Old Deposits, TA-39, HF Digestion

Element	Coarse Channel Sands, Average (ppm) *	Old Channel Sands (ppm) **	Bulk Floodplain Deposit, Average (ppm) ***	Old Floodplain Deposits (ppm) ****
Al	49500 ± 2121	63000 ± 6300 a	60750 ± 354	69000 ± 6900 c
As	4.2 ± 2.9	7.5 ± 1.5	6.8 ± 0.6	10.4 ± 2.1 a
Ba	125 ± 7	290 ± 29 b	276 ± 63	340 ± 34
Be	1.0 ± 0.1	1.5 ± 0.15 a	3.4 ± 0.1	4 ± 0.4
Ca	1900 ± 141	8100 ± 810 b, c	4350 ± 636	6100 ± 610 a
Co	0.9 ± 0.2	7 ± 0.7 b, c	3.0 ± 0.7	3.9 ± 0.5
Cr	1.8 ± 1.0	23 ± 2.3 b	11.8 ± 3.8	15 ± 1.5
Cu	1.1 ± 0.1	2.6 ± 0.5 a	7.0 ± 2.0	7.6 ± 0.8
Fe	4500 ± 566	52000 ± 5200 b, c?	14500 ± 1414	17000 ± 1700
K	25000 ± 1414	25000 ± 2500	26550 ± 2121	27000 ± 2700
Mg	500 ± 42	2500 ± 250 b	2200 ± 566	3300 ± 330
Mn	155 ± 35	1300 ± 130 b	435 ± 14	450 ± 45
Na	19000 ± 1414	20000 ± 2000	17750 ± 2475	18000 ± 1800
Ni	< 2	14 ± 2 b	8.5 ± 3.5	8 ± 2
Pb	< 4	< 4	12 ± 0.4	14 ± 4
Sb	< 5	< 5	< 5	< 5
Ta	1.1 ± 0.2	2.6 ± 0.3 a	4.8 ± 0.5	4.4 ± 0.4
Th	3.6 ± 0.4	9.4 ± 0.4 a	14 ± 1.4	15 ± 0.6
Tl	0.3 ± 0.1	0.4 ± 0.2	0.7 ± 0.2	0.8 ± 0.2
U	0.9 ± 0.3	1.5 ± 0.2	4.1 ± 0.3	4.7 ± 0.4
V	3.4 ± 0.9	84 ± 8.4 b	22 ± 6	27 ± 2.7
Zn	30 ± 6	210 ± 21 b	66 ± 1	72 ± 7.2

Notes

* Samples FS2224 and FS2233.

** Sample FS2228; a = beyond range of modern channel sands, but within range of medium to coarse sand separate of floodplain deposits; b = beyond range of medium to coarse sand separate of floodplain deposits; c = maximum value from this data set.

*** Samples FS2220, FS2223 (duplicate), FS2229, and FS2232 (duplicate)

**** Sample FS2227; a = beyond range of modern bulk floodplain deposits, but within range of fine sand to clay separates of floodplain deposits; b = beyond range of fine sand to clay separates of floodplain deposits; c = maximum value from this data set.

Table 11
Summary Statistics For Background Sediment Samples *

Analyte	Number of Outliers	Minimum Value (ppm)	Median Value (ppm)	Mean Value (ppm)	Standard Deviation (ppm)	Maximum Value (ppm)	utl95**
Al	0	740	5400	5023.12	2665.26	8400	11747.57
As	0	<0.5	2	1.65	0.91	3.0	3.94
Ba	0	8	62.5	59.52	32.44	100	141.37
Be	0	<0.08	0.68	0.59	0.32	1.1	1.40
Ca	0	180	1400	1451.88	746.67	2600	3335.73
Co	1	0.6	3	2.57	1.01	3.8	5.16
Cr	1	0.8	4.95	4.15	1.80	5.9	8.77
Cu	1	0.8	4.35	4.21	2.20	7.5	9.85
Fe	2	1400	8400	6971.43	2845.90	9600	14410.60
K	0	180	1250	1171.88	664.49	2200	2848.39
Mg	0	170	1110	1029.38	508.90	1700	2313.33
Mn	1	46	240	240.60	97.21	380	490.04
Na	0	34	93	96.31	39.02	190	194.77
Ni	0	<2	4.5	4.81	2.07	9	10.04
Pb	1	<4	7.5	7.13	2.61	11	13.84
Th	1	0.9	5.9	5.24	2.28	8	11.09
U	1	<0.3	0.6	0.58	0.27	1.0	1.29
V	1	1.0	9.5	8.91	4.82	20	21.27
Zn	1	9	33.5	32.00	11.74	48	62.11
SO4	2	<5	NA	NA	NA	10	NA

Notes:

* Statistics only presented for results of HNO₃ and deionized digestion procedures, and were calculated after outliers were deleted. Outliers presented in Table 12. No values are presented for Cl because only two analyses were above detection limits, and these are excluded as outliers.

** utl95 is a (.95,.95) UTL, computed using estimated mean and standard deviation and normal assumptions (i.e., selecting a "k-factor" appropriate for a sample of size 16 (0 outliers, k=2.523), 15 (1 outlier, k=2.566) or 14 (2 outliers, k=2.614). Then utl95 = mean + k*standard deviation).

Table 12
Outliers in Background Sediment Data Set *

Sample Number	Sample Description	Analyte	Concentration (ppm)
FS 2225	black magnetite-rich sands	Co	6
		Cr	12
		Fe	57000
		Mn	1200
		Th	14
		V	66
		Zn	300
FS 2226	recent mud deposit	Cu	12
		Pb	16
		U	1.6
FS 2227	prehistoric floodplain deposit	Cl	8.5
		SO ₄	35
FS 2228	prehistoric channel sands	Cl	10.3
		Fe	13000
		V	20
		SO ₄	26.5

Notes:

* Outliers only calculated for HNO₃ and deionized water digestions.
Outliers identified as values that would inflate the estimate of the mean by more than 10%.

NATURAL BACKGROUND GEOCHEMISTRY OF THE BANDELIER TUFF AND OTHER ROCK UNITS, LOS ALAMOS, NEW MEXICO

by

David E. Broxton¹, Randall T. Rytz², Steven L. Reneau¹,
Clarence Duffy³, and Patrick Longmire³

ABSTRACT

Background elemental concentrations were determined for inorganic constituents of the Bandelier Tuff as part of Environmental Restoration investigations conducted at Los Alamos National Laboratory. A total of 251 bulk-rock samples was collected from outcrops across the Laboratory and borehole 49-2-700-1 at TA-49. Total elemental concentrations were determined for 208 samples by x-ray fluorescence and for 38 samples by instrumental neutron activation analyses to determine the chemical variability of rock units on the Pajarito Plateau. Then, based on the XRF and INAA results, a representative suite of 106 samples was selected for analyses by EPA SW846 methods for their leachable concentrations of inorganic analytes by inductively coupled plasma mass spectrometry, inductively coupled plasma emission spectroscopy, electrothermal vapor atomic absorption spectroscopy, or ion chromatography.

The Wilcoxon rank sum test and box plots were used to determine if there is a significant chemical difference between units of the Tshirege Member as well as between the Tshirege Member and other rock units. UTLs were calculated for all inorganic elements, except for iron and sulfate which have unusual distributions. The background screening value for inorganic analytes is the 95th percentile upper tolerance limit (UTL), which is the 95% upper confidence limit of the 95th percentile of the data distribution. For the elements that are normally distributed without any data transformation and the elements that are normally distributed after a square root transformation, UTLs were calculated using the following equation:

$$UTL_{0.95,0.95} = \text{mean} + \text{standard deviation} * k_{0.95,0.95}$$

The k-factor is dependent on the number of background samples. The UTLs for log normally distributed elements were estimated by a simulation process. The calculated UTL results were screened to ensure that the estimated UTLs were not artificially inflated due to a small sample size. Maximum detected concentrations were used to define background screening

¹ Geology/Geochemistry Group
² Neptune and Company, Inc.
³ Environmental Geochemistry

values for the rarely detected elements antimony, arsenic, chromium, copper, nickel, radium, silver, tantalum, and thallium as well as for iron and sulfate. Maximum concentrations are used to define background screening values for units Tt, Qbo, Qct, and Qbt 4 because they are represented by fewer than 10 samples. Background screening values for naturally occurring potassium, thorium, and uranium isotopes are calculated from total elemental concentration data.

The spatial coverage and population size of background chemistry samples are considered adequate for defining background screening values for units Qbt 1g, Qbt 1v, Qbt 2, and Qbt 3 of the Tshirege Member. These tuffs are the most widespread rock units on the Pajarito Plateau and make up the bedrock at the majority of the Laboratory's potential release sites. No additional background data are needed for these units. We recommend additional characterization of Qbt 4 because so few samples of this unit are included in the present data set. Preliminary background screening data are presented for pre-Tshirege rock units (tephras and volcanoclastic sediments of the Cerro Toledo interval, the upper part of the Otowi Member of the Bandelier Tuff, and dacitic lavas of the Tschicoma Formation); we recommend that these data be supplemented by local background data on an as needed basis.

INTRODUCTION

Background elemental concentrations were determined for inorganic constituents of the Bandelier Tuff as part of Environmental Restoration (ER) investigations conducted at Los Alamos National Laboratory (LANL). These background investigations conform with guidelines set forth in Task IV of the Laboratory's Hazardous and Solid Waste and Amendments (HSWA) permit to "...describe the extent of contamination (qualitative/quantitative) in relation to the background levels indicative for the area". The background data supplements information from earlier background soil and tuff investigations by Longmire et al. (1995a) and the companion report to this study (Longmire et al., 1995b). These background data support Resource Conservation and Recovery Act (RCRA) investigations at the Laboratory and will be used as baseline data for RCRA facilities investigations (RFI). The data set provides regional coverage of the bedrock geologic units and can be used for identifying areas of contamination, performing baseline risk assessments, and planning remedial actions. The data can also be used to assess how local background data compares to regional background.

This report presents background chemical data primarily for the Tshirege Member of the Bandelier Tuff. The Tshirege Member is the most widespread rock unit on the Pajarito Plateau, and it is the bedrock unit at the majority of the Laboratory's potential release sites. The Tshirege data are considered complete except for unit 4. The western part of the Laboratory, where unit 4 is the major surface bedrock unit, was little characterized at the time samples were collected for stratigraphic studies of the Bandelier Tuff, and only 4 samples of this unit were available for background characterization. The presence of a thick sequence of unit 4 tuffs in borehole 49-2-700-1 at TA-49 was not discovered until after background samples were submitted for analysis of leachable inorganic analytes.

Additional background data are presented for some of the pre-Tshirege rock units including, in descending stratigraphic order: tephra and volcanoclastic sediments of the Cerro Toledo interval, the upper part of the Otowi Member of the Bandelier Tuff, and dacitic lavas of the Tschicoma Formation. Background data for the pre-Tshirege rock units are preliminary because of the low number of samples representing the units; however, these data provide useful bounding information on the geochemistry of these deeper units.

Two types of analytical data for inorganic constituents are presented in this report. *Leachable elemental concentrations* are provided to determine the bioavailability of elements for risk assessment calculations. Leachable elemental concentrations were determined by first leaching the loosely bound inorganic constituents of the rocks in a water or acid solution, and then analyzing the leachate. The leachable elemental concentrations are the primary focus of this report because RFI soils and rocks also are analyzed for their leachable elemental concentrations.

Total elemental concentrations also are discussed in this report and refer to the total concentration of an inorganic element in a rock, including the insoluble forms of the elements tightly bound in mineral structures as well as acid leachable (bioavailable) forms. Total elemental concentrations provide important information about: (1) the natural geochemical variability of the rock units, (2) the leachability behavior of inorganic constituents in different geologic settings, (3) discrimination of contaminated vs. uncontaminated media, and (4) geochemical processes controlling contaminant transport. In addition, background screening values for naturally occurring potassium, thorium, and uranium isotopes are calculated from total elemental concentration data. Data for total elemental concentrations are presented graphically, and comparisons between leachable elemental concentrations and total elemental concentrations are made on an analyte by analyte basis. The total elemental concentrations are not treated statistically and are used as supporting data for understanding the distribution of inorganic elements in the rock units.

This report summarizes the results of background chemistry investigations for rocks of the Pajarito Plateau. Field, analytical, and statistical methods used to describe background element concentrations are described, and geologic factors that control elemental distributions are discussed. Background elemental values are determined for each rock unit, and background screening values are calculated based on upper threshold limits or maximum reported concentrations. The data are summarized in tables and figures, and the underlying data will be available through the Facility for Information Management and Display (FIMAD).

METHODS

A total of 251 bulk-rock samples was collected from rock units across the Pajarito Plateau. One hundred and eighty-seven of the samples were collected from outcrops as part of stratigraphic studies of the Bandelier Tuff and older units, and details about sample collection as well as other relevant information about the geologic setting of the samples are given elsewhere (Broxton et al., 1995a, 1995b, 1995c; Longmire, 1995a). Sixty four samples were collected from background geology borehole 49-2-700-1 at TA-49 (Stimac et al., 1995). Areas where samples were collected are shown in Fig. 1.

In general, field work was performed using the procedure Characterization of Lithologic Variations within the Rock Outcrops of a Volcanic Field (LANL-ER-SOP-03.07). Typically, samples were collected in vertical stratigraphic sections at a nominal vertical spacing of 5 m or at major changes in lithology. Metal tags mark sample sites in the field. Vertical control was maintained by Jacob staff and Abney level in the field, and locations and elevations were estimated from maps or were surveyed by a professional surveying company. Site observations generally included descriptions of rock type, unit thickness, type and degree of alteration, welding and compaction, phenocryst assemblage and abundance, color of fresh and weathered surfaces, pumice size and abundance, and weathering characteristics. Bedding characteristics, fractures and their filling materials, and lithic assemblage, size, and abundance were also noted.

Table I summarizes the analytical methods, analytes, and numbers of samples collected in this study. First, total elemental concentrations were determined for 208 samples by x-ray fluorescence (XRF) and 38 samples by instrumental neutron activation analyses (INAA) to determine the chemical variability of rock units on the Pajarito Plateau. Then, based on the XRF and INAA results, a representative suite of 106 samples was selected for analyses by EPA SW846 methods for their leachable concentrations of inorganic analytes. These included 5 outcrop samples from the Tschicoma Formation that were analyzed only for their inorganic analytes.

SW846 leachable elemental concentrations were determined by inductively coupled plasma mass spectrometry (ICPMS), inductively coupled plasma emission spectroscopy (ICPES), and electrothermal vapor atomic absorption spectroscopy (ETVAA). Aliquots of crushed rock powders were treated with a solution of concentrated HNO_3 ($\text{pH} < 1$), and the leachate was analyzed by ICPMS and ICPES. Separate aliquots of crushed rock powders were treated with de-ionized water and the leachate was analyzed for chlorine and sulfate by ion chromatography (IC). Thirteen untreated samples were analyzed for Radium-226 activities by gamma-ray spectroscopy (G).

Total elemental concentrations were made using an automated Rigaku wavelength-dispersive X-ray fluorescence (XRF) spectrometer located in the Geology/Geochemistry Group (EES-1) at LANL. Details about XRF analytical conditions are summarized in Broxton et al. (1995b, 1995c). Total elemental concentrations by INAA (Table I) were performed at the Omega West reactor facility at LANL. Minor et al. (1982) and Garcia et al. (1982) provide additional infor-

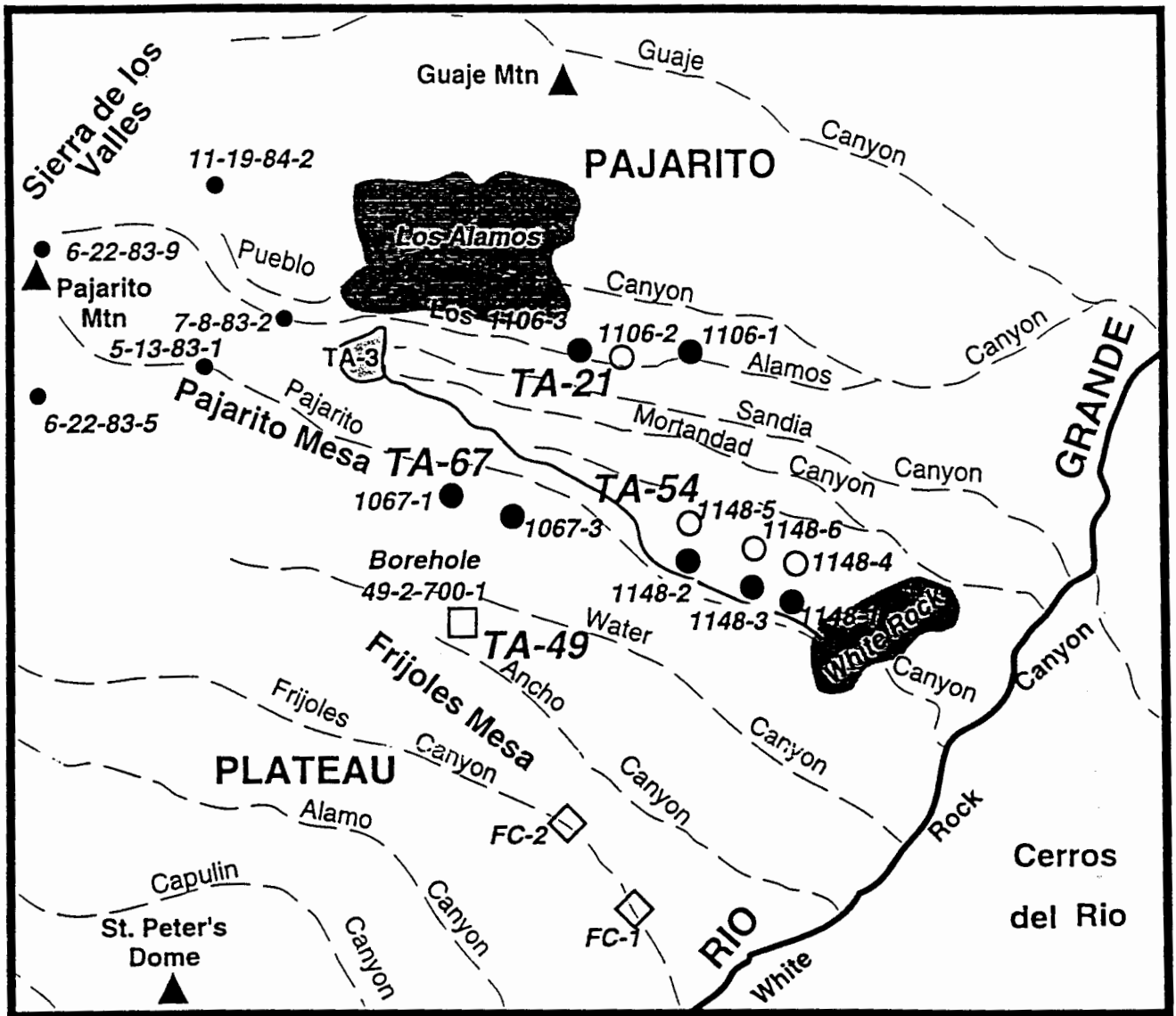


Fig. 1. Map showing location of sites where background chemistry samples were collected from outcrops and a borehole. Large filled circles indicate sites of outcrop samples that were analyzed for both leachable and total elemental concentrations. Open circles are sites of outcrop samples analyzed for total elemental concentrations by XRF only. Open diamonds are sites of Frijoles Canyon outcrop samples analyzed for total elemental concentrations by INAA only. Small filled circles are outcrop sites where samples of the Tschicoma Formation were sampled and analyzed for leachable elemental concentrations. The name of the stratigraphic sections are shown in italics next to the symbols described above. Borehole 49-2-700-1 at TA-49 (open box) was also sampled, and total elemental concentrations were determined by XRF.

mation about analytical uncertainties, conditions of analysis, and detection limits for elements analyzed by INAA. Total radium was determined for 13 samples by gamma-ray spectrometry. Loss on ignition (LOI) was determined by measuring the difference in sample weight at room temperature and after heating at 1000°C for one hour.

TABLE I.

ANALYTES, ANALYTICAL METHODS, AND NUMBERS OF SAMPLES FOR BACKGROUND CHEMISTRY INVESTIGATION OF ROCK UNITS ON THE PAJARITO PLATEAU

Analysis Method	Leachate Analyses				Total Rock Analyses			
	ICPES	ICPMS	IC	ETVAA	G	XRF	INAA	
Number of Analyses	106	106	106	106	13	208	38	
Analytes	Ag	Pb	SO ₄	As	Ra	Si	Na	Sb
	Al	Sb	Cl			Ti	Mg	I
	Ba	Ta				Al	Al	Cs
	Be	Th				Fe	Cl	Ba
	Ca	Tl				Mn	K	La
	Co	U				Mg	Ca	Ce
	Cr					Na	Sc	Nd
	Cu					K	Ti	Sm
	Fe					P	V	Eu
	K					V	Cr	Tb
	Mg					Cr	Mn	Dy
	Mn					Ni	Fe	Yb
	Na					Zn	Co	Lu
	Ni					Rb	Cu	Hf
	V					Sr	Zn	Ta
	Zn					Y	Ga	W
						Zr	As	Au
						Nb	Se	Hg
						Ba	Br	Th
							Rb	U
							Sr	Be
							Zr	Cd
							Ag	Pb
							In	

GEOLOGIC SETTING

The stratigraphic nomenclature for the Bandelier Tuff used in this investigation follows the usage of Broxton and Reneau (1995). Figure 2 shows the stratigraphic relations of the units discussed, and Figure 3 shows Bandelier Tuff nomenclature as used in other Laboratory reports dating back to the early 1960s. In descending stratigraphic order, the rock units represented in this background study include: the Tshirege Member of the Bandelier Tuff, tephra and volcanoclastic sediments of the Cerro Toledo interval, the upper part of the Otowi Member of the Bandelier Tuff, and dacitic lavas of the Tschicoma Formation.

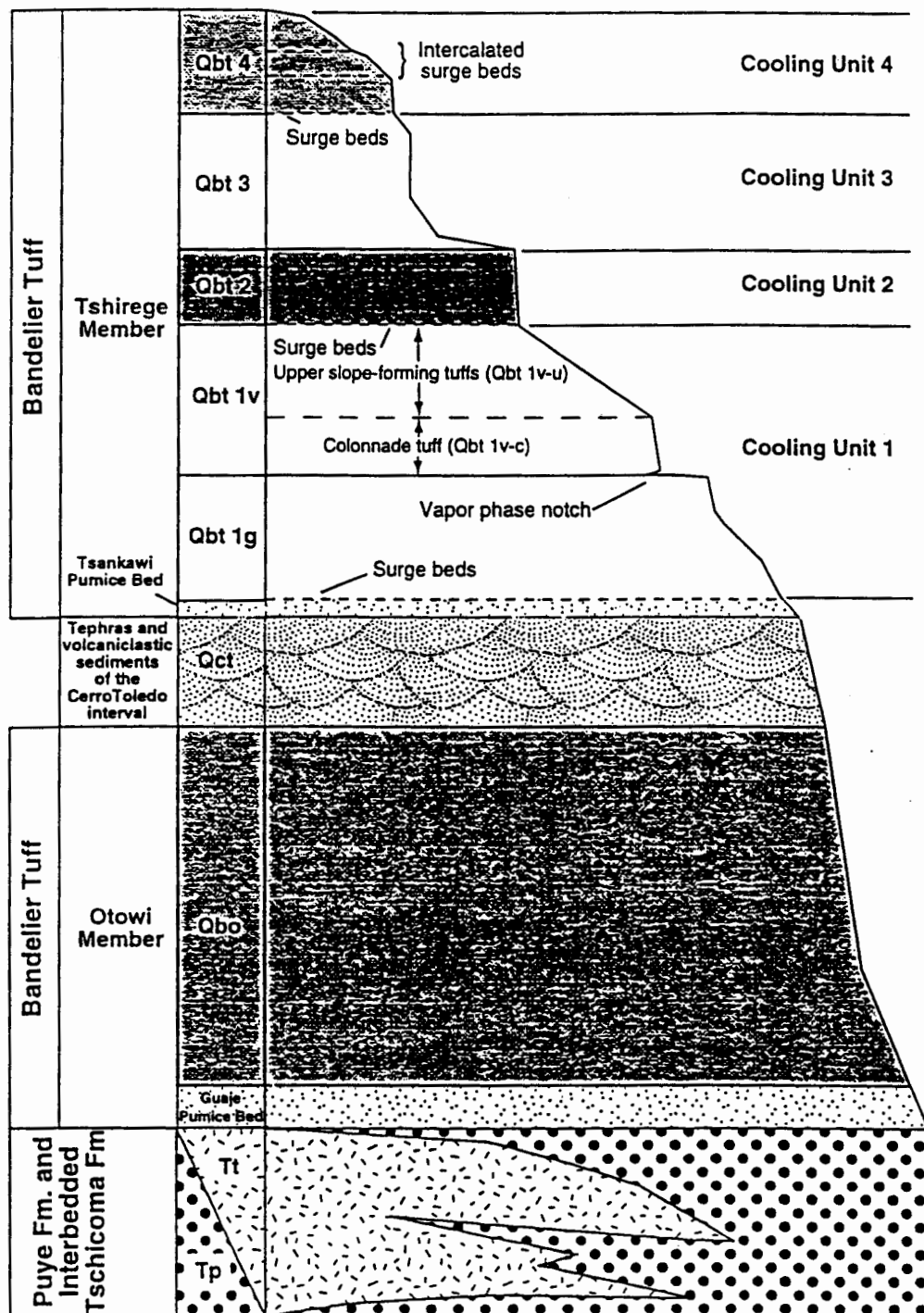


Fig. 2 Schematic stratigraphic section showing rock units sampled for background chemistry. Modified from Broxton and Reneau (1995).

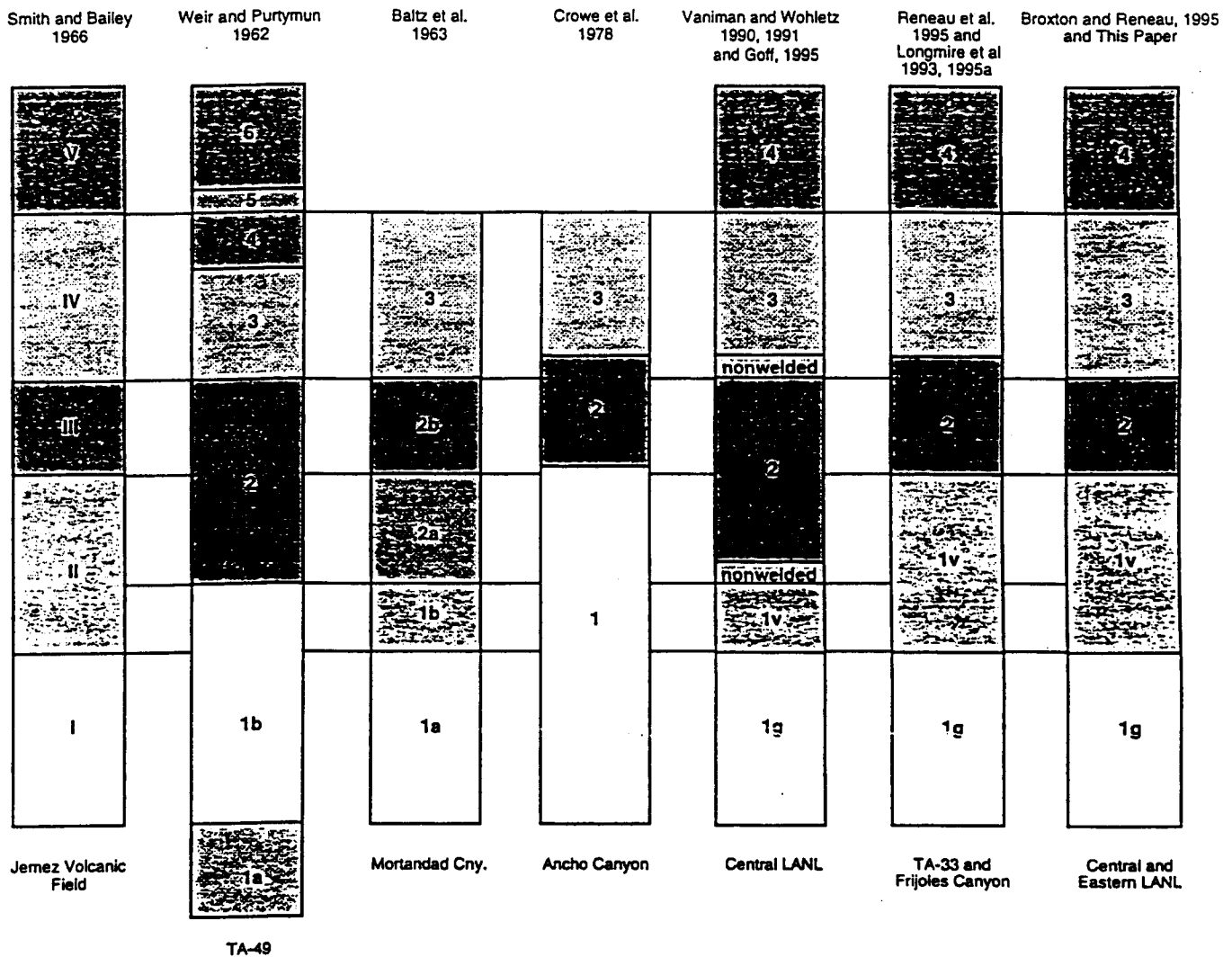


Fig. 3 Chart showing correlation of rock unit names applied to the Tshirege Member of the Bandelier Tuff by various investigators. From Broxton and Reneau (1995).

The Tshirege Member is a thick ignimbrite sheet that was erupted from the Valles caldera 1.21 Ma (Smith, 1960; Smith and Bailey, 1968, Izett and Obradovich, 1994). Because of its complex cooling history, the Tshirege Member forms a compound cooling unit divided into the basal Tsankawi Pumice Bed and four overlying ignimbrite cooling units. Consequently, the physical properties of the Tshirege Member vary both vertically and laterally. The lower three cooling units crop out in the central and eastern part of the Laboratory, and the fourth is present only in the western part. These cooling units, labeled 1 through 4 in ascending order (Fig. 2), represent episodes of ash-flow deposition that were separated by partial cooling breaks.

The Tshirege Member is a chemically zoned ignimbrite sheet, and the concentrations of minor and trace elements vary with stratigraphic height above the base of the unit. Chemical zonations in the Tshirege Member represent the compositional zonations that existed in the Bandelier

magma chamber before eruption (Smith and Bailey, 1968; Smith, 1979). The earliest erupted magmas mainly tapped the top of the magma body and were deposited as the stratigraphically lowest ignimbrites. Further eruptions continued to draw down the magma body, tapping generally deeper compositional zones of the magma body; these later eruptions resulted in the deposition of stratigraphically higher parts of the Tshirege ignimbrite sheet. Thus the chemical zonation in the Tshirege Member represents in inverted order the general compositional zonation of the Tshirege magma chamber before eruption, although some mixing of different levels of magma occurred during in each eruptive event.

Tephros and volcanoclastic sediments of the Cerro Toledo interval is an informal name given to a sequence of epiclastic sediments and tephros of mixed provenance that lies between the two members of the Bandelier Tuff (Broxton and Reneau, 1995). The age of this unit is bracketed by the ages of the Tshirege and Otowi Members (1.22-1.61 Ma; Izett and Obradovich, 1994). This unit contains some deposits normally assigned to the Cerro Toledo Rhyolite, including tuffaceous sandstones and siltstones and primary ash-fall and pumice-fall deposits (Smith et al., 1970; Heiken et al., 1986). The Cerro Toledo interval also includes poorly sorted coarse-grained volcanoclastic sediments derived from lava flows of the Tschicoma Formation. In most cases, both types of volcanoclastic deposits are intercalated, and it is not practical to separate them. Samples for this investigation were collected only from primary fallout deposits. This allowed us to characterize one end-member (high-silica rhyolite tuffaceous material) within this complex assemblage. The other end member composition is represented by analyses from the dacitic lavas of the Tschicoma Formation, which are described below.

The Otowi Member of the Bandelier Tuff is a relatively homogenous unit made up of a succession of ignimbrites. The ignimbrites are nonwelded to partially welded in the areas studied, and the entire sequence of tuffs apparently forms a simple cooling unit. Only the upper part of the Otowi Member was accessible at the sites studied, therefore the elemental data presented los Valles. Tschicoma Formation rocks represent end member compositions for the gravel component of stream-transported sediments in these larger drainage systems. These Tschicoma-derived stream sediments and soils Bandelier Tuff as the streams cross the Pajarito Plateau.

STATISTICAL APPROACH

Statistical Analysis of Bandelier Tuff and Other Geologic Units

The goal of the statistical analysis of the background tuff data is to develop a technically defensible set of data for Environmental Restoration (ER) Project decision-making. The key to technical defensibility is ensuring that the rock analyses represent the natural variation found within each of the Laboratory's geological rock units. Thus the background rock samples were collected from areas that were not affected by Laboratory operations.

The background data are used to support the RFI screening process ("Screening Assessment Methodology at Los Alamos National Laboratory", LANL ER Project, January 1995, draft). As a part of the RFI process, data for most sites are compared to natural background concentration of inorganic analytes. The screening action level (SAL) comparison step fol-

lows the background comparison in the screening assessment process. The SALs cited in this report are based on EPA Region 9 Preliminary Remediation Goals (PRGs). The background screening value for inorganic analytes is the 95th percentile upper tolerance limit (UTL), which is the 95% upper confidence limit of the 95th percentile of the data distribution. The type of data distribution for each inorganic analyte must be estimated to calculate these UTLs.

The statistical analysis of the background data is a step-wise process involving the following steps:

- a) determine if there is a significant chemical difference between units of the Tshirege Member as well as between the Tshirege Member and other rock units.
- b) estimate the type of data distribution for each inorganic analyte so that UTLs can be calculated.
- c) calculate background screening values for each analyte by stratigraphic unit using either UTLs or the maximum reported values for infrequently detected analytes or sparsely sampled stratigraphic units.

Initial Data Analysis Steps

Some of the inorganic results in the combined background rock data set are reported as less than the detection level (<DL). To facilitate statistical analysis of the data, all values reported as <DL were replaced by one-half of the detection limit. This replacement approach is recommended in the EPA risk assessment guidance (EPA 1992, 1166). Concentrations below detection limits commonly occurred for antimony, arsenic, chromium, copper, nickel, radium, silver, tantalum, and thallium. These analytes are excluded from further statistical analyses.

Three samples (field sample numbers 1106-3-12, 1106-3-13, and 1106-3-14) from the Tshirege Qbt 1g/Qbt 1v contact from a stratigraphic section at TA-21 were excluded from the statistical analyses of these two units. This contact, which coincides with a feature called the vapor-phase notch (Broxton et al., 1995), contains anomalous elemental concentrations that significantly skew some statistical parameters when included with the data sets for these units. Exclusion of the samples is justified because they represent a relatively thin zone (~2 m) of chemical alteration specific to the vapor phase notch at one locality, and they are not representative of the chemical characteristics of units 1g and 1v as a whole.

Comparison of Units of the Tshirege Member as well as between the Tshirege Member and other rock units

The statistical analyses first compared rock units represented by 10 or more samples. Because of the sampling bias which focused this study on the Tshirege Member, only units of the Tshirege Member are represented by 10 or more samples. These units included unit 1g (Qbt 1g), unit 1v (Qbt 1v), unit 2 (Qbt 2), and unit 3 (Qbt 3) (Fig. 4). The box plots show the actual values (as filled circles) for each stratigraphic unit. The ends of the box represent the "inter-

quartile" range of the data distribution. The inter-quartile range is specified by the 25th percentile and 75th percentile of the data distribution. The line within the box plot is the median (50th percentile) of the data distribution. Thus the box indicates concentration values for the central half of the data, and concentration shifts can be readily assessed by comparing the boxes. If the majority of the data is represented by a single concentration value (usually the detection limit), the box is reduced to a single line. The solid line spanning the series of box plots is the mean value for the entire data set. Unit 4 (Qbt 4) of the Tshirege Member, tephra and volcanoclastic sediments of the Cerro Toledo interval (Qct), the Otowi Member (Qbo) of the Bandelier Tuff, and the Tschicoma Formation (Tt) were represented by fewer than ten samples and were excluded from the statistical comparisons. Background screening values were developed from the maximum observed value in Qbt 4, Qct, Qbo, and Tt.

Units 1g, 1v, 2, and 3 of the Tshirege Member were statistically compared by the Wilcoxon rank sum test. The Wilcoxon rank sum test is one of the "distribution shift" methods discussed in the LANL ER Project Policy Paper on background comparisons (Environmental Restoration Project Assessments Council 1995, 1218). The statistical comparisons were conducted in a stepwise manner to be consistent with the geological relationships between these rock units. The first step involves a test for a statistically significant difference between units Qbt 1g and Qbt 1v. If these units were not statistically different, these data were lumped in a single data group (Qbt 1), and subsequent statistical comparisons were made between the pooled Qbt 1 data and the other Tshirege units. If Qbt 1g and Qbt 1v were significantly different, we compared each of these units separately to the other Tshirege units.

Estimating Data Distributions for Bandelier Tuff Background Data

The distribution properties of the rock units were summarized, and the results are presented in the Results and Discussion. The visual data displays presented by box plots were used to assign Tshirege unit results to data groups. Statistical distributions that best model the data were used to calculate the UTLs.

Calculation of Background Screening Values for Bandelier Tuff and Other Geologic Units

UTLs were calculated for all inorganic elements, except for iron and sulfate, where enough values were detected to allow estimation of the statistical distribution. Iron and sulfate have unusual distributions, which do not allow use of a simple statistical distribution model. Therefore, we propose use of the maximum detected value as a background screening value for iron and sulfate as well as for the rarely detected elements (antimony, arsenic, chromium, copper, nickel, radium, silver, tantalum, and thallium).

For the elements that are normally distributed without any data transformation and the elements that are normally distributed after a square root transformation¹, we calculated parametric tolerance limits by using the following equation:

$$UTL_{0.95,0.95} = \text{mean} + \text{standard deviation} * k_{0.95,0.95}^1$$

¹ For square root transformed data, the UTL is calculated from the mean and standard deviation of the transformed data, and the resulting estimate of the UTL is squared to facilitate comparisons to site results.

The k-factor depends on the number of background samples; complete tables of k-factors are published in the RCRA ground water statistical analysis document (EPA 1989, 1141) and Gilbert (1987, 0312). Readers are referred to the LANL ER Project policy paper on background comparisons for example k-factors.

The UTLs for log normally distributed elements were estimated by a simulation process. These simulations were run in the S-plus statistical programming environment. The S-plus code is presented in Appendix I. These simulations were run for 10,000 trials, which were sufficient to estimate the lognormal UTLs to two to three significant digits.

The raw calculated UTL results were screened to ensure that the estimated UTLs were not artificially inflated due to a small sample size.

We compared the relative value of the median, mean and calculated UTLs for the cooling unit subgroups and the overall combined background data set. If the mean and the median for a cooling unit were less than the combined data set mean or median and the UTL for the subset was greater than the combined data set, we substituted the overall data UTL for the unit subgroup UTL. We propose that these trimmed UTL values, and the sample maximum for the analytes discussed above, be used as the LANL-wide background screening values.

RESULTS AND DISCUSSION

Table II summarizes the detection limits, number of samples above and below detection limits, and the minimum, maximum, and mean value of samples above detection limits for all leachable inorganic analytes. Box plot summaries of all leachable inorganic analytes by rock units are presented in Figure 4, and samples ranges for these analytes are summarized in Table III.

The significance levels for the pairwise Wilcoxon rank sum test are presented in Table IV. Four inorganic analytes (barium, beryllium, lead and sulfate) showed no consistent statistical difference between the cooling units. The data for these analytes were collapsed into one group Qbt 123, and the remaining statistical analyses were performed on this single data group. All other analytes were partitioned into two, three or four data groups based on the results of the Wilcoxon rank sum test, and the remaining statistical analyses were performed on these data subgroups.

Table V summarizes the distribution properties of the Bandelier Tuff inorganic analytes. Distributions were either normally distributed or were transformed to normality with either a log- or square root transformation.

The raw calculated UTLs for inorganic constituents are presented in Table VI and the summary of background screening values (trimmed UTL values or strata maximums) is presented in Table VII. Trimmed UTL values or strata maximums should be used as the LANL-wide background screening values for the Bandelier Tuff units Qbt 1, Qbt 2 or Qbt 3. Maximum concentrations are used to define background screening values for units Tt, Qbo, Qct, and Qbt 4 because they are represented by fewer than 10 samples.

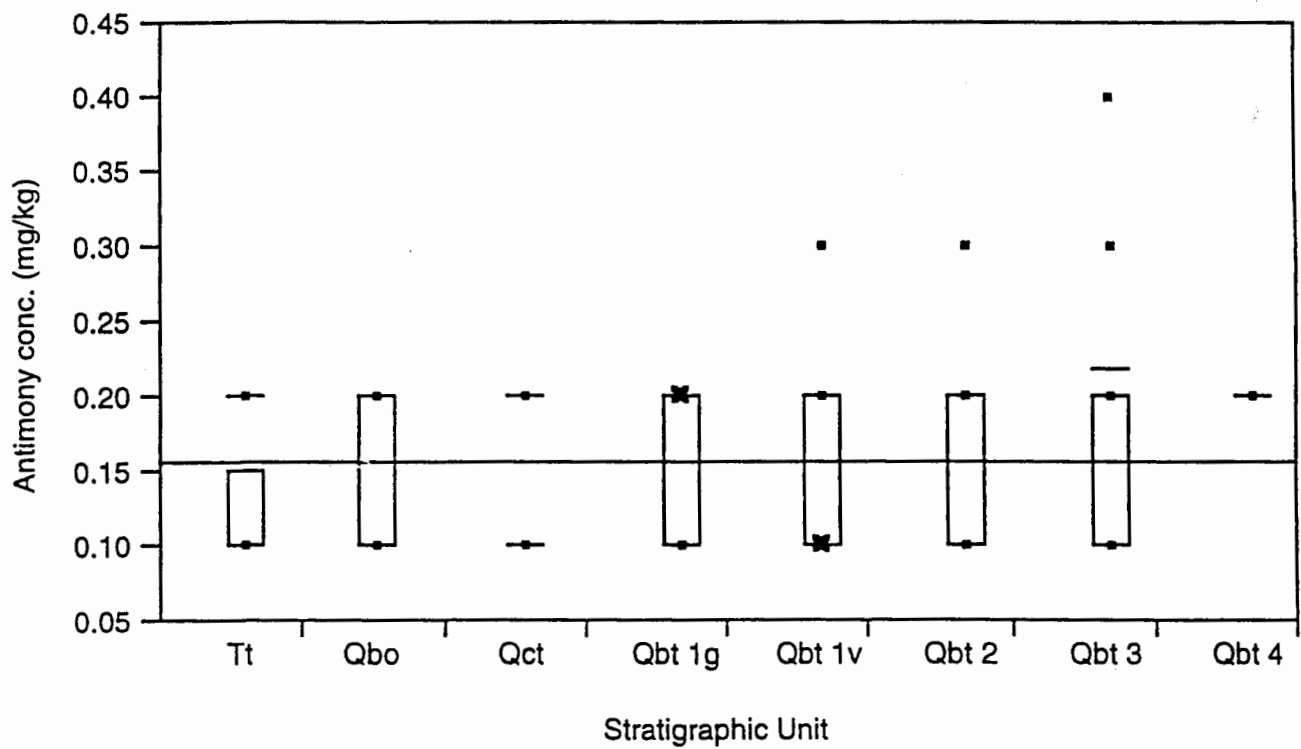
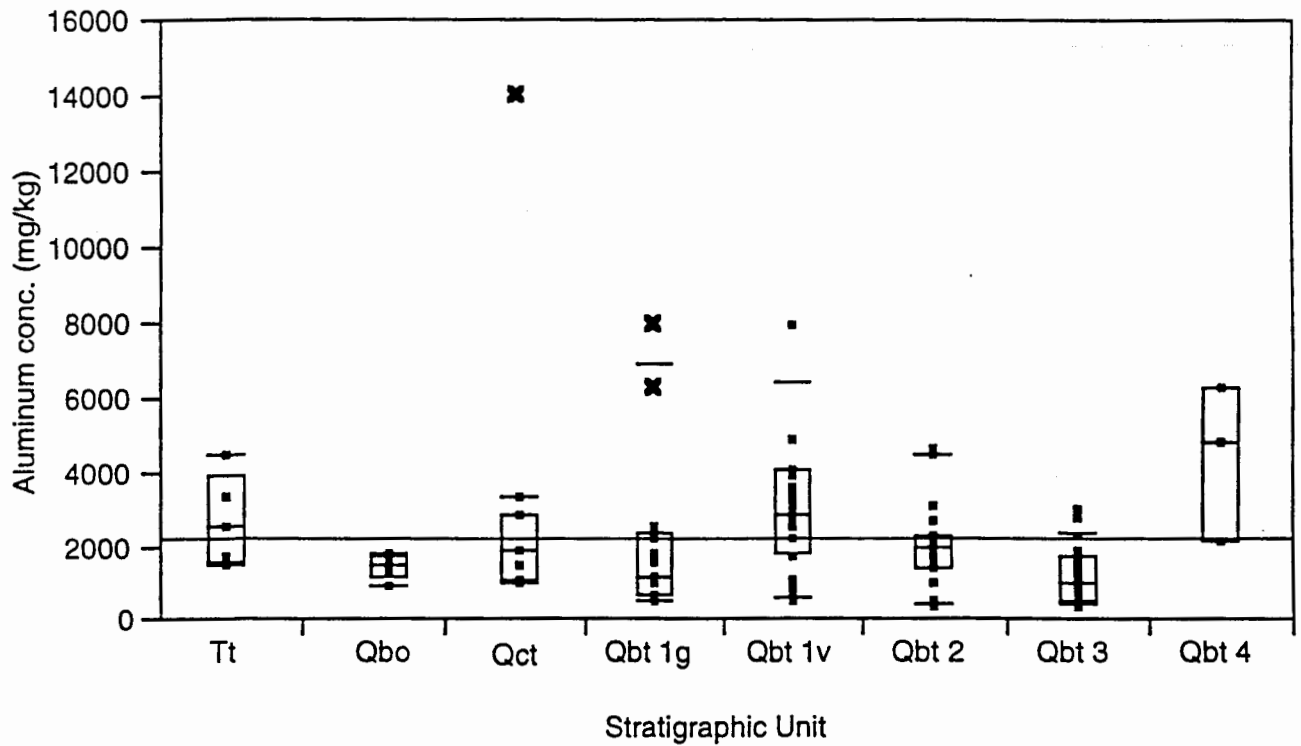


Fig. 4 Box plot summaries of leachable inorganic analytes by geologic unit. See Figure 2 for explanation of geologic unit labels. Explanation of box plots symbols is given in the text. The "x" values in these plots are vapor phase notch samples from stratigraphic section 3 at TA-21.

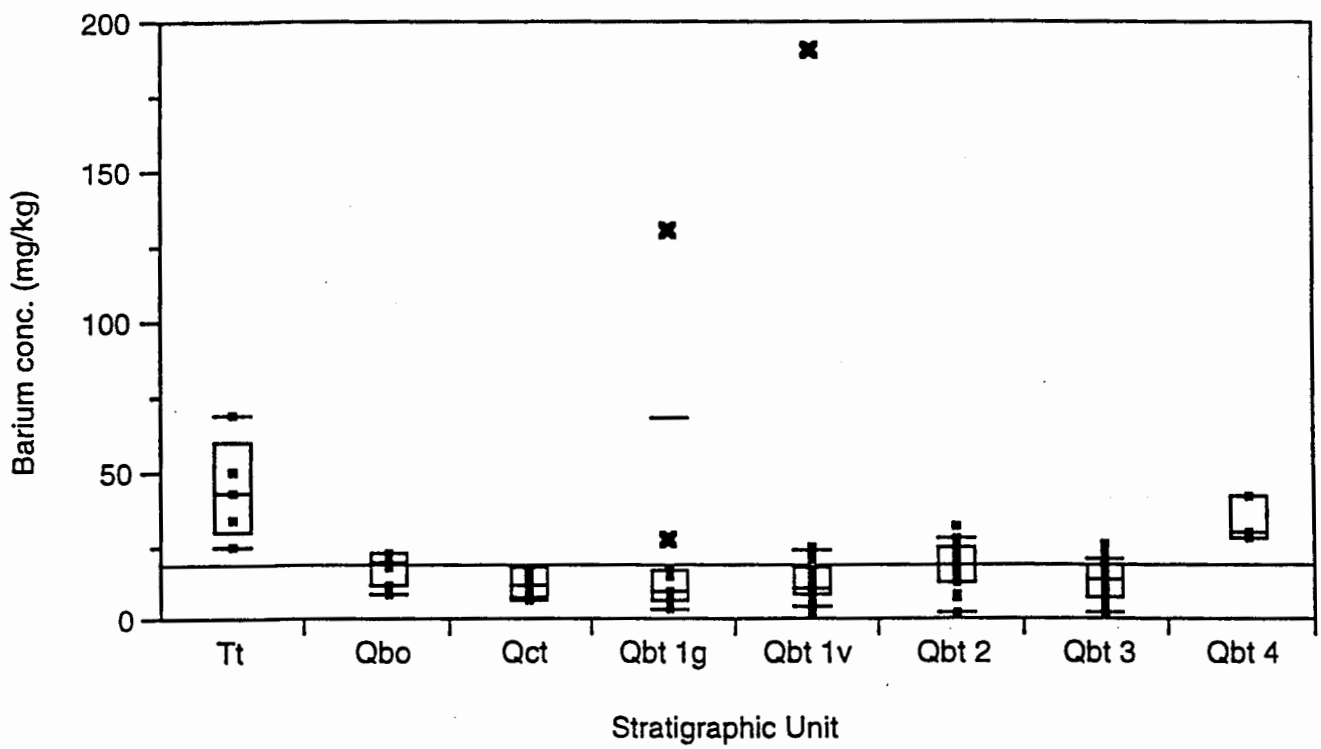
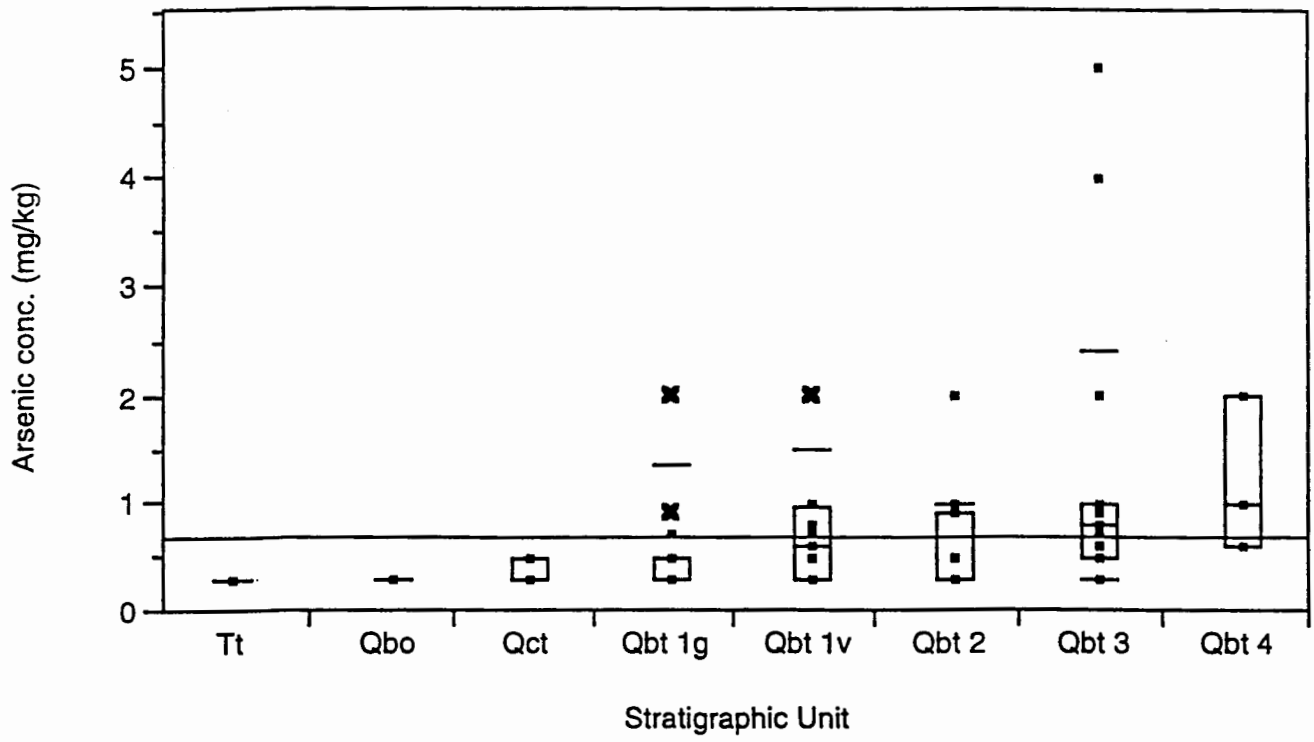


Fig. 4 (Continued)

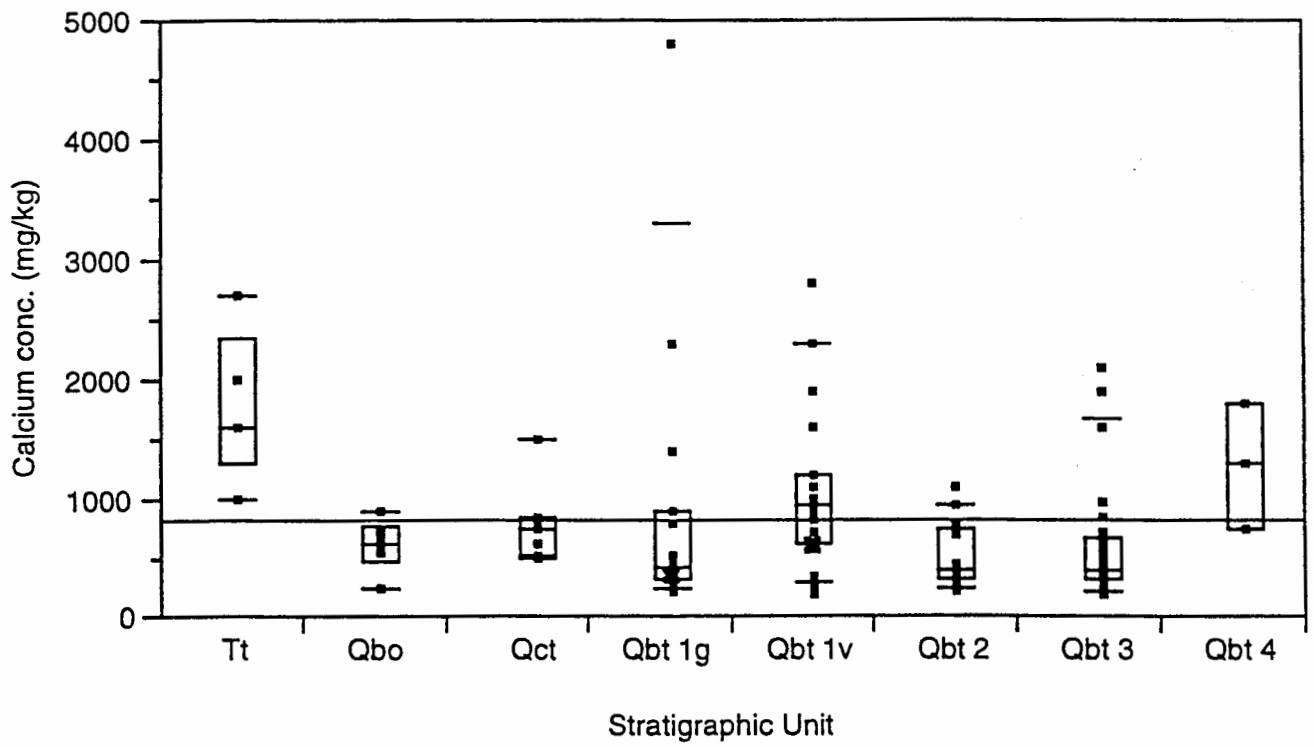
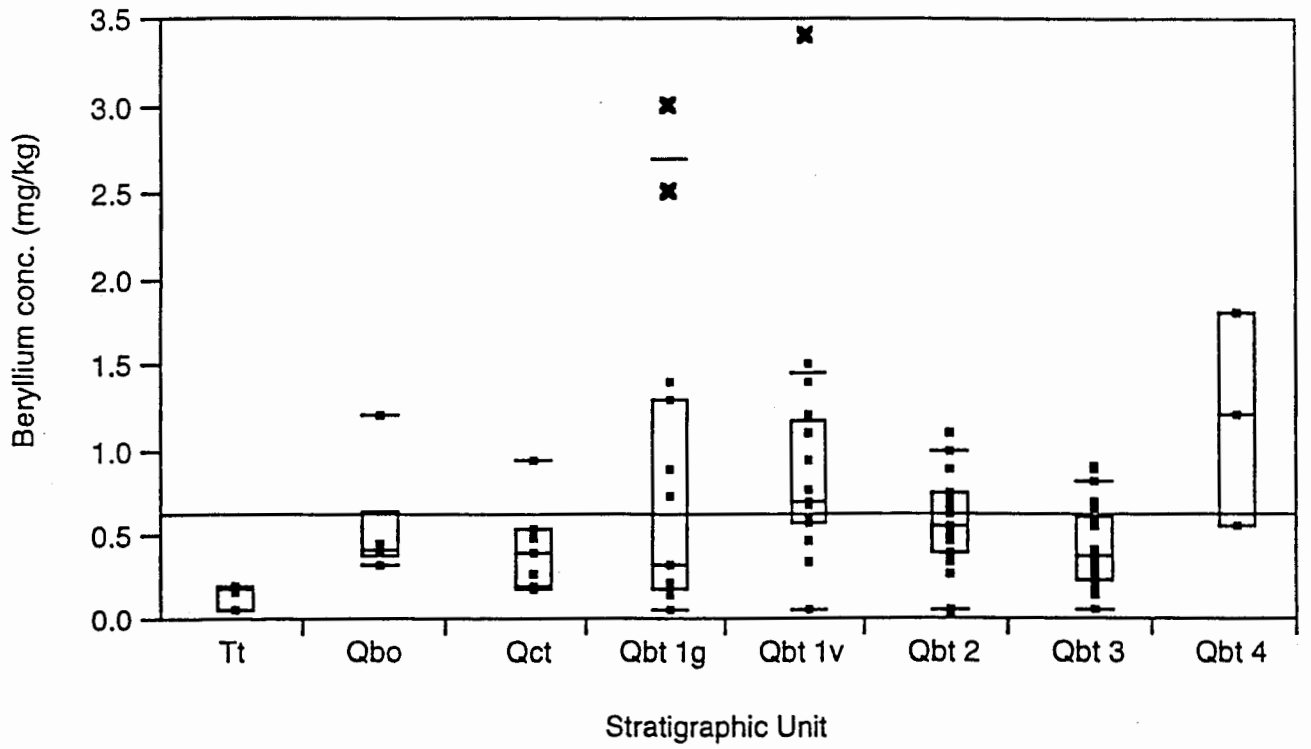


Fig. 4 (Continued)

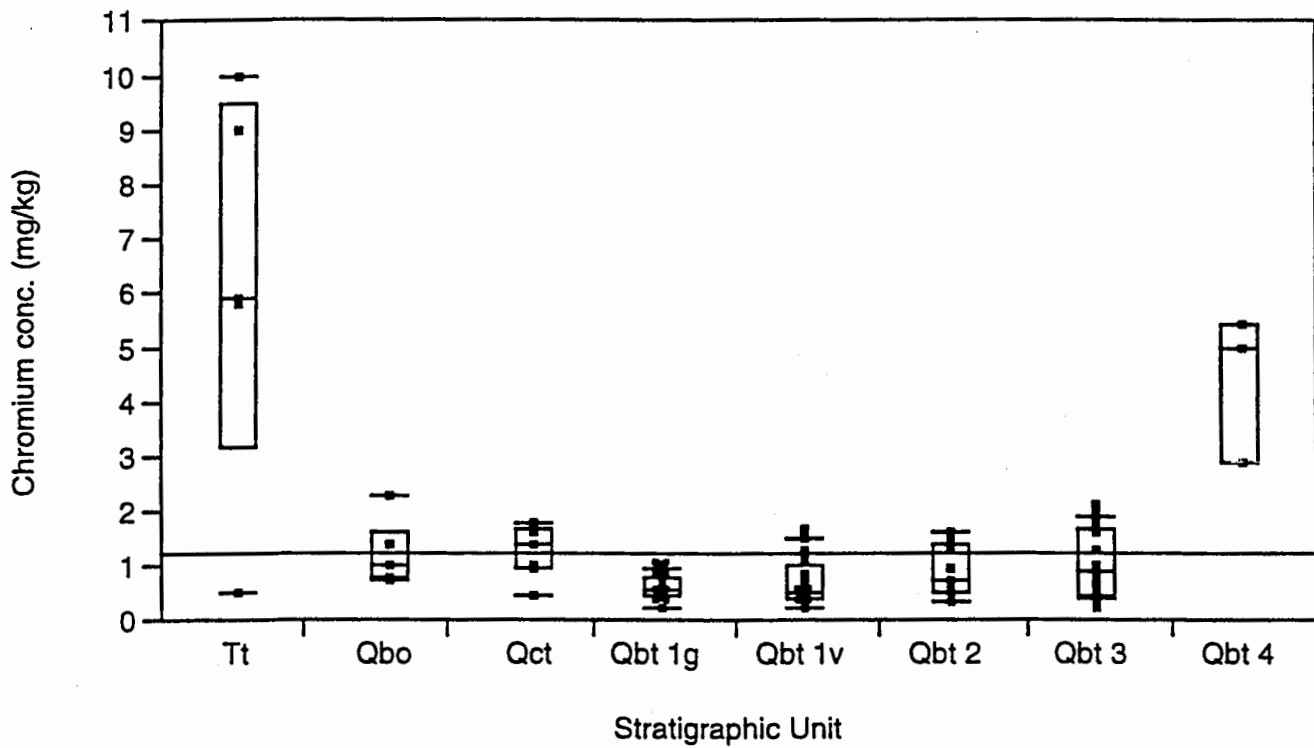
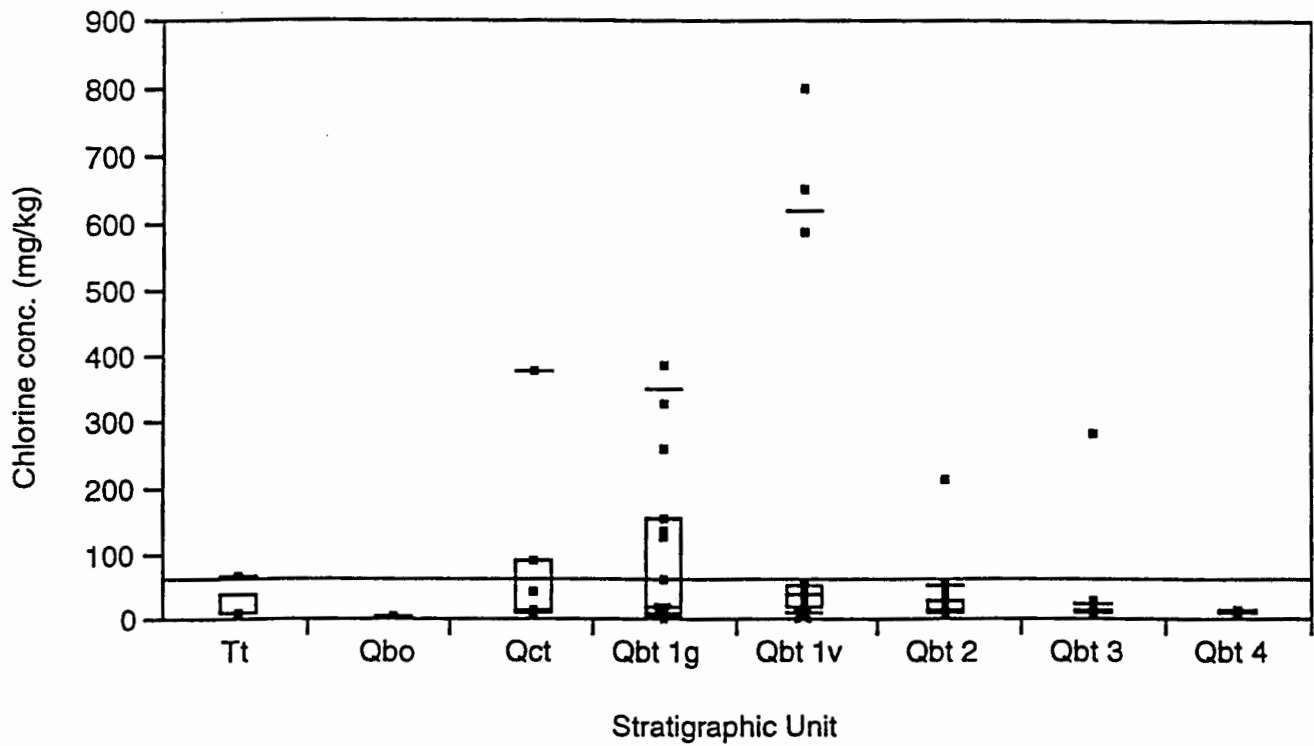


Fig. 4 (Continued)

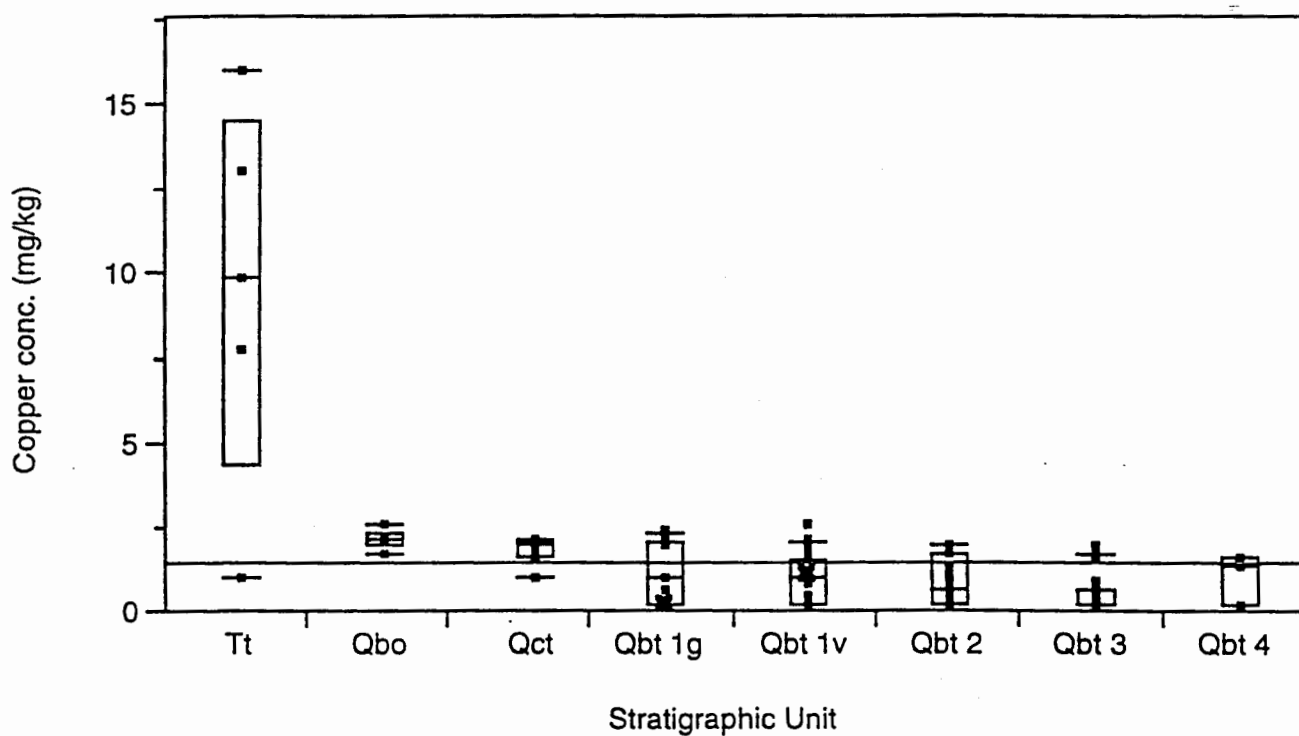
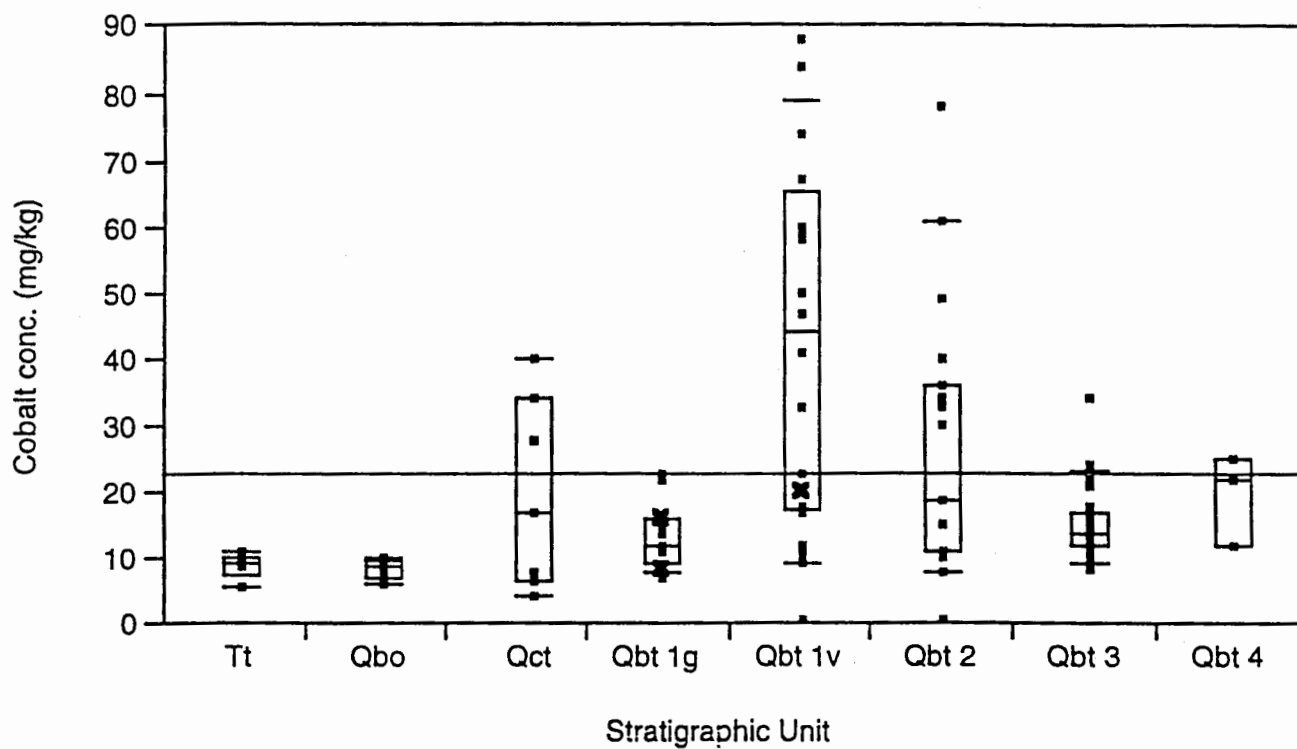


Fig. 4 (Continued)

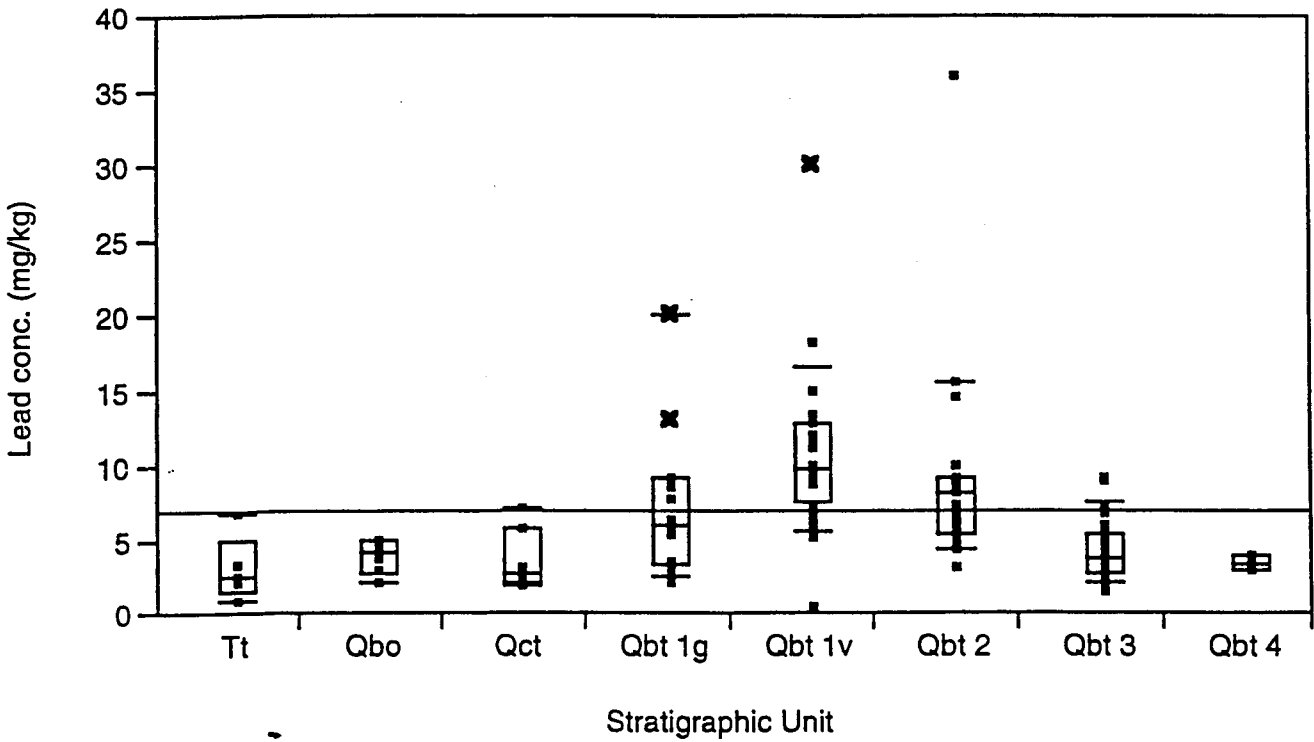
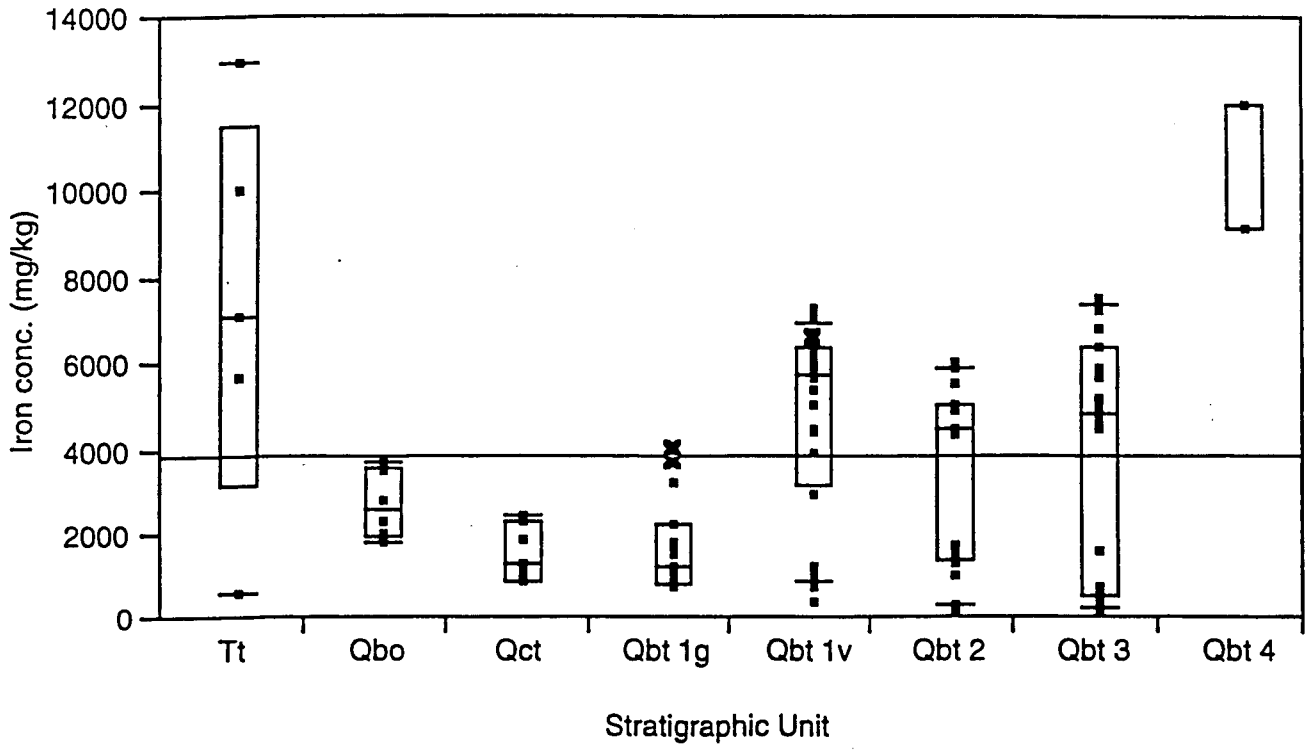


Fig. 4 (Continued)

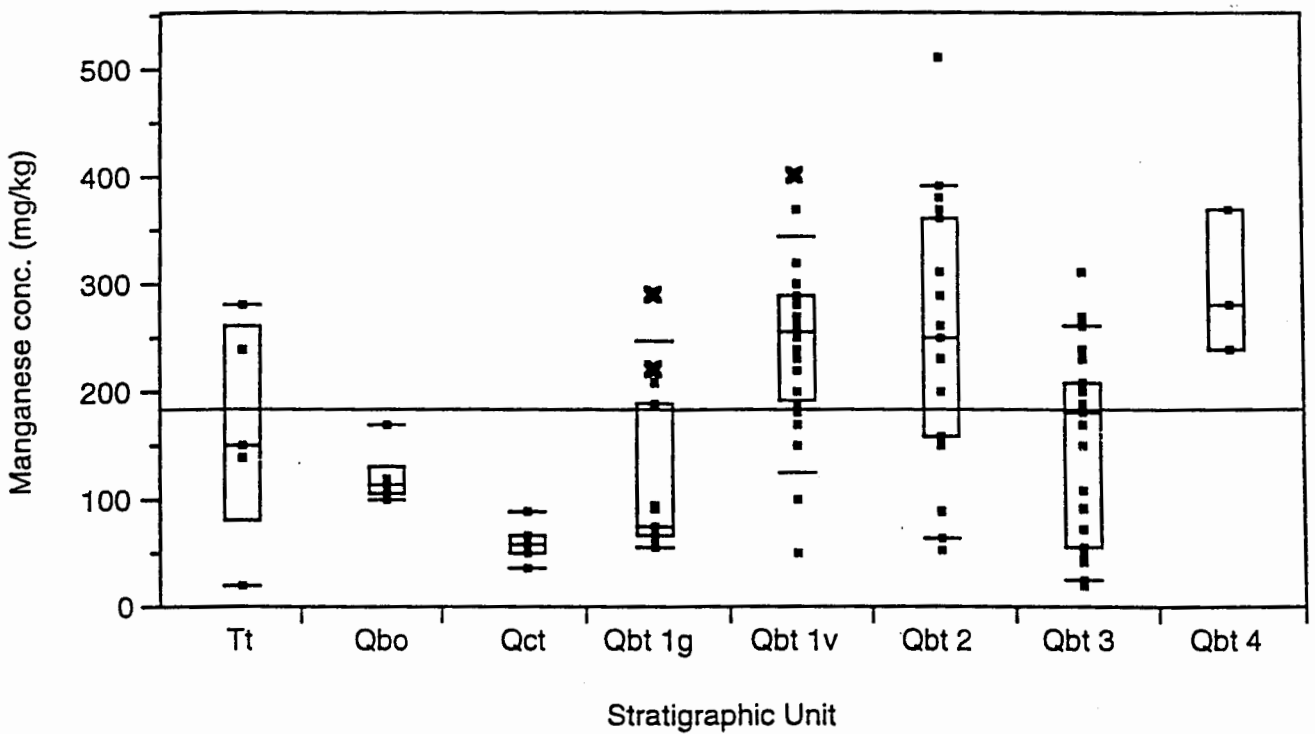
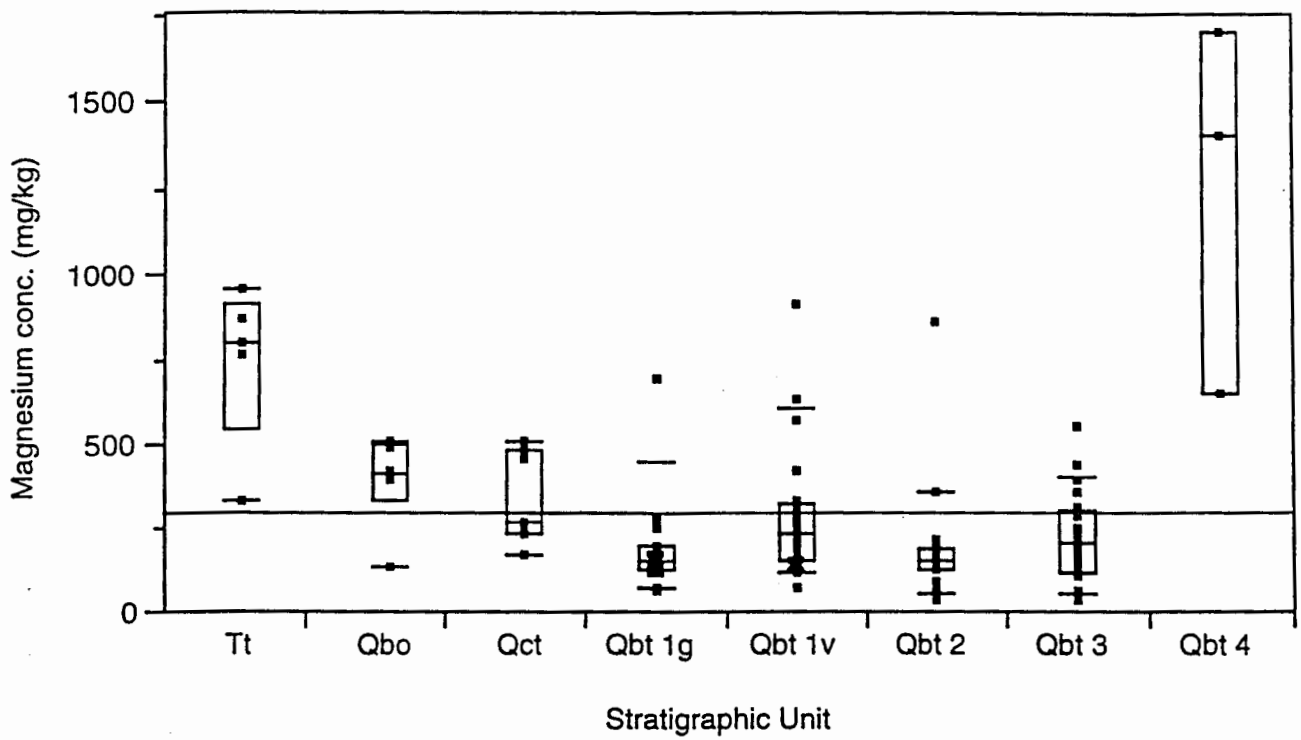


Fig. 4 (Continued)

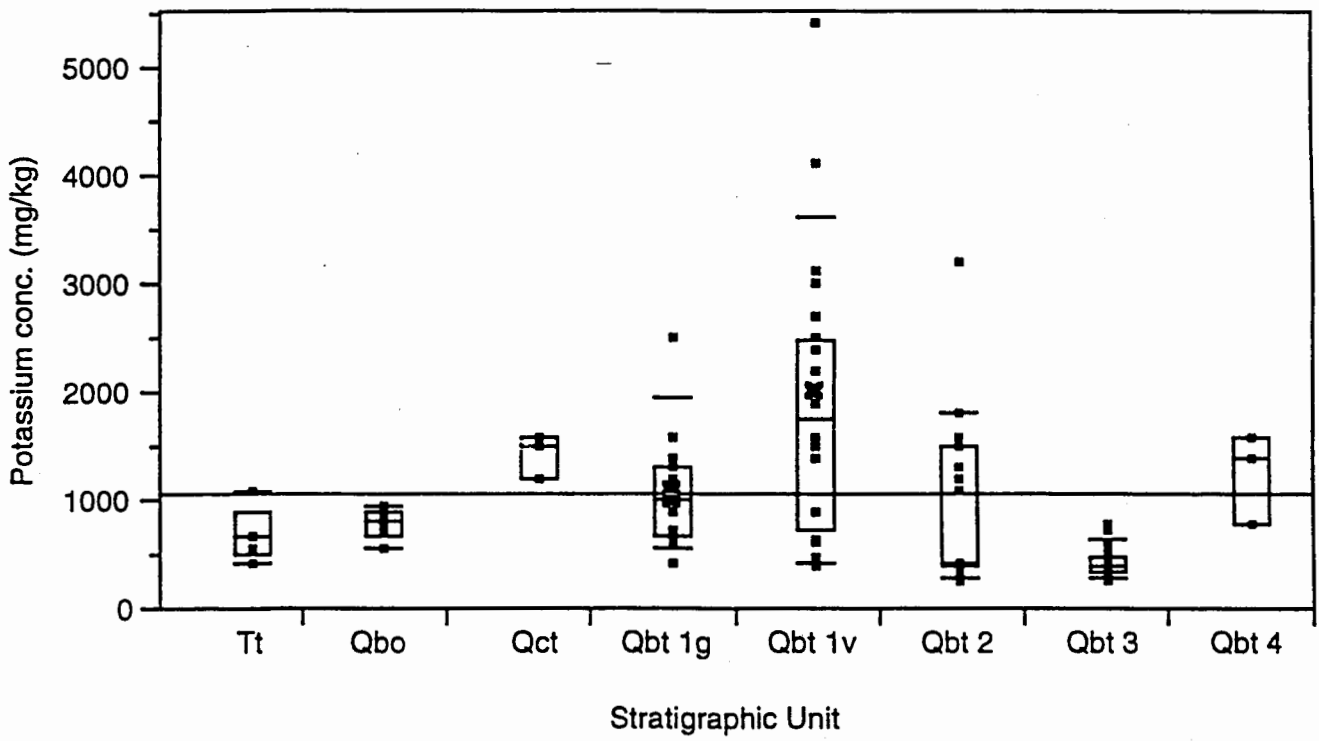
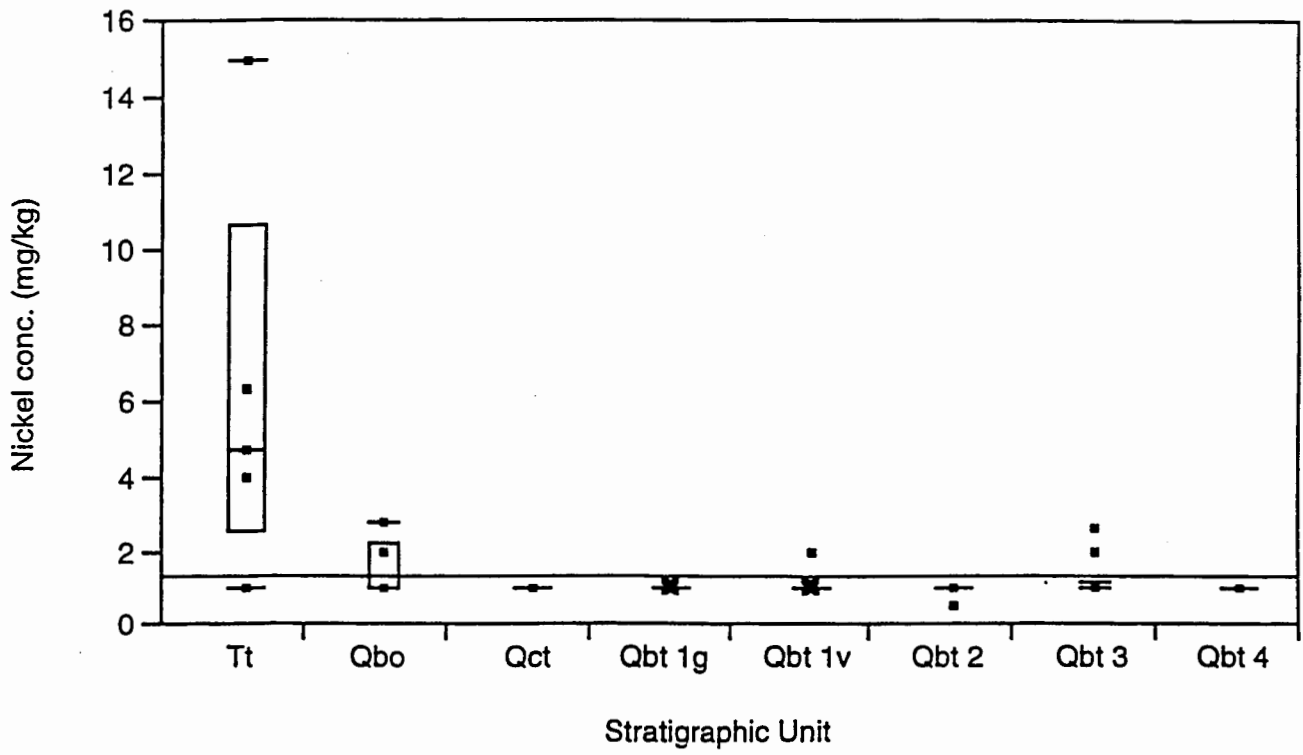


Fig. 4 (Continued)

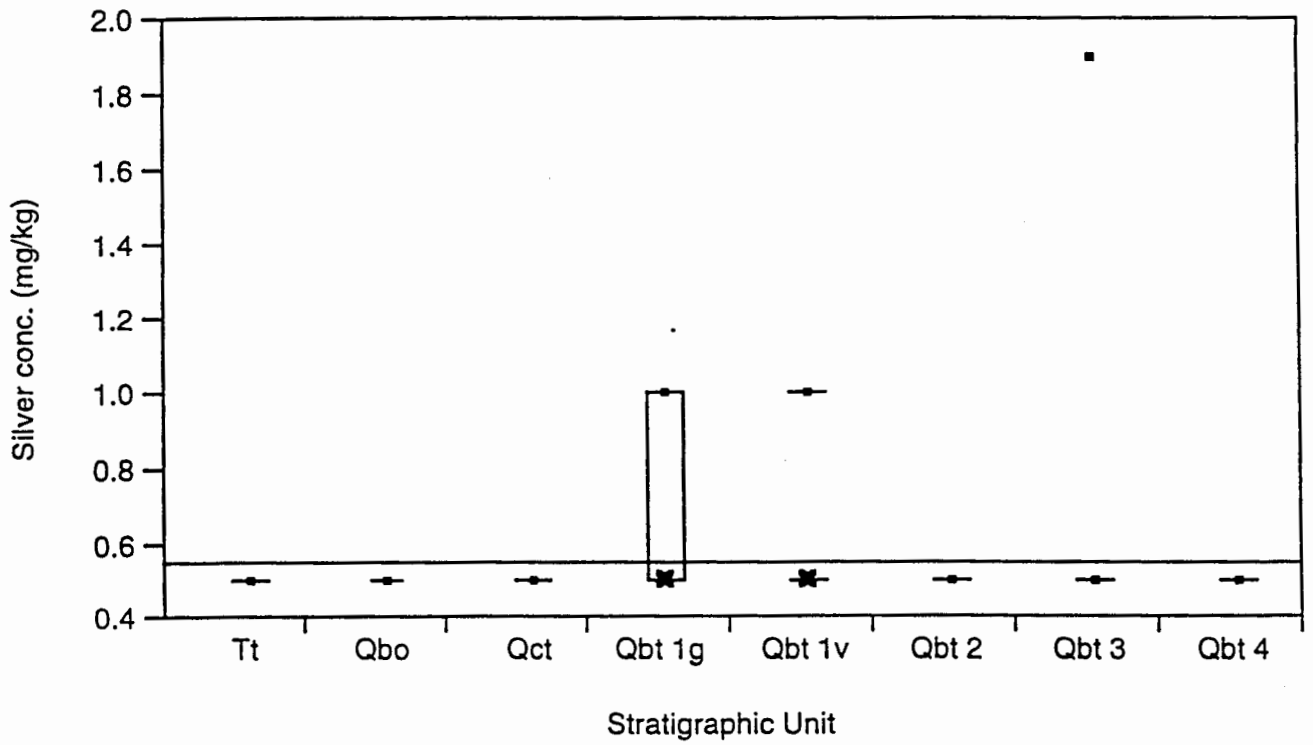
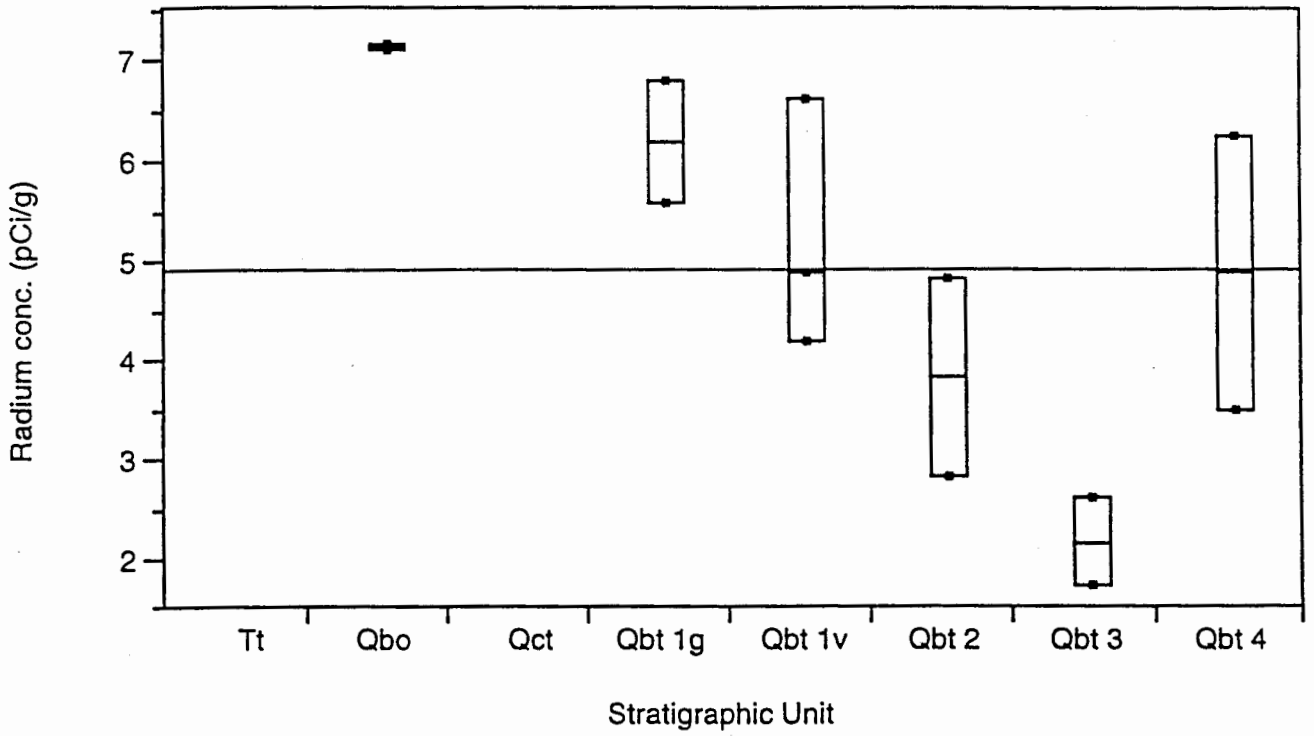


Fig. 4 (Continued)

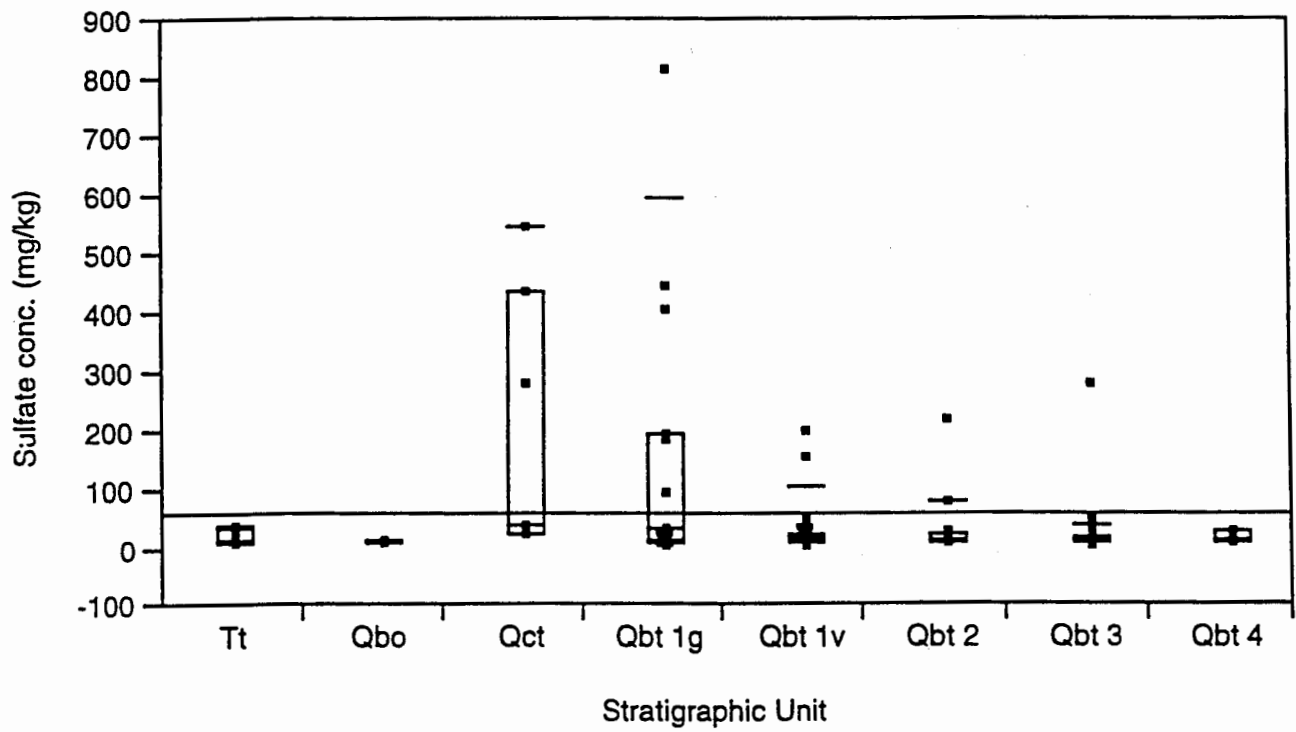
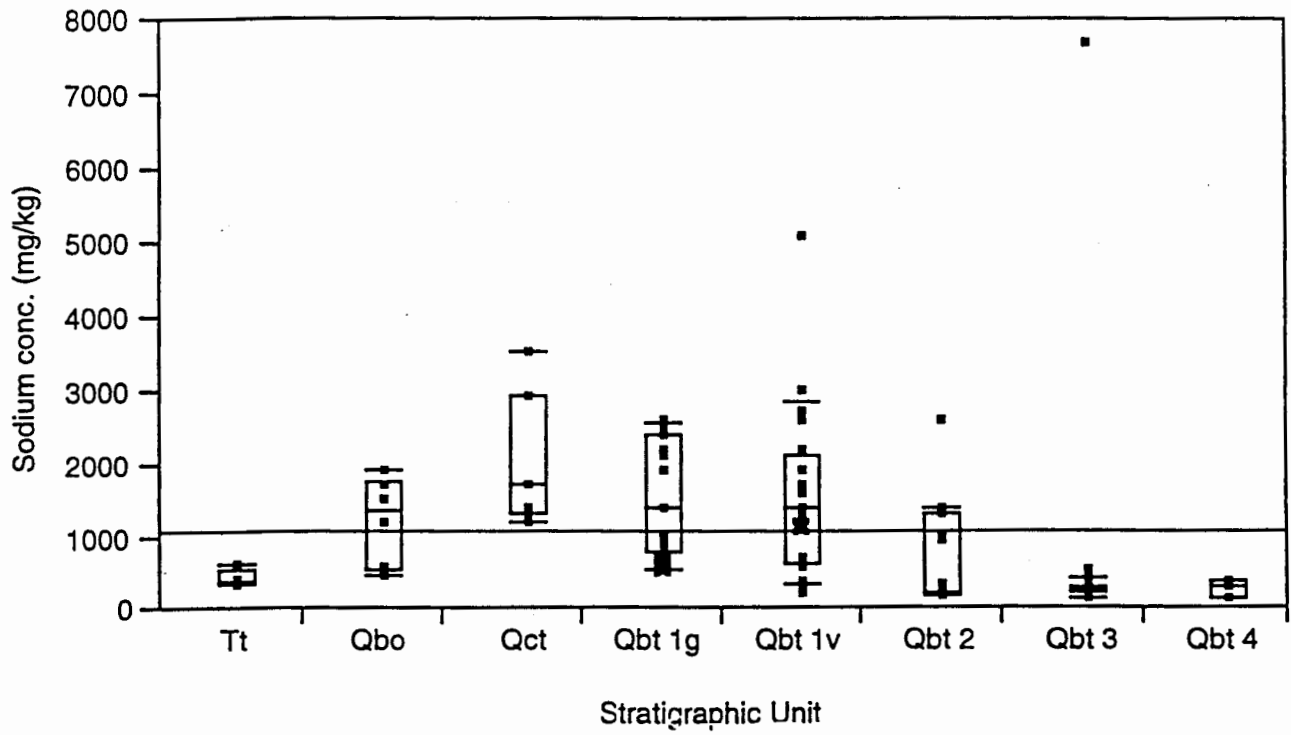


Fig. 4 (Continued)

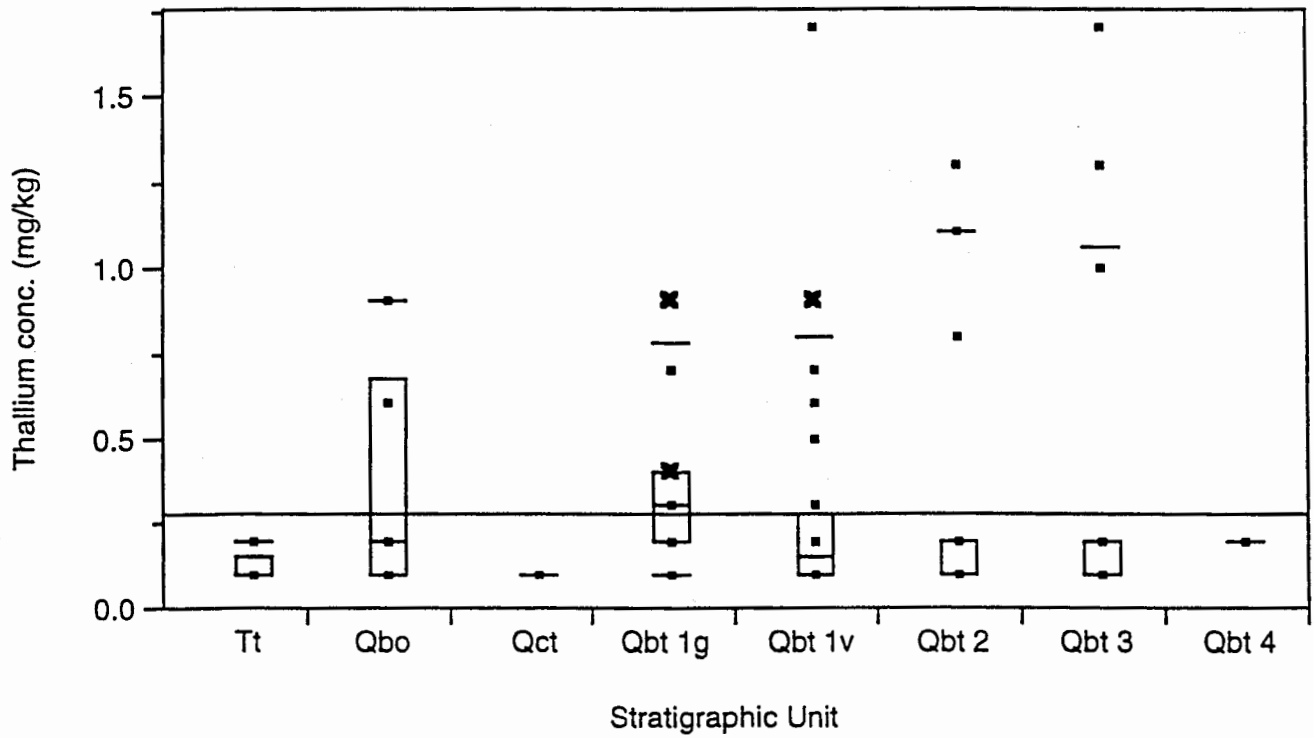
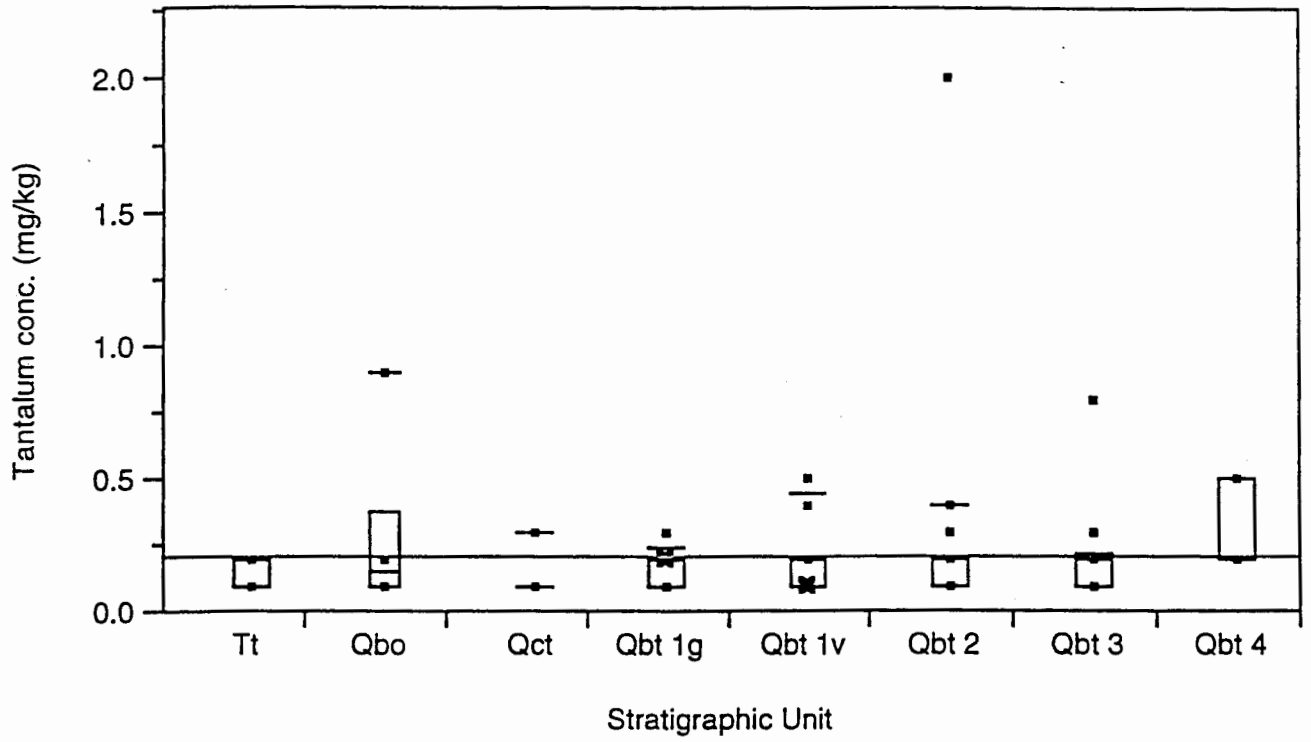


Fig. 4 (Continued)

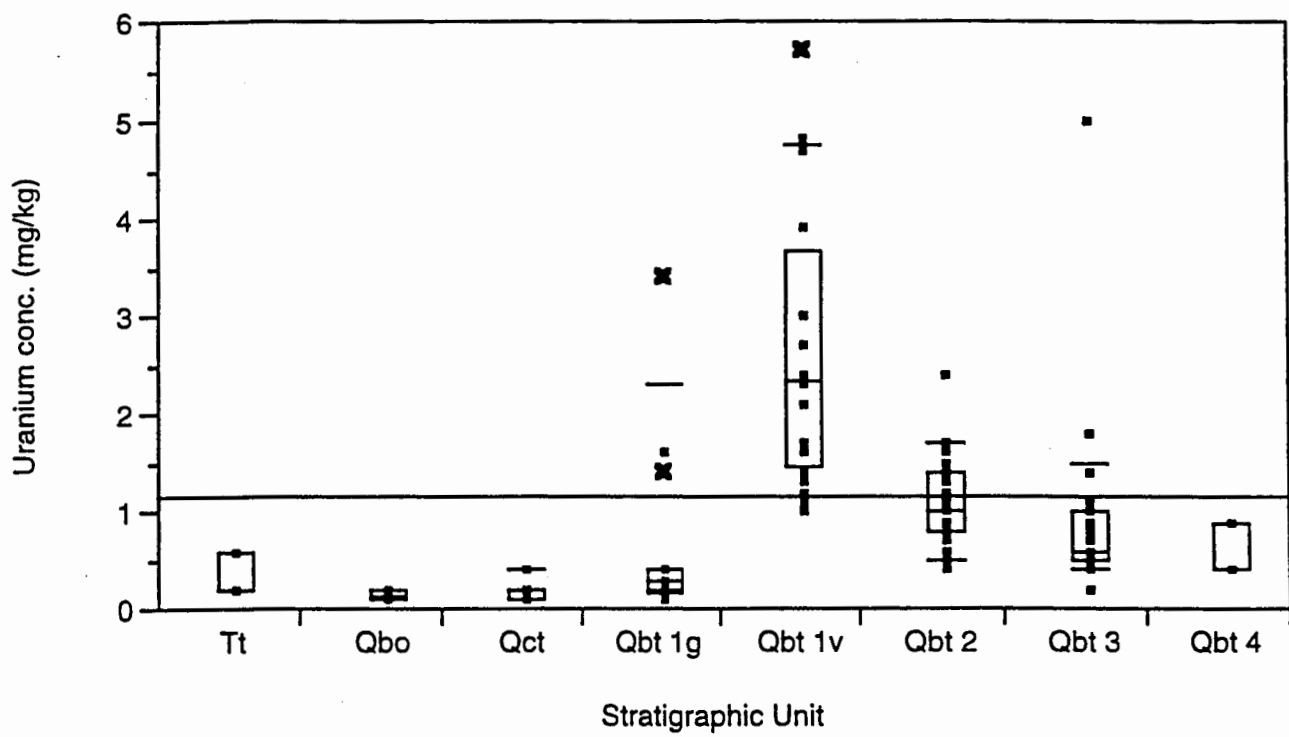
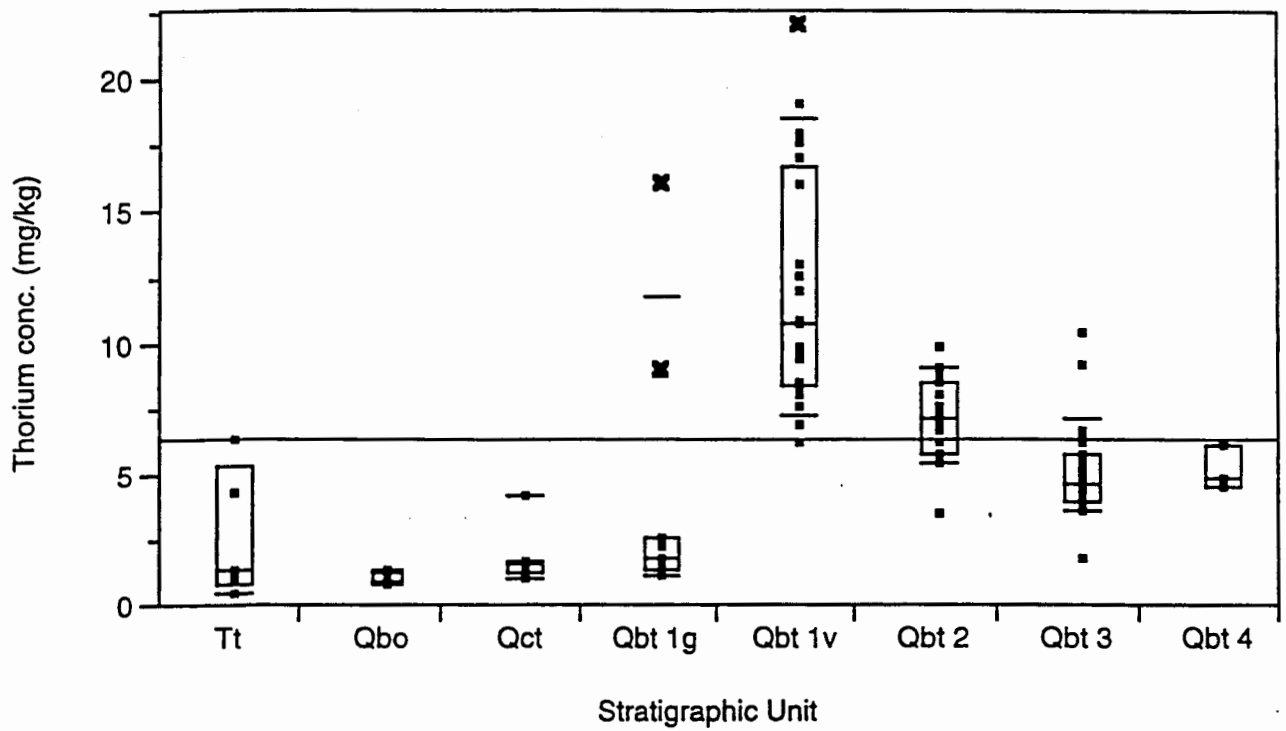


Fig. 4 (Continued)

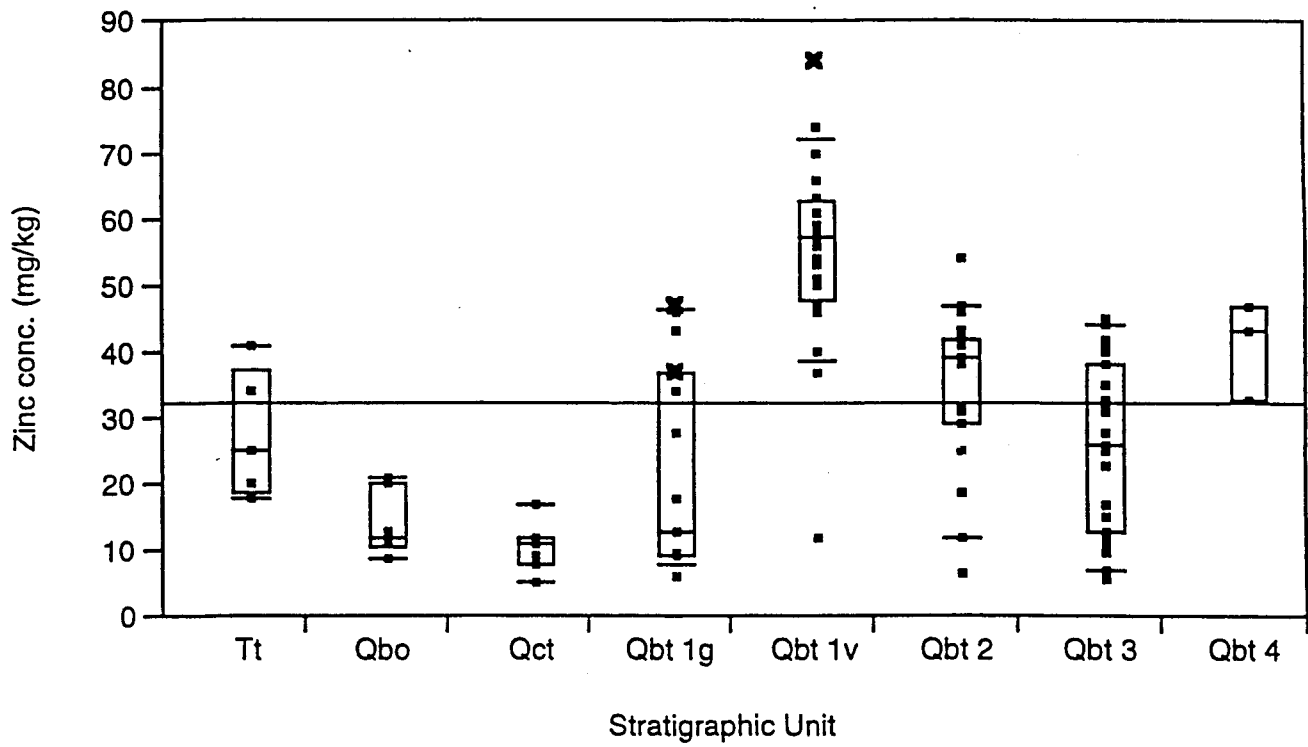
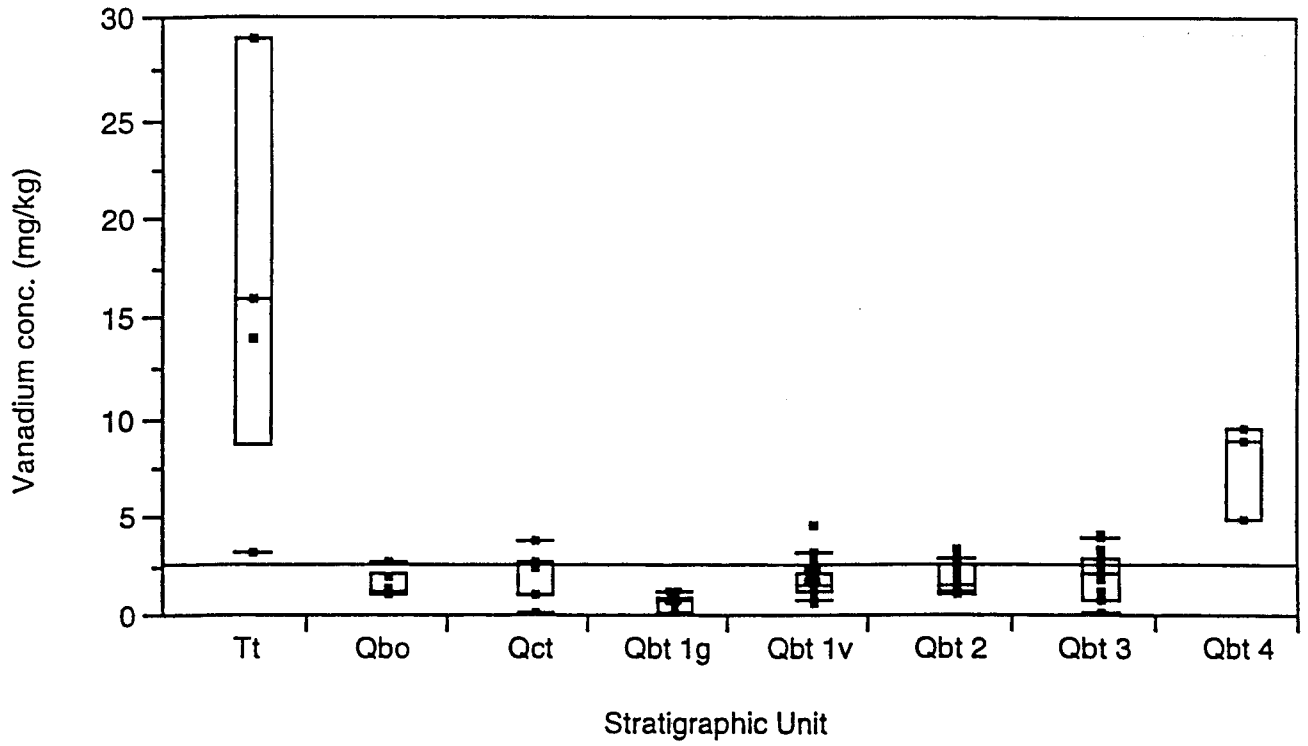


Fig. 4 (Continued)

TABLE II.

SUMMARY OF POPULATION STATISTICS FOR LEACHABLE INORGANIC ANALYTES
IN BACKGROUND ROCK SAMPLES.

Analyte	Non-detects			Detects			
	Count	Min	Max	Count	Min	Max	Average
Aluminum	0			106	350	14000	2187
Antimony	97	0.2	0.3	9	0.2	0.4	0.256
Arsenic	52	0.5	0.5	53	0.5	5	1.08
Barium	0			106	1.4	190	18.5
Beryllium	13	0.08	0.14	93	0.15	3.4	0.700
Calcium	0			106	200	4800	825
Chloride	0			106	3.65	802	59.9
Chromium	38	0.5	2	68	0.57	10	1.70
Cobalt	1	1	1	105	0.89	88	23.1
Copper	49	0.5	2	57	0.6	16	2.38
Iron	0			106	190	13000	3867
Lead	0			106	0.6	36	6.95
Magnesium	0			106	39	1700	296
Manganese	0			106	21	510	184
Nickel	97	1	2	9	2	15	4.60
Potassium	0			106	250	5400	1055
Potassium- Total	0			47	28760	47920	38137
Radium-226 (b)	0			13	1.72	7.15	4.92
Silver	105	1	2	1	1.9	1.9	1.9
Sodium	0			106	130	7700	1059
Sulfate	0			106	1.5	815	56.9
Tantalum	85	0.2	0.3	21	0.2	2	0.429
Thallium	82	0.2	0.3	24	0.2	1.7	0.729
Thorium	0			106	0.5	22	6.31
Thorium- Total	0			47	12.7	37.1	22.7
Uranium	14	0.2	0.3	92	0.2	5.7	1.28
Uranium- Total	0			47	2.83	10.1	5.89
Vanadium	16	0.4	1.4	90	0.8	29	3.08
Zinc	0			106	5.3	84	32.1

(a) Includes the three samples from the vapor phase notch.

(b) Radium-226 concentration is a total concentration.

All analyses reported as mg/kg except for radium-226, which is reported as pCi/g.

TABLE III.

Summary of population statistics for leachable elemental concentrations in background samples by stratigraphic unit

Analyte (1)	Qct		Qbt 1g		Qbt 1v		Qbt 2		Qbt 3		Qbt 4		Qbo		Tt	
	min	max	min	max	min	max	min	max	min	max	min	max	min	max	min	max
Aluminum	1100	3400	490	2500	490	7900	350	4600	400	3000	2100	6200	900	1800	1500	4500
Antimony	<0.2	0.2	<0.2	<0.3	<0.2	0.3	<0.2	0.3	<0.2	0.4	<0.3	<0.3	<0.2	<0.3	<0.2	<0.3
Arsenic	<0.5	0.5	<0.5	0.7	<0.5	2	<0.5	2	<0.5	5	0.6	2	<0.5	<0.5	<0.5	<0.5
Barium	6.7	18	3.6	17	2.4	25	1.4	32	1.7	26	28	42	8.4	23	25	69
Beryllium	0.19	0.95	<0.14	1.4	<0.14	1.5	<0.08	1.1	<0.14	0.91	0.56	1.8	0.32	1.2	<0.14	0.21
Calcium	490	1500	210	4800	200	2800	210	1100	200	2100	730	1800	250	890	990	2700
Chloride	10.1	379	3.65	384	8.2	802	13.5	212	11	279	10.8	14.9	6.7	7.7	9.7	67
Chromium	<0.9	1.8	<0.5	0.94	<0.5	1.7	<0.7	1.6	<0.5	2.1	2.9	5.4	0.73	2.3	<1	10
Cobalt	4.5	40	7.2	23	0.89	88	<1	78	8.6	34	12	25	6.3	10	5.7	11
Copper	<2	2.2	<0.5	2.4	<0.5	2.6	<0.5	2	<0.5	2	<0.5	1.6	1.7	2.6	0.97	16
Iron	880	2400	730	3200	360	7300	200	6000	190	7500	9100	12000	1800	3700	570	13000
Lead	2	7.1	2.2	20	0.6	18.3	3.2	36	1.6	9.1	2.9	4	2.1	5	1	6.7
Magnesium	170	510	69	690	78	910	39	860	42	550	650	1700	140	510	330	950
Manganese	38	90	57	210	52	370	54	510	22	310	240	370	100	170	21	280
Nickel	<2	<2	<2	<2	<2	2	<1	<2	<2	2.6	<2	<2	<2	2.8	<2	15
Potassium	1200	1600	440	2500	390	5400	250	3200	250	800	800	1600	560	960	430	1100
Radium (2)	ND	ND	ND	6.78	ND	6.61	ND	4.82	ND	2.6	ND	6.23	ND	7.15	ND	ND
Silver	<1	<1	<1	<2	<1	<2	<1	<1	<1	1.9	<1	<1	<1	<1	<1	<1
Sodium	1200	3500	530	2600	210	5100	170	2600	150	7700	130	390	450	1900	350	610
Sulfate	22.4	548	1.64	815	1.5	199	9.9	217	3.8	277	10.2	26.4	8.5	12.7	10.5	38.6
Tantalum	<0.2	0.3	<0.2	0.3	<0.2	0.5	<0.2	2	<0.2	0.8	<0.3	0.5	<0.3	0.9	<0.2	0.2
Thallium	<0.2	<0.2	<0.2	0.7	<0.2	1.7	<0.2	1.3	<0.2	1.7	<0.3	<0.3	<0.2	0.9	<0.2	<0.3
Thorium	1.1	4.2	1.2	8.8	6.2	19.1	3.5	9.9	1.9	10.4	4.6	6.1	0.9	1.4	0.5	6.4
Uranium	<0.2	0.4	<0.2	1.6	1	4.8	0.4	2.4	0.2	5	0.4	0.9	<0.2	0.2	<0.3	0.6
Vanadium	<0.5	3.8	<0.4	1.3	<1.4	4.6	1.2	3.4	<0.5	4.2	5	9.5	1.1	2.8	3.3	29
Zinc	5.3	17	6.1	46	12	74	6.7	54	5.5	45	33	47	8.9	21	18	41

Sample sizes are: Qct, n=7; Qbt 1g, n=13; Qbt 1v, n=23; Qbt 2, n=19; Qbt 3, n=27; Qbt 4, n=3; Qbo, n=6, except arsenic n=5; Tt, n=5.

(1) - All values are in mg/kg unless otherwise noted.

(2) - Units are pCi/g.

ND - Not determined.

TABLE IV.

SUMMARY OF MANN-WHITNEY SIGNIFICANCE LEVELS FOR COMPARISONS BETWEEN UNITS OF THE TSHIREGE MEMBER

Analyte	Qbt1g vs Qbt1v	Qbt1g vs Qbt2	Qbt1v vs Qbt2	Qbt1g vs Qbt3	Qbt1v vs Qbt3	Qbt 1 vs Qbt 2	Qbt 1 vs Qbt 3	Qbt 2 vs Qbt 3	Data groups
Aluminum	0.00	0.09	0.04	0.79	0.00	0.49	0.00	0.01	Qbt 1g23 Qbt 1v
Barium	0.28	0.00	0.02	0.09	0.39	0.00	0.16	0.05	Qbt 123
Beryllium	0.22	0.45	0.18	0.87	0.01	0.55	0.09	0.09	Qbt 123
Calcium	0.11	0.38	0.00	0.63	0.00	0.00	0.04	0.70	Qbt 1 Qbt 23
Chloride	0.88	0.26	0.03	0.02	0.00	0.05	0.00	0.00	Qbt 1 Qbt 2 Qbt 3
Cobalt	0.00	0.04	0.06	0.21	0.00	0.69	0.10	0.09	Qbt 1g3 Qbt 1v2
Iron	0.00	0.00	0.06	0.14	0.34	0.94	0.99	0.49	Qbt 1g Qbt 1v23
Lead	0.00	0.07	0.06	0.08	0.00	0.63	0.00	0.00	Qbt 123
Magnesium	0.04	0.73	0.00	0.40	0.26	0.04	0.69	0.19	Qbt 1g2 Qbt 1v3
Manganese	0.00	0.00	0.67	0.03	0.00	0.06	0.27	0.02	Qbt 1g Qbt 1v2 Qbt 3
Potassium	0.07	0.14	0.00	0.00	0.00	0.00	0.00	0.08	Qbt 1g2 Qbt 1v Qbt 3
Sodium	0.48	0.00	0.00	0.00	0.00	0.00	0.00	0.74	Qbt 1 Qbt 23
Sulfate	0.09	0.10	0.68	0.00	0.00	0.30	0.00	0.07	Qbt 123
Thorium	0.00	0.00	0.00	0.00	0.00	0.33	0.07	0.00	Qbt 1g Qbt 1v Qbt 2 Qbt 3
Uranium	0.00	0.00	0.00	0.00	0.00	0.30	0.13	0.03	Qbt 1g Qbt 1v Qbt 2 Qbt 3
Vanadium	0.00	0.00	0.80	0.00	0.79	0.02	0.13	0.95	Qbt 1g Qbt 1v23
Zinc	0.00	0.00	0.00	0.11	0.00	0.09	0.00	0.08	Qbt 1g23 Qbt 1v

TABLE V.

STATISTICAL DISTRIBUTION OF THE BANDELIER TUFF BACKGROUND DATA SET INORGANIC ANALYTES. THESE DATA ARE FOR THE NITRIC ACID DISSOLUTION EXTRACTION METHOD (EPA METHOD 3050)

Analyte	Statistical Distribution
Aluminum	Square root transformed data are approximately normally distributed.
Antimony	Only 9 of 106 total values are detects, no distribution was estimated.
Arsenic	Only 53 of 105 total values are detects, no distribution was estimated.
Barium	Data are approximately normally distributed.
Beryllium	Square root transformed data are approximately normally distributed.
Calcium	Log transformed data are approximately normally distributed.
Chloride	Log transformed data are approximately normally distributed.
Chromium	Only 68 of 106 total values are detects, no distribution was estimated.
Cobalt	Square root transformed data are approximately normally distributed.
Copper	Only 57 of 106 total values are detects, no distribution was estimated.
Iron	Each data subgroup was bimodally distributed, instead of estimating a mixture distribution, we will use the maximum value per subgroup as a background screening value.
Lead	Square root transformed data are approximately normally distributed, which include a statistical outlier that was not deleted from the combined data group (36 mg/kg).
Magnesium	Square root transformed data are approximately normally distributed.
Manganese	Data are approximately normally distributed.
Nickel	Only 9 of 106 total values are detects, no distribution was estimated.
Potassium	Square root transformed data are approximately normally distributed.
Potassium-Total	Data are approximately normally distributed.
Radium	Only 13 of 106 total values are detects, no distribution was estimated.
Silver	Only 1 of 106 total values is a detect, no distribution was estimated.
Sodium	For data group Qbt 1, square root transformed data are approximately normally distributed. For data group Qbt 23, log transformed data are approximately normally distributed.
Sulfate	Each data subgroup was bimodally distributed, instead of estimating a mixture distribution, we will use the maximum value per subgroup as a background screening value.
Tantalum	Only 21 of 106 total values are detects, no distribution was estimated.
Thallium	Only 24 of 106 total values are detects, no distribution was estimated.
Thorium	Square root transformed data are approximately normally distributed.
Thorium-Total	Statistical distribution was not evaluated due to a small sample size per stratigraphic unit.
Uranium	Square root transformed data are approximately normally distributed.
Uranium-Total	Statistical distribution was not evaluated due to a small sample size per stratigraphic unit.
Vanadium	Data are approximately normally distributed.
Zinc	Data within each subgroup are approximately normally distributed.

TABLE VI.

SUMMARY OF CALCULATED RAW UTLs AND MAXIMUM CONCENTRATIONS FOR BANDELIER TUFF
UNITS QBT 123 GROUPS AND SUBGROUPS

Aluminum								
Data group	Count	minimum	median	maximum	Mean	Std Dev	Prob>ChiSq (1)	UTL _{95th} (sqrt)
Qbt 1g23	59	350	1300	4600	1467	959	0.0001	3698
Qbt 1v	23	490	2700	7900	2945	1716		8173
All Qbt 123 data	82	350	1700	7900	1882	1380		5066

Antimony								
Data group	Count	minimum	median	maximum	Mean	Std Dev	Prob>ChiSq (1)	Max. detect
Qbt 1g	13	0.1	0.2	0.2	0.169	0.048	0.0568	ND
Qbt 1v	23	0.1	0.1	0.3	0.135	0.057		0.3
Qbt 2	19	0.1	0.2	0.3	0.168	0.058		0.3
Qbt 3	27	0.1	0.2	0.4	0.178	0.070		0.4
All Qbt 123 data	82	0.1	0.2	0.4	0.162	0.062		0.4

Arsenic								
Data group	Count	minimum	median	maximum	Mean	Std Dev	Prob>ChiSq (1)	Max. detect
Qbt 1g	13	0.3	0.3	0.7	0.362	0.126	0.0013	0.7
Qbt 1v	23	0.3	0.6	2	0.626	0.398		2
Qbt 2	19	0.3	0.3	2	0.547	0.441		2
Qbt 3	27	0.3	0.8	5	1.085	1.112		5
All Qbt 123 data	82	0.3	0.5	5	0.717	0.748		5

Barium								
Data group	Count	minimum	median	maximum	Mean	Std Dev	Prob>ChiSq (1)	UTL _{95th}
All Qbt 123 data	82	1.4	14	32	13.4	7.17	NA	28.0

Beryllium								
Data group	Count	minimum	median	maximum	Mean	Std Dev	Prob>ChiSq (1)	UTL _{95th} (sqrt)
All Qbt 123 data	82	0.04	0.57	1.5	0.570	0.371	NA	1.53

Calcium								
Data group	Count	minimum	median	maximum	Mean	Std Dev	Prob>ChiSq (1)	UTL _{95th} by sim
Qbt 1	36	200	885	4800	1073	926	0.0017	4139
Qbt 23	46	200	400	2100	560	416		1524
All Qbt 123 data	82	200	520	4800	785	729		2431

TABLE VI (CONTINUED).

SUMMARY OF CALCULATED RAW UTLs AND MAXIMUM CONCENTRATIONS FOR BANDELIER TUFF UNITS QBT 123 GROUPS AND SUBGROUPS

Chloride								
Data group	Count	minimum	median	maximum	Mean	Std Dev	Prob>ChiSq (1)	UTL _{95th} by sim
Qbt 1	36	3.65	42.5	802	118.0	194.7	0	404.9
Qbt 2	19	13.5	18	212	33.0	44.7		107.2
Qbt 3	27	11	13.1	279	25.2	51.0		64.8
All Qbt 123 data	82	3.65	19.65	802	67.8	140.2		237.0

Chromium								
Data group	Count	minimum	median	maximum	Mean	Std Dev	Prob>ChiSq (1)	Max. detect
Qbt 1g	13	0.25	0.6	0.94	0.556	0.230	0.0391	0.94
Qbt 1v	23	0.25	0.6	1.7	0.733	0.451		1.7
Qbt 2	19	0.35	0.76	1.6	0.913	0.461		1.6
Qbt 3	27	0.25	0.9	2.1	1.051	0.596		2.1
All Qbt 123 data	82	0.25	0.705	2.1	0.851	0.507		2.1

Cobalt								
Data group	Count	minimum	median	maximum	Mean	Std Dev	Prob>ChiSq (1)	UTL _{95th}
Qbt 1g3	40	7.2	14	34	14.9	5.53	0.0002	27.4
Qbt 1v2	42	0.5	31.5	88	35.5	25.5		106.7
All Qbt 123 data	82	0.5	15.5	88	25.5	21.2		72.5

Copper								
Data group	Count	minimum	median	maximum	Mean	Std Dev	Prob>ChiSq (1)	Max. detect
Qbt 1g	13	0.25	2	2.4	1.488	0.810	0.0011	2.4
Qbt 1v	23	0.25	1	2.6	1.020	0.724		2.6
Qbt 2	19	0.25	0.65	2	0.887	0.689		2
Qbt 3	27	0.25	0.25	2	0.582	0.605		2
All Qbt 123 data	82	0.25	0.65	2.6	0.919	0.745		2.6

Iron								
Data group	Count	minimum	median	maximum	Mean	Std Dev	Prob>ChiSq (1)	UTL _{95th}
Qbt 1v23	69	190	4900	7500	4075	2453	0.0039	9035
Qbt 1g	13	730	1200	3200	1390	698		3254
All Qbt 123 data	82	190	4500	7500	3650	2469		8642

Lead								
Data group	Count	minimum	median	maximum	Mean	Std Dev	Prob>ChiSq (1)	UTL _{95th} (sqrt)
Qbt 1g23	59	1.6	5.3	36	6.33	5.23	0	16.2
Qbt 1v	23	0.6	9.6	18.3	9.85	3.69		21.9
All Qbt 123 data	82	0.6	6.35	36	7.32	5.08	NA	18.1

TABLE VI (CONTINUED).

SUMMARY OF CALCULATED RAW UTLs AND MAXIMUM CONCENTRATIONS FOR BANDELIER TUFF
UNITS QBT 123 GROUPS AND SUBGROUPS

Magnesium								
Data group	Count	minimum	median	maximum	Mean	Std Dev	Prob>ChiSq (1)	UTL _{95th} (sqrt)
Qbt 1g2	32	39	150	860	195	167	0.0245	548
Qbt 1v3	50	42	230	910	252	164		628
All Qbt 123 data	82	39	190	910	229	166		582

Manganese								
Data group	Count	minimum	median	maximum	Mean	Std Dev	Prob>ChiSq (1)	UTL _{95th}
Qbt 1v2	42	52	250	510	245.5	98.2	0	533
Qbt 1g	13	57	72	210	93.4	49.2		273
Qbt 3	27	22	180	310	155.0	87.0		426
All Qbt 123 data	82	22	200	510	191.6	105.7		488

Nickel								
Data group	Count	minimum	median	maximum	Mean	Std Dev	Prob>ChiSq (1)	Max. detect
Qbt 1g	13	1	1	1	1	0	0.262	ND
Qbt 1v	23	1	1	2	1.043	0.209		2
Qbt 2	19	0.5	1	1	0.974	0.115		ND
Qbt 3	27	1	1	2.6	1.096	0.357		2.6
All Qbt 123 data	82	0.5	1	2.6	1.038	0.241		2.6

Potassium								
Data group	Count	minimum	median	maximum	Mean	Std Dev	Prob>ChiSq (1)	UTL _{95th} (sqrt)
Qbt 1g2	32	250	720	3200	977	688	0	2725
Qbt 1v	23	390	1600	5400	1872	1256		5541
Qbt 3	27	250	390	800	420	132		735
All Qbt 123 data	82	250	615	5400	1045	970		3099

Potassium-Total								
Data group	Count	minimum	median	maximum	Mean	Std Dev	Prob>ChiSq (1)	UTL _{95th}
All Qbt 123 data	47	28760	38090	47920	38137	3347	NA	45102

Radium (pCi/g)								
Data group	Count	minimum	median	maximum	Mean	Std Dev	Prob>ChiSq (1)	Max. detect
Qbt 1g	2	5.58	6.18	6.78	6.180	0.849	0.0965	6.78
Qbt 1v	3	4.18	4.89	6.61	5.227	1.249		6.61
Qbt 2	2	2.81	3.815	4.82	3.815	1.421		4.82
Qbt 3	2	1.72	2.16	2.6	2.160	0.622		2.60
All Qbt 123 data	9	1.72	4.82	6.78	4.443	1.780		6.78

TABLE VI (CONTINUED).

SUMMARY OF CALCULATED RAW UTLs AND MAXIMUM CONCENTRATIONS FOR BANDELIER TUFF
UNITS QBT 123 GROUPS AND SUBGROUPS

Silver								
Data group	Count	minimum	median	maximum	Mean	Std Dev	Prob>ChiSq (1)	Max. detect
Qbt 1g	13	0.5	0.5	1	0.692	0.253	0.0041	ND
Qbt 1v	23	0.5	0.5	1	0.565	0.172		ND
Qbt 2	19	0.5	0.5	0.5	0.5	0		ND
Qbt 3	27	0.5	0.5	1.9	0.552	0.269		1.9
All Qbt 123 data	82	0.5	0.5	1.9	0.566	0.211		1.9

Sodium								
Data group	Count	minimum	median	maximum	Mean	Std Dev	Prob>ChiSq (1)	UTL _{95th}
Qbt 1 (sqrt)	36	210	1500	5100	1613	998	0	4289
Qbt 23 (by sim)	46	150	255	7700	607	1174		1941
All Qbt 123 data (by sim)	82	150	470	7700	1048	1204		4604

Sulfate								
Data group	Count	minimum	median	maximum	Mean	Std Dev	Prob>ChiSq (1)	Max. detect
All Qbt 123 data	82	1.5	14.55	815	53.3	118	NA	815

Tantalum								
Data group	Count	minimum	median	maximum	Mean	Std Dev	Prob>ChiSq (1)	Max. detect
Qbt 1g	13	0.1	0.2	0.3	0.177	0.060	0.975	0.3
Qbt 1v	23	0.1	0.2	0.5	0.200	0.117		0.5
Qbt 2	19	0.1	0.2	2	0.274	0.425		2
Qbt 3	27	0.1	0.2	0.8	0.189	0.134		0.8
All Qbt 123 data	82	0.1	0.2	2	0.210	0.227		2

Thallium								
Data group	Count	minimum	median	maximum	Mean	Std Dev	Prob>ChiSq (1)	Max. detect
Qbt 1g	13	0.1	0.3	0.7	0.277	0.154	0.1385	0.7
Qbt 1v	23	0.1	0.1	1.7	0.270	0.355		1.7
Qbt 2	19	0.1	0.2	1.3	0.300	0.354		1.3
Qbt 3	27	0.1	0.2	1.7	0.289	0.392		1.7
All Qbt 123 data	82	0.1	0.2	1.7	0.284	0.339		1.7

Thorium								
Data group	Count	minimum	median	maximum	Mean	Std Dev	Prob>ChiSq (1)	UTL _{95th} (sqrt)
Qbt 1g	13	1.2	1.7	8.8	2.33	2.01	0	7.69
Qbt 1v	23	6.2	10.7	19.1	11.68	4.00		22.14
Qbt 2	19	3.5	7.1	9.9	7.15	1.56		11.50
Qbt 3	27	1.9	4.7	10.4	5.11	1.72		9.29
All Qbt 123 data	82	1.2	6.35	19.1	6.99	4.16		16.85

TABLE VI (CONTINUED).

SUMMARY OF CALCULATED RAW UTLs AND MAXIMUM CONCENTRATIONS FOR BANDELIER TUFF UNITS QBT 123 GROUPS AND SUBGROUPS

Thorium-Total Data group	Count	minimum	median	maximum	Mean	Std Dev	Prob>ChiSq (1)	Max. detect
Qbt1g	9	21.32	29.39	37.06	29.29	4.267	0	37.06
Qbt1v	18	19.14	26.46	30.08	25.73	3.286		30.08
Qbt2	5	16.25	19.67	25.93	20.39	3.503		25.93
Qbt3	6	12.89	15.05	16.32	14.61	1.402		16.32
All Qbt 123 data	47	12.66	22.56	37.06	22.68	6.343		37.06

Uranium Data group	Count	minimum	median	maximum	Mean	Std Dev	Prob>ChiSq (1)	UTL _{95th} (sqrt)
Qbt 1g	13	0.1	0.2	1.6	0.362	0.384	0	1.39
Qbt 1v	23	1	2.3	4.8	2.474	1.270		5.93
Qbt 2	19	0.4	1	2.4	1.105	0.484		2.48
Qbt 3	26	0.2	0.55	1.8	0.727	0.356		1.64
All Qbt 123 data	81	0.1	1	4.8	1.253	1.100		3.68

Uranium-Total Data group	Count	minimum	median	maximum	Mean	Std Dev	Prob>ChiSq (1)	Max. detect
Qbt1g	9	5.977	7.853	10.13	7.908	1.239	0	10.13
Qbt1v	18	4.713	7.142	7.592	6.869	0.807		7.592
Qbt2	5	4.322	4.728	7.123	5.135	1.146		7.123
Qbt3	6	3.173	3.3345	4.371	3.467	0.454		4.371
All Qbt 123 data	47	2.832	6.737	10.13	5.890	1.980		10.13

Vanadium Data group	Count	minimum	median	maximum	Mean	Std Dev	Prob>ChiSq (1)	UTL _{95th}
Qbt 1v23	69	0.25	1.7	4.6	1.929	1.030	0	4.01
Qbt 1g	13	0.2	0.5	1.3	0.662	0.377		1.67
All Qbt 123 data	82	0.2	1.4	4.6	1.728	1.062		3.88

Zinc Data group	Count	minimum	median	maximum	Mean	Std Dev	Prob>ChiSq (1)	UTL _{95th}
Qbt 1g23	59	5.5	28	54	26.8	14.1	0	55.5
Qbt 1v	23	12	57	74	53.8	13.3		84.6
All Qbt 123 data	82	5.5	37.5	74	34.4	18.4		71.6

(1) Probability that the Qbt 1, Qbt 2, and Qbt 3 data are drawn from the same distribution, or are statistically not different, as measured the Wilcoxon/Kruskal-Wallis test. The Kruskal-Wallis is a three or more data group extension of the Wilcoxon rank sum test. Probabilities less than 0.05 indicate that there is a statistically significant difference between strata, and a probability greater than 0.05 indicates that there is no statistically significant difference between strata.

UTL_{95th} - 95% upper tolerance limit of the 95th percentile calculated using normal theory.

UTL_{95th} (sqrt) - 95% upper tolerance limit of the 95th percentile calculated using normal theory on square root transformed data.

UTL_{95th} by sim - 95% upper tolerance limit of the 95th percentile calculated using log-transformed data and computer simulation.

Max. detect. - maximum detected value is proposed as a background screening value due to a small Count of detects.

NA - Not applicable.

ND - Not detected.

TABLE VII.

BACKGROUND SCREENING VALUES FOR INORGANIC ANALYTES COMPILED BY GEOLOGICAL UNITS

Analyte ¹	Qct	Qbt 1g	Qbt 1v	Qbt 2	Qbt 3	Qbt 4	Qbo	Tt
Aluminum	3400	3700	8170	3700	3700	6200	1800	4500
Antimony	0.2	<0.3	0.3	0.3	0.4	<0.3	<0.3	<0.3
Arsenic	0.5	0.7	2	2	5	2	<0.5	<0.5
Barium	18	28.0	28.0	28.0	28.0	42	23	69
Beryllium	0.95	1.53	1.53	1.53	1.53	1.8	1.2	0.21
Calcium	1500	4140	4140	1520	1520	1800	890	2700
Chloride	379	405	405	107	64.8	14.9	7.7	67
Chromium	1.8	0.94	1.7	1.6	2.1	5.4	2.3	10
Cobalt	40	27.4	107	107	27.4	25	10	11
Copper	2.2	2.4	2.6	2	2	1.6	2.6	16
Iron	2400	3250	9040	9040	9040	12000	3700	13000
Lead	7.1	16.2	21.9	16.2	16.2	4	5	6.7
Magnesium	510	548	628	548	628	1700	510	950
Manganese	90	273	533	533	426	370	170	280
Nickel	<2	<2	2	<2	2.6	<2	2.8	15
Potassium	1600	2730	5540	2730	735	1600	960	1100
Potassium- Total	NA	45100	45100	45100	45100	45300	37200	33800
Radium-226 ²	NA	6.78	6.61	4.82	2.6	6.23	7.15	NA
Silver	<1	<2	<2	<1	1.9	<1	<1	<1
Sodium	3500	4290	4290	1940	1940	390	1900	610
Sulfate	548	815	815	815	815	26.4	12.7	38.6
Tantalum	0.3	0.3	0.5	2	0.8	0.5	0.9	0.2
Thallium	<0.2	0.7	1.7	1.3	1.7	<0.3	0.9	<0.3
Thorium	4.2	7.69	22.1	11.5	9.29	6.1	1.4	6.4
Thorium- Total	NA	37.1	30.1	25.9	16.3	15.6	19.9	NA
Uranium	0.4	1.39	5.93	2.48	1.64	0.9	0.2	0.6
Uranium- Total	NA	10.1	7.59	7.12	4.37	2.93	5.61	NA
Vanadium	3.8	1.67	4.01	4.01	4.01	9.5	2.8	29
Zinc	17	55.5	84.6	55.5	55.5	47	21	41

(a) - The maximum detected or non-detected value is reported for units Qct, Qbt 4, Qbo, and Tt. Readers are referred to Table VI for the derivation of the background screening values for Qbt1g1v23.

(1) - All values are in mg/kg unless otherwise noted.

(2) - Units are pCi/g.

ND - Not detected.

NA - Not available.

Inorganic Analytes

Aluminum (Al)

All of the 106 leachable aluminum concentrations were above ICPEES detection limits. Square root transformed aluminum data are approximately normally distributed. Aluminum concentrations for all geologic units range from 350 to 14000 mg/kg and average 2187 mg/kg.

Population characteristics from the Wilcoxon rank sum test (Table IV) and box plots (Fig. 4) resulted in pooling the aluminum data for Qbt 1g, Qbt 2, and Qbt 3 (as Qbt 1g23) and Qbt 1v as a separate data group. Box plots comparing acid leachable aluminum by geologic unit show that medians, arithmetic means, and middle 50 percent ranges are distinctly greater for units Qbt 1v and Qbt 4 than for the other units (Fig. 4). Plots of leachable aluminum from individual stratigraphic sections show aluminum concentrations increase up section towards Qbt 1v before decreasing in the overlying tuffs (Fig. 5).

The background screening values for leachable aluminum are 4500 mg/kg for Tt, 1800 mg/kg for Qbo, 3400 mg/kg for Qct, 8170 mg/kg for Qbt 1v, 3700 mg/kg for Qbt 1g, Qbt 2, and Qbt 3, and 6200 mg/kg for Qbt 4. These background screening values are lower than the aluminum SAL of 77000 mg/kg.

Total aluminum concentrations by XRF and INAA tend to increase up section through the Tshirege Member (Fig. 5). Aluminum concentrations in the upper Otowi Member are slightly elevated with respect to the lower Tshirege Member. Comparison of acid leachable and total aluminum data for the Bandelier Tuff shows that approximately 10% to 25% of the total aluminum in the rock is leachable by nitric acid at a pH of 1.

Antimony (Sb)

Nine of the 106 leachable antimony concentrations were above ICPMS detection limits of 0.2 to 0.3 mg/kg. No statistical distribution of the antimony was estimated because of the limited number of detects. For samples above detection limits, leachable antimony concentrations range from 0.2 to 0.4 mg/kg and average 0.256 mg/kg.

The background screening values for leachable antimony are based on maximum detected concentrations in each rock unit. Background screening values are <0.3 mg/kg for Tt, <0.3 mg/kg for Qbo, 0.2 mg/kg for Qct, <0.3 mg/kg for Qbt 1g, 0.3 mg/kg for Qbt 1v, 0.3 mg/kg for Qbt 2, 0.4 mg/kg for Qbt 3, and <0.3 mg/kg for Qbt 4. Background screening values for antimony in all rock units are well below the SAL of 31 mg/kg for soils and rock.

Only two of 38 samples analyzed by INAA had total antimony concentrations above detection limits which ranged between 0.2 and 0.7 mg/kg. The maximum detected total antimony concentration was 0.7 mg/kg.

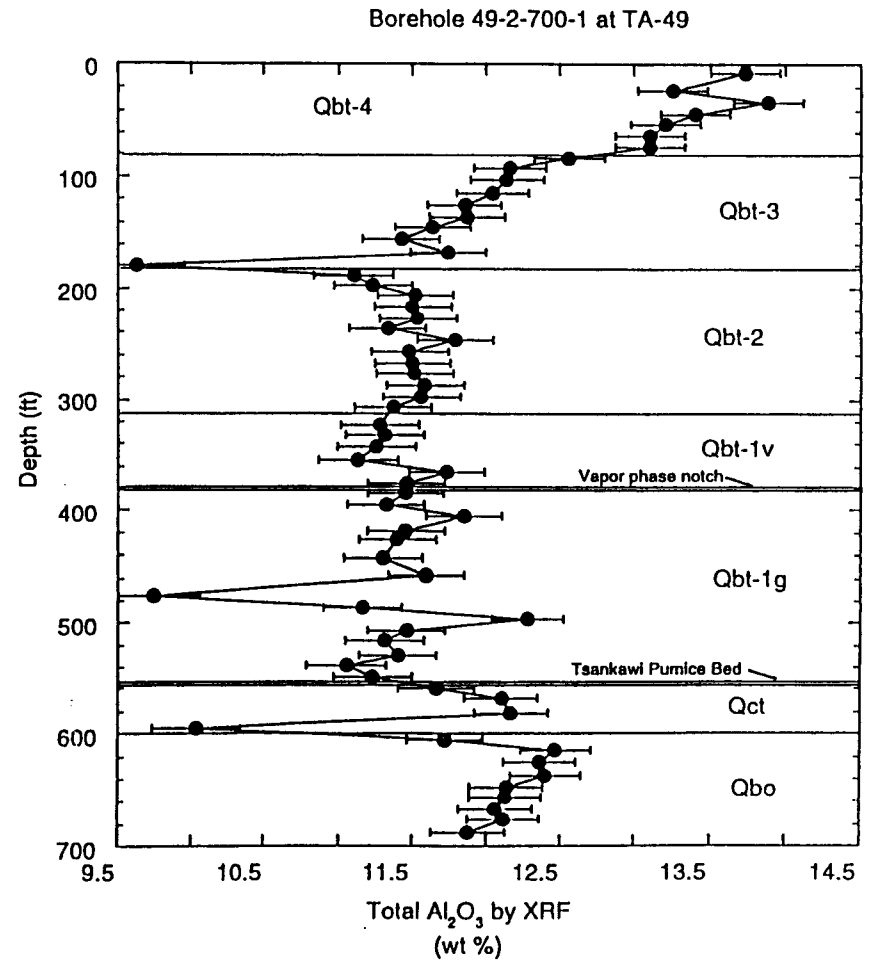
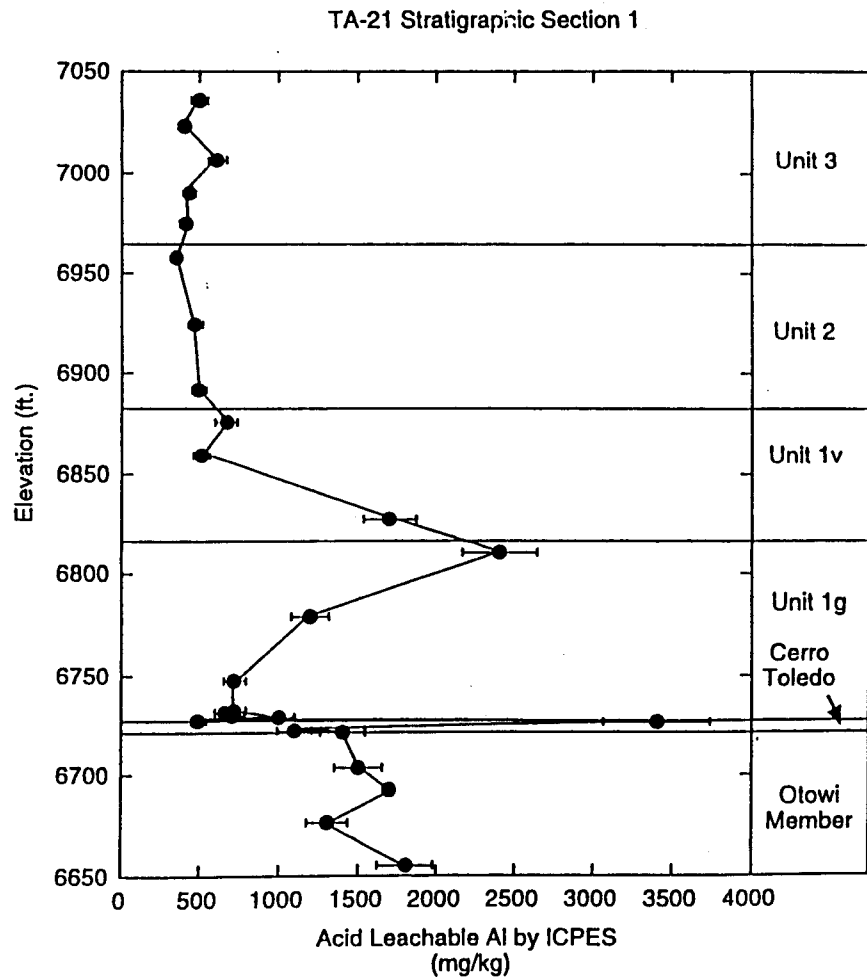


Fig. 5 Plots showing examples of acid leachable aluminum concentrations at TA-21 and total aluminum concentrations at TA-49 as a function of stratigraphic height in the Bandelier Tuff.

Arsenic (As)

Fifty-three of the 105 leachable antimony concentrations were above ETVAA detection limit of 0.5 mg/kg. No statistical distribution of the antimony was estimated because of the large number of non detects. For samples above detection limits, leachable antimony concentrations range from 0.5 to 5 mg/kg and average 1.08 mg/kg.

Box plots comparing acid leachable arsenic by geologic unit show that the middle 50 percent ranges are somewhat greater for units Qbt 3 and Qbt 4 than for the other units (Fig. 4). However, plots of leachable arsenic from individual stratigraphic sections fail to show any clear pattern of arsenic concentration variation as a function of stratigraphic height (Fig. 6).

The background screening values for leachable arsenic are based on maximum detected concentrations in each rock unit. Background screening values are <0.5 mg/kg for Tt, <0.5 mg/kg for Qbo, 0.5 mg/kg for Qct, 0.7 mg/kg for Qbt 1g, 2 mg/kg for Qbt 1v, 2 mg/kg for Qbt 2, 5 mg/kg for Qbt 3, and 2 mg/kg for Qbt 4. All of the background screening values exceed the SAL of 0.32 mg/kg.

Total arsenic concentrations by INAA were below detection limits for 61% of the samples. Concentrations ranged from 1.0 to 3.1 mg/kg for samples with total arsenic above the detection limit. Detection limits ranged from 1 to 4 mg/kg.

Barium (Ba)

All of the 106 leachable barium concentrations were above ICPEES detection limits. Leachable barium data are approximately normally distributed. Barium concentrations for all geologic units range from 1.4 to 190 mg/kg and average 18.5 mg/kg.

Population characteristics from the Wilcoxon rank sum test (Table IV) and box plots (Fig. 4) resulted in pooling the barium data for Qbt 1g, Qbt 1v, Qbt 2, and Qbt 3 (as Qbt 123). Box plots comparing acid leachable barium by geologic unit show that medians, arithmetic means, and middle 50 percent ranges are greater for units Tt and Qbt 4 than for the other units (Fig. 4). Plots of leachable barium at individual stratigraphic sections supports the pooling of the leachable data set Qbt 123 (Fig. 7).

The background screening values for leachable barium are 69 mg/kg for Tt, 23 mg/kg for Qbo, 18 mg/kg for Qct, 42 mg/kg for Qbt 4, and 28 mg/kg for Qbt 1g, Qbt 1v, Qbt 2, and Qbt 3. Background screening values for barium in these rock units are well below the SAL of 5300 mg/kg.

Total barium concentrations by XRF tend to increase up section through the Tshirege Member (Fig. 7). The highest concentrations of total barium occur in Qbt 4 which contains about three times as much barium as the base of the Tshirege Member. Barium concentrations in the upper Otowi Member are about twice that found in the lower Tshirege Member. Comparison of acid leachable and total barium data for the Bandelier Tuff shows that approximately 5 to 30% of the total barium in the rock is leachable by nitric acid at a pH of 1.

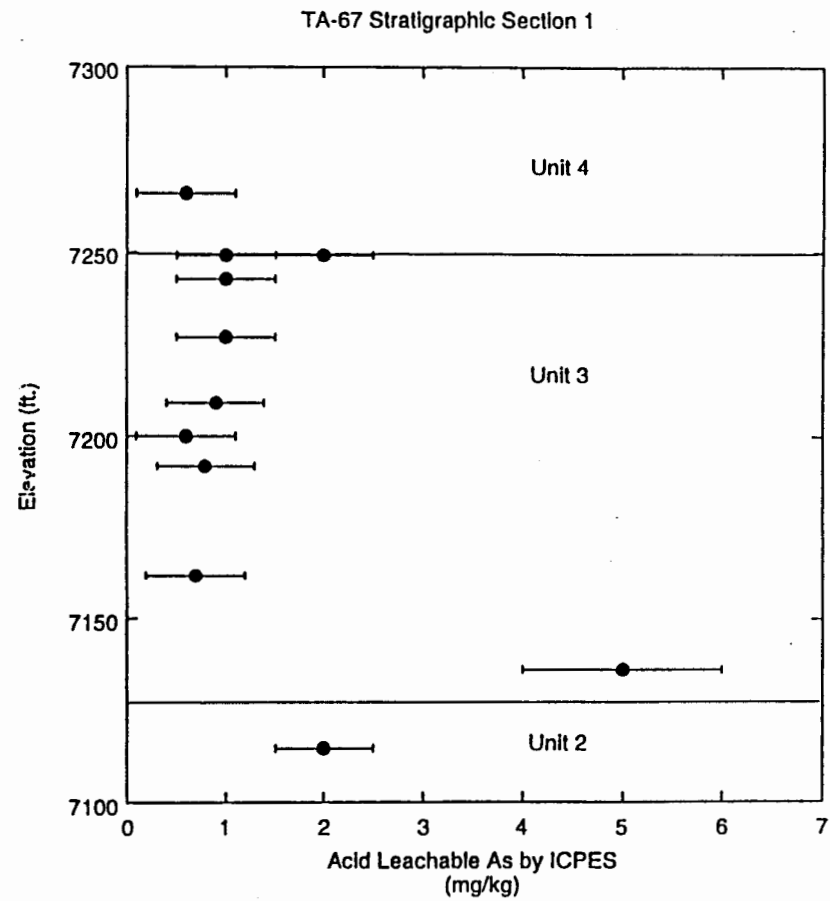
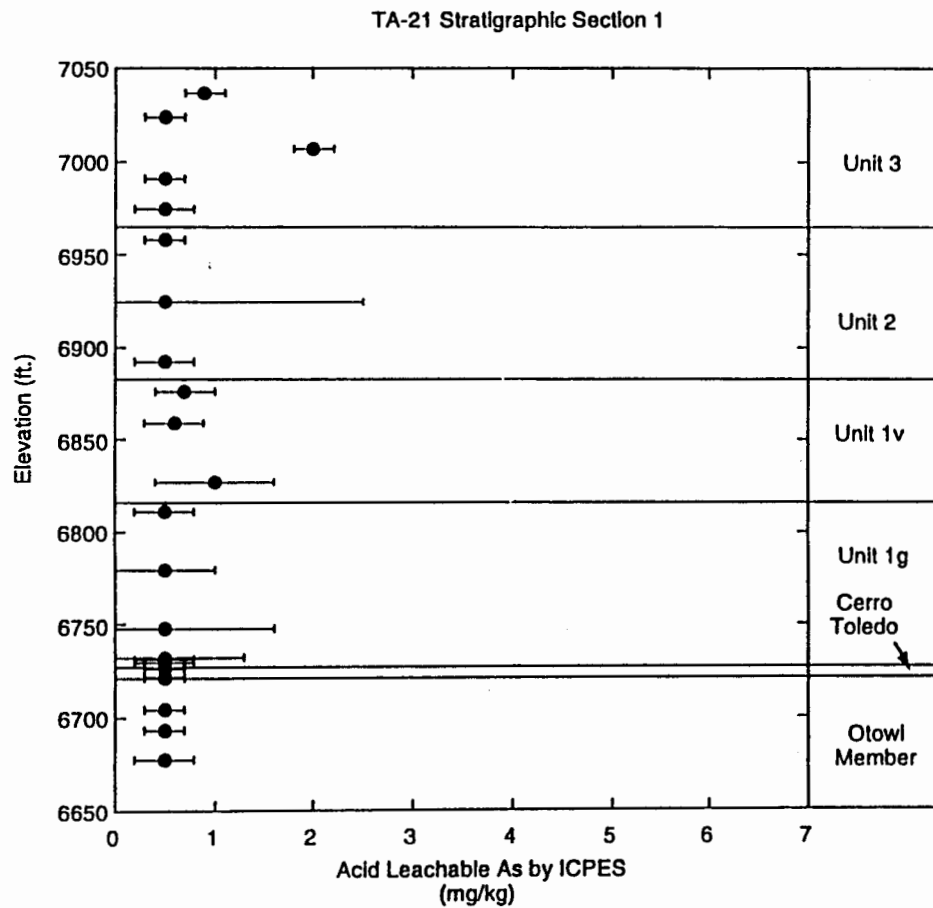


Fig. 6 PLOTS SHOWING EXAMPLES OF ACID LEACHABLE ARSENIC CONCENTRATIONS AS A FUNCTION OF STRATIGRAPHIC HEIGHT IN THE BANDELIER TUFF AT TA-21 AND TA-67.

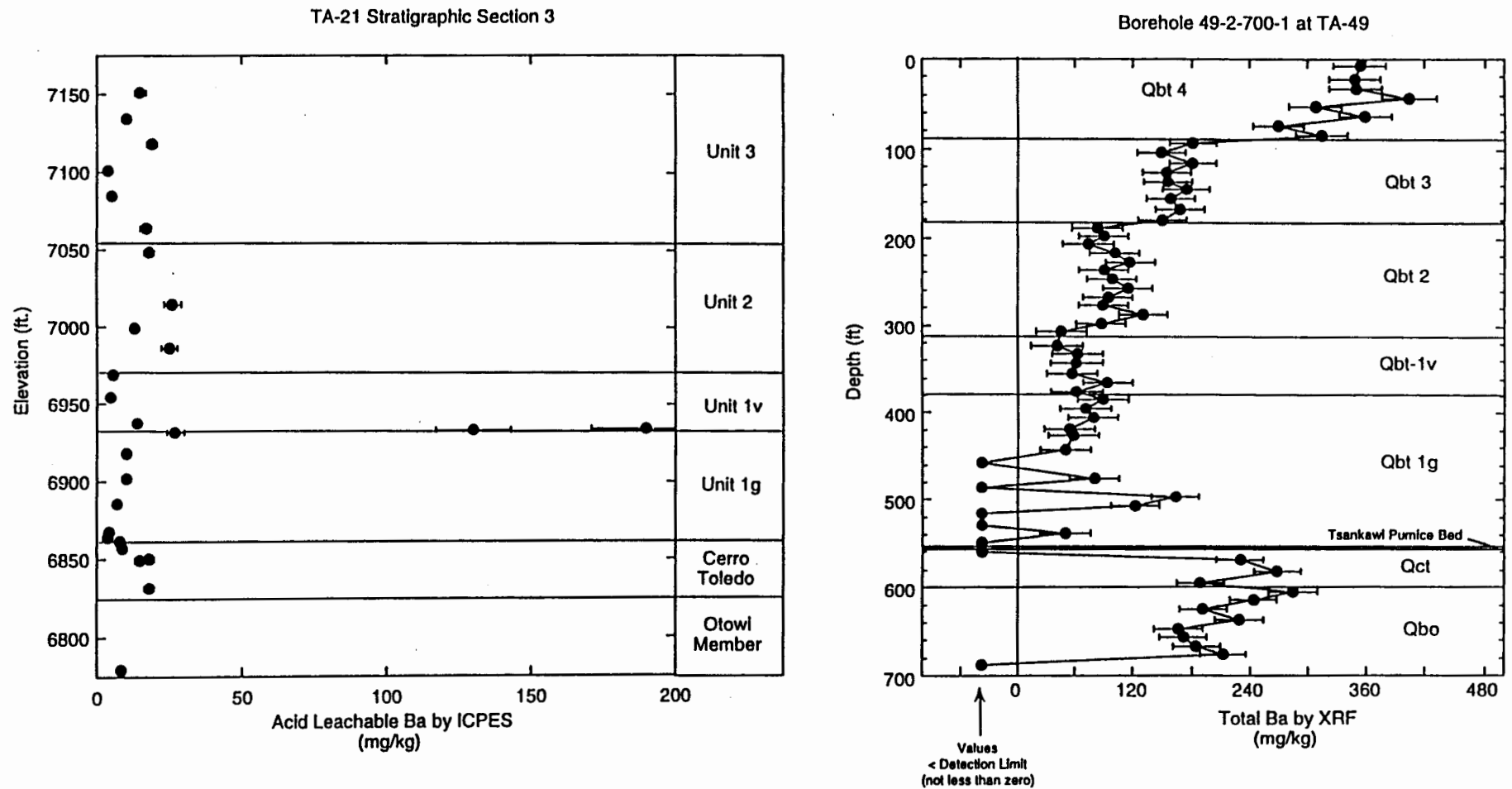


Fig. 7 PLOTS SHOWING EXAMPLES OF ACID LEACHABLE BARIUM CONCENTRATIONS AT TA-21 AND TOTAL BARIUM CONCENTRATIONS AT TA-49 AS A FUNCTION OF STRATIGRAPHIC HEIGHT IN THE BANDELIER TUFF. NOTE THE ENRICHMENT OF LEACHABLE BARIUM ASSOCIATED WITH THE QBT 1G/QBT 1V CONTACT IN STRATIGRAPHIC SECTION 3 AT TA-21. THIS BARIUM ENRICHMENT IS A LOCAL PHENOMENA ASSOCIATED WITH SECONDARY ALTERATION AT THE VAPOR PHASE NOTCH. ITS IS REPRESENTED BY SAMPLE 1106-3-12, 1106-3-13, AND 1106-3-14.

Beryllium (Be)

Ninety-three of the 106 leachable beryllium concentrations were above ICPES detection limits of 0.0 to 0.14 mg/kg. Square root transformed beryllium data are approximately normally distributed. For samples above detection limits, beryllium concentrations for all geologic units range from 0.15 to 3.4 mg/kg and average 0.70 mg/kg.

Population characteristics from the Wilcoxon rank sum test (Table IV) resulted in pooling the beryllium data for Qbt 1g, Qbt 1v, Qbt 2, and Qbt 3 (as Qbt 123). Box plots comparing acid leachable beryllium by geologic unit show that medians, arithmetic means, and middle 50 percent ranges are generally less for units Tt, Qbo, Qct, Qbt 3 and Qbt 4 than for the other units (Fig. 4). Plots of leachable beryllium from individual stratigraphic sections show that in the Tshirege Member, beryllium concentrations increase up section from the base of the unit towards the Qbt 1g/Qbt 1v contact before decreasing in the overlying tuff units (Fig. 8). Enrichment of leachable beryllium at the Qbt 1g/Qbt 1v contact coincides with the vapor phase notch that separates two units. The vapor phase notch frequently has an unusual geochemistry suggestive of secondary alteration concentrated along a boundary of contrasting rock lithologies.

The background screening values for leachable beryllium are 0.21 mg/kg for Tt, 1.2 mg/kg for Qbo, 0.95 mg/kg for Qct, 1.8 mg/kg for Qbt 4, and 1.53 mg/kg for Qbt 1g, Qbt 1v, Qbt 2, and Qbt 3. All of the background screening values exceed the SAL of 0.14 mg/kg.

Total beryllium concentrations by INAA decrease up section through the Tshirege Member (Fig. 8). The highest concentrations of total beryllium occur in units Qbt 1g and Qbt 1v which contain approximately twice as much beryllium as units 3 and 4. Beryllium concentrations in the upper Otowi Member are slightly lower than those found in the lower part of the Tshirege Member. Comparison of acid leachable and total beryllium data for the Bandelier Tuff shows that approximately 15 to 50% of the total beryllium in the rock is leachable by nitric acid at a pH of 1.

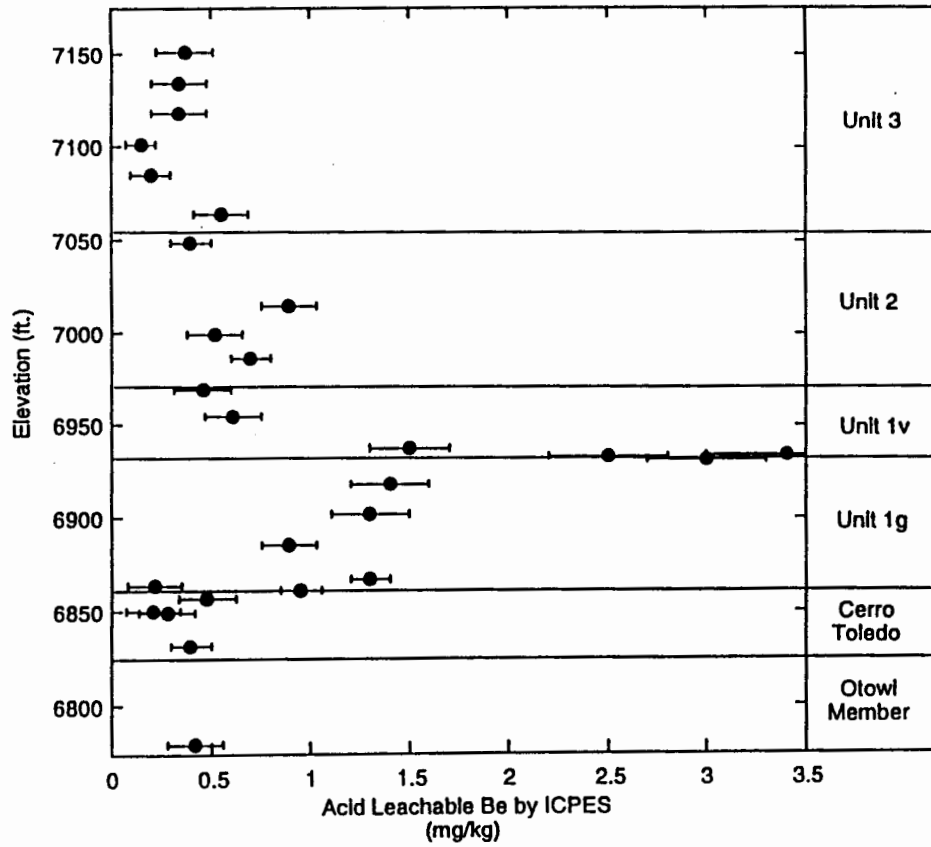
Cadmium (Cd)

Leachable cadmium concentrations were not determined for this investigation because total cadmium was not detected in the samples analyzed by INAA. All 38 of the samples analyzed by INAA had total cadmium concentrations below the detection limit of 1 mg/kg. Thus naturally cadmium concentrations are well below the SAL of 38 mg/kg.

Calcium (Ca)

All of the 106 leachable calcium concentrations were above ICPES detection limits. Log transformed calcium data are approximately normally distributed. Calcium concentrations for all geologic units range from 200 to 4800 mg/kg and average 825 mg/kg.

TA-21 Stratigraphic Section 3



Frijoles Canyon Stratigraphic Section 2

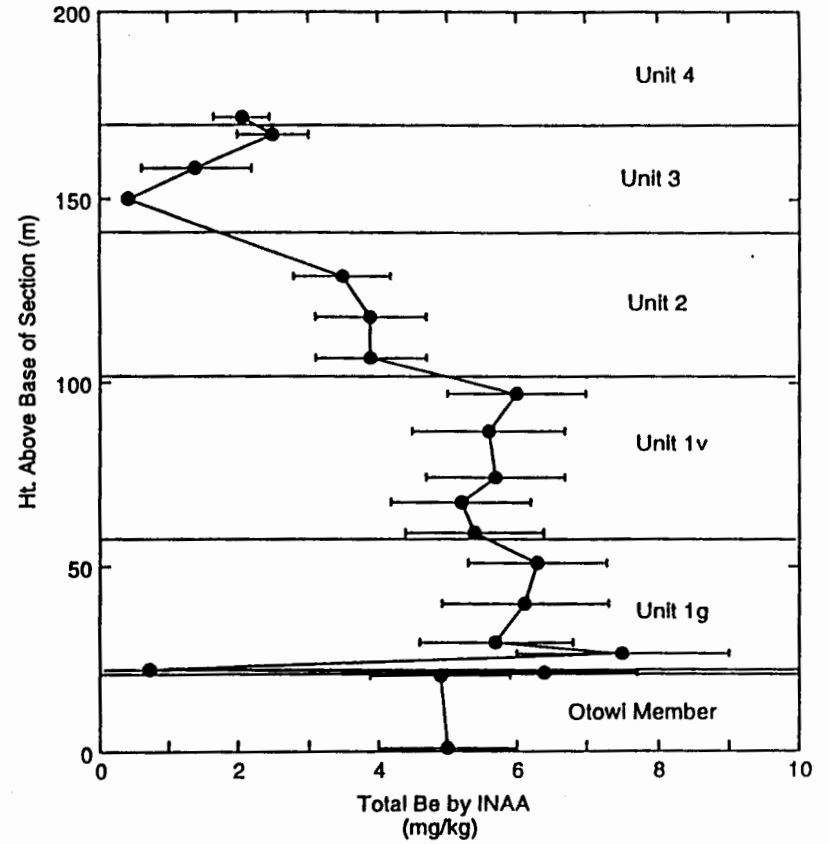


Fig. 8 PLOTS SHOWING EXAMPLES OF ACID LEACHABLE BERYLLIUM CONCENTRATIONS AT TA-21 AND TOTAL BERYLLIUM CONCENTRATIONS AT FRIJOLES CANYON AS A FUNCTION OF STRATIGRAPHIC HEIGHT IN THE BANDELIER TUFF.

Population characteristics from the Wilcoxon rank sum test (Table IV) resulted in pooling the calcium data for Qbt 1g and Qbt 1v (as Qbt 1) and pooling the calcium data for Qbt 2 and Qbt 3 (as Qbt 23). Box plots comparing acid leachable calcium by geologic unit show that medians, arithmetic means, and middle 50 percent ranges are generally greater for units Tt and Qbt 4 than for the other units (Fig. 4). Plots of leachable calcium from individual stratigraphic sections show that in the Tshirege Member, calcium concentrations are highly variable, particularly in units Qbt 1g and Qbt 1v (Fig. 9). The greatest enrichments or depletions of leachable calcium seem to be associated with unit boundaries and may represent secondary alteration along preferential ground water pathways.

The background screening values for leachable calcium are 2700 mg/kg for Tt, 890 mg/kg for Qbo, 1500 mg/kg for Qct, 4140 mg/kg for Qbt 1g and Qbt 1v, 1520 mg/kg for Qbt 2 and Qbt 3, and 1800 for Qbt 4.

Except for higher concentrations in Qbt 4, total calcium concentrations by XRF and INAA are relatively constant in the Tshirege Member (Fig. 9). Calcium concentrations in the upper Otowi Member tend to increase up section, and they are slightly elevated with respect to the lower Tshirege Member. Because of its low abundance, calcium concentrations in the Bandelier Tuff are easily affected by diagenetic alteration, particularly in the near-surface environment and near fractures where calcite (CaCO_3) is commonly deposited by infiltrating ground water.

Chlorine (Cl)

Leachable chlorine concentrations were determined for rock samples on aliquots extracted in deionized water and analyzed by IC. All of the 106 leachable chlorine concentrations were above detection limits. Log transformed chlorine data are approximately normally distributed. Chlorine concentrations for all geologic units range from 3.65 to 802 mg/kg and average 59.9 mg/kg.

Population characteristics from the Wilcoxon rank sum test (Table IV) resulted in pooling the chlorine data for Qbt 1g and Qbt 1v (as Qbt 1), and Qbt 2 and Qbt 3 were each treated as separate data groups. Box plots comparing leachable chlorine by geologic unit show that chlorine concentration ranges are distinctly greater for units Tt and Qbt 4 than for the other units (Fig. 4). Plots of leachable chlorine from individual stratigraphic sections show that leachable chlorine concentrations vary little throughout the Otowi and Tshirege Members with the exception of high chlorine concentrations along some unit contacts (e.g., Fig. 10).

Particularly high concentrations of soluble chlorine are associated with the lower Tshirege Member (including the Tsankawi Pumice Bed) and the tephra and volcanoclastic sediments of the Cerro Toledo interval in stratigraphic section 1 at TA-21 (Fig. 10). The presence of elevated chlorine concentrations in these tuffs suggests that they acted as preferential ground water pathways at some time after their deposition. These tuffs are now well above the canyon floor and there is no evidence of present-day ground water perching in these units. Most likely these units were preferential ground water pathways when Los Alamos Canyon was shallower, and these units were below the level of potential perched alluvial ground water bodies on the canyon floor.

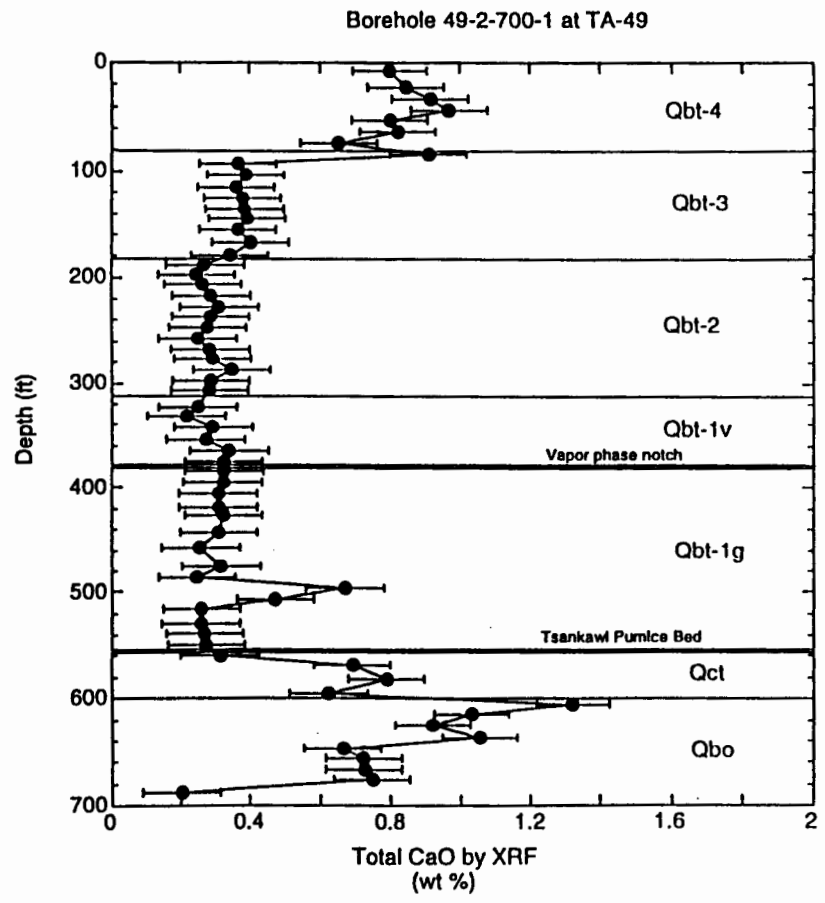
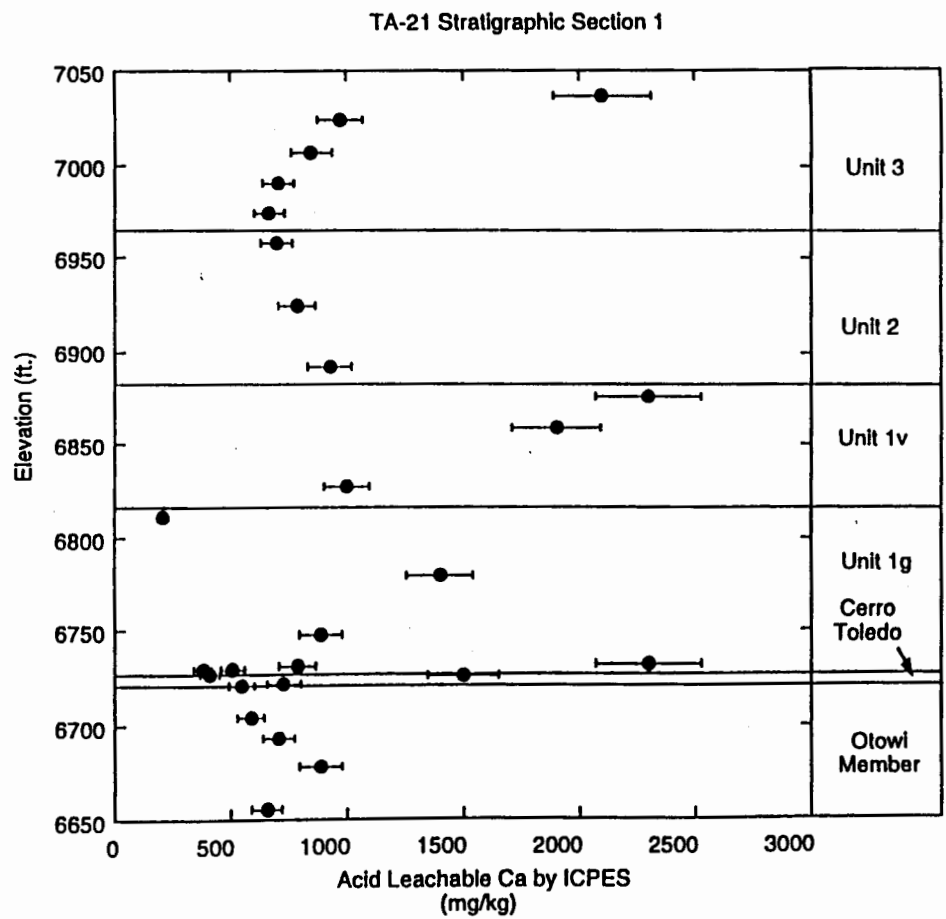


Fig. 9 PLOTS SHOWING EXAMPLES OF ACID LEACHABLE CALCIUM CONCENTRATIONS AT TA-21 AND TOTAL CALCIUM CONCENTRATIONS AT FRIJOLE CANYON AS A FUNCTION OF STRATIGRAPHIC HEIGHT IN THE BANDELIER TUFF.

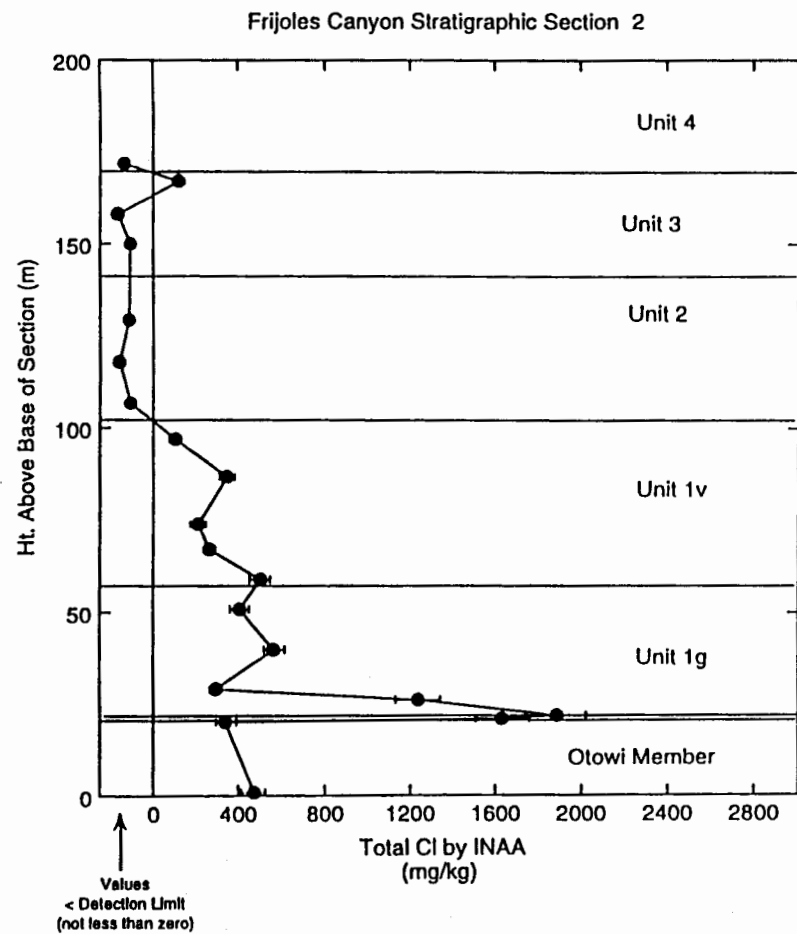
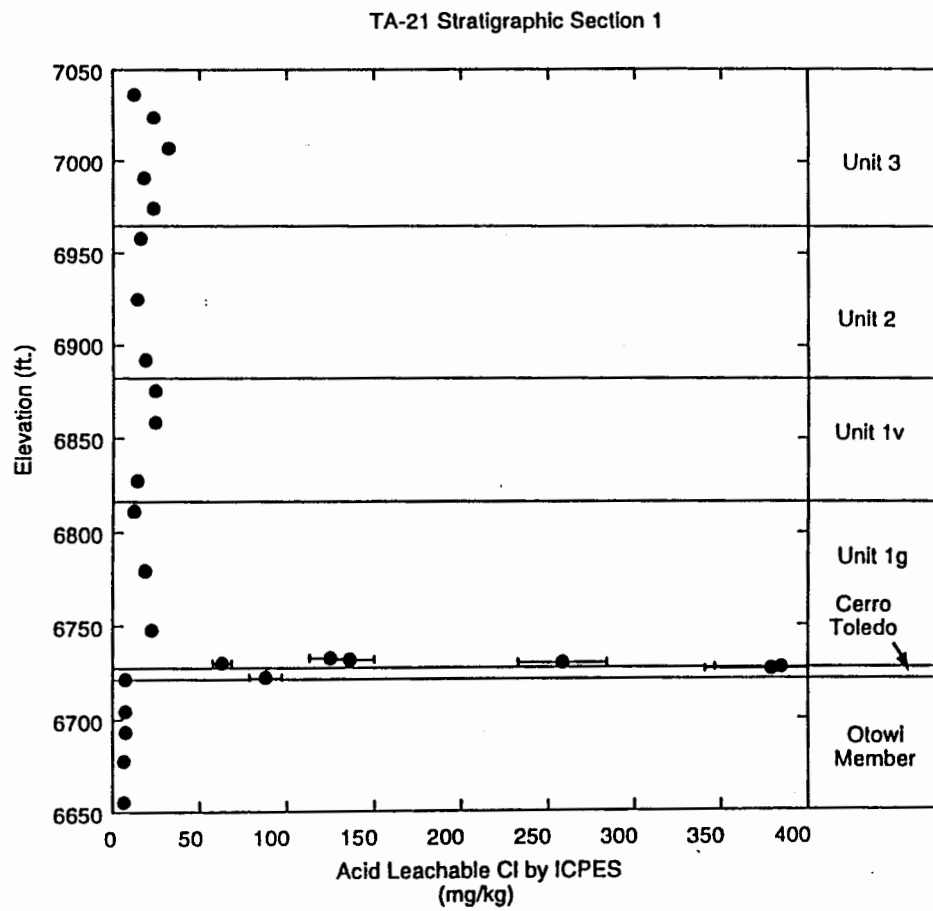


Fig. 10 PLOTS SHOWING EXAMPLES OF ACID LEACHABLE CHLORINE CONCENTRATIONS AT TA-21 AND TOTAL CHLORINE CONCENTRATIONS AT FRIJOLETS CANYON AS A FUNCTION OF STRATIGRAPHIC HEIGHT IN THE BANDELIER TUFF.

In addition to the vertical variations in leachable chlorine concentrations described above, there are also lateral variations in leachable chlorine across the Pajarito Plateau (Fig. 11). Median leachable chlorine concentrations for the Bandelier Tuff typically are 14 mg/kg in the central part of the Laboratory (e.g., TA-21, TA-67) and 44 mg/kg in the eastern part of the Laboratory. These lateral differences in median soluble Cl concentrations probably reflect increased evapotranspiration and/or decreased moisture flux within bedrock eastwards across the Laboratory due to higher average temperatures and to lower rain fall and snow fall.

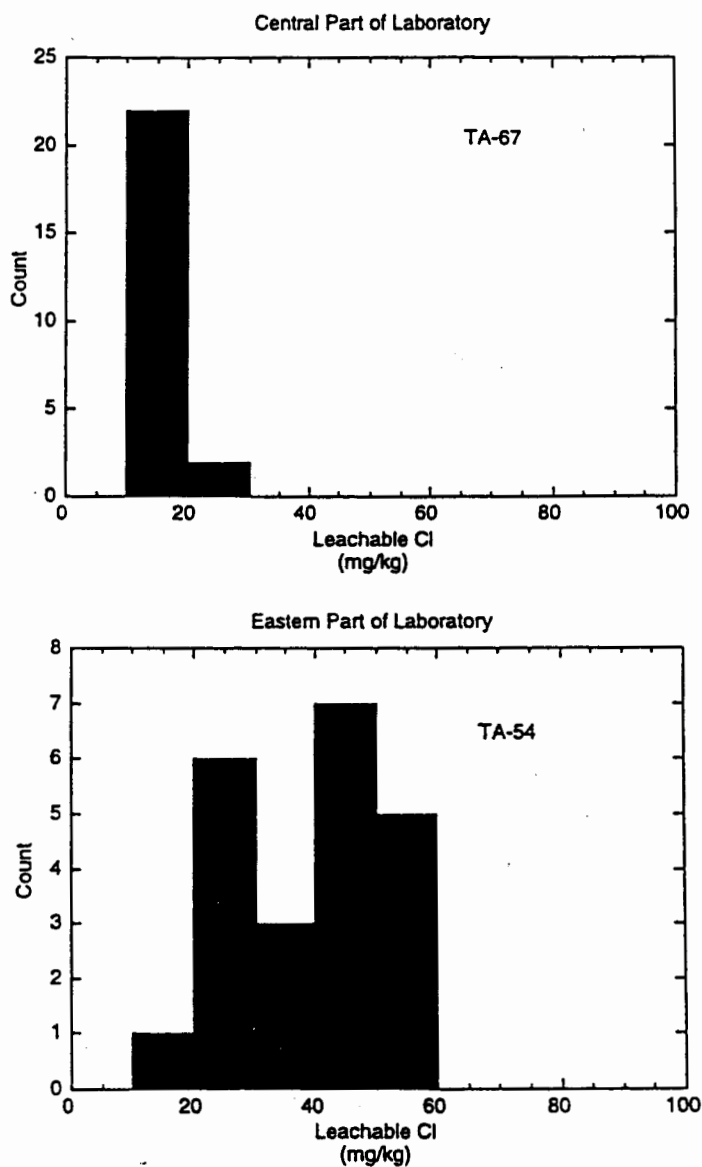


Fig. 11 Histogram of acid leachable chlorine concentrations in Bandelier Tuff as a function of lateral position. Chlorine concentrations generally increase eastward across the Pajarito Plateau. The few anomalous Cl concentrations above 100 mg/kg are not shown.

The background screening values for leachable chlorine are 67 mg/kg for Tt, 7.7 mg/kg for Qbo, 379 mg/kg for Qct, 405 mg/kg for Qbt 1g and Qbt 1v, 107 mg/kg for Qbt 2, 64.8 mg/kg for Qbt 3, and 14.9 mg/kg for Qbt 4. The background screening values are lower than the chlorine SAL of 7700 mg/kg.

Total chlorine concentrations by INAA systematically decrease up section from Qbt 1g to Qbt 4 in the Tshirege Member (Fig. 10). The highest total chlorine concentrations occur at the base of Qbt 1g and in the Tsankawi Pumice Bed. These high chlorine concentrations may represent secondary enrichment of chlorine by ground water along a preferential pathway. Chlorine concentrations are below detection limits in the upper part of Qbt 1v and in overlying units.

Chromium (Cr)

Sixty-eight of the 106 leachable chromium concentrations were above the ICPES detection limits of 0.5 to 2 mg/kg. No statistical distribution of the chromium was estimated because of the large number of non detects. For samples above detection limits, leachable chromium concentrations range from 0.57 to 10 mg/kg and average 1.70 mg/kg.

Box plots comparing acid leachable chromium by geologic unit show that the leachable chromium concentration ranges are greater for units Tt and Qbt 4 than for the other units (Fig. 4). The background screening values for leachable chromium are based on maximum detected concentrations in each rock unit. Background screening values are 10 mg/kg for Tt, 2.3 mg/kg for Qbo, 1.8 mg/kg for Qct, 0.94 mg/kg for Qbt 1g, 1.7 mg/kg for Qbt 1v, 1.6 mg/kg for Qbt 2, 2.1 mg/kg for Qbt 3, and 5.4 mg/kg for Qbt 4. Background screening values are less than the total chromium SAL of 210 mg/kg.

Cobalt (Co)

Artificially high concentrations of cobalt were introduced into the samples analyzed by ICPES during sample preparation. Cobalt contamination was added to the samples during powdering the samples in a tungsten-carbide shatter box. The median acid leachable cobalt in the Tshirege Member is 16 mg/kg. This median concentration is more than an order of magnitude greater than the median total cobalt value (0.85 mg/kg) determined by INAA (Fig. 12), and it is significantly greater than 1 mg/kg, the average cobalt value for rocks of granitic compositions (Carr and Turekian, 1961). Because of the potential for introduced contamination, we recommend that a ceramic shatter box be used to prepare rock samples for cobalt (and tungsten) analysis.

Because acid leachable cobalt concentrations by ICPES are suspected of being in error, background screening levels for cobalt in the Bandelier Tuff (Table VII) are based on the maximum total cobalt concentration for each unit. Total concentrations were determined by INAA for samples powdered in a ceramic shatter box. Total cobalt concentrations by INAA range from <0.3 to 8.8 mg/kg and average 1.3 mg/kg. Total cobalt values are relatively constant in the Tshirege Member, except for a single cobalt determination for Qbt 4 which was

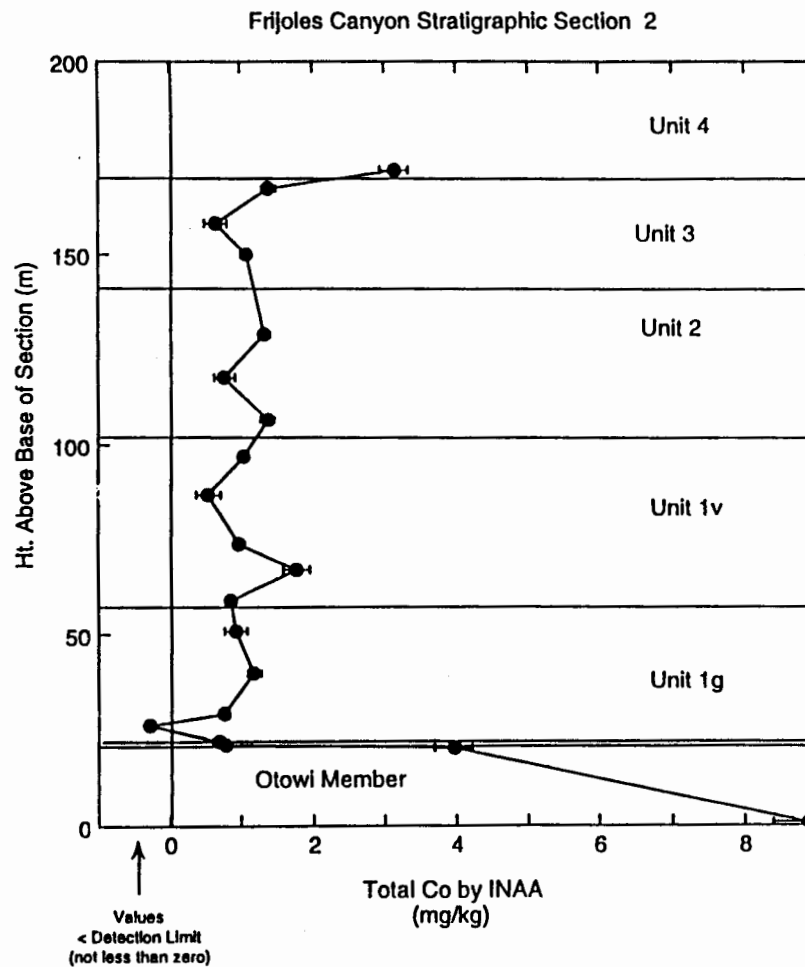
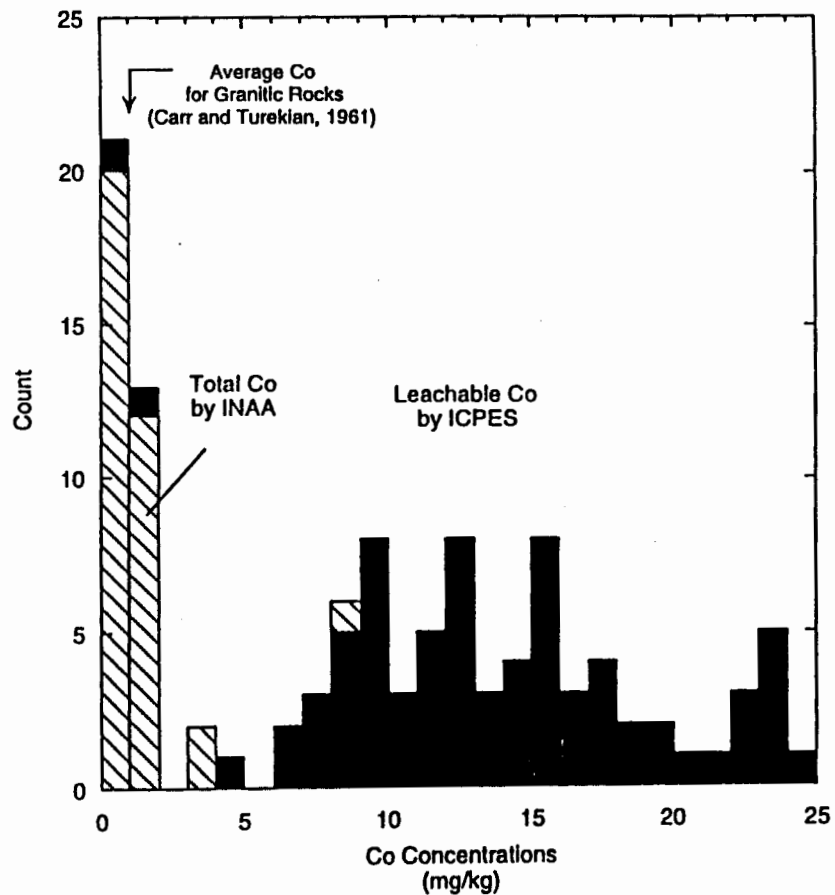


Fig. 12 ON LEFT, HISTOGRAM OF TOTAL CO CONCENTRATIONS BY INAA VS LEACHABLE COBALT CONCENTRATIONS BY ICPES FOR THE BANDELIER TUFF (OUTLIERS ABOVE 25 MG/KG NOT SHOWN). ON RIGHT, TOTAL COBALT CONCENTRATIONS AT FRIJOLES CANYON AS A FUNCTION OF STRATIGRAPHIC HEIGHT IN THE BANDELIER TUFF. BECAUSE OF PROBABLE ANALYTICAL ERRORS, LEACHABLE COBALT VALUES ARE NOT USED TO DETERMINE BACKGROUND SCREENING VALUES.

three times greater than the underlying tuffs (Fig. 12). The highest concentrations of total cobalt occur in two samples of Qbo. The two cobalt determinations for Qbo are four to eight times greater than those in Qbt 1g.

Background screening values are 8.8 mg/kg for Qbo, 1.27 mg/kg for Qbt 1g, 1.78 mg/kg for Qbt 1v, 1.38 mg/kg for Qbt 2, 1.39 mg/kg for Qbt 3, and 3.14 mg/kg for Qbt 4.

Copper (Cu)

Fifty-seven of the 106 leachable copper concentrations were above the ICPES detection limits of 0.5 to 2 mg/kg. No statistical distribution of the copper was estimated because of the large number of non detects. For samples above detection limits, leachable copper concentrations range from 0.6 to 16 mg/kg and average 2.38 mg/kg.

Box plots comparing acid leachable copper by geologic unit show that the leachable copper concentration ranges are relatively constant for all rock units except for Tt, which has distinctly greater concentrations of leachable copper than the other units (Fig. 4). The background screening values for leachable copper are based on maximum detected concentrations in each rock unit. Background screening values are 16 mg/kg for Tt, 2.6 mg/kg for Qbo, 2.2 mg/kg for Qct, 2.4 mg/kg for Qbt 1g, 2.6 mg/kg for Qbt 1v, 2 mg/kg for Qbt 2, 2 mg/kg for Qbt 3, and 1.6 mg/kg for Qbt 4. Background screening values for leachable copper in the Bandelier Tuff are well below the SAL of 2800 mg/kg.

Total copper concentrations by INAA for the Bandelier Tuff were below the detection limits, which ranged from about 250 to 400 mg/kg. These detection limits are much greater than average copper concentrations in granitic rocks of about 10 mg/kg (Turekian and Wedepohl, 1961).

Iron (Fe)

All of the 106 leachable iron concentrations were above ICPES detection limits. Iron concentrations for all geologic units range from 190 to 13000 mg/kg and average 3867 mg/kg.

Population characteristics from the Wilcoxon rank sum test (Table IV) resulted in pooling the leachable iron data for Qbt 1g as one data group and pooling the data for Qbt 1v, Qbt 2 and Qbt 3 (as Qbt 1v23) as another data group. Each data group was bimodally distributed. Box plots comparing acid leachable iron by geologic unit show that medians, arithmetic means, and middle 50 percent ranges are generally greater for units Tt and Qbt 4 than for the other units (Fig. 4). The distribution of acid leachable iron concentrations in the Tshirege Member is complex. The greatest concentrations of acid leachable iron occur at the Qbt 1g/Qbt 1v contact, and generally iron concentrations decrease up section (Fig. 13). In contrast to iron in stratigraphic section 1 at TA-21 (Fig. 13), relatively high concentrations of leachable iron occur up section to the top of Qbt 2 in stratigraphic section 3 at TA-21.

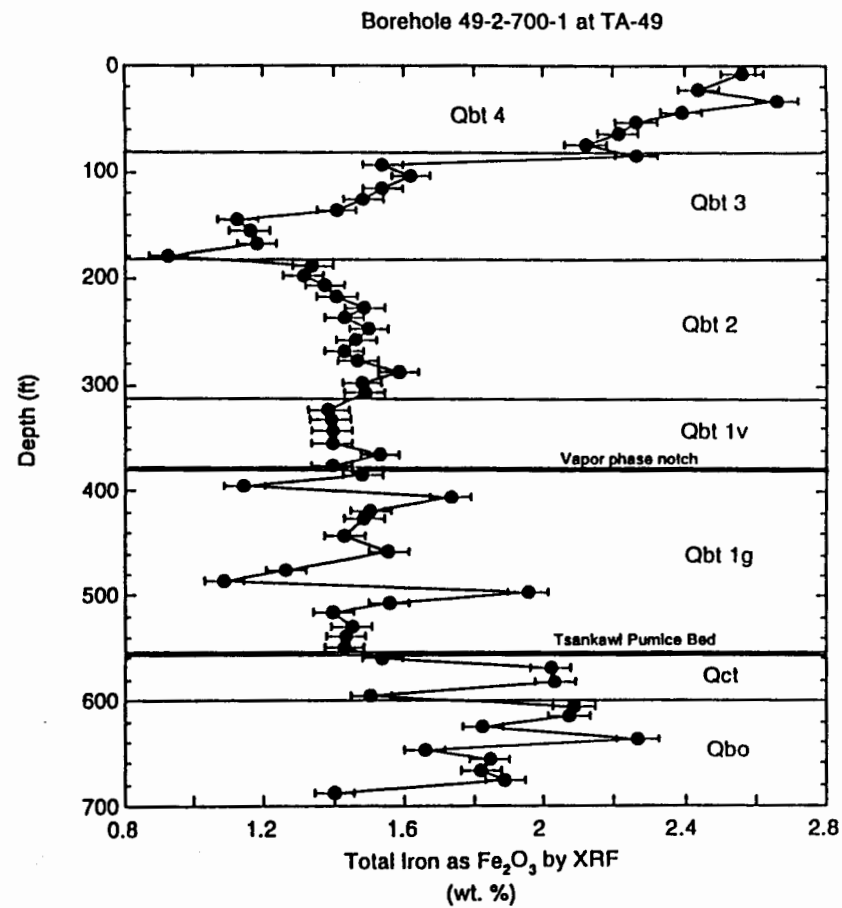
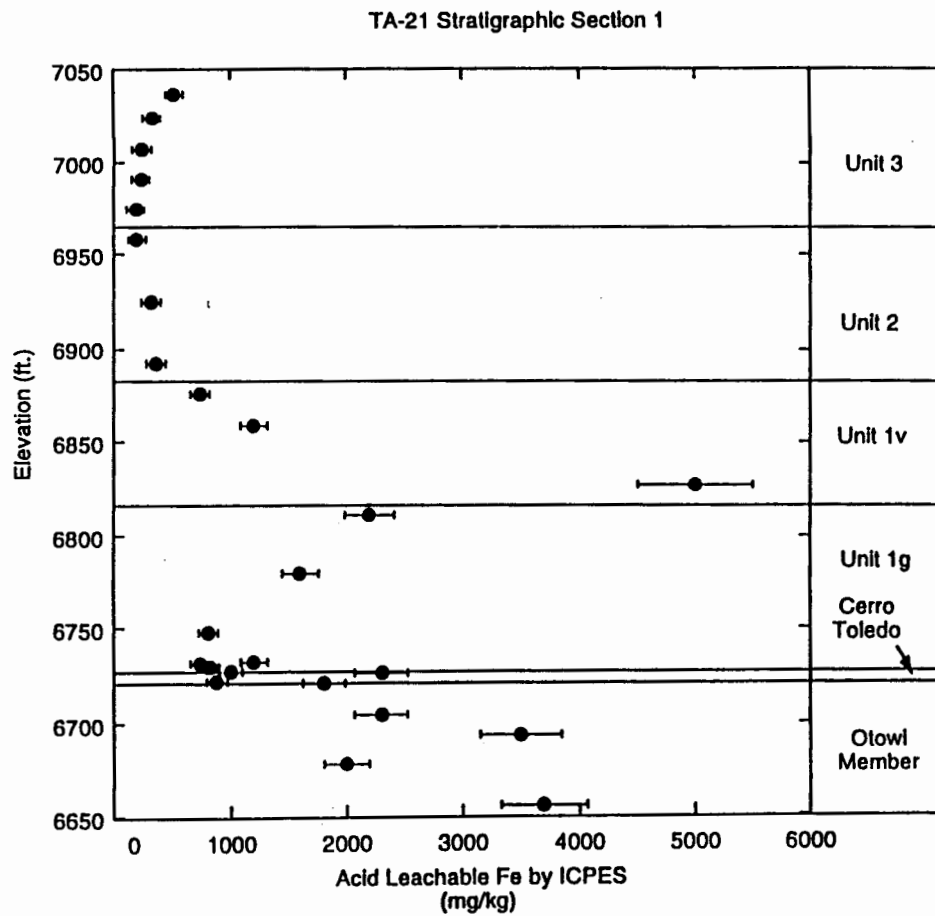


Fig. 13 PLOTS SHOWING EXAMPLES OF ACID LEACHABLE IRON CONCENTRATIONS AT TA-21 AND TOTAL IRON CONCENTRATIONS AT TA-49 AS A FUNCTION OF STRATIGRAPHIC HEIGHT IN THE BANDELIER TUFF.

Instead of estimating a mixture distribution because of the bimodality in each data group, we use the maximum leachable iron concentration for each data group for the background screening values. The background screening values are 13000 mg/kg for Tt, 3700 mg/kg for Qbo, 2400 mg/kg for Qct, 3250 mg/kg for Qbt 1g, 12000 mg/kg for Qbt 4, and 9040 mg/kg for Qbt 1v, Qbt 2 and Qbt 3.

Total iron concentrations by XRF and INAA vary little in Qbt 1g, Qbt 1v, and Qbt 2 (Fig. 13). Total iron concentrations initially decrease up section across the Qbt 2/Qbt 3 contact, but then increase up section through Qbt 3. Total iron concentrations increase abruptly across the Qbt 3/Qbt 4 contact and concentrations increase up section through Qbt 4. The top of Qbo contains about twice as much total iron as the Qbt 1g tuffs at the base of the Tshirege Member (Fig. 13).

Lead (Pb)

All of the 106 leachable lead concentrations were above ICPMS detection limits. Square root transformed lead data are approximately normally distributed. Lead concentrations for all geologic units range from 0.6 to 36 mg/kg and average 6.95 mg/kg.

Population characteristics from the Wilcoxon rank sum test (Table IV) resulted in pooling all of the lead data for Qbt 1g, Qbt 1v, Qbt 2 and Qbt 3 (as Qbt 123). There was a significant difference between Qbt 1v and Qbt 1g, however this difference was not consistent with other Wilcoxon comparisons, which lead to pooling data across all data groups. Box plots comparing acid leachable lead by geologic unit show that medians, arithmetic means, and middle 50 percent ranges are generally greater for unit Qbt 1v than for the other units (Fig. 4). Plots of leachable lead from individual stratigraphic sections show that in the Tshirege Member, leachable lead concentrations are greatest in the center of the unit, particularly near the vapor phase notch at the unit Qbt 1g/Qbt 1v contact (Fig. 14).

The background screening values for leachable lead are 6.7 mg/kg for Tt, 5 mg/kg for Qbo, 7.1 mg/kg for Qct, 21.9 mg/kg for Qbt 1v, 4 mg/kg for Qbt 4, and 16.2 mg/kg for Qbt 1g, Qbt 2, and Qbt 3. Background screening values for lead in all rock units are well below the SAL of 400 mg/kg.

Total lead concentrations by INAA generally decrease up section in the Tshirege Member (Fig. 14). Two total lead concentrations were determined for Qbo; both were about 35% lower than total lead concentrations determined for Qbt 1g of the Tshirege Member. The percentage of total lead that is susceptible to acid leaching in the Bandelier Tuff varies with stratigraphic position. Approximately 25% to 75% of the lead near the Qbt 1g/Qbt 1v contact is released by leaching in a solution of nitric acid at a pH of 1. However, only 10% to 15% of the lead in the remainder of the Bandelier Tuff is dissolved by the nitric acid solution.

Magnesium (Mg)

All of the 106 leachable magnesium concentrations were above ICPEs detection limits. Square root transformed magnesium data are approximately normally distributed. Magnesium concentrations for all geologic units range from 39 to 1700 mg/kg and average 296 mg/kg.

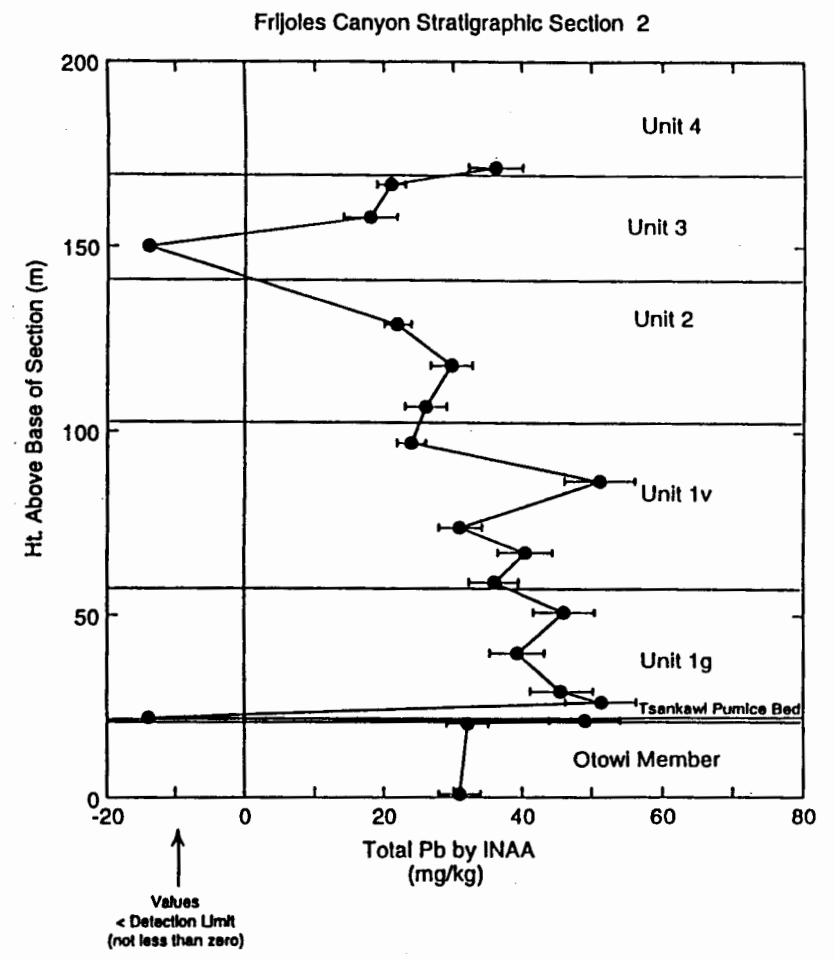
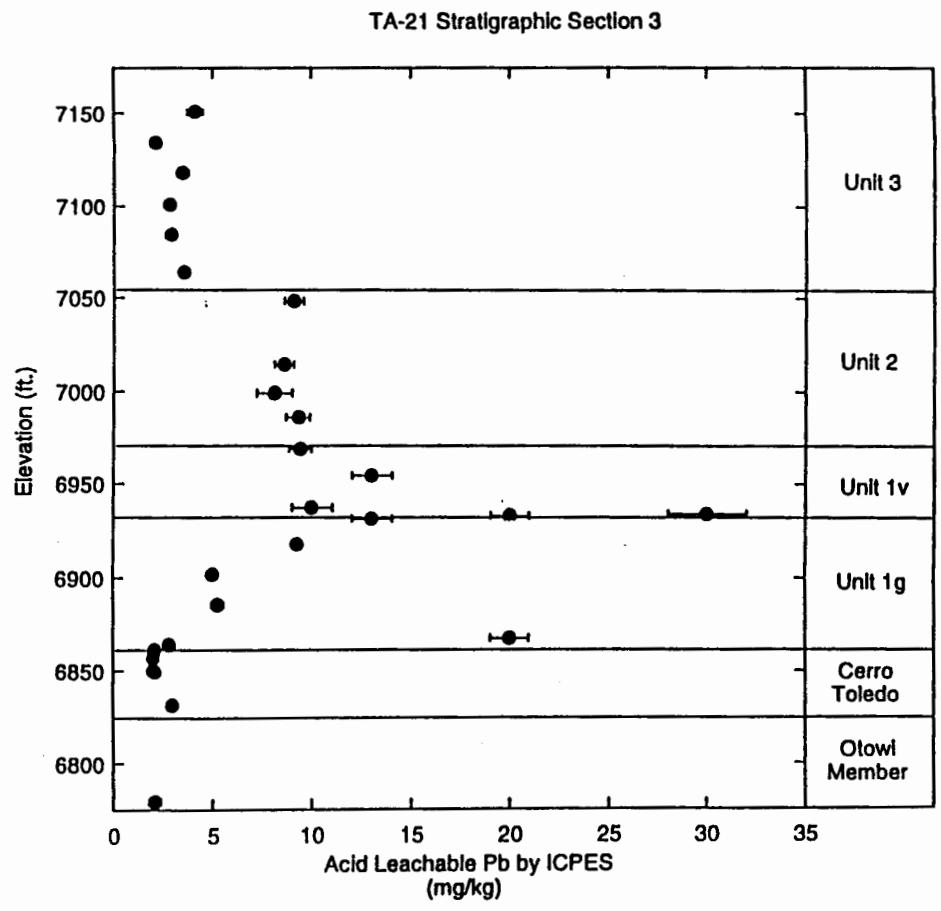


Fig. 14 PLOTS SHOWING EXAMPLES OF ACID LEACHABLE LEAD CONCENTRATIONS AT TA-21 AND TOTAL LEAD CONCENTRATIONS AT FRIJOLES CANYON AS A FUNCTION OF STRATIGRAPHIC HEIGHT IN THE BANDELIER TUFF. NOTE THE HIGH CONCENTRATIONS OF LEACHABLE LEAD ASSOCIATED WITH THE CONTACT BETWEEN UNITS QBT 1G AND QBT 1V (VAPOR PHASE NOTCH) REPRESENTED BY SAMPLES 1106-3-12, 1106-3-13, AND 1106-3-14.

Population characteristics from the Wilcoxon rank sum test (Table IV) resulted in pooling all of the magnesium data for Qbt 1g and Qbt 2 (as Qbt1g2) and Qbt 1v and Qbt 3 (as Qbt 1v3). Box plots comparing acid leachable magnesium by geologic unit show that medians, arithmetic means, and middle 50 percent ranges are generally greater for units Tt and Qbt 4 than for the other units (Fig. 4). Plots of leachable magnesium from individual stratigraphic sections show no clear relation of concentrations to stratigraphic position (Fig. 15). Because of its low abundance and its chemical mobility, magnesium concentrations in the Bandelier Tuff are easily affected by diagenetic alteration, particularly in the near-surface environment.

The background screening values for leachable magnesium are 950 mg/kg for Tt, 510 mg/kg for Qbo, 510 mg/kg for Qct, 548 mg/kg for Qbt 1g and Qbt 2, 628 mg/kg for Qbt 1v and Qbt 3, and 1700 mg/kg for Qbt 4.

Although approximately half of the total magnesium concentrations by XRF and INAA are below detection limits, the greatest magnesium concentrations are clearly related to units Qbo and Qct (Fig. 15).

Manganese (Mn)

All of the 106 leachable manganese concentrations were above ICPEES detection limits. Square root transformed manganese data are approximately normally distributed. Manganese concentrations for all geologic units range from 21 to 510 mg/kg and average 184 mg/kg.

Population characteristics from the Wilcoxon rank sum test (Table IV) resulted in pooling all of the manganese data for Qbt 1g as a data group, Qbt 1v and Qbt 2 as a data group (as Qbt1v2), and Qbt 3 as a data group. Box plots comparing acid leachable manganese by geologic unit show that medians, arithmetic means, and middle 50 percent ranges are generally greater for units Qbt 1v, Qbt 2, and Qbt 4 than for the other units (Fig. 4). Plots of leachable manganese from individual stratigraphic sections show that leachable manganese concentrations are greater in Qbt 1v and Qbt 2 than the rest of the Tshirege Member (Fig. 16).

The background screening values for leachable manganese are 280 mg/kg for Tt, 170 mg/kg for Qbo, 90 mg/kg for Qct, 273 mg/kg for Qbt 1g, 533 mg/kg for Qbt 1v and Qbt 2, 426 mg/kg for Qbt 3, and 370 mg/kg for Qbt 4. These background screening values are roughly equal to or greater than the manganese SAL of 380 mg/kg.

Total manganese concentrations by XRF and INAA vary little as a function of stratigraphic position (Fig. 16). There is a slight tendency for total manganese concentrations to decrease up section in the Tshirege Member, except for Qbt 4 which is characterized by an abrupt increase in manganese concentrations relative to underlying units. At TA-49, total manganese concentrations systematically decrease up section in the upper part of Qbo (Fig. 16).

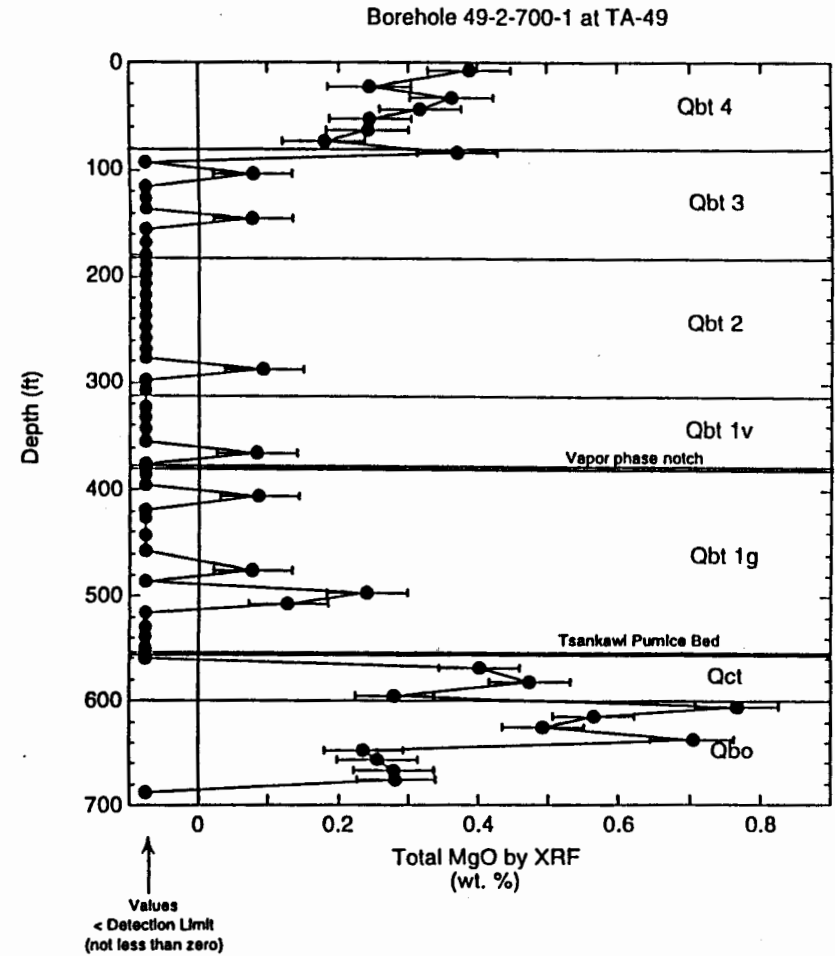
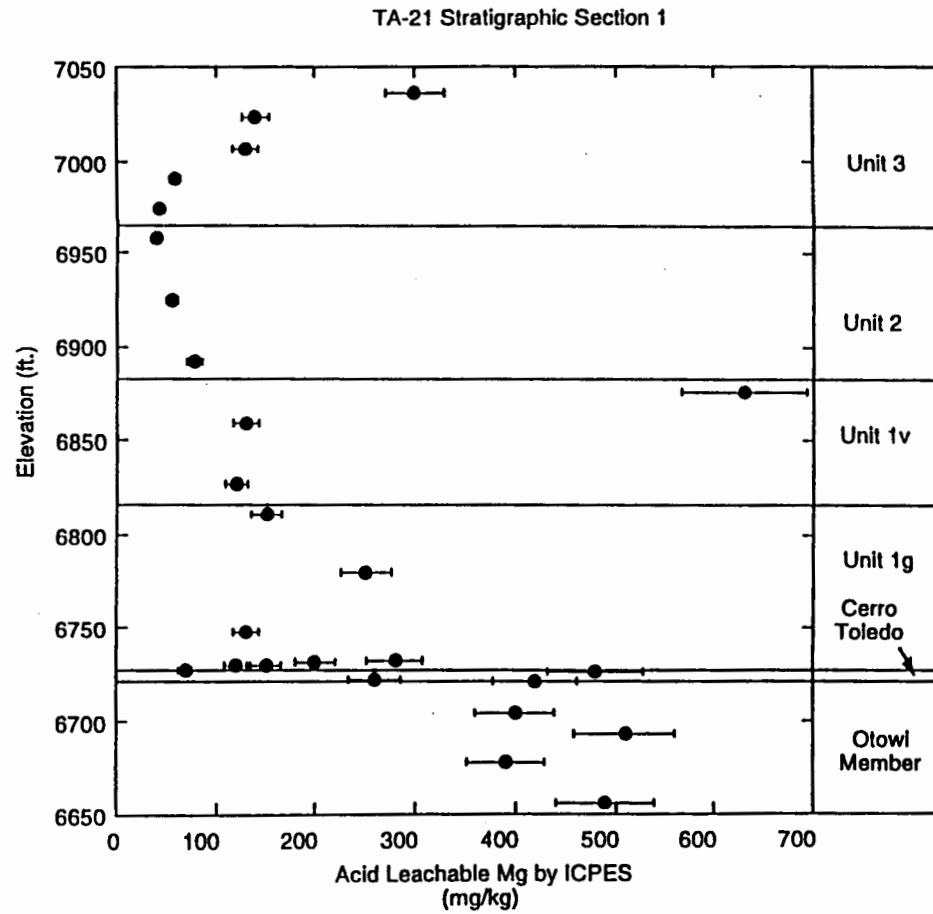


Fig. 15 PLOTS SHOWING EXAMPLES OF ACID LEACHABLE MAGNESIUM CONCENTRATIONS AT TA-21 AND TOTAL MAGNESIUM CONCENTRATIONS AT TA-49 AS A FUNCTION OF STRATIGRAPHIC HEIGHT IN THE BANDELIER TUFF.

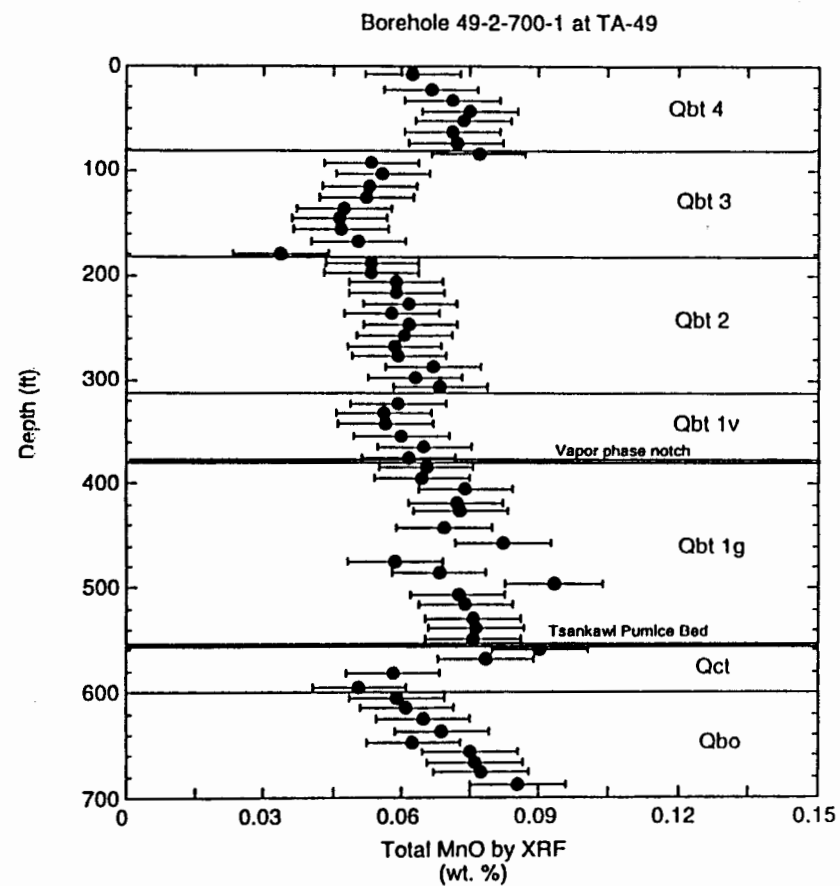
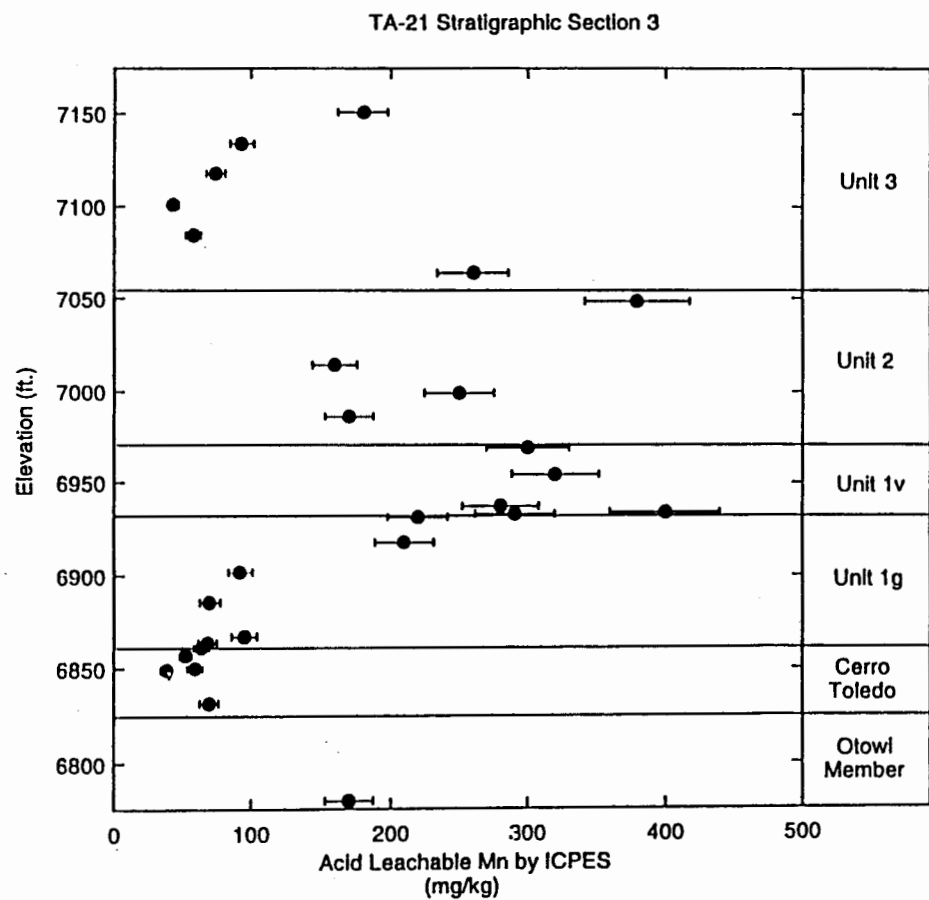


Fig. 16 PLOTS SHOWING EXAMPLES OF ACID LEACHABLE MANGANESE CONCENTRATIONS AT TA-21 AND TOTAL MANGANESE CONCENTRATIONS AT TA-49 AS A FUNCTION OF STRATIGRAPHIC HEIGHT IN THE BANDELIER TUFF.

Mercury (Hg)

Leachable mercury concentrations were not determined for this investigation because mercury was not detected in the INAA analyses. All 38 of the samples analyzed by INAA had total mercury concentrations below detection limits, which range from 0.3 to 0.7 mg/kg. Thus naturally mercury concentrations are well below the SAL of 23 mg/kg.

Nickel (Ni)

Only 9 of the 106 leachable nickel concentrations were above ICPEs detection limits of 1 to 2 mg/kg. No statistical distribution of the nickel was estimated because of the large number of non detects. For samples above detection limits, leachable nickel concentrations range from 2 to 15 mg/kg and average 4.6 mg/kg.

Box plots comparing acid leachable nickel by geologic unit show that the highest leachable nickel concentrations are associate with unit Tt (Fig. 4). The background screening values for leachable nickel are based on maximum detected concentrations in each rock unit. Background screening values are 15 mg/kg for Tt, 2.8 mg/kg for Qbo, <2 mg/kg for Qct and Qbt 1g, 2 mg/kg for Qbt 1v, <2 mg/kg for Qbt 2, 2.6 mg/kg for Qbt 3, and <2 mg/kg for Qbt 4. Background screening values for all rock units are well below the SAL of 1500 mg/kg.

Total nickel concentrations by XRF were generally below detection limits which ranged between 6 and 7 mg/kg.

Potassium (K)

All of the 106 leachable potassium concentrations were above ICPEs detection limits. Square root transformed potassium data are approximately normally distributed. Potassium concentrations for all geologic units range from 250 to 5400 mg/kg and average 1055 mg/kg.

Population characteristics from the Wilcoxon rank sum test (Table IV) resulted in pooling all of the potassium data for Qbt 1g and Qbt 2 (as data group Qbt 1g2). Qbt 1v and Qbt 3 were pooled as two separate data groups. Box plots comparing acid leachable potassium by geologic unit show generally high concentrations for units Qbt 1g and generally low concentrations for units Qbo, Qbt 3, and Tt (Fig. 4). Plots of leachable potassium from individual stratigraphic sections show that leachable potassium concentrations are greatest in the glassy tuffs (units Qbo, Qct, and Qbt 1g), and concentrations decrease up section in the overlying devitrified tuffs (Fig. 17).

The background screening values for leachable potassium are 1100 mg/kg for Tt, 960 mg/kg for Qbo, 1600 mg/kg for Qct, 2730 mg/kg for Qbt 1g and Qbt 2, 5540 mg/kg for Qbt 1v, 735 mg/kg for Qbt 3, and 1600 mg/kg for Qbt 4.

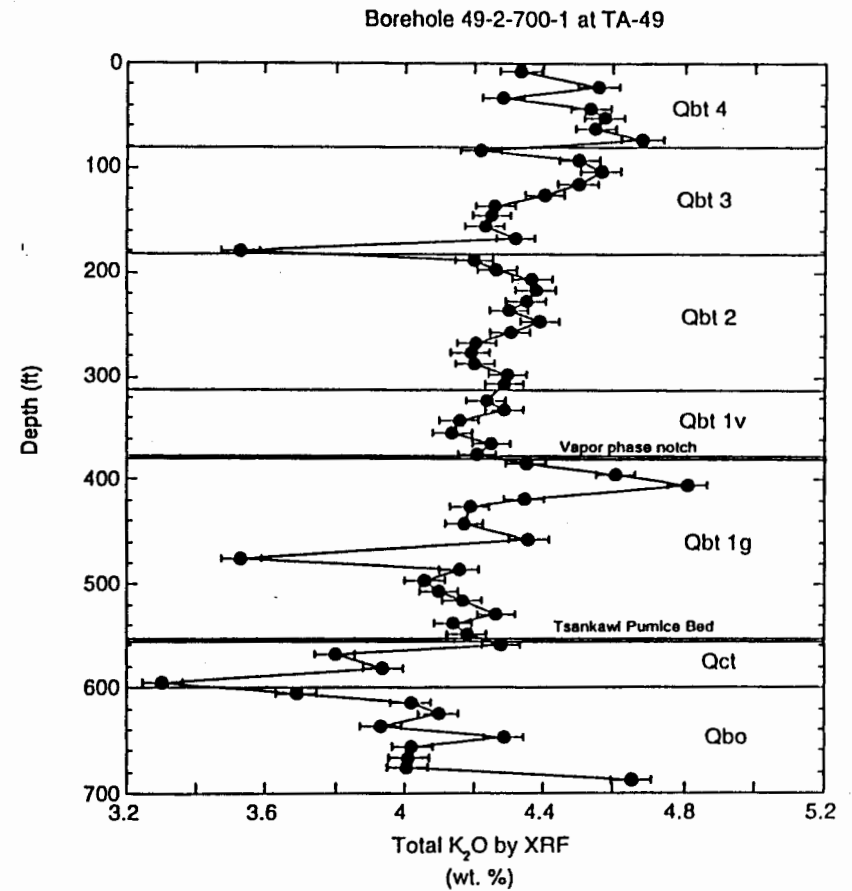
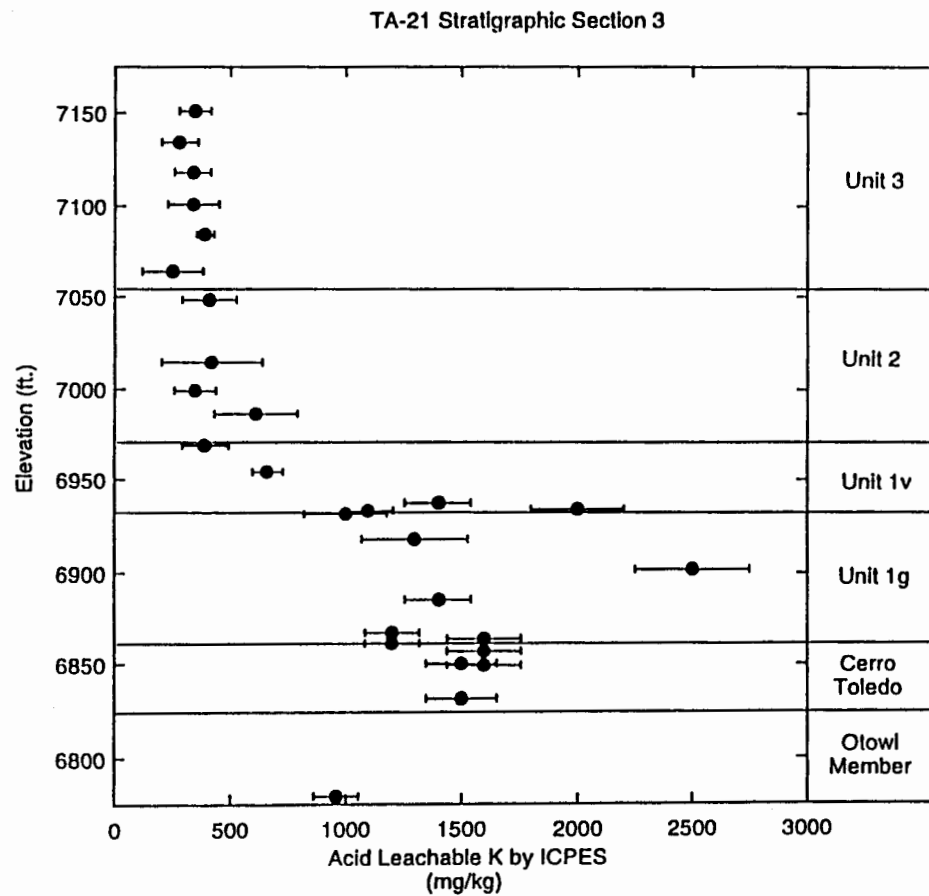


Fig. 17 PLOTS SHOWING EXAMPLES OF ACID LEACHABLE POTASSIUM CONCENTRATIONS AT TA-21 AND TOTAL POTASSIUM CONCENTRATIONS AT TA-49 AS A FUNCTION OF STRATIGRAPHIC HEIGHT IN THE BANDELIER TUFF.

There is slight increase up section in total potassium concentrations by XRF and INAA in the Bandelier Tuff. Increasing total potassium up section is opposite of the general decrease in soluble potassium up section in the Tshirege Member (Fig. 17). Total potassium concentrations at the top of Qbo are somewhat lower than those found in the basal tuffs of the Tshirege Member (e.g., Qbt 1g). Potassium in the Bandelier Tuff is relatively insoluble, and only 1% to 10% of the total potassium in the rock is released by leaching in a solution of nitric acid at a pH of 1.

Selenium (Se)

Leachable selenium concentrations were not determined for this investigation because total selenium was not detected by INAA, and these detection limits were consistently less than the SAL. All 38 of the samples analyzed by INAA had total selenium concentrations below detection limits, which range from 1.1 to 4.9 mg/kg. Thus leachable selenium concentration should be well below the SAL of 380 mg/kg.

Silver (Ag)

Only 1 of the 106 leachable silver concentrations was above ICPES detection limits of 1 to 2 mg/kg. The single detected silver concentration, which occurred in unit Qbt 3, was 1.9 ± 1.0 mg/kg.

Except for unit Qbt 1v, background screening values for leachable silver are based on maximum detection limits in each rock unit. Background screening values are <1 mg/kg for Tt, Qbo, Qct, Qbt 2, and Qbt 4, <2 mg/kg for Qbt 1g and Qbt 1v, and 1.9 mg/kg for Qbt 3. Background screening values for all rock units are well below the SAL of 380 mg/kg.

Total silver concentrations by INAA were below detection limits which ranged between 1 and 3 mg/kg.

Sodium (Na)

All of the 106 leachable sodium concentrations were above ICPES detection limits. Sodium concentrations for all geologic units range from 130 to 7700 mg/kg and average 1059 mg/kg.

Population characteristics from the Wilcoxon rank sum test (Table IV) resulted in pooling all of the sodium data for Qbt 1g and Qbt 1v (as data group Qbt 1). Qbt 2 and Qbt 3 were pooled as data group Qbt 23. Square root transformed sodium data are approximately normally distributed for data group Qbt 1. Log transformed sodium data are approximately normally distributed for data group Qbt 23. Box plots comparing acid leachable sodium by geologic unit show generally low concentrations for units Qbt 3, Qbt 4, and Tt relative to the other rock units (Fig.

4). Plots of leachable sodium from individual stratigraphic sections show that leachable sodium concentrations are greatest in the glassy tuffs (units Qbo, Qct, and Qbt 1g), and concentrations decrease up section in the overlying devitrified tuffs (Fig. 18).

The background screening values for leachable sodium are 610 mg/kg for Tt, 1900 mg/kg for Qbo, 3500 mg/kg for Qct, 4290 mg/kg for Qbt 1g and Qbt 1v, 1940 mg/kg for Qbt 2 and Qbt 3, and 390 mg/kg for Qbt 4.

Total sodium concentrations by XRF and INAA vary systematically as a function of stratigraphic position, but in sense opposite to that of the leachable sodium concentrations (Fig. 18). In the Tshirege Member, total sodium concentrations increase systematically up section through the tuff. Thus, tuffs that contain the lowest total sodium concentrations have the greatest concentrations of soluble sodium. At TA-49, total sodium concentrations tend to decrease up section in the upper part of the Qbo in the overlying tuffaceous sediments of Qct (Fig. 18).

Strontium (Sr)

Leachable strontium concentrations were not determined for this investigation because the total strontium results are consistently several orders of magnitude below the strontium SAL of 46000 mg/kg. Total strontium concentrations for the Bandelier Tuff range from below the detection limit of 5 mg/kg to 368 mg/kg and average 33 mg/kg.

In the Tshirege Member, total strontium concentrations increase slightly up section from Qbt 1g to Qbt 3 (Fig. 19). There is an abrupt increase in strontium concentrations above the Qbt 3/Qbt 4 contact. Total strontium concentrations in the upper part of Qbo increase upsection and total strontium concentrations tend to be greater than in the overlying tuffs of Qct and Qbt 1g (Fig. 19). Strontium concentrations in the upper part of Qbo at TA-49 are notably greater than in the upper part of Qbo at TA-21 (Fig. 19). These differences probably reflect different patterns of Qbo deposition and erosion at the two sites. Based on its chemical characteristics, Qbo was probably either: 1) more deeply eroded at TA-21 than at TA-49 before being buried by the Tshirege Member or 2) stratigraphically higher Sr-rich tuffs were deposited at TA-49 but not at TA-21.

Sulfate (SO₄)

Sulfate concentrations were determined for rock samples on aliquots extracted in deionized water and analyzed by IC. All of the 106 leachable sulfate concentrations were above IC detection limits. Sulfate concentrations for all geologic units range from 1.5 to 815 mg/kg and average 56.9 mg/kg.

Population characteristics from the Wilcoxon rank sum test (Table IV) resulted in pooling the leachable sulfate data for Qbt 1g and Qbt 1v into one data group (Qbt 1) and then pooling the Qbt 1 data group with data for units Qbt 2 and Qbt 3 into a single data group (as Qbt 123). The

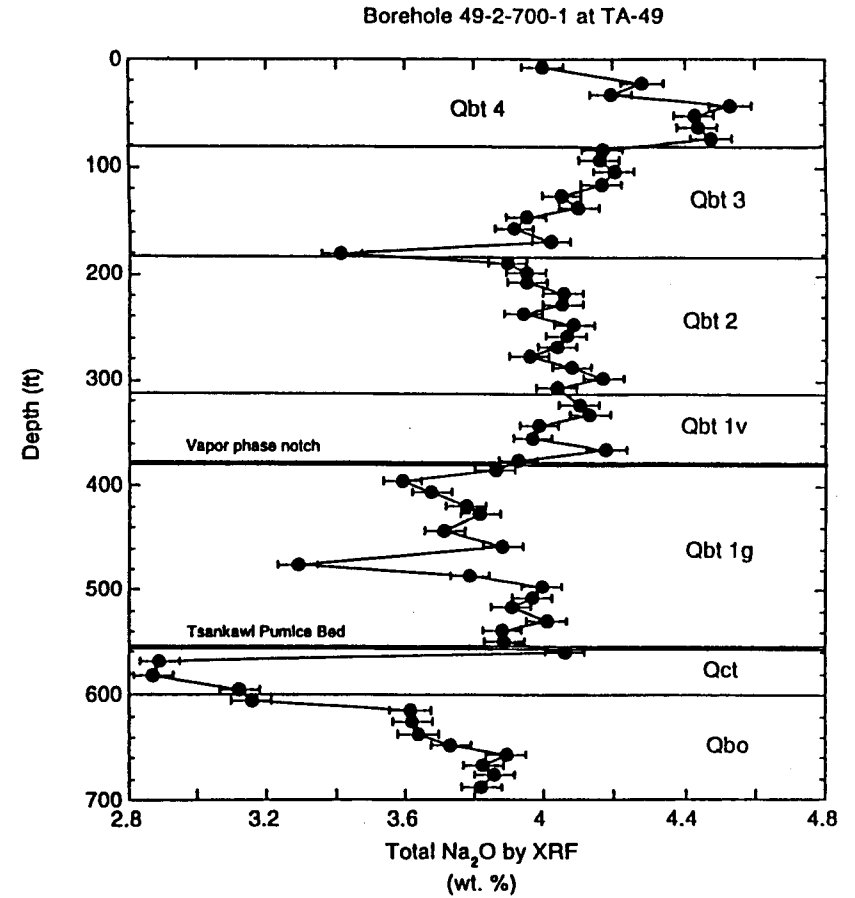
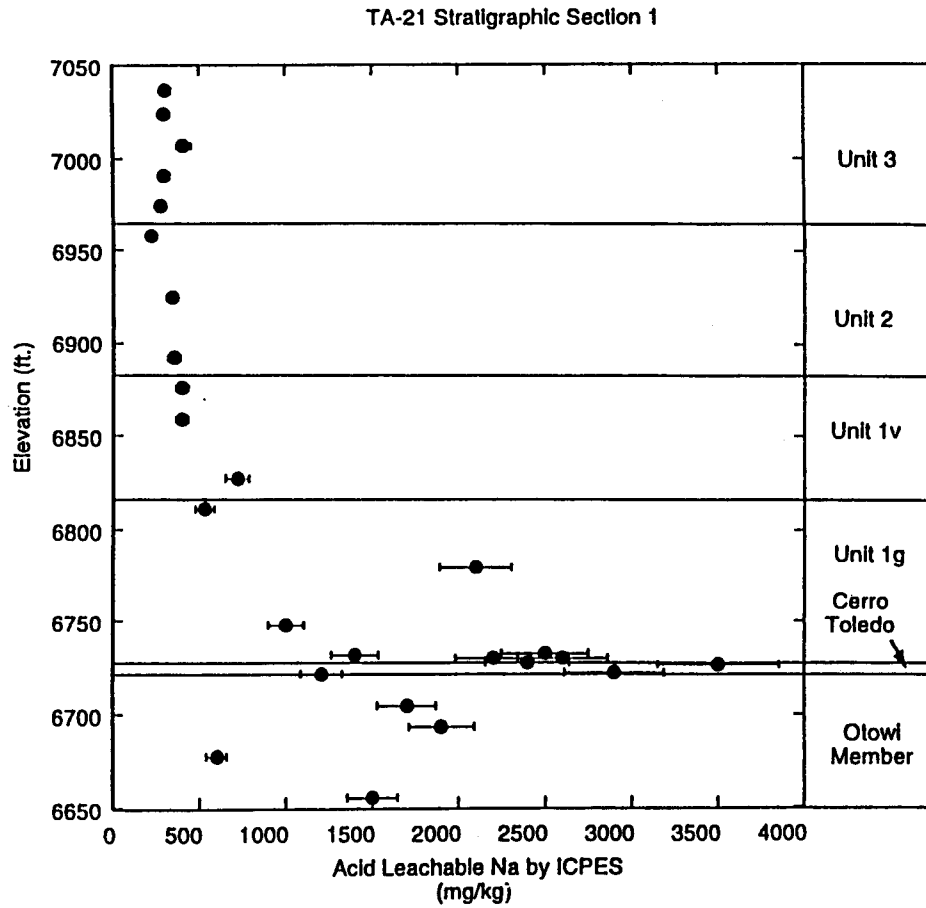


Fig. 18 PLOTS SHOWING EXAMPLES OF ACID LEACHABLE SODIUM CONCENTRATIONS AT TA-21 AND TOTAL SODIUM CONCENTRATIONS AT TA-49 AS A FUNCTION OF STRATIGRAPHIC HEIGHT IN THE BANDELIER TUFF.

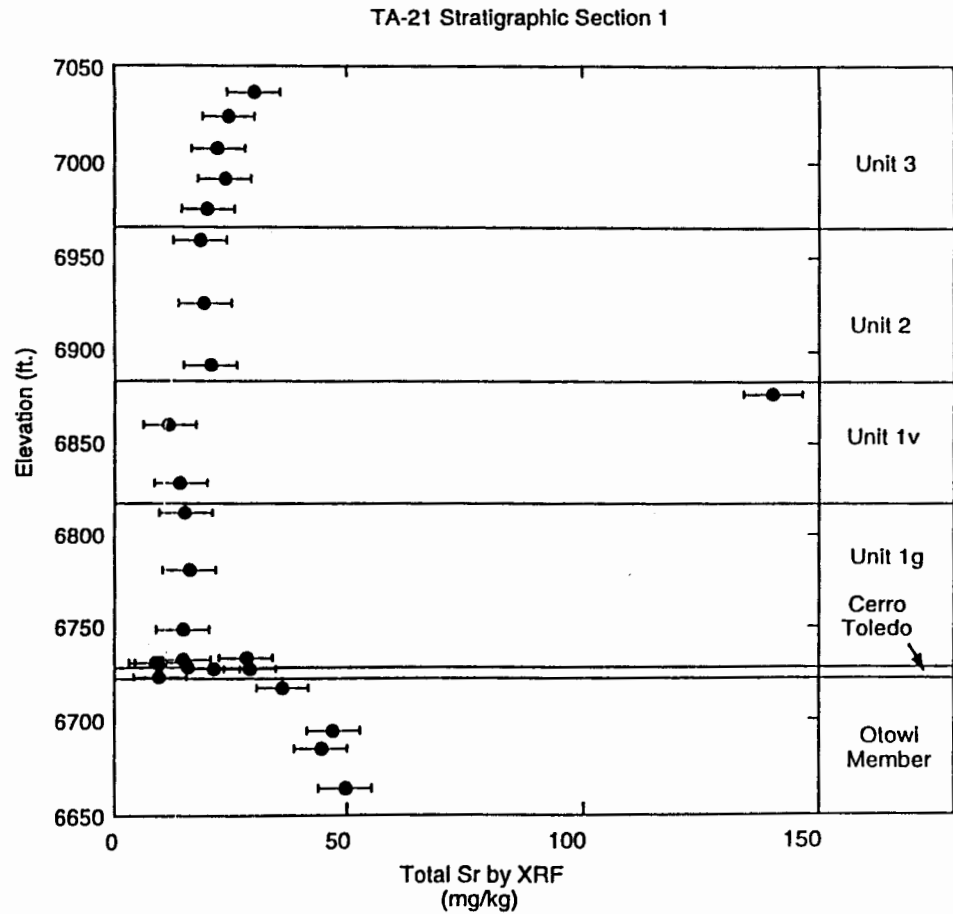
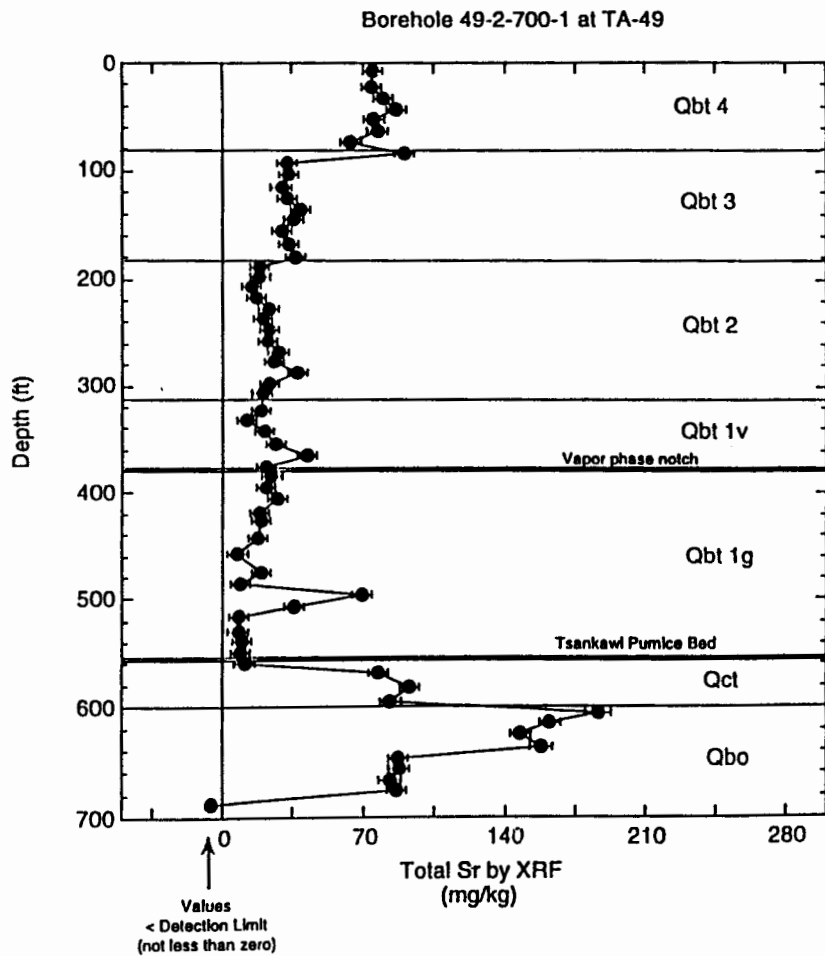


Fig. 19 PLOTS SHOWING TOTAL STRONTIUM CONCENTRATIONS AT TA-49 AND TA-21 AS A FUNCTION OF STRATIGRAPHIC HEIGHT IN THE BANDELIER TUFF.

resulting data group was bimodally distributed. Box plots comparing leachable sulfate by geologic unit show that medians, arithmetic means, and middle 50 percent ranges are generally greater for units Qct and Qbt 1g than for the other units (Fig. 4).

The greatest concentrations of sulfate are associated with the contact between the lower Tshirege Member (including the Tsankawi Pumice Bed) and the tephra and volcanoclastic sediments of the Cerro Toledo interval (Fig. 20). Soluble chlorine concentrations are also elevated in this interval. The presence of elevated concentrations of water soluble species such as sulfate and chlorine in these tuffs suggest that they have acted as preferential ground water pathways at some point after their deposition. These tuffs are now well above the canyon floor, and there is no evidence of perching of present-day ground water in these units. It is possible that these units were preferential ground water pathways when Los Alamos Canyon was shallower, and these units were below the level of perched alluvial ground water bodies on the canyon floor. Elevated sulfate also occurs at the Qbt 2/Qbt 3 contact at TA-67 (Fig. 20).

Instead of estimating a mixture distribution because of the bimodality in each data group, we use the maximum leachable sulfate concentration for each data group for the background screening values. The background screening values are 38.6 mg/kg for Tt, 12.7 mg/kg for Qbo, 548 mg/kg for Qct, 26.4 mg/kg for Qbt 4, and 815 mg/kg for Qbt 1g, Qbt 1v, Qbt 2, and Qbt 3.

Tantalum (Ta)

Twenty-one of the 106 leachable tantalum concentrations were above ICPMS detection limits. No statistical distribution of the tantalum was estimated because of the small sample population. For samples above detection limits, tantalum concentrations for all geologic units range from 0.2 to 2 mg/kg and average 0.43 mg/kg.

Box plots comparing acid leachable tantalum by geologic unit show concentrations above detection limits occur most often in Qbo and Qbt 4 relative to the other rock units (Fig. 4). Plots of leachable tantalum from individual stratigraphic sections showed no clear relation between above detection limit tantalum concentrations and stratigraphic height. In two cases, above detection limit leachable tantalum concentrations are associated with crystal-rich surge deposits at unit contacts (Fig. 21).

The background screening values for leachable tantalum are based on maximum detected concentrations in each rock unit. Background screening values are 0.2 mg/kg for Tt, 0.9 mg/kg for Qbo, 0.3 mg/kg for Qct, 0.3 mg/kg for Qbt 1g, 0.5 mg/kg for Qbt 1v, 2 mg/kg for Qbt 2, 0.8 mg/kg for Qbt 3, and 0.5 mg/kg for Qbt 4.

Total tantalum concentrations by INAA decrease systematically up section in the Tshirege Member (Fig. 21). Total tantalum in the upper Tshirege Member is about one-third of that in the lower part. Tantalum concentrations in the upper Otowi Member are about half of those found in the lower Tshirege Member.

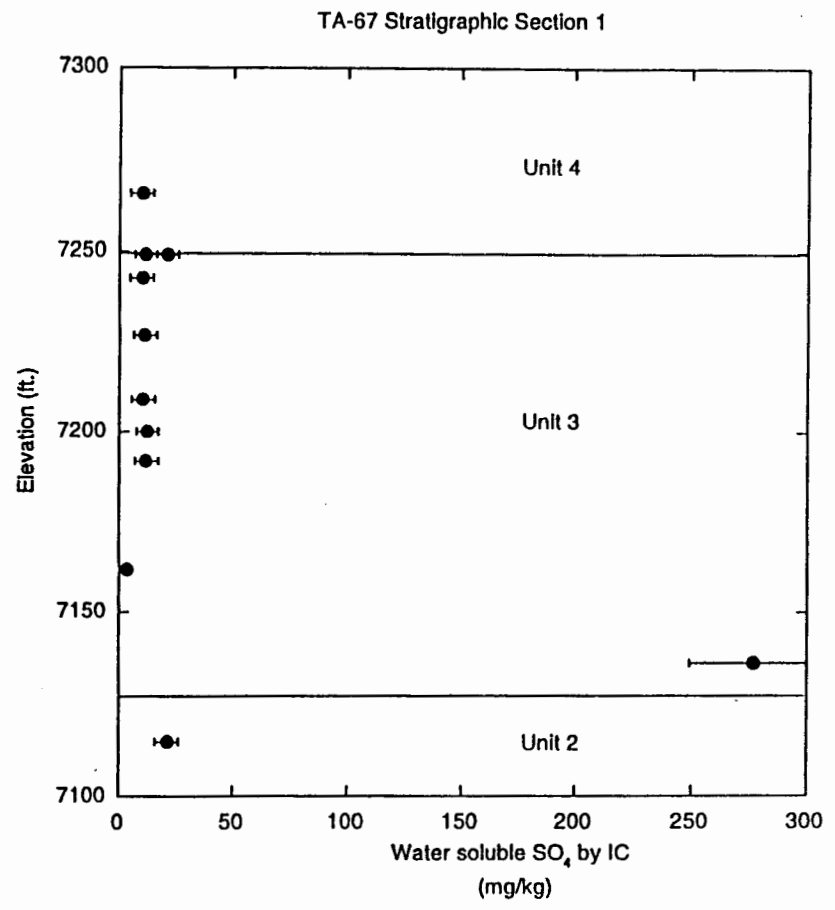
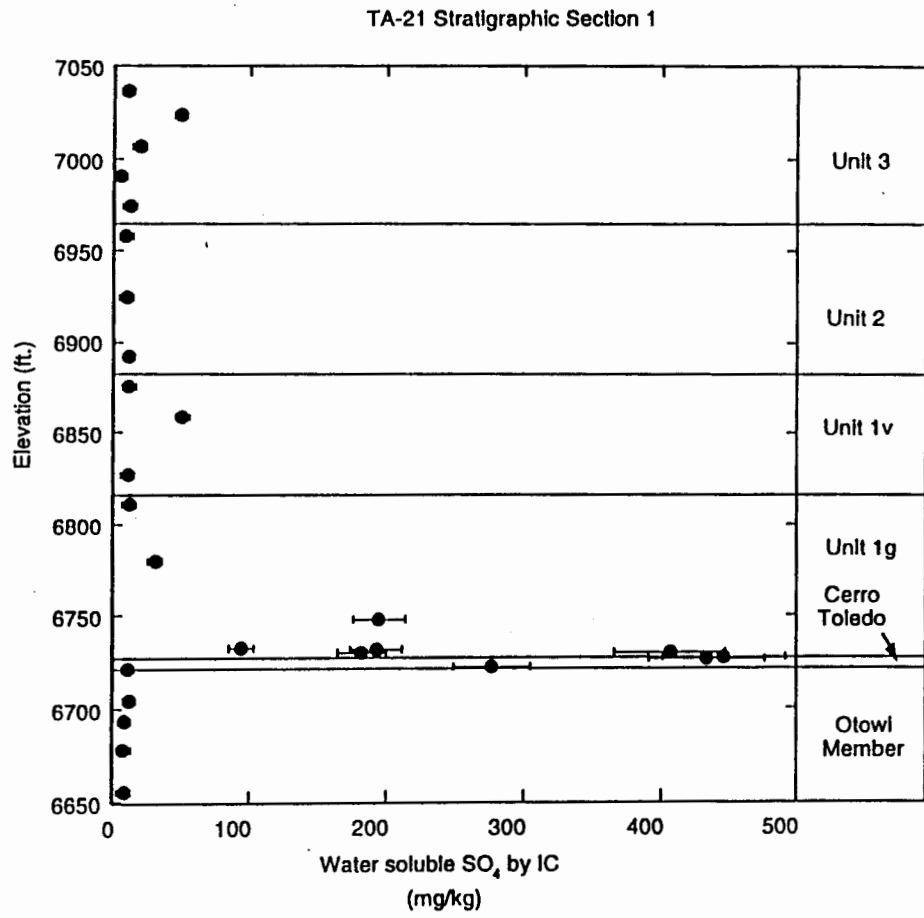


Fig. 20 PLOTS SHOWING EXAMPLES OF WATER SOLUBLE SULFATE CONCENTRATIONS AT TA-21 AND AT TA-67 AS A FUNCTION OF STRATIGRAPHIC HEIGHT IN THE BANDELIER TUFF.

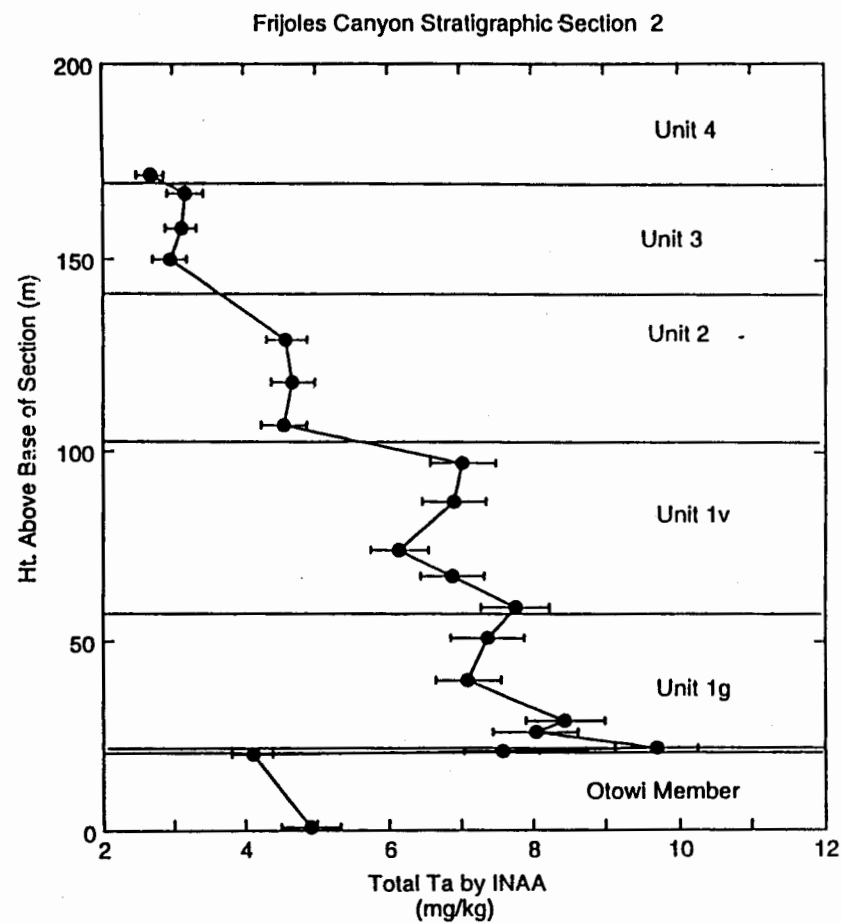
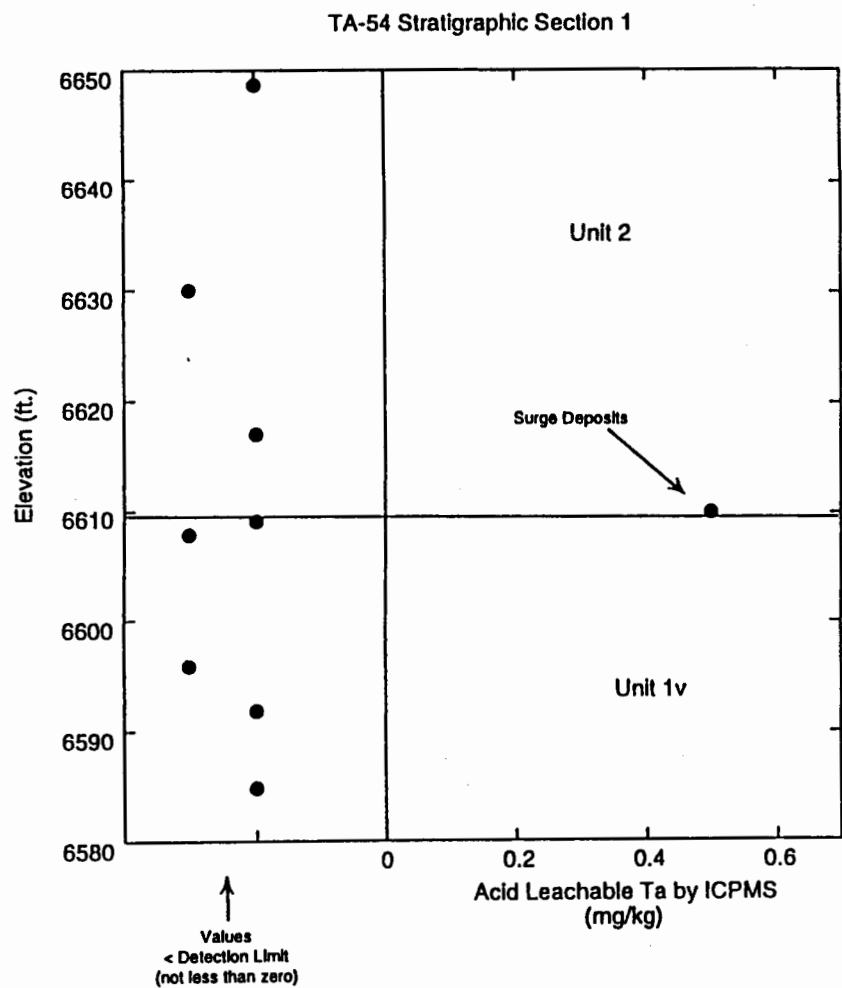


Fig. 21 PLOTS SHOWING EXAMPLES OF ACID LEACHABLE TANTALUM CONCENTRATIONS AT TA-54 AND TOTAL TANTALUM CONCENTRATIONS AT FRIJOLES CANYON AS A FUNCTION OF STRATIGRAPHIC HEIGHT IN THE BANDELIER TUFF.

Thallium (Tl)

Twenty-four of the 106 leachable thallium concentrations were above ICPMS detection limits. No statistical distribution of the thallium was estimated because of the small sample population. For samples above detection limits, thallium concentrations for all geologic units range from 0.2 to 1.7 mg/kg and average 0.73 mg/kg.

Box plots comparing acid leachable thallium by geologic unit generally show concentrations above detect limits occur most often in Qbo and Qbt 1g relative to the other rock units (Fig. 4). Plots of leachable thallium from individual stratigraphic sections show that above detection limit thallium concentrations are associated with the Qbt 1g/Qbt 1v contact or with tuffs near the base of Qbt 1g and in the upper part of Qbo (Fig. 22).

The background screening values for leachable thallium are based on maximum detected concentrations in each rock unit. Background screening values are <0.3 mg/kg for Tt, 0.9 mg/kg for Qbo, <0.2 mg/kg for Qct, 0.7 mg/kg for Qbt 1g, 1.7 mg/kg for Qbt 1v, 1.3 mg/kg for Qbt 2, 1.7 mg/kg for Qbt 3, and <0.3 mg/kg for Qbt 4. The background screening values are less than the thallium SAL of 5.4 mg/kg.

Thorium (Th)

All of the 106 leachable thorium concentrations were above ICPMS detection limits. Square root transformed thorium data are approximately normally distributed. Thorium concentrations for all geologic units range from 0.5 to 22 mg/kg and average 6.31 mg/kg.

Population characteristics from the Wilcoxon rank sum test (Table IV) resulted in pooling the thorium data for Qbt 1g, Qbt 1v, Qbt 2 and Qbt 3 as four separate data groups. Box plots comparing acid leachable thorium by geologic unit show generally high concentrations for units Qbt 1v and Qbt 2 and low concentrations for units Qbo, Qbt 1g, Qct, and Tt relative to the other rock units (Fig. 4). Plots of leachable thorium from individual stratigraphic sections show that leachable thorium concentrations typically are low in the glassy tuffs in Qbo and in the basal part of the Tshirege Member (Fig. 23). However, leachable thorium concentrations abruptly increase by about an order of magnitude in the crystalline tuffs above the Qbt 1g/Qbt 1v contact. Above this contact, thorium concentrations decrease up section (Fig. 23).

The background screening values for leachable thorium are 6.4 mg/kg for Tt, 1.4 mg/kg for Qbo, 4.2 mg/kg for Qct, 7.69 mg/kg for Qbt 1g, 22.1 mg/kg for Qbt 1v, 11.5 mg/kg for Qbt 2, 9.29 mg/kg for Qbt 3, and 6.1 mg/kg for Qbt 4.

Total thorium concentrations by INAA decrease systematically up section from the base of the Tshirege Member (Fig. 23). Total thorium in the upper Tshirege Member is about one-third of that in the lower part. Thorium concentrations in the upper Otowi Member are about half of that found in the lower Tshirege Member. Comparison of acid leachable and total thorium data shows that approximately 10% to 40% of the thorium in the Bandelier Tuff is susceptible to leaching by nitric acid at a pH of 1.

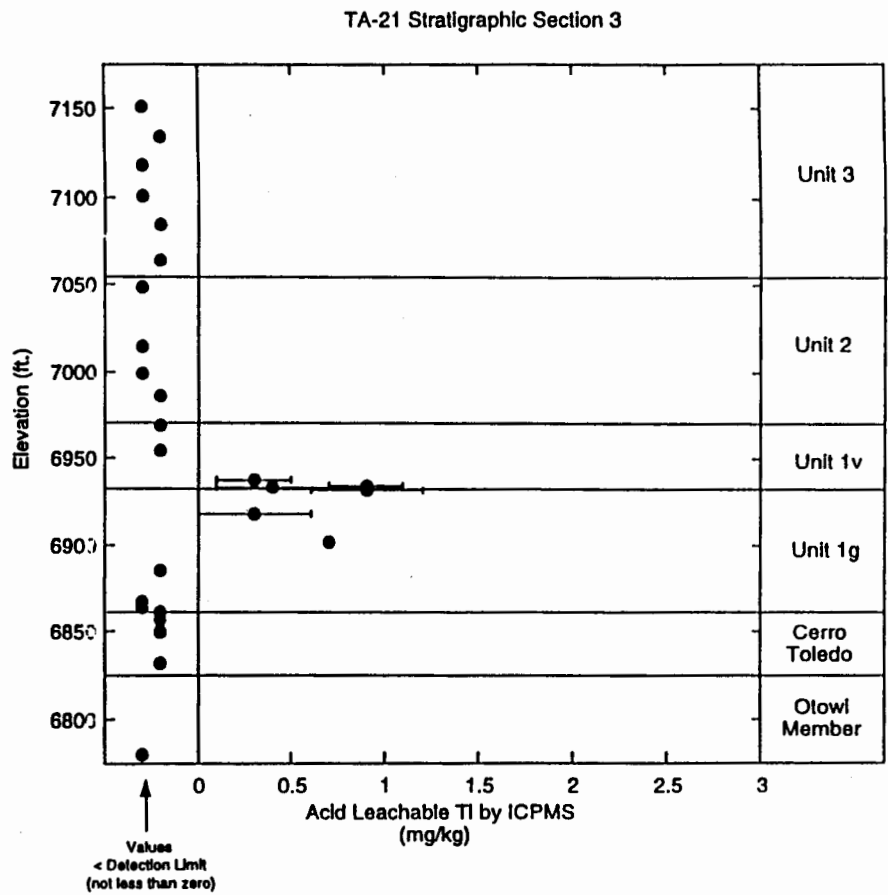
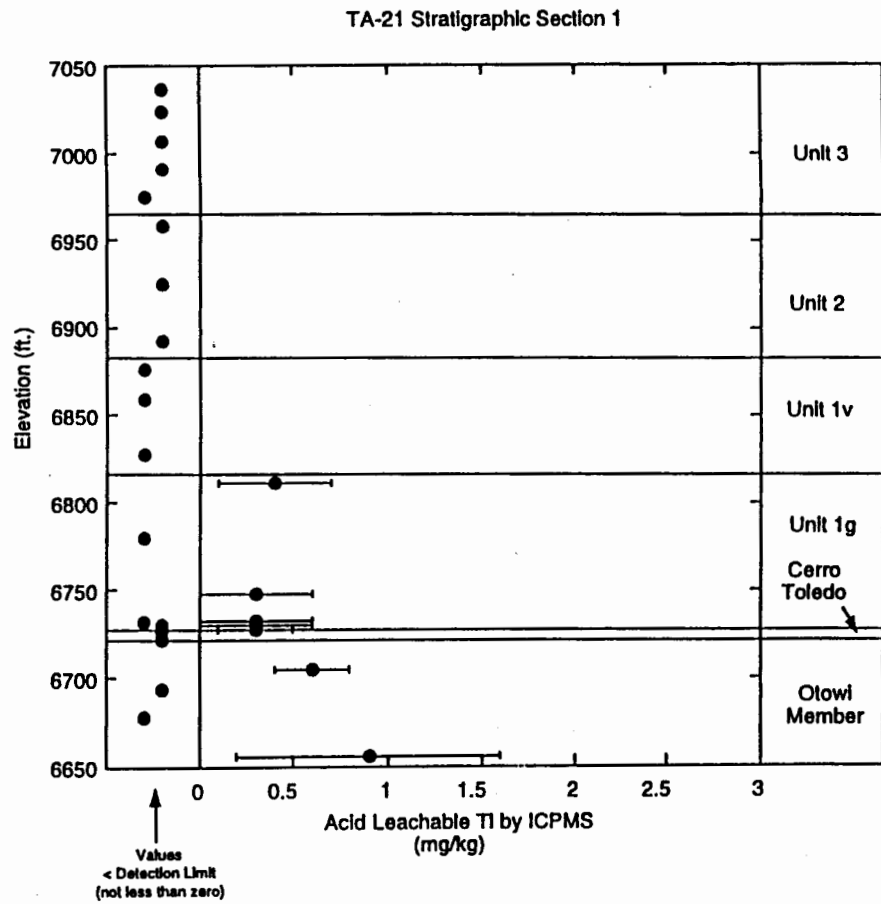


Fig. 22 PLOTS SHOWING EXAMPLES OF ACID LEACHABLE THALLIUM CONCENTRATIONS AT TA-21 AS A FUNCTION OF STRATIGRAPHIC HEIGHT IN THE BANDELIER TUFF.

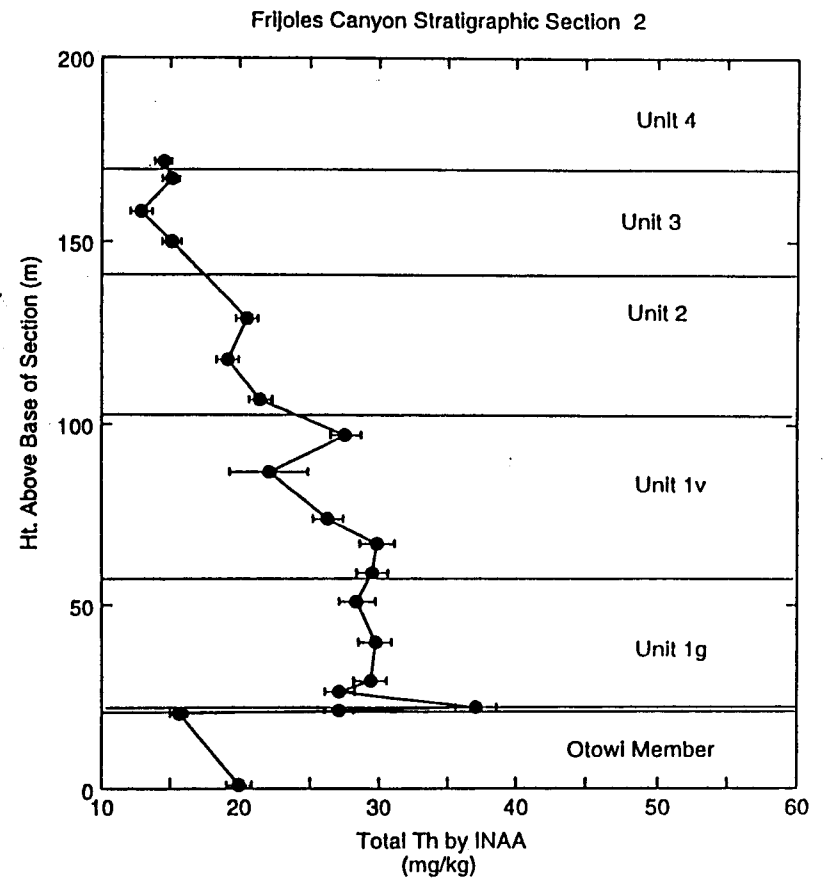
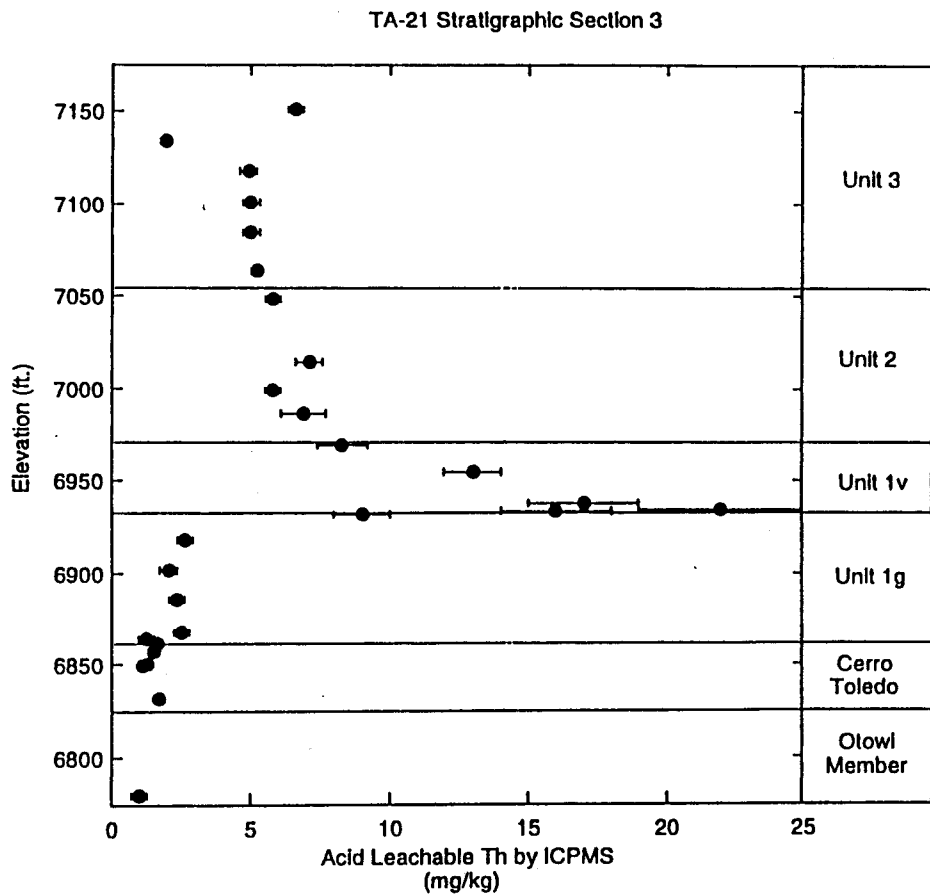


Fig. 23 PLOTS SHOWING EXAMPLES OF ACID LEACHABLE THORIUM CONCENTRATIONS AT TA-21 AND TOTAL THORIUM CONCENTRATIONS AT FRIJOLETS CANYON AS A FUNCTION OF STRATIGRAPHIC HEIGHT IN THE BANDELIER TUFF.

Uranium (U)

Ninety-two of the 106 leachable uranium concentrations were above ICPMS detection limits. Square root transformed uranium data are approximately normally distributed. Uranium concentrations for all geologic units range from 0.2 to 5.7 mg/kg and average 1.28 mg/kg.

Population characteristics from the Wilcoxon rank sum test (Table IV) resulted in pooling the uranium data for Qbt 1g, Qbt 1v, Qbt 2 and Qbt 3 as four separate data groups. Box plots comparing acid leachable uranium by geologic unit show generally high concentrations for unit Qbt 1v and low concentrations for units Qbo, Qbt 1g, Qct, and Tt relative to the other rock units (Fig. 4). Plots of leachable uranium from individual stratigraphic sections show that leachable uranium concentrations typically are low in the glassy tuffs in Qbo and in the basal part of the Tshirege Member, and they abruptly increase above the Qbt 1g/Qbt 1v contact (Fig. 24). Above this contact, uranium concentrations decrease up section.

The background screening values for leachable uranium are 0.6 mg/kg for Tt, 0.2 mg/kg for Qbo, 0.4 mg/kg for Qct, 1.39 mg/kg for Qbt 1g, 5.93 mg/kg for Qbt 1v, 2.48 mg/kg for Qbt 2, 1.64 mg/kg for Qbt 3, and 0.9 mg/kg for Qbt 4. Background screening values for uranium in all rock units are well below the SAL of 95 mg/kg.

Total uranium concentrations by INAA decrease systematically up section from the base of the Tshirege Member (Fig. 24). Total uranium in the upper Tshirege Member is about one-half of that in the lower part. Uranium concentrations in the upper Otowi Member are about 25% less than those found in the lower Tshirege Member. Comparison of acid leachable and total uranium data shows that between 5% and 50% of the total uranium in the Bandelier Tuff is susceptible to leaching by nitric acid at a pH of 1.

Vanadium (V)

Ninety of the 106 leachable vanadium concentrations were above ICPES detection limits of 0.4 to 1.4 mg/kg. The vanadium data are approximately normally distributed. Vanadium concentrations for all geologic units range from 0.8 to 29 mg/kg and average 3.08 mg/kg.

Population characteristics from the Wilcoxon rank sum test (Table IV) resulted in pooling the vanadium data for Qbt 1g as a separate data group and Qbt 1v, Qbt 2, and Qbt 3 as another data group (Qbt1v,2,3). Box plots comparing acid leachable aluminum by geologic unit show that medians, arithmetic means, and middle 50 percent ranges are distinctly greater for units Tt and Qbt 4 than for the other units (Fig. 4). Plots of leachable vanadium from individual stratigraphic sections show that leachable vanadium concentrations are relatively constant in units Qct 1g through Qbt 3 of the Tshirege Member (Fig. 25). Soluble vanadium concentrations in Qbt 4 are approximately four times greater than those in the underlying tuffs of the Tshirege Member.

The background screening values for leachable vanadium are 29 mg/kg for Tt, 2.8 mg/kg for Qbo, 3.8 mg/kg for Qct, 1.67 mg/kg for Qbt 1g, 9.5 mg/kg for Qbt 4, and 4.01 mg/kg for Qbt 1v, Qbt 2, and Qbt 3. Background screening values for vanadium in all rock units are well below the SAL of 540 mg/kg.

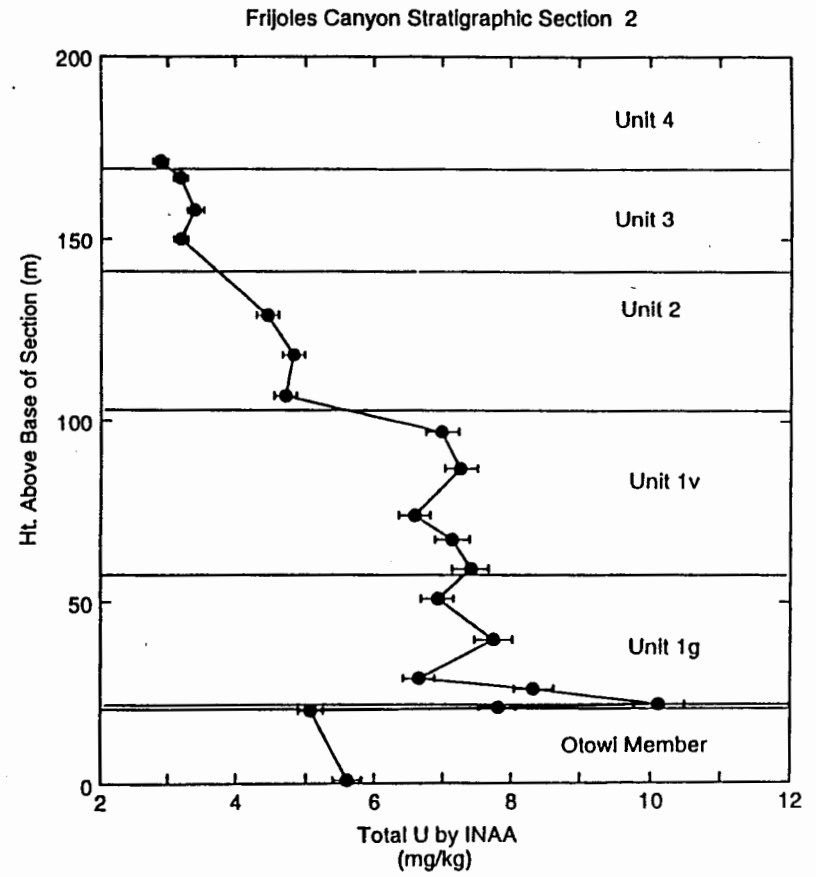
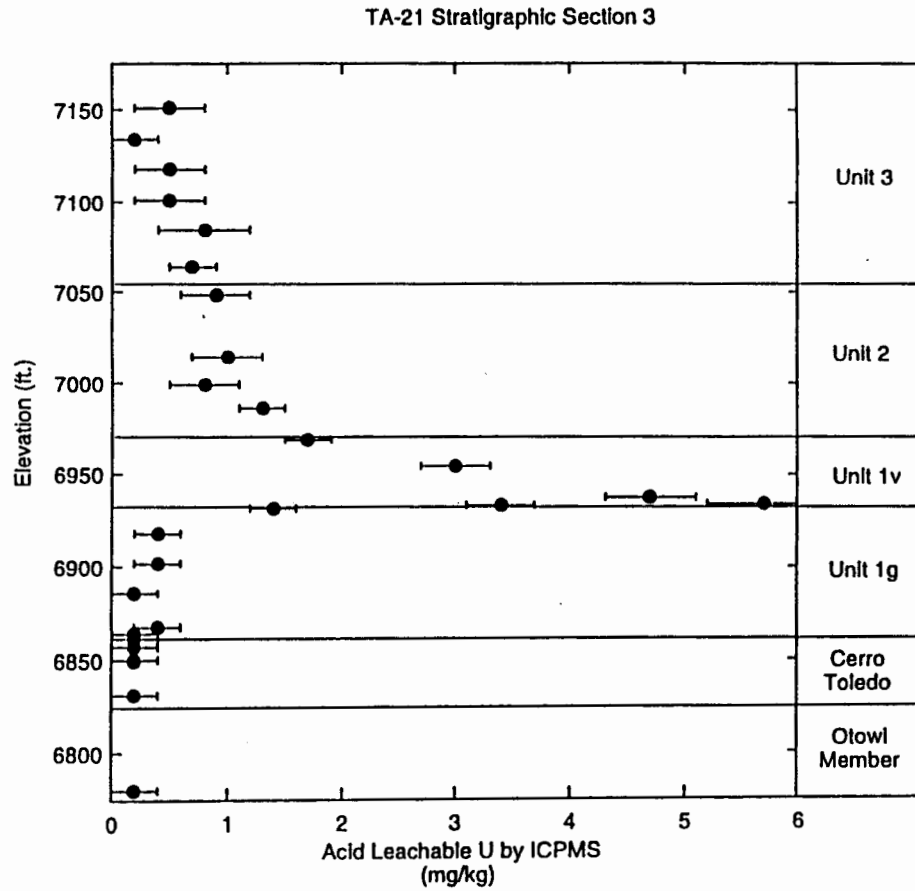


Fig. 24 PLOTS SHOWING EXAMPLES OF ACID LEACHABLE URANIUM CONCENTRATIONS AT TA-21 AND TOTAL URANIUM CONCENTRATIONS AT FRIJOLES CANYON AS A FUNCTION OF STRATIGRAPHIC HEIGHT IN THE BANDELIER TUFF.

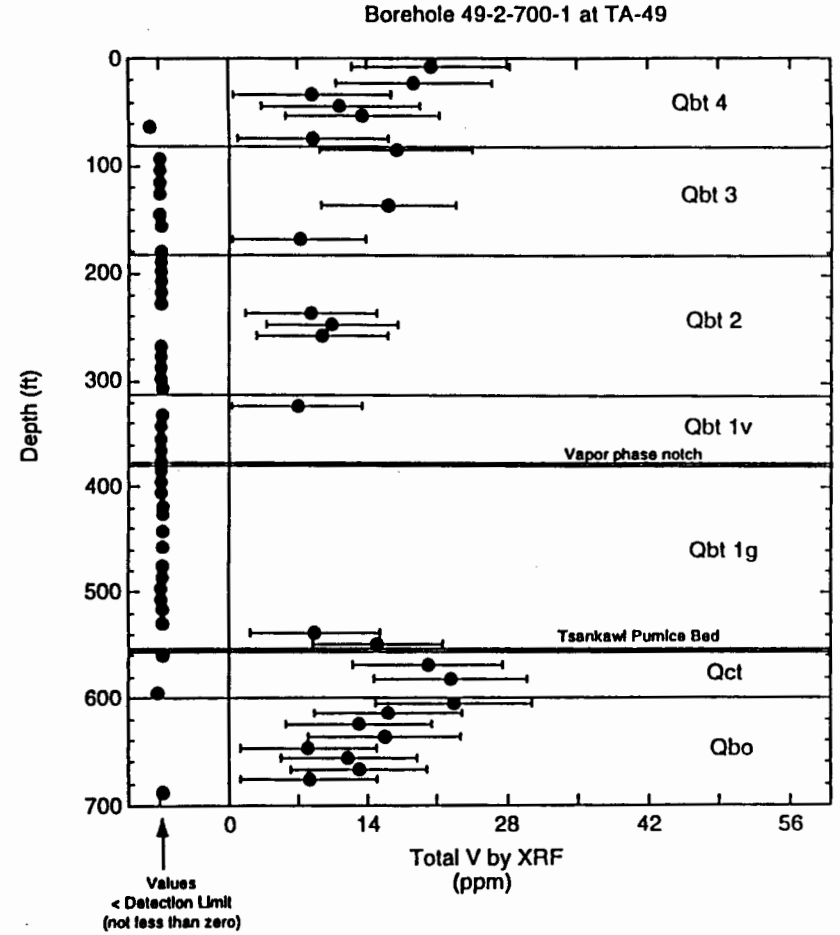
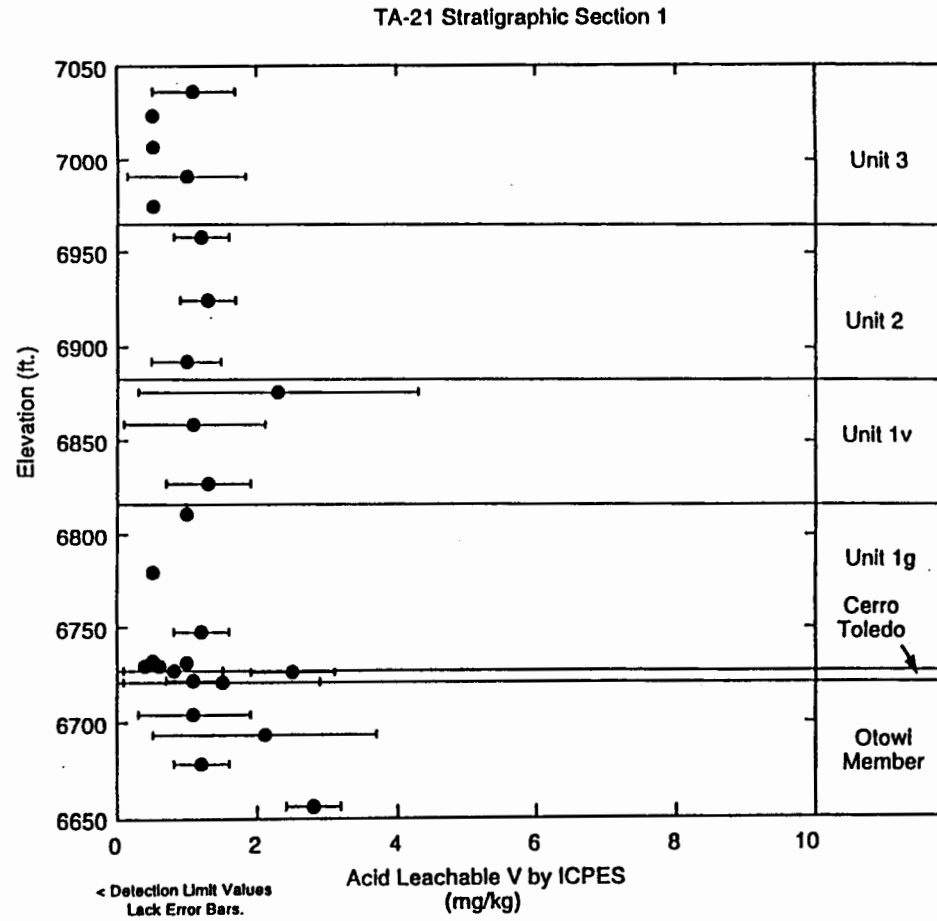


Fig. 25 PLOTS SHOWING EXAMPLES OF ACID LEACHABLE VANADIUM CONCENTRATIONS AT TA-21 AND TOTAL VANADIUM CONCENTRATIONS AT TA-49 AS A FUNCTION OF STRATIGRAPHIC HEIGHT IN THE BANDELIER TUFF.

About 40% of total vanadium concentrations by XRF are above the detection limit of approximately 7 mg/kg (Fig. 25). Total vanadium concentrations in the vitric tuffs at the base of the Tshirege Member (Qbt 1g) were generally below the detection limit whereas about half of the vanadium concentrations in overlying tuffs were above the detection limit, with the greatest concentrations occurring in Qbt 4 (Fig. 25). Total vanadium concentrations in Qbo are similar to those in upper part of the Tshirege Member.

Zinc (Zn)

All of the 106 leachable zinc concentrations were above ICPEES detection limits. Zinc concentrations for all geologic units range from 5.3 to 84 mg/kg and average 32.1 mg/kg.

Population characteristics from the Wilcoxon rank sum test (Table IV) resulted in pooling the zinc data for Qbt 1g, Qbt 2 and Qbt 3 as data group Qbt 1g23; Qbt 1v was treated as a separate data group. Box plots comparing acid leachable zinc by geologic unit show generally high concentrations for unit Qbt 1v and low concentrations for units Qbo and Qct relative to the other rock units (Fig. 4). Plots of leachable zinc from individual stratigraphic sections show that leachable zinc concentrations typically are low in the glassy tuffs Qbo and in the basal part of Qbt 1g (Fig. 26). Leachable zinc increases up section in Qbt 1g, reaching a maximum at the Qbt 1g/Qbt 1v contact (at the vapor phase notch). Above this contact, zinc concentrations decrease up section.

The background screening values for leachable zinc are 41 mg/kg for Tt, 21 mg/kg for Qbo, 17 mg/kg for Qct, 84.6 mg/kg for Qbt 1v, 47 mg/kg for Qbt 4, and 55.5 mg/kg for Qbt 1g, Qbt 2, and Qbt 3. Background screening values for zinc in all rock units are well below the SAL of 23000 mg/kg.

Total zinc concentrations by XRF decrease slightly up section from Qbt 1g to the middle of Qbt 3 (Fig. 26). Zinc concentrations abruptly increase in the middle of Qbt 3 and remain relatively constant up section into Qbt 4. Total zinc concentrations tend to increase up section in the upper part of the Qbo, and the top of Qbo is generally depleted in zinc relative to the lower part of Qbt 1g. The percentage of total zinc susceptible to acid leaching in the Bandelier Tuff varies with stratigraphic position. Approximately 50% to 80% of the zinc in upper Qbt 1g and in Qbt 1v is released by leaching in a solution of nitric acid at a pH of 1. However, only 10% to 20% of the zinc in other parts of the Bandelier Tuff is dissolved by the nitric acid solution.

Radionuclide Background Screening Values

Background screening values for activities of naturally occurring potassium, thorium, and uranium isotopes were calculated using total elemental concentrations and assuming secular isotopic equilibrium in the tuffs. Isotopic screening activities were calculated by multiplying the total element background screening value by the percent natural abundance of the iso-

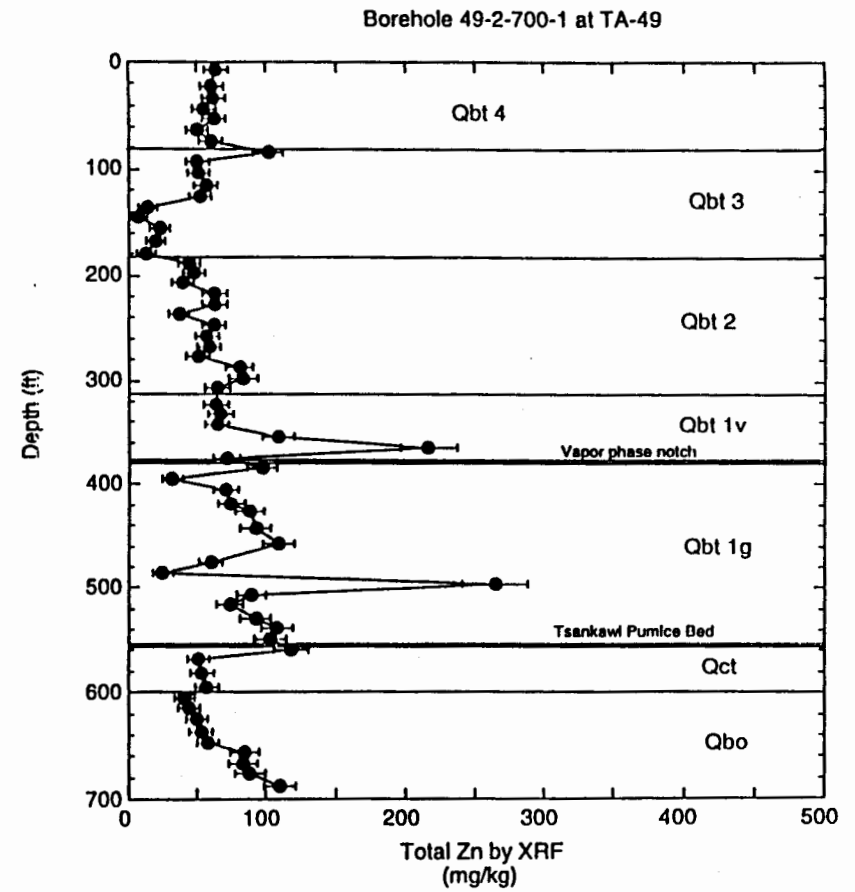
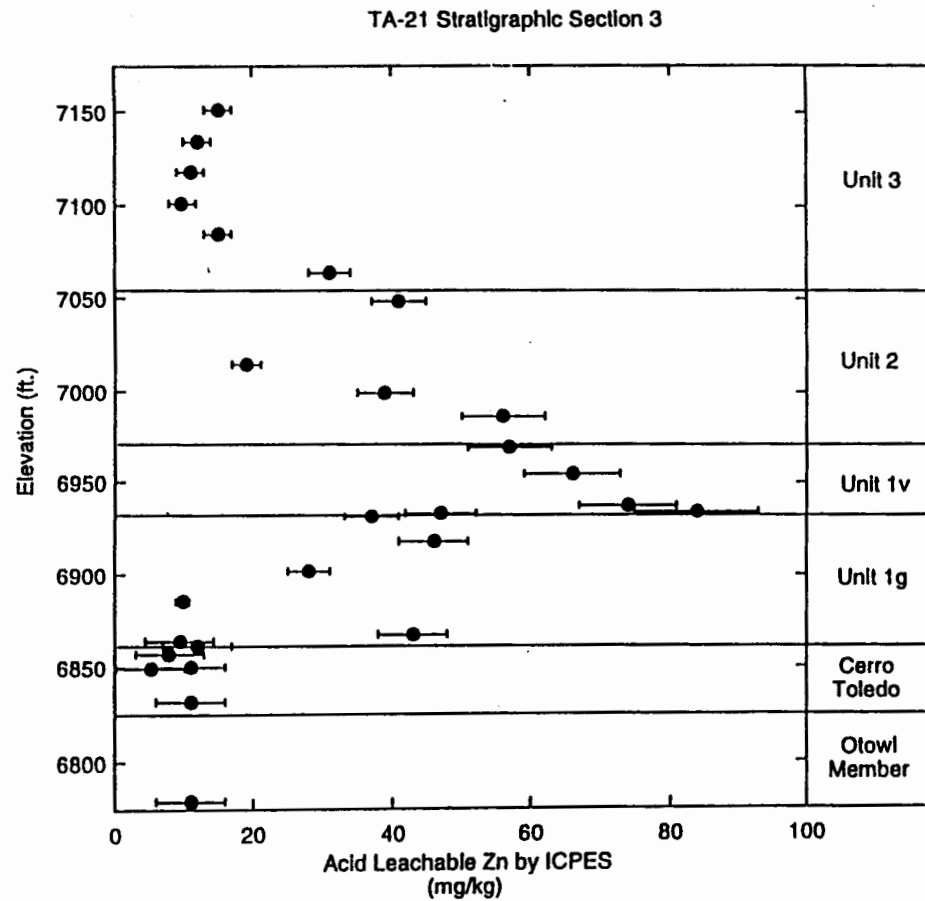


Fig. 26 PLOTS SHOWING EXAMPLES OF ACID LEACHABLE ZINC CONCENTRATIONS AT TA-21 AND TOTAL ZINC CONCENTRATIONS AT TA-49 AS A FUNCTION OF STRATIGRAPHIC HEIGHT IN THE BANDELIER TUFF.

top of interest and the specific activity of that isotope. Radium-226 activities were measured for a limited suite of samples, and background screening values for this isotope are also discussed.

The radionuclide background screening activities were calculated using INAA data for 47 samples of Bandelier Tuff collected at two sections in Frijoles Canyon. A summary of background screening activities for radionuclides is presented in Table VIII.

Potassium-40

All of the total potassium concentrations were above INAA detection limits. Potassium concentrations for all geologic units range from 28760 to 47920 mg/kg and average 38137 mg/kg. The potassium data are approximately normally distributed. Population characteristics from the Wilcoxon rank sum test resulted in pooling all of the potassium data for Qbt 1g, Qbt 1v, Qbt 2, and Qbt 3 (as data group Qbt 123). Qbt 4 was pooled as a separate data group.

The background screening activities for potassium-40 are 30.4 pCi/g for Qbo, 36.9 pCi/g for Qbt 1g, Qbt 1v, Qbt 2, and Qbt 3, and 37.0 pCi/g for Qbt 4 (Table VIII).

Radium (Ra)

Thirteen Bandelier Tuff samples were analyzed for Radium-226 activities by gamma-ray spectroscopy. No statistical distribution of the radium-226 was estimated because of the small sample population. Radium activities range from 1.72 to 7.15 pCi/g and average 4.92 in the 13 samples analyzed.

Box plots comparing radium-226 activities by geologic unit show that radium-226 activities tend to decrease up section, with the highest activities occurring in unit Qbo and the lowest in Qbt 3 (Fig. 4). Radium-226 activities increase in Qbo 4 relative to the underlying tuffs. Radium-226 activities were not determined for units Qct and Tt.

The background screening values for radium-226 are based on maximum activities in each rock unit. Background screening values are 7.15 pCi/g for Qbo, 6.78 pCi/g for Qbt 1g, 6.61 pCi/g for Qbt 1v, 4.82 pCi/g for Qbt 2, 2.6 pCi/g for Qbt 3, and 6.23 pCi/g for Qbt 4. Six of the thirteen tuff samples analyzed in this study have ²²⁶Ra activities that exceed the SAL of 5 pCi/g.

Thorium-232

All of the total thorium concentrations were above INAA detection limits. Thorium concentrations for all geologic units range from 12.7 to 37.1 mg/kg and average 22.7 mg/kg. Statistical distributions for total thorium were not evaluated because of the small sample size for each stratigraphic unit. Maximum concentrations are used to calculate background screening activities for all units.

TABLE VIII.

COMPUTED BACKGROUND SCREENING VALUES FOR NATURALLY OCCURRING RADIONUCLIDES COMPILED BY GEOLOGICAL UNITS

Analyte ¹	Qbo	Qbt 1g	Qbt 1v	Qbt 2	Qbt 3	Qbt 4	SAL
Total Potassium (mg/kg)	37200	45100	45100	45100	45100	45300	NA
Potassium-40 (pCi/g)	30.4	36.9	36.9	36.9	36.9	37.0	NA
Radium-226 (pCi/g measured)	7.15	6.78	6.61	4.82	2.6	6.23	5
Total Thorium (mg/kg)	19.9	37.1	30.1	25.9	16.3	15.6	NA
Thorium-232 (pCi/g)	2.17	4.05	3.29	2.83	1.78	1.70	5
Total Uranium (mg/kg)	5.61	10.1	7.59	7.12	4.37	2.93	95
Uranium-234 (pCi/g)	1.99	3.59	2.70	2.53	1.55	1.04	86
Uranium-235 (pCi/g)	0.086	0.155	0.116	0.109	0.067	0.045	18
Uranium-238 (pCi/g)	1.87	3.37	2.53	2.37	1.46	0.98	59
Total Uranium (pCi/g)	3.95	7.12	5.34	5.01	3.08	2.06	66

NA - Not available.

The background screening activities for thorium-232 are 2.17 pCi/g for Qbo, 4.05 pCi/g for Qbt 1g, 3.29 pCi/g for Qbt 1v, 2.83 pCi/g for Qbt 2, 1.78 pCi/g for Qbt 3, and 1.70 pCi/g for Qbt 4 (Table VIII). The background screening activities for thorium-232 are below the SAL of 5 pCi/g.

Uranium Isotopes

All of the total uranium concentrations were above INAA detection limits. Uranium concentrations for all geologic units range from 2.8 to 10.1 mg/kg and average 5.89 mg/kg. Statistical distributions for total uranium were not evaluated because of the small sample size for each stratigraphic unit. Maximum concentrations are used to calculate background screening activities for all units. Uranium background screening activities are summarized by isotope in Table VIII. The background screening activities for uranium isotopes are below SALs.

Use of Bivariate Plots in Background Comparisons

In addition to their use in deriving background screening values, the background data in this report also can be used to define natural geochemical trends in rock units. These trends provide another tool for evaluating whether elemental concentrations determined during an RFI are naturally occurring or if their geochemical signature is outside the normal range found in the bedrock units. The background element pairs of uranium vs. thorium, lead vs. zinc, and zinc vs. thorium show the greatest degree of correlation for the leachable inorganic elements (Fig. 27).

The leachable uranium and thorium concentrations are the most strongly correlated elements in the data set, and they are the best element pair for defining the natural geochemistry of the Bandelier Tuff. Samples with leachable elemental concentrations significantly outside the uranium and thorium data trend should be considered as potentially contaminated and evaluated further. The lead vs. zinc and zinc vs. thorium regression curves are not correlated as well, but they still may be useful in identifying obvious data outliers (Fig. 27).

Data evaluations must be done with caution because some outliers to the main data trends may be naturally occurring. Naturally occurring outliers can be present where primary magmatic trends are overprinted by secondary alteration. The potassium vs. sodium plot (Fig. 27) provides a good example where two naturally occurring geochemical trends are defined by the data set. Most samples fall along the lower linear regression line and probably represent the leachable compositions of the tuff soon after emplacement. The upper linear regression curve represents glassy tuffs from stratigraphic section 1 at TA-21. Glassy tuffs are susceptible to diagenetic alteration, and as the chlorine and sulfate data discussed above show, the tuffs at this location were probably altered by ground water sometime after their deposition.

CONCLUSIONS AND RECOMMENDATIONS

Background elemental concentrations were determined for inorganic constituents of the Bandelier Tuff and for some older rock units as baseline data for RCRA facilities investigations. These data meet the requirements for characterizing the chemistry of uncontaminated rock units for use in comparisons to identify areas of contamination, perform baseline risk assessments, and plan remedial actions. These data supplement information from earlier background soil and tuff investigations by Longmire et al. (1994a) and the companion report to this study (Longmire et al., 1995b).

Two types of analytical data for inorganic constituents are presented. Leachable elemental concentrations provide information about the bioavailability of elements for risk assessment calculations. The leachable elemental concentrations are treated statistically and are the primary focus of this investigation. Total elemental concentrations are used for calculating background screening values for naturally occurring potassium, thorium, and uranium isotopes, and they provide supporting data for understanding the distribution of inorganic elements in the rock units.

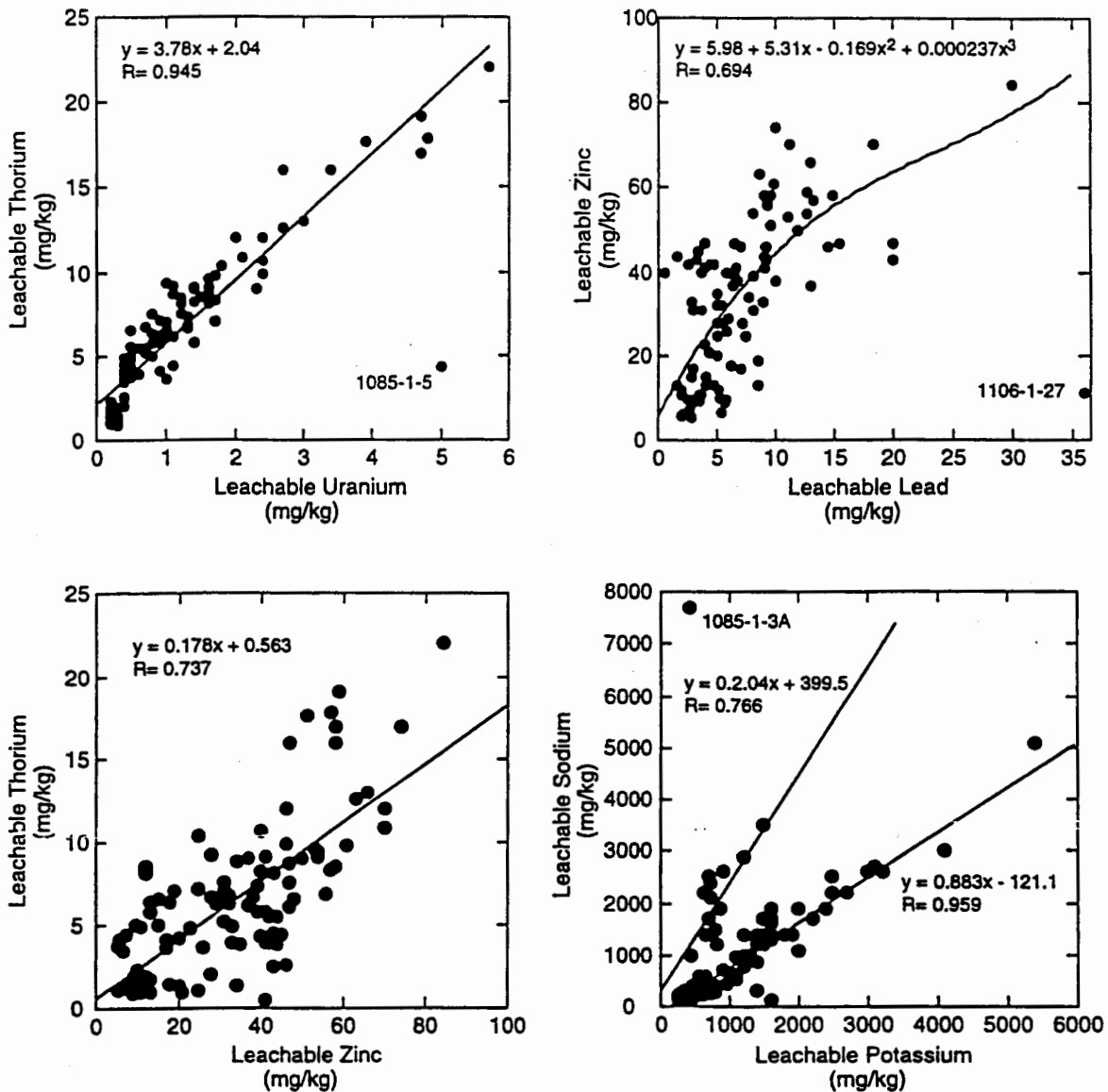


Fig. 27 Bivariant plots showing natural elemental distribution for leachable analytes in the Bandelier Tuff. Outliers, which are labeled with their sample numbers, were not used to calculate regression curves. The background data can be used to define natural geochemical trends in rock units as shown in the uranium vs. thorium, lead vs. zinc, and zinc vs. thorium plots. Such plots should be interpreted with caution because some outliers to the main data trends may be naturally occurring. The potassium vs. sodium plot provides a good example where two naturally occurring geochemical trends are defined by the data set. The samples falling along the lower linear regression line probably represent the leachable compositions of the tuff soon after emplacement whereas the upper linear regression curve represents glassy tuffs that were probably altered by ground water sometime after their deposition.

The field, analytical, and statistical methods used in this investigation are sufficient for defining background element concentrations for inorganic contaminants of concern. The spatial coverage and population size of background chemistry samples are adequate for defining background screening values for units Qbt 1g, Qbt 1v, Qbt 2, and Qbt 3 of the Tshirege

Member. These tuffs are the most widespread rock units on the Pajarito Plateau and make up the bedrock at the majority of the Laboratory's potential release sites. No additional background data are needed for these units.

We recommend additional background characterization of Qbt 4 because so few samples of this unit are included in the present data set. Qbt 4 is an important geologic unit because it has unique geochemical characteristics compared to other parts of the Tshirege Member and because it is the surface bedrock unit underlying potential release sites in the western part of the Laboratory. The need for additional Qbt 4 background data will be mitigated in part by ongoing local background investigations being done in support of clean closure of MDA P at TA-16. We recommend that characterization of Qbt 4 be completed by analyzing samples from the background geology borehole 49-2-700-1 at TA-49 which penetrated 25 m of Qbt 4 at the top of the section.

Additional background data are presented for some of the pre-Tshirege rock units including, in descending stratigraphic order: tephra and volcanoclastic sediments of the Cerro Toledo interval, the upper part of the Otowi Member of the Bandelier Tuff, and dacitic lavas of the Tschicoma Formation. These background data provide useful bounding information on the geochemistry of these deeper units, but they are considered preliminary because so few samples of these units are included in the present data set. Because these rock units directly underlie so few potential release sites, we recommend that local background data be collected for these units on an as needed basis.

REFERENCES

Baltz, E.H., Abrahams, J.H., Sr., and Purtymun, W.D., 1963, Preliminary report on geology and hydrology of Mortandad Canyon near Los Alamos, New Mexico, with reference to disposal of liquid low-level radioactive wastes, U.S. Geol. Survey open-file report (Albuquerque, NM), 105 p.

Broxton, D.E., Heiken, G., Chipera, S.J., and Byers, F.M., 1995a, Stratigraphy, Petrography, and Mineralogy of Bandelier Tuff and Cerro Toledo deposits, *in* D.E. Broxton and P.G. Eller, eds., *Earth Science Investigations for Environmental Restoration—Los Alamos National Laboratory Technical Area 21*, Los Alamos National Laboratory Report LA-12934-MS pp. 33-64.

Broxton, D.E., Vaniman, D., Byers, F.M., Jr., Chipera, S.J., Kluk, E.C., and Warren, R.G., 1995b, Stratigraphy, mineralogy, and chemistry of bedrock tuffs at Pajarito Mesa, Los Alamos National Laboratory, New Mexico, Los Alamos National Laboratory report, in press, 29p

Broxton, D.E., LaDelfe, C., Chipera, S.J., and Kluk, E.C., in review, Stratigraphy, mineralogy, and chemistry of bedrock tuffs at Mesita del Buey, Los Alamos National Laboratory, New Mexico, Los Alamos National Laboratory LAMS report, 32p., in review.

Broxton, D.E. and Reneau, S.L., 1995, Stratigraphic nomenclature of the Bandelier Tuff for the Environmental Restoration Project at Los Alamos National Laboratory, Los Alamos National Laboratory Report LA-13010-MS, 21p.

Carr, M.H. and Turekian, K.K., 1961, The geochemistry of cobalt, *Geochem. et Cosmochim. Acta*, 26, pp. 411-416.

Crowe, B., Linn, G., Heiken, G., and Bevier, M., 1978, Stratigraphy of the Bandelier Tuff in the Pajarito Plateau, applications to waste management, Los Alamos National Laboratory report LA-7225-MS, 57 p.

Doell, R.R., Dalrymple, G.B., Smith, R.L., and Bailey, R.A., 1968, Paleomagnetism, potassium-argon ages, and geology of rhyolites and associated rocks of the Valles caldera, New Mexico, *Geol. Soc. America Memoir* 116, pp. 211-248.

EPA (US Environmental Protection Agency), April 1989, "Statistical Analysis of Ground-Water Monitoring Data at RCRA Facilities. Interim Final Guidance," Office of Solid Waste, Waste Management Division, US Environmental Protection Agency, Washington DC. (EPA 1989, 1141)

EPA (US Environmental Protection Agency), April 1992, "Guidance for Data Useability in Risk Assessment (Part A)," Office of Emergency Remedial Response, US Environmental Protection Agency, Washington DC. (EPA 1992, 1166)

Environmental Restoration Project Assessments Council, March 28, 1995. Statistical Comparisons to Background, Part I," Los Alamos National Laboratory Report LA-UR-95-1217, Los Alamos, New Mexico. (Environmental Restoration Project Assessments Council 1995, 1218)

Garcia, S.R., Hensley, W.K., Minor, M.M., Denton, M., and Fuka, M. A., 1982, An automated multidetector system for instrumental neutron activation analysis, of geologic and environmental materials, *in* R.H. Filby, B.S. Carpenter, and R.C. Ragaini, eds., *Atomic and Nuclear Methods in Fossil Energy Research*, Plenum, New York, pp. 133-140.

Gilbert, R.O., 1987, *Statistical Methods for Environmental Pollution Monitoring.*, Von Nostrand Reinhold Company Inc., New York, 320 pp.

Goff, Fraser, 1995, Geologic Map of Technical Area 21, *in* D.E. Broxton and P.G. Eller, eds., *Earth Science Investigations for Environmental Restoration—Los Alamos National Laboratory Technical Area 21*, Los Alamos National Laboratory Report LA-12934-MS pp. 33-64.

Heiken, G., Goff, F., Stix, J., Tamanyu, S., Shafiqullah, S., Garcia, S., and Hagan, R, 1986, Intracaldera volcanic activity, Toledo caldera and embayment, Jemez Mountains, New Mexico, *J. Geophys. Res.*, 91, (B2), pp. 1799-1815.

Izett, G.A. and Obradovich, J.D., 1994, $^{40}\text{Ar}/^{39}\text{Ar}$ age constraints for the Jaramillo Normal Subchron and the Matuyama-Brunhes geomagnetic boundary, *J. Geophys. Res.* 99 (B2), pp. 2925-2934.

Longmire, O., Duffy, C., and Reneau, S., 1993, Preliminary Background Elemental Concentrations in Bandelier Tuff and Selected Soils Series, 1993, Los Alamos National Laboratory, Letter Report.

Longmire, P., Reneau, S., Watt, P., McFadden, L., Gardner, J., Duffy, C., and Rytí, R., 1995a, Natural Background Geochemistry, Geomorphology, and Pedogenesis of Selected Soil Profiles and Bandelier Tuff, Los Alamos, New Mexico, Los Alamos National Laboratory Report LA-12913-MS, 158p.

Longmire, P., McDonald, E., Reneau, S., Rytí, R., and Watt, P., 1995b, Natural Background Geochemistry, Geomorphology, and Pedogenesis of Fourteen Soil Profiles, Los Alamos, New Mexico, this report.

Minor, M.M., Hensley, W.K., Denton, M., and Garcia, S.R., 1982, An automated activation analysis system, *J. Radioanal. Chem.*, 70, pp. 459-471.

Reneau, S.L., Dethier, D.P., and Carney, J.S., 1995, Landslides and other mass movements at Technical Area 33, Los Alamos National Laboratory Report LA-12955-MS, 48 p.

Smith, R.L., 1960, Zones and zonal variations in welded ash flows, *U.S. Geol. Survey Prof. Paper 354-F*, pp. 149-159.

Smith, R.L. and Bailey, R.A., 1966, The Bandelier Tuff: a study of ash-flow eruption cycles from zoned magma chambers, *Bull. Volcanologique*, v. 29, pp. 83-104.

Smith, R.L., Bailey, R.A., and Ross, C.S., 1970, Geologic map of the Jemez Mountains, New Mexico, *U.S. Geol. Survey Map I-571*, scale 1:125,000.

Smith, R. L., 1979, Ash flow magmatism, *Geol. Soc. America Spec. Paper 180*, p. 5-27.

Stimac, J.A., Broxton, D.E. Klug, E., and Chipera, S., 1995, Preliminary stratigraphy of tuffs from borehole 49-2-700-1 at Technical Area 49, Los Alamos National Laboratory, New Mexico, Los Alamos National Laboratory Report, in review.

Turekian K.K. and Wedepohl, K.H., 1961, Distribution of the elements in some major rock units of the Earth's crust, *Geol. Soc. America Bull.*, v. 72, pp. 175-192.

Vaniman, D. and Wohletz, K., 1990, Results of geological mapping/fracture studies, TA-55 area, Los Alamos National Laboratory Seismic Hazards Memo EES1-SH90-17, 25 pp, 3 Plates, 23 figures.

Vaniman, D., and Wohletz, K., 1991, Revisions to report EES1-SH90-17, Los Alamos National Laboratory Seismic Hazards Memo EES1-SH91-12, 2 pp.

Weir, J.E. and Purtymun, W.D., 1962, Geology and hydrology of Technical Area 49, Frijoles Mesa, Los Alamos County, New Mexico, *U.S. Geol. Survey Admin. Release Report*, Albuquerque, NM, 225 p.

APPENDIX I

S-PLUS CODE USED TO CALCULATE LOGNORMAL UTLS

File: Inorm_utl1.s

```
function(q,p,n,ave,sd,nt)
{
# Inorm_utl1.s is used as function LUTL1 in Splus
# This function is used to estimate the upper 95% CI of the 95th
# percentile for a lognormal distribution. Uses Gilbert's MBE of LN.
# q = the quantile to estimate
# p = the confidence limit of q
# n = number of values sampled
# ave = mean of logtransformed data
# sd = st. dev. of logtransformed data
# nt = number of simulation trials
#.....

# Calculate the qth quantile of the normal distribution
q1_qnorm(q)

# Initialize arrays
t1_rep(-1,n)
t2_rep(-1,nt)

i_0

repeat

{ i_i+1

# Get the "n" lognormal samples
t1_rlnorm(n,ave,sd)

# Calculate the mean and sd the "Gilbert" way
dummy_InormUMV.s(t1)
ave1_dummy$mu
sd1_sqrt(dummy$s2)

# Calculate an estimate of the 95th percentile
t2[i]_exp(ave1+q1*sd1)
if(i>=nt) break
}
}
```

APPENDIX I (CONT)

```
# Find the upper p*100% of the qth percentile
quantile(t2,p)
}
```

File: InormUMV.s

```
function(x)
{
# InormUMV.s (Splus function)
# Calls: psi.s
# Min Variance Unbiased ests of parameters of lognormal(mu,var=s2) distn
# for X~lognorm(mu,s2), Y=log(X)~normal(mu,s2)
# returns:E=mean(X), V=var(X)
#      mu=mean(Y),s2=var(Y)
# ref:Gilbert('87),Stat Methods for Env Pollution Mon, pp165-166
  n <- length(x)
  y <- log(x)
  ymu <- mean(y)
  vy <- var(y)
  psi1 <- psi.s(vy/2, n)
  psi2 <- psi.s(2 * vy, n)
  psi3 <- psi.s((vy * (n - 2))/(n - 1), n)
  E <- exp(ymu) * psi1
  V <- exp(2 * ymu) * (psi2 - psi3)
  mu <- log(E^2/(V + E^2)^0.5)
  s2 <- log(V/E^2 + 1)
  return(E, V, mu, s2)
}
```

File: psi.s

```
function(t, n)
{
# psi.s (Splus function)
# called by InormUMV.s
# psi function in Gilbert('87) Stat. Meth. Env. Pollution. Mon, pp 165
# for Min Variance Unbiased ests of parameters of lognormal(mu,var=s2) distn
  psi <- 0
  psi[1] <- ((n - 1) * t)/n
  for(i in 1:25) {
    psi[i + 1] <- (psi[i] * (n - 1)^2 * t)/((i + 1) * n * (n + (2 *
      i - 1)))
    if(abs((psi[i + 1] - psi[i])/psi[i]) < 1e-09)
      break
  }
  psi <- 1 + sum(psi)
  psi
}
```